AD-E301242

AD-A134 722

(1)

DNA 2028H

TREE PREFERRED PROCEDURES

Selected Electronic Parts

Kaman Tempo, DASIAC
816 State Street (P.O. Drawer QQ)
Santa Barbara, California 93102

31 January 1982

Handbook

CONTRACT No. DNA 001-82-C-0069

APPROVED FOR PUBLIC RELEASE;
DISTRIBUTION UNLIMITED.

THIS WORK WAS SPONSORED BY THE DEFENSE NUCLEAR AGENCY
UNDER RDT&E RMSS CODE B337082466 P99QAXDC00005 H2590D.

DTIC FILE COPY

Prepared for
Director
DEFENSE NUCLEAR AGENCY
Washington, DC 20305

DTIC
ELECTE
S NOV 15 1983 D
B

83 10 21 004

Destroy this report when it is no longer needed. Do not return to sender.

PLEASE NOTIFY THE DEFENSE NUCLEAR AGENCY, ATTN: STTI, WASHINGTON, D.C. 20305, IF YOUR ADDRESS IS INCORRECT, IF YOU WISH TO BE DELETED FROM THE DISTRIBUTION LIST, OR IF THE ADDRESSEE IS NO LONGER EMPLOYED BY YOUR ORGANIZATION.

DNA PRINTING PLANT

UNCLASSIFIED

SECURITY CLASSIFICATION OF THIS PAGE *(When Data Entered)*

REPORT DOCUMENTATION PAGE		READ INSTRUCTIONS BEFORE COMPLETING FORM
1. REPORT NUMBER DNA 2028H	2. GOVT ACCESSION NO. AD-A134 722	3. RECIPIENT'S CATALOG NUMBER
4. TITLE *(and Subtitle)* TREE PREFERRED PROCEDURES Selected Electronic Parts		5. TYPE OF REPORT & PERIOD COVERED Handbook 6. PERFORMING ORG. REPORT NUMBER
7. AUTHOR(s) M. A. Espig, Editor		8. CONTRACT OR GRANT NUMBER(s) DNA 001-82-C-0069
9. PERFORMING ORGANIZATION NAME AND ADDRESS Kaman Tempo, DASIAC 816 State Street (P.O. Drawer QQ) Santa Barbara, California 93102		10. PROGRAM ELEMENT, PROJECT, TASK AREA & WORK UNIT NUMBERS Subtask P99QAXDC000-05
11. CONTROLLING OFFICE NAME AND ADDRESS Director Defense Nuclear Agency Washington, DC 20305		12. REPORT DATE 31 January 1982 13. NUMBER OF PAGES 208
14. MONITORING AGENCY NAME & ADDRESS(*if different from Controlling Office*)		15. SECURITY CLASS *(of this report)* UNCLASSIFIED 15a. DECLASSIFICATION DOWNGRADING SCHEDULE N/A since UNCLASSIFIED

16. DISTRIBUTION STATEMENT *(of this Report)*

Approved for public release; distribution unlimited.

17. DISTRIBUTION STATEMENT *(of the abstract entered in Block 20, if different from Report)*

18. SUPPLEMENTARY NOTES

This work was sponsored by the Defense Nuclear Agency under RDT&E RMSS Code B337082466 P99QAXDC00005 H2590D.

19. KEY WORDS *(Continue on reverse side if necessary and identify by block number)*

Radiation Effects Testing	Transistors	Integrated Circuits
Test Design and Documentation	Diodes	Transient Radiation
Dosimetry	Capacitors	Standard Test Procedures

20. ABSTRACT *(Continue on reverse side if necessary and identify by block number)*

This handbook provides recommended test procedures that have been agreed upon as standards for determining the effects of transient radiation on electronic parts. It is intended to assist personnel who have responsibility for conducting radiation effects tests using available simulation facilities.

DD FORM 1 JAN 73 1473 EDITION OF 1 NOV 65 IS OBSOLETE

UNCLASSIFIED

SECURITY CLASSIFICATION OF THIS PAGE *(When Data Entered)*

PREFACE

Preparation of this document has been carried out under the direction of the Defense Nuclear Agency (DNA). Grateful acknowledgment is made for the constructive review of the material by William Alfonte (Kaman Tempo), George Messenger (Consultant), Robert McCoskey (Kaman Tempo), Arthur Namenson (NRL), Harry Schafft (NBS), Dr. E.A. Wolicki (NRL), and also to the many other individuals who have helped to develop the DNA Approved Hardness Assurance Procedures on which this document is based.

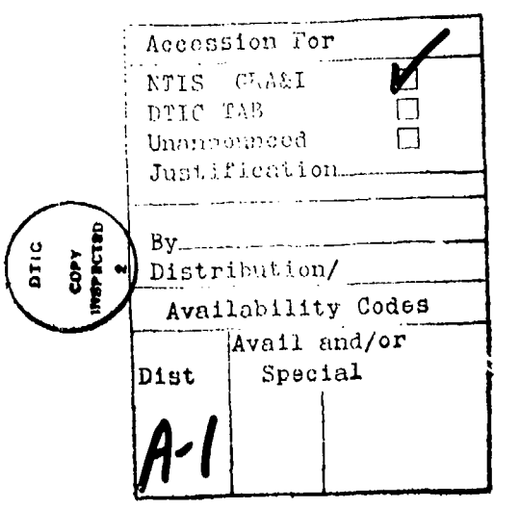

TABLE OF CONTENTS

TABLE OF CONTENTS (Continued)

TABLE OF CONTENTS (Continued)

TABLE OF CONTENTS (Continued)

TABLE OF CONTENTS (Continued)

LIST OF ILLUSTRATIONS

LIST OF ILLUSTRATIONS (Continued)

LIST OF ILLUSTRATIONS (Continued)

LIST OF TABLES

CHAPTER 1

INTRODUCTION

1.1 BACKGROUND

The technology of Transient Radiation Effects on Electronics (TREE) covers a wide range of scientific and engineering disciplines. It is a specialized field that incorporates concepts and terms from solid-state physics, radiation and nuclear physics, nuclear-weapon technology, and electronic and systems engineering. Most electronic systems must meet some kind of nuclear radiation specifications; hence, there is a need for device testing to gather data to fill the gap between available state-of-the-art information and the requirements of a specific system. It is important that test data be obtained and recorded in such a way that tests can be repeated and the data can be correlated with other work in the same area.

It is the purpose of the TREE Preferred Procedures to bring to the attention of the electronic engineer and the system designer those procedures in testing that will yield useful results for these purposes. Numerous standard procedures have been formulated as part of the Defense Nuclear Agency (DNA) hardness assurance program for TREE. This handbook describes the principles and philosophy involved in applying a set of standard procedures to obtain data for both discrete and integrated circuit devices.

1.2 PHILOSOPHY

The recommendations in this document are based on the applicable ASTM and Military Standards that have been developed for device parameter measurements. The object has been to formulate and recommend procedures by which radiation test data on electronic components and radiation environments may be obtained and reported. They provide a means of communicating useful information among workers in a large multidisciplined technology so that people in different but related specialties (e.g., dosimetry, circuit design, component testing, system specification, or component fabrication) will be able to use one common term in place of various specialty terms to better understand one another.

It is assumed that the users of this document will have access to the Design Handbook for TREE (Reference 1). The proper use of these preferred procedures relies on the user being familiar with the information contained in that handbook. A review of the pertinent subjects is strongly recommended when planning any TREE testing programs.

1.3 USE OF THIS DOCUMENT

This document will be of assistance to four principal types of users:

1. Circuit and system designers who use component data
2. System specifiers--those who perform tradeoffs to formulate environment criteria, system performance specifications, and system-failure criteria
3. Component manufacturers who can provide basic physical and electrical data and have the fabrication techniques and process controls needed for the development of radiation hardened components
4. The primary users of this document--those who define and perform tests to obtain and record radiation response data on electronic devices for use in circuit and system design.

The material in this document reflects the present ASTM and Military Standards for device testing; additional standards will be developed as electronics technology advances. This document will be updated as necessary to incorporate the latest standards. Therefore, it is the responsibility of the user to make certain he is using the most recent edition and to take an active part in supplying new information to effect improvements. The user should also realize that he bears the responsibility when simplifying or deviating from the suggested procedures.

1.4 DOCUMENT CONTENTS AND LIMITATIONS

This document is divided into eight related chapters. Chapter 2 discusses the principles of test design, analysis and prediction requirements, test data, and test procedure requirements. Also covered are test hardware considerations and general testing techniques such as device characterization and interference suppression. Chapter 3 covers general documentation requirements for testing programs.

A brief survey of the radiation sources used in TREE testing is presented in Chapter 4. General characteristics of radiation sources are discussed and the important parameters are summarized in tabular form. Source selection guidelines are also presented.

Chapter 5 covers dosimetry and environmental correlation procedures. Neutron measurements, photon and electron measurements, and pulse shape monitoring techniques are discussed for each type of the major simulation techniques.

Chapter 6 covers specific test procedures for measuring parameter variations due to radiation for transistors, diodes, and field-effect devices. Neutron, total dose, and transient ionizing radiation measurements are discussed.

Chapter 7 deals with test procedures for determining the currents and voltages in charged and uncharged capacitors due to radiation exposure. The most important capacitor effects are transient.

Chapter 8 presents test procedures for making permanent degradation and transient response measurements on integrated circuit devices. Both digital and linear circuit responses are discussed and specific test procedures are given for both types.

The principles presented in this document are applicable to high-volume testing as well as individual device testing. There are a number of high-volume electronic device testers in use. However, this equipment is often specially designed and is also expensive. Unless the radiation facility to be used already has such equipment and it is applicable to the test program, the test engineer will have to supply his own test fixtures.

It is not recommended that the measurement procedures described in this document be used in connection with decisions between buyers and sellers unless the precision of each has been evaluated by interlaboratory comparison and is approved for procurement purposes.

CHAPTER 2

TEST DESIGN

2.1 INTRODUCTION

Careful organization of the test efforts related to a development program is essential to avoid waste of test facility and financial resources. It also helps to reduce the time required for system development. Use of proven standardized test and documentation procedures is necessary if one is to obtain reliable, repeatable test data.

A well-documented test program provides much of the input information needed for scheduling, financing, and managing the total system development program as well as the test work. It not only specifies the tests to be accomplished and the expected results, but also provides a basis for efficient and effective integration of the test program into the total system development program. A good test design document will contain much of the information needed for the final report that describes the test results. It is a good practice to anticipate the final report format in the test planning documentation, since much effort must be spent in preparing and documenting the test program before any results can be published.

In all branches of science and technology, there are principles and techniques that are pertinent to the task of designing engineering tests. The basic principles and techniques applicable to designing tests for determination of transient-radiation effects on electronic parts are discussed in this chapter.

2.2 TEST DESIGN PRINCIPLES

Radiation effects data on electronic components are available from many different sources. There has been considerable variation in the techniques and simulation facilities used. Proper interpretation of such data requires some knowledge of the techniques and problems encountered in testing. This section considers the principles of test design with the objective of standardizing test procedures in accordance with established ASTM and Military Standards. Standardization of the test procedures will result in data that have much greater design application.

The following must be considered in developing a comprehensive test program for electronic components:

1. Purpose of the test--what is the problem and what information is needed to solve the problem?

2. Pretest analysis and prediction requirements--what analysis or other methods can be used to obtain this information? Is the theory valid?

3. Data requirements--what test data are needed to solve the problem?

4. Test procedures--what tests must be done to obtain the data?

5. Application of the data--how can the data be best analyzed and applied to solve the problem?

The documentation of a test program should contain the answers to these questions.

2.2.1 Purpose of the Test

Defining the problem to be solved often leads to optimal approaches for solution. Therefore, the statement of the problem--the purpose of the test--is an important part of the test design. In very brief form, the purpose of most TREE tests to which these preferred procedures are applicable will be to support either some TREE-hardened system design or the TREE assessment of a system. System design support might involve determination of radiation responses of a group of devices for design application data or it might take the form of screening tests for acceptance. The definition of the problem for a pretest document, then, would include:

1. A clear statement of the test objectives to ensure that the necessary results will be achieved

2. The system design or assessment radiation criteria

3. A statement as to how the system design or assessment program has been organized

4. A statement as to how the tests about to be described and performed will be integrated into the overall program

5. A statement of the data required and the required accuracy of the data.

2.2.2 Pretest Analysis and Prediction Requirements

Most TREE testing to which this document applies measures electronic device parameters before, during, and/or after radiation exposure. Since these electrical parameters are related to an application requirement or a response model, some predictive analysis may be made as a basis upon which test results may be judged. In the test design, pretest analysis methods should be described in detail and approximate expected test results should be predicted. This will ease the measurement process and also demonstrate applicability of the expected results to the system task at hand. Pretest

analysis may lead to significant changes in the test design if unexpected results are found. This is normal and proper, since design is inherently a dynamic process, subject to revision as new data or understanding become available. Any changes should be documented.

Analysis procedures for TREE phenomena are outlined in this handbook. Detailed procedures can be found in the Design Handbook for TREE (Reference 1). Discussions of the validity of the underlying theory for the pretest analysis may be necessary for some parameters. The significant assumptions should be set down, especially those related to the system problem of which the test is to be a part. (For example, environmental synergistic effects may be important.) These questions should be addressed in pretest analysis and in its documentation.

2.2.3 Test Data Requirements

Data requirements for a test program are derived from the test objectives, the amount of existing information, and the planned analysis methods. Specific requirements are also defined in the applicable ASTM and Military Standards (References 2 through 4). These requirements should be observed in all testing. A basic list of data requirements includes:

1. The format
2. A list of required parameters and their dependencies
3. Accuracies
4. The number of test items
5. Environmental ranges
6. Contractual requirements such as traceability of calibration standards.

Some compromises will need to be made when establishing data requirements. For example, at a particular test facility, the radiation environments may be mixed or separated in certain ways or the number of data points may be limited for nontechnical reasons.

Statistical test design should be used when suitable to provide controls, proper numbers of test groups, and sample sizes to meet system confidence requirements. The assignment of test-sample sizes is not a trivial problem, nor can statistical methods be blindly applied to TREE test design. One reason for this is that the distributions of semiconductor-device parameters are probably not normal but rather truncated by manufacturers' process controls and screening tests. Log-normal distributions are generally used instead. Another reason is that most of the tests envisioned will be designed to determine device parameters as functions of operating conditions and environments rather than in terms of a "failure level" or "go-no-go" criteria; screening tests are an obvious exception. These points are discussed in detail in Section 2.4.

The other elements of the test data requirements (1 through 3 and 5 above) are discussed in the succeeding chapters of this document.

2.2.4 Test Procedures

Detailed test procedures must be developed as an integral part of the test plan. Existing ASTM and Military Standards must be followed and must be used as the basis for electronic component test procedures (References 2 through 4). The test engineer must also consider availability of personnel, equipment, radiation facilities, or even of test items. Ultimately, the test engineer should apply the physical principles of TREE technology within whatever other constraints he may have. This document contains specific recommended "preferred" procedures, based on existing standards, for many types of TREE tests on transistors, diodes, integrated circuits, and capacitors as aids to the test engineer.

The test procedures section of a test plan should include:

1. Specific means for eliminating or controlling sources of systematic errors
2. Description of each of the test tasks and how these integrate into the whole test to produce the desired results
3. Required measurement-equipment lists including calibrations and accuracy requirements
4. Specific, detailed procedures including circuit diagrams, operating ranges, environment ranges, etc.
5. Radiation source characterization details and means of obtaining the desired exposures
6. Specific plans for data analysis.

2.2.5 Application of the Data

The raw TREE test data will generally be in the form of oscilloscope photographs, punched cards or tape from an automated semiconductor test set, or tabulated sets of meter readings. A posttest analysis and data reduction are required to translate the raw data into useful information that can be used as a measure of the expected performance of a system containing the tested components when operated in a specified radiation environment. The posttest data analysis involves three processes:

1. Interpretation of the raw data in terms of electrical quantities and units including reading errors and equipment accuracies
2. Interpretation of the electrical quantities in terms of the test objectives, required parameters, device models, predicted responses, etc., including the

experimental uncertainties arising from the procedures and sample sizes

3. Interpretation of unexpected data points in terms of testing errors or some uncontrolled or unknown phenomenon.

The appropriate posttest analysis methods should be specified in the pretest documentation for the particular test.

2.3 ANALYSIS OF TEST DATA

Selection and specification of the analysis procedures for a test program is primarily an engineering responsibility. The general rule for selecting analysis techniques for inclusion in the analysis procedures section of the test program document is to select the simplest technique that will fulfill the stated objectives and purpose of the test. Actually, the only restrictions placed on the selection of analytical techniques is that they must be sufficient to:

1. Satisfy the test objectives
2. Determine the confidence associated with any conclusions reached
3. Estimate the test accuracy for all numerical results.

For any type of test, the objectives will require that the analysis procedures produce an orderly arrangement (tabular and/or graphic) of the test data as measured and, where appropriate, in reduced form. Detailed procedures should be specified for data reduction.* A description of the procedures for evaluating measurement precision and system test error and the methods for combining these to estimate the test error and accuracies should be included. Error bands should be included and identified (e.g., ranges, standard deviation, etc.) on all graphs. Accuracies should be stated in all tables of numeric data.

For the preferred measurement procedures given in this document, the data reduction and analysis techniques are usually inherently defined by

---

* Data reduction here denotes the derivation of more meaningful parameters by combining the values of measured parameters. For example, resistivity may be derived by combining measured voltage, current, and dimensional values; neutron fluence expressed as neutrons per cm^2 (E > 1 MeV) may be derived combining activation dosimetry values, reactor spectra information, and shielding data. Data reduction may also mean the computation of descriptive statistics, the normalization of data by taking ratios, etc. Making value judgments or predictions of any kind are not included in data reduction.

the test. Thus, if transistor gain as a function of collector current and neutron fluence is needed, the test procedures would result in raw data that can be reduced by straightforward methods to obtain the desired gain data. In the process of data reduction, it is important to track the sources of uncertainty and error, such as measurement errors in currents, counting errors in dosimetry, etc. Then the results and probable errors are quoted. This data reduction process is clear for the problem of determining response of one or a few devices.

The test objective might be to determine the expected radiation response distribution of a population of devices of which a sample population was tested. The test design must then provide for proper sampling of the population, measures to control errors, and the analysis of the response data of the irradiated groups of devices. In this case, some statistical interpretations will have to be made. For example, for a given neutron fluence, the gains as functions of collector current may be analyzed to find, for several specific values of I_c, the mean observed gain and the observed standard deviation of the gain for the sample. From this, assuming proper randomizing of the sample and assuming fixed process controls, a statistical inference may be made with specified confidence concerning the parts-population mean gain and variance for this fluence at these collector currents. This process could be repeated for other fluence values. Alternatively, the gain versus fluence, or damage constant data, could be analyzed for specified I_c values to arrive at the same result. More complex statistical inferences concerning multiparameter distributions could also be determined, but they may not be worth the effort. A specialist in statistical inference should assist in their use.

An assumption normally made that may not be valid is that the parts response distributions are gaussian. Instead, the response distributions are log-normal. It may be one function of the test to determine the actual population distribution with some degree of certainty. This may lead to use of "non-parametric" statistical analysis of data--again, an area for specialists.

One desired engineering result for TREE test data is often curves of gain, photocurrent, etc. plotted as functions of an electrical or radiation parameter. This involves fitting a curve to the measured (and reduced) data. It is convenient to express the data in terms that could theoretically be plotted linearly, e.g., reciprocal gain versus fluence or peak photocurrent versus dose rate. Then, least squares and regression analysis can be used to determine how well the data fit, what slopes and intercepts are given with confidence, etc. More simply, such curves can be visually examined if the statistical detail is not needed. When the curves are not linear and/or the functional relations are not analytic, the purpose of the test will usually determine what effort is worthwhile in performing more complex statistical analyses.

For "go-no-go" tests, such as acceptance screening of parts by testing for a certain parameter, the statistical design of the test is generally

easier to establish. Here, the distribution of data is binomial and the techniques are well established. The part either passes or fails a test, depending on the radiation response, but the parts-response distribution itself is not the entity in view. The data are the "passes" or "fails," a "go" or a "no-go" for a given test item, or a fraction passing, p, and failing, q = 1 - p, in the population. Based on the number of failures in a sample drawn from the parts lot being accepted and on the system requirements, determination of the probability that the population failure rate will be within specified limits, using binomial distribution statistics, is straightforward (References 5 and 6).

For system assessment work, it is more likely that only a few parts can be found for tests and the analysis technique must glean the most information from the test. This calls for careful test design and, perhaps, the use of "small-sample" statistics and tolerance factors--an area for a specialist.

2.4 SAMPLE SIZE DETERMINATION

In TREE test design, the selection of the sample for test depends strongly on the purpose of the test. As indicated earlier, screening tests use the binomial distribution,

$$P\ (x \leq c) = \sum_{x=0}^{c} \binom{N}{x} p^x\ q^{N-x}\ , \qquad (2\text{-}1)$$

where $P(x \leq c)$ is the probability that the number of passed items, x, is no greater than the acceptance test level number, c, for the test sample size, N, and p is the actual probability of a single item's passing the test, with q = 1 - p. Curves and nomographs of this distribution may be used to decide on sample size, N, and acceptance test level, c. The test engineer should consult statistical texts or specialists for details of application to his problem. The Military and ASTM Standards for TREE testing specify a minimum sample size of 10 devices randomly selected from the parent population (References 2 and 3). MLD-STD-19500 and MIL-STD-38510 may also be used for sampling plans and acceptance criteria (References 7 and 8).

For parametric design data on components and devices, the accuracy with which the data must be known for the specific system design applications will determine the sample sizes for tests. Also, the spreads in the data themselves and the uniformity of parts responses will influence the sample size, as will the actual shapes of the distributions. This implies that there needs to be some processing control of parts manufacturing to provide reasonable uniformity of response and that the sample set selected for test must adequately represent the parts population to be used in the system design.

To be much more specific than the last paragraph requires a detailed discussion of statistical methods considering confidence (or tolerance) limits for the system design data, allocation of parts for tests depending on their design margins in the system, etc. These factors are system dependent and complex and general mathematical approaches shall not be pursued here. However, as a rule of thumb and as a matter of common practice, many test engineers have found between 10 and 30 samples adequate to define the parameters of principal interest to system designers for neutron and gamma ray effects on semiconductor parts (References 2 and 3). Mean damage constants or photocurrent slopes (in the linear range) do not usually become appreciably better known by increasing test sample size above 30 for those parts types that have been fabricated with the same technologies and controls.* Normally, system designers invoke enough margins so that the mean values of radiation-affected parameters and their distributions (variance or higher moments) need not be known to high accuracy. In addition, for system hardness assurance, samples for irradiation tests are often picked from selected production lots of a particular device type. The variations of device response from lot to lot and from manufacturer to manufacturer are important considerations when evaluating system hardness assurance. Typically, a sample size between 10 and 30 is considered adequate for radiation sampling tests of a particular production lot. In some cases, such as the statistical evaluation of systems performance, an analysis might show the need for more parts tests or the data spreads in the test itself might indicate such a need.

2.5 TEST HARDWARE CONSIDERATIONS AND TECHNIQUES

2.5.1 Introduction

General test hardware considerations and testing techniques for electronic components are discussed in this section. In the normal case, the test engineer must consider the following:

1. How to characterize the device to be tested. This characterization may be repeated one or more times after the test.
2. Selection of the proper irradiation facility to meet the test objectives (Chapter 4).
3. Measurement of the selected response of the device being irradiated. The proper operating mode for the device during irradiation must be selected. A choice of pre- and post- or in-situ measurements must be made.

---

* For 90-percent confidence, 90 percent of a normal population will differ from the sample mean by no more than a tolerance factor, K, times the sample variance, with K decreasing only by about 25 percent (from 2.0 to 1.7) as N goes from 10 to 30).

4. Electrical- and radiation-induced interferences and thermal effects during testing.

5. Selection of the dosimetry techniques to properly characterize the radiation to which the device is exposed (Chapter 5).

2.5.2 Characterizing the Test Device

Two types of measurements should be performed on the test device before exposure to radiation. The first are measurements of those parameters that are expected to change due to radiation exposure, such as transistor gain. Secondly, it is desirable to perform additional measurements that will characterize the particular device type. Within a particular device type number, there are sometimes large variations in individual device characteristics. These variations are usually within the parameter specification, but occasionally there are devices whose characteristics fall outside of the specification (the maverick problem). In practice, it is very useful and cost effective to perform electrical measurements that can be correlated with the expected radiation response of a device. The gain-bandwidth product, f_T, of a transistor is an example of such a measurement. Therefore, the preirradiation characterization should include those parameters.

There are also other basic considerations unrelated to actual parameter measurements when planning radiation tests. One is that the construction of semiconductor devices with the same electrical specifications device number may be substantially different if obtained from separate manufacturers or even from different production lots of one manufacturer. These differences in production procedure may have a significant effect on the radiation responses of the devices. The effect of processing details on radiation response is particularly important when evaluating radiation-induced surface effects. Therefore, the characterization of samples from various production lots is advisable to obtain results that are truly representative of the radiation response of a particular device type. A second consideration is that data requirements may make it necessary to exercise some control over the samples obtained from the device manufacturer. Samples with identical construction but with tighter initial-parameter spreads may be required to satisfy system specifications for the intended application and to obtain greater internal consistency in the test results. If controlled samples are used, it is important to identify them as accurately as possible when reporting test results.

There are several ways to conduct permanent-damage tests. One of the simplest, most convenient, and least expensive ways is to perform pre- and postexposure measurements on devices that are exposed to radiation in an unbiased state per Method 1017 of Reference 2. Each set of measurements establishes the device response at a single irradiation level. This procedure permits the effective use of automated testers in a laboratory environment and it is possible to test a statistically significant number of

samples. Such tests are useful as proof tests to establish adequate device performance at a given radiation level, as long as time and bias dependence are not important. Usually, there is a wait for the radioactivity of the test devices to decay to a safe level before testing.

Data may be obtained at several irradiation levels by repeating a test as many times as desired or by exposing different groups of samples to various radiation levels. The first procedure is more time-consuming and, since it usually involves repeated physical orientation in the radiation environment, may be subject to errors. Due to differences in the radiation response of different samples, data obtained by the second method may exhibit a lack of internal consistency (i.e., there may not be a smooth pattern of parameter change with increasing irradiation exposure). Also, when extended periods without irradiation occur during a test, the sample parameter values sometimes change (due to annealing) so that data taken before and after the cessation do not correlate well. Therefore, measurements should be made at the beginning and end of such periods, if possible (Method 1019 of Reference 2).

Devices may be remotely instrumented at the test facility to permit in-situ parameter measurements. The radiation response at various exposure levels and/or at specific time intervals during and after exposure can be obtained in this way on a single group of devices (Method 1019 of Reference 2). Use of automated test equipment helps to eliminate the errors due to sample repositioning and the time delays involved in laboratory measurements. The requirement for test equipment and extensive cabling at the test facility makes in-situ testing more complicated and more expensive than pre- and postexposure testing, especially if a significant number of samples are tested.

Normally, more than one parameter will be measured in a test. The sequence of parameter and operating-point measurements should be carefully considered since this affects the duration of the measurement period and the device temperature. Automatic testers are useful if a large number of samples are to be tested. The test engineer should consult References 2 and 4 for measurement configurations.

Transient effect data measurements must be performed during and immediately after the radiation pulse (Reference 3). The response of a device under test depends upon the radiation pulse width. For pulses much shorter than the device electrical response time, the magnitude of the response usually depends upon total dose and its duration is a function of the device recovery time. For pulses long compared to the device response time, the instantaneous response tends to follow the dose rate. The test circuit can affect the observed response time by intentional or inadvertent capacitive loading of the terminals of semiconductor devices which have high impedance circuits in series with this capacitance. In establishing a transient effects test program, it is necessary to understand the role played by the intrinsic device response time, such as inherent conductivity

relaxation, and the response times influenced by external parameters. Therefore, the electrical loading of the device under test must always be accurately recorded.

2.5.2.1 Transistors and Diodes

The basic methods of making parametric measurements on transistors and diodes are the steady-state method and the pulsed method. The most common and simplest technique is to apply steady-state sources (either dc or ac) to the test circuit and observe the desired response while varying one or more of the sources in discrete steps. Unfortunately, as power dissipation increases, the junction temperatures increase, altering many of the parameters of the device. If the ultimate application of a particular device is in the pulsed mode, the data taken at the higher levels using the steady-state technique will yield inapplicable results. The pulsed method of parameter measurement minimizes changes in junction temperature and may also be used to simulate actual operating conditions for a particular circuit design. Applied pulses must have sufficient duration to ensure that responses have reached the electrical steady state (not thermal). The pulse repetition rate (duty cycle) should be kept low to minimize device heating.

For matched-pair devices, it is desirable to determine the changes in differential device parameters. The most satisfactory technique is to make a differential measurement. Although such techniques are not detailed here, the test engineer can readily modify suggested measurement circuitry to provide for differential measurements (Reference 4).

An example of a simple and relatively fast method of obtaining many parameters at many operating points is by using a curve tracer to sweep out a family of device characteristics and display them on an oscilloscope. Both steady-state and pulse measurements can be made using this method. The displayed characteristics should be photographed to provide a permanent record for pre- and posttest comparisons. This method typically yields data with an uncertainty of at least 5 percent so it is not recommended for critical design-data purposes. It should be used only when device parameter changes of more than 15 percent of preirradiation values are expected.

The choice of a particular measurement method must involve consideration of the ultimate circuit application of the device (if known), accuracy requirements, cost limitations, the number of measurements to be made, and methods of data reduction. If the application of a particular device is not unique, it is wise to employ several of the above-mentioned techniques to acquire several kinds of data. Regardless of the particular methods chosen, conditions should be as identical as possible for pre- and posttest measurements. If a large number of measurements are planned, consideration should be given to automating the measurements and the data-reduction procedure. Although such methods are not described here, the suggested measurement circuitry can be modified to allow for automated measurement schemes and machine-oriented data reduction.

Sometimes the leads of a sample are shortened after pretest measurements to facilitate subsequent test purposes. The shorter leads may affect the relation between pre- and posttest measurements in two ways. First, at high currents, the voltage drops in the leads may be significantly different in the two cases; this can be measured and a correction made. Second, changing the lead length may change the case-to-ambient thermal resistance; this can readily change the case temperature by 20°C or more and cannot be easily compensated. Therefore, every effort should be made to keep the lead lengths constant and the device should be well heat-sinked for measurements.

Unwanted oscillations during an electrical measurement can render the measurement invalid. The following are suggested ways to eliminate oscillations of test circuits:

1. Use shielded or coaxial cable to minimize coupling between the transistor elements
2. Locate an appreciable part of the collector-circuit resistance as close to the transistor as possible
3. Place ferrite beads on the leads of the transistor
4. Bypass with a capacitor the collector to the emitter and/or the base to the emitter
5. Provide degenerative feedback through a pulse transformer.

2.5.2.2 Integrated Circuits

The radiation response of integrated circuits can be quite complex. Many medium-scale integrated (MSI) and large-scale integrated (LSI) devices have a large number of possible states or complex feedback loops. As a result, the output is not a direct function of the input; that is, a change of state on an input signal lead does not result in a corresponding output change. This makes detailed evaluation of the interaction between the various elements on a given chip impractical, if not impossible.

The choice of a potential measurement method for integrated circuits must involve consideration of the ultimate application (Reference 2). If the application of a particular device is not unique, it is wise to employ several techniques to acquire the kinds of data that are needed. Regardless of the particular methods chosen, conditions should be as identical as possible for pre- and postirradiation measurements. If a large number of measurements are planned, consideration should be given to automating the measurements and the data-reduction procedure. Although such methods are not described here, the suggested measurement circuitry can be modified to allow for automated measurement schemes and machine-oriented data reduction.

A very critical step in the process of testing integrated circuits is determining what constitutes a significant response and failure of a device. The specific system requirements must be used as one of the criteria to define component failure. The failure criteria for the components of a given system must be carefully determined by considering all electrical parameters of a device in its system application. These failure criteria are usually much lower than would normally be expected because of the circuit tolerances which are used to establish worst-case failure criteria. Logic circuits are usually not the limiting factor in displacement effects radiation hardness of a system.

Since logic circuits are relatively hard, use of one worst-case failure criterion for all the logic circuits is conservative and cost effective. This eliminates the necessity of developing failure criteria for each logic circuit application.

Linear circuits, however, are almost always softer than logic circuits, and it is often both advantageous and necessary to examine each application in detail to determine failure criteria. The necessity of each specification limit must be carefully considered because if the required specification is too strict, a heavy cost may result when circuits that are hard to the required level are selected.

2.5.3 Measuring the Response to Radiation

Radiation response measurements should be made in accordance with the procedures specified in References 2, 3, and 4. These procedures define the requirements for testing sealed semiconductor devices for specific types of exposure. These include:

1. Test setup and site requirements
2. The radiation source requirements
3. Bias fixtures and requirements
4. Sample selection criteria
5. Electrical parameter measurements
6. Dosimetry requirements
7. Safety requirements
8. Documentation
9. Data requirements.

Specification of the operating mode of the test device is one of the first decisions to be made when developing a test plan. The bias conditions must be set and properly controlled during irradiation and wherever the test devices are connected to the test fixture. Neutron exposure nests are often conducted with the device leads open or shorted during irradiation. Measurements are then made on a pre- and posttest basis (Method 1017

of Reference 2). Total dose exposure tests require the devices to be biased during irradiation and throughout the postirradiation measurements for the observation of surface effects. In-situ measurements are often used (Method 1019 of Reference 2). Transient effects measurements also require the devices to be biased in an operating region of interest. These measurements must be taken rapidly, so only one bias point can be checked per exposure. Exposures can be repeated at different bias points with no change in inherent device characteristics (Method F448 of Reference 3).

The irradiation levels at which data are taken depend upon the end purpose of the data. For data analysis and presentation purposes, it is desirable to obtain data at approximately equal logarithmic intervals of radiation exposure, such as $2 \times 10^{(x)}$, $5 \times 10^{(x)}$, and $10^{(x+1)}$.

Adequate dosimetry is essential for all radiation testing. Reactor irradiation should include both neutron and gamma dose measurements. At pulsed reactors, the n/γ ratio can be measured for a particular test configuration. At steady-state reactors, provision should be made for a low-power gamma dosimetry run. The value obtained can be scaled to the experimental power level. This run can sometimes be performed several days in advance of the actual test. If an attenuating shield is to be introduced during the test, spectral measurements should be made with and without the shield (Methods E720, E721, E722 of Reference 3). For experiments performed at gamma radiation sources, the gamma dose rate can be monitored and the total dose determined from the total irradiation time, or an integrating dosimeter can be used to measure the total dose (Methods F526, E665, E666, and E668 of Reference 3).

The selection of the number of dose rates at which to make measurements will depend on the data requirements, the particular device type, and the intended application. In the absence of detailed application information, measurements should be made at each decade of dose rate, $\dot{\gamma}$, over a dose rate range from 3×10^5 to 3×10^{10} rads (Si)/s. This extends from a low range where the response is usually linear to a higher value where the device is saturated in many circuit applications. Justification for measurements over such a wide range of dose rates is that some devices do not conform to a linear dependence of I_{pp} on $\dot{\gamma}$, and such a series of measurements will reveal the range of rates over which these nonlinearities exist.

When repetitive pulsing is employed or when high dose rates and/or long pulse widths are involved, it is easy to build up large doses in the sample. Above 10^4 rads (Si), some devices may incur significant permanent damage. Such damage is evidenced as an increase in junction leakage. When this threshold is exceeded, the sample dose should be reported and a clear identification made of the data that were obtained above the threshold. Justification should be given for using such data.

To some extent, the photocurrent response of a device is dependent upon the energy spectrum of the ionizing-radiation source, especially for spectral components with energies less than 0.5 MeV. Therefore, an effort should be made to control and/or measure the spectrum as well as the dose rate. This is particularly important if it is suspected that the incident spectrum at the sample location has changed (e.g., due to the interposition of shields).

Most transistors and diodes are in the class of "thin samples" and their responses are independent of orientation in a homogeneous, high-energy radiation beam. High-power devices, however, may have thick-walled cases or mounting studs that, in some orientations, act to shield the active device volume (semiconductor chip) from the radiation. If such orientations cannot be avoided, the orientation used should be recorded and an effort made to determine the actual dose received by the active volume. Dose enhancement effects due to the differences in materials must be accounted for in the dose measurements.

Semiconductor device characteristics are dependent on junction temperature; hence, the ambient temperature of the test must be controlled. References 2, 3, and 4 specify room temperature testing for most cases. If other temperatures are required, these must be carefully specified and controlled to keep the devices within their maximum ratings.

2.5.4 Interference Suppression

Conducting transient radiation effects tests presents some severe problems. These tests usually require transmitting small signals over long cables in the vicinity of a powerful pulsed radiation source. Careless handling of the signals can result in the loss of data or questionable data. Therefore, it is mandatory to maintain the signal-to-noise ratio as high as possible.

2.5.4.1 Interference Coupling Modes

Interference can be injected into a test setup in a number of ways. The pulsed radiation source is a large noise generator. It has an associated electromagnetic field that can propagate through shielding into the measuring circuitry. The radiation source can also introduce noise on the 60-Hz power line that couples the noise into the test equipment.

Use of multiple ground points can result in ground loops or common-mode return paths that permit noise from the pulsed radiation source, or any other source, to enter the measuring system. Capacitive coupling can act as a high-frequency ground connection.

In the case of a pulsed source of ionizing radiation, such as a linear accelerator (LINAC) or flash X-ray, another source of noise is the charge transferred between the source and the test box and test circuitry. An illustration of charge transfer in Figure 2.5-1 shows that the charge is not

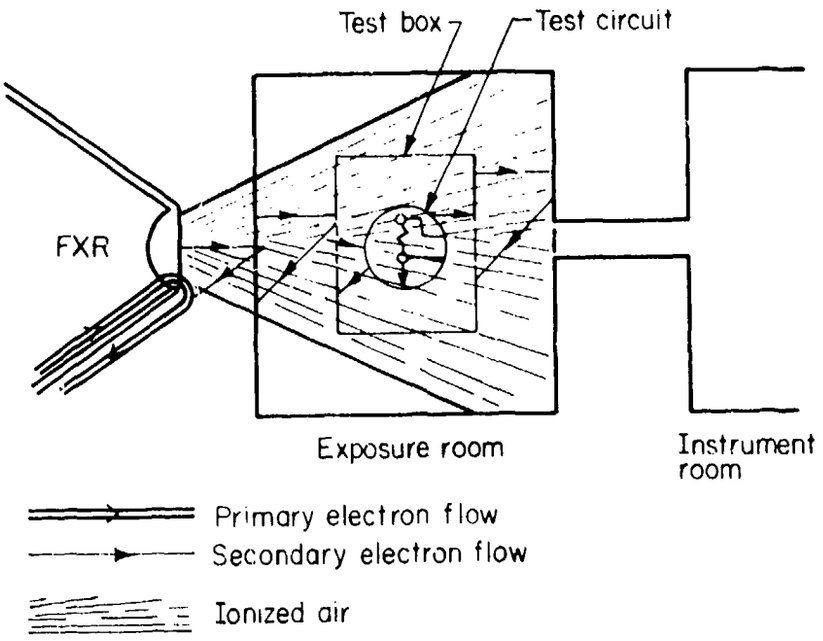

Figure 2.5-1. Charge transfer paths.

only transferred from the main beam source but also between the sample and its surrounding environment. The charge transfer is maximized in the electron-beam mode but is also significant in the bremsstrahlung mode due to the production of energetic electrons by Compton and photoelectric interactions. Values of the currents generated by this charge transfer range between 10^{-13} and 10^{-12} amp-sec/cm^2-rad. Use of a scatter plate with an intense beam may increase this current.

Another example of charge transfer occurs in coaxial cables. The effects are shown for various cable types in Table 2.5-1. The actual responses are also dependent on the cable's irradiation and voltage history.

Air ionization caused by the radiation sources can also introduce spurious and misleading signals. Typical air-ionization leakages due to short pulses yield a conductivity of $\sim 10^{-14}\ \dot{\gamma}$ (mhos/cm), where $\dot{\gamma}$ is the ionization dose rate in rads/s. This can be minimized by making the measurements in a vacuum or by encapsulating the test sample in an insulator. However, secondary electrons produced in the potting material can also introduce erroneous signals. When a test is being conducted in a vacuum chamber or cassette, the effects of the secondary electrons produced by the bremsstrahlung radiation entering and leaving the test box can be minimized, but not eliminated, by using thin low-Z window material. If this proves insufficient, a magnet can be used to sweep the electrons away from the test sample.

Table 2.5-1. Cable effects in an ionization environment for 30-MeV electrons (10^{10} rad/sec) (Reference 9).

Cable	Type	Replacement Current 10^{-14} $\frac{\text{amps-sec}}{\text{cm-rad}}$	Induced Conductance 10^{-17} $\frac{\text{mho-sec}}{\text{cm-rad}}$
RG-58	Solid	+3	1
RG-59	Solid	-2.4	1.2 (prompt) -2.5 (delayed to 1 ms)
RG-62	Foamed	+8	25
RG-62	Semisolid	-2.4	50

Notes:

1. Replacement current flows in center conductor (shield is at ground.
2. Conductivity of dielectric is also affected.
3. Above numbers are per cm of cable exposed to ionizing radiation.

An[illegible] source of potential noise interference is the pulsed magnetic field p[illegible]ced by the electron current associated with a photon beam. The field i[illegible]nerally solenoidal about the direction of the photon beam and can be e[illegible]imated from the known equilibrium between photon and electron currents. The effect of this field can be eliminated by proper shielding and avoidance of loops in cabling configurations.

Figure 2.5-2 depicts some of the ways described above in which noise can be int[illegible]uced into a system.

2.5.4.2 Noise Minimizing

Techniques used to minimize noise in electronic systems are fairly well understood, although often disregarded. As few ground points as possible should be used, preferably only one. High-frequency signals should be handled in a coaxial configuration with continuous shielding and, where possible, differential measurement techniques should be used. If a high-frequency differential measurement is to be made, coaxial cables for each side should be used. The two cables should be the same length and tied together so that any noise picked up in the cables will be of the same phase and magnitude and cancel each other in the differential mode. At lower frequencies, twinaxial cables or shielded-twisted pairs provide better common-mode signal rejection. In extreme electromagnetic fields, the test devices should be enclosed in a cassette, with the interconnecting cables between the exposure and instrumentation rooms enclosed in a continuous

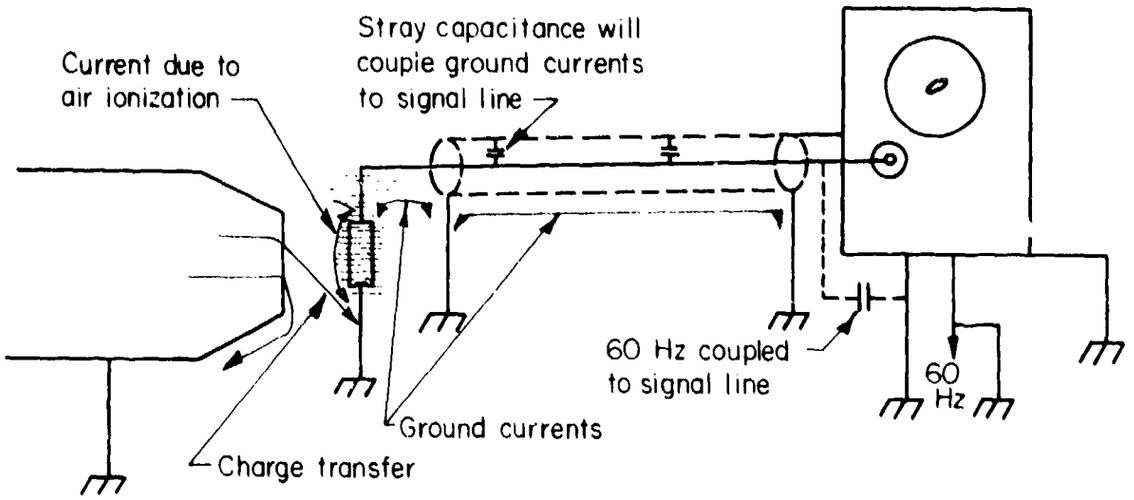

Figure 2-5.2. Typical noise sources.

shield such as "zip" tubing, again grounded at only one point. Triaxial cable can also be used. Grounding of the shielding and the low side of the measuring circuit should be located as close to each other as possible to prevent ground loops. Where it is necessary to provide 60-Hz power to some portion of the test setup, the low side of the 60-Hz power should not be connected to or used as the signal return line. An improved test setup is shown in Figure 2.5-3.

In general, when selecting a ground point, it is not advisable to use the pulsed radiation source for this purpose since it is probably the largest source of noise in the vicinity of the test. However, in the case where charge transferred from the radiation source to the test setup is a noise problem, a ground or connection between the two may become necessary to avoid persistent noise oscillations. LINACs or flash X-ray machines used in the electron beam mode must have a ground return. This connection must have a very low inductance; otherwise, there will be a significant voltage buildup during the pulse which can then be coupled to the measuring circuit.

An example of a setup in which separate shield rooms enclose the target and recording equipment is shown in Figure 2.5-4. The charge transfer to the cassette is transferred back to the wall of the target shield room via the outer shield of a triaxial cable, a zipper tube, or at best a solid shield pipe. The test specimen is floated inside the cassette (but inevitably couples to it capacitively) and is connected via coaxial cable to the recording station, at which the circuit common is connected to a master earth. This system can also be used with balanced cable pairs and line drivers.

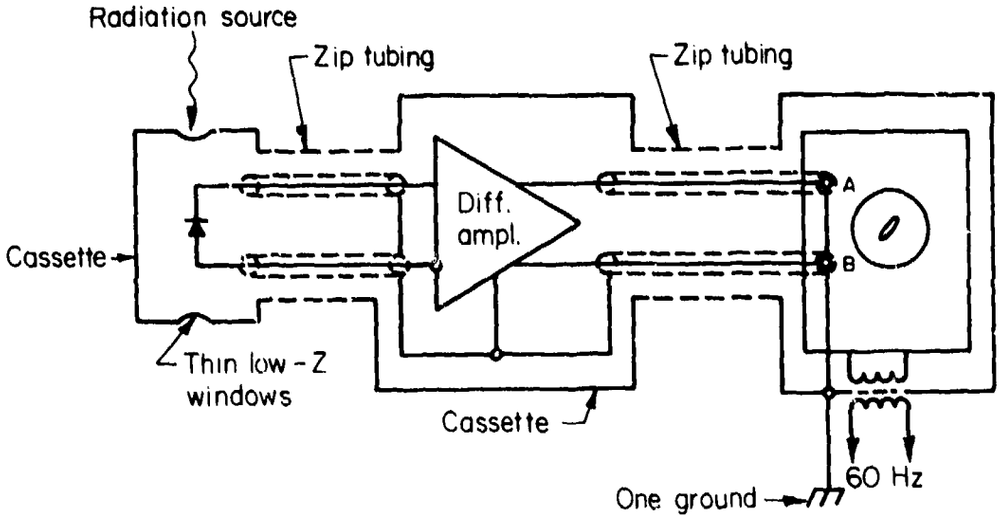

Figure 2.5-3. Improved test setup.

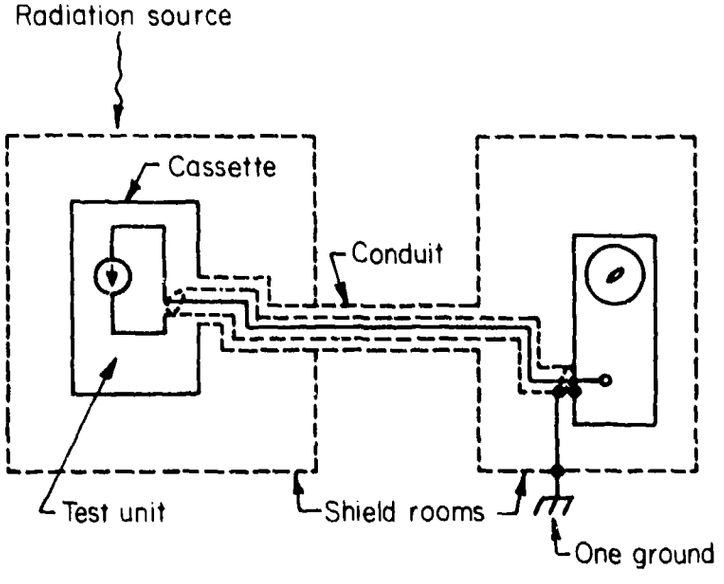

Figure 2.5-4. Typical use of shield rooms.

Sometimes it is necessary to connect a number of pieces of equipment together, e.g., bias supplies, checkout equipment, and recording devices. Generally, these items will be capacitively coupled to their environment, even though they may be deliberately isolated from earth. Multiple-capacitive ground loops could occur. An effective approach is to lay out the

instrumentation system along a ground path, taking care not to introduce loops between the plane, the equipment, and the cables. Low-inductance coupling of the units in the plane (e.g., bolting racks together) is important. In this case, the cabling system to the test unit is looked at as an extension to the ground plane. Allowing cables to take two different routes from the recording station to the test unit would be a violation of the ground plane principle.

If noise is being injected into the system through the 60-Hz line, a well-designed filter or an isolation transformer may be sufficient to suppress the noise. In cases where these solutions fail, a motor-generator set with a low-capacitance insulated mechanical coupling should be used.

Cables used to periodically monitor conditions of the test in the exposure room, but not part of the active measuring circuitry, should be disconnected prior to taking data. These cables act as additional antennas and pump noise into the system. When required, they can be connected via relays or switches. Cables used to operate remotely controlled relays, motors, etc. should be carefully filtered at the point where they penetrate the test enclosure.

2.5.4.3 Circuit Considerations

Transmitting high-frequency signals over long coaxial cable runs between the exposure room and the instrumentation room requires that the cables be properly terminated in their characteristic impedances. In many cases, there is a mismatch between the test equipment and the cable. Therefore, some impedance-matching method must be employed, such as a line driver or, if the signal is large enough, a simple voltage divider network may suffice. Care must be taken in the design of impedance-matching devices to ensure that they faithfully reproduce the desired signal and that they are not susceptible to the radiation environment, contributing erroneous signals to the measuring circuits (References 2, 3, and 4).

In measuring currents, the choice of series resistance is important. For the highest frequencies, current probes can be used. They have low insertion impedance and operate into terminated 50-Ω cables, but they have rather low sensitivity (~1 V/amp) and do not operate well at lower frequencies. If higher sensitivity is required, a series resistor is useful, but at a cost in insertion impedance and frequency response. For example, with a very low-capacitance preamplifier (~20 pF), the rise time across a 1-kΩ resistor is 20 ns. If the 1-kΩ resistor is connected with 3 feet of coaxial cable to the preamplifier, the rise time would be almost 100 ns.

Coaxial cables must be used with care in a radiation environment since they are also susceptible to the radiation and can produce large unwanted noise signals. Where it is necessary to use coaxial cable in the exposure area, it should be kept to a minimum length, with coils or loops of cable avoided. In some cases, where noise is repeatable from one radiation

pulse to the next, methods of subtracting out the noise can be used. However, with coaxial cables, many types exhibit a radiation response that is dependent on the voltage and radiation history of the cable. Solid dielectric coaxial cables with a low capacitance per foot are preferable.

The most effective way of eliminating spurious currents due to the cables is by careful collimation of the beam and by proper shielding to prevent them from being irradiated. By these techniques, it is usually possible to reduce cable currents to negligible values in LINAC and flash X-ray tests.

Component cabling at a pulsed-reactor facility must extend up to the machine so that a portion of the cable is always irradiated. The signal produced in the cable during the reactor pulse may have little or no reproducibility for subsequent pulses. Polarity of the cable response appears to be influnced by the type of cable and the magnitude of the applied voltage, and may not have the same polarity as the applied signal. Tests should be conducted to determine the extent of the cable effects in the system.

Another source that can affect the quality of the data is the response time of the measuring equipment. If the response time of the test circuitry is approximately the same as the radiation pulse width or the relaxation time of the irradiated test specimen, the resulting signal is not a true representation of what the signal would have been if the measuring circuit had not been connected. As a rule of thumb, the measuring system should have a response time at least a factor of 10 faster than the relaxation time of the test sample, if the signal must be reproduced with less than 1-percent distortion. Another alternative is to integrate the signal. For this type of measurement, the integrating circuit should have a time constant at least a factor of three longer than the sample relaxation time. Longer integrating time constants will improve data quality.

CHAPTER 3

DOCUMENTATION REQUIREMENTS

3.1 INTRODUCTION

The inherent, unstated objective of any report should be to make clear to the reader the value and accuracy of the information contained in it. The entire effort of a properly conducted test program can be nullified if time and space are not taken to report the test results in a manner that can be critically evaluated--by indicating the way in which the test program was planned and performed, how the data were analyzed, and establishing a basis for the conclusions reached.

This chapter covers the general information normally required in a radiation-effects test report. No attempt is made to detail all the specific information that may be required; certainly a good deal of judgment in this regard is required of the report writer as he assesses his particular test circumstances. However, some of the following sections do point out many minimum specific details that normally should be reported.

It is assumed that the person preparing the report is familiar with technical writing and the typical structure of a technical report. The sponsoring agency will often have a standard report format that must be followed. Minimum data recording requirements and formats are often specified by the applicable ASTM or Military Standard (References 2 through 4, 7, and 8). In all cases, the report should contain clear statements of the test purposes and objectives, a description of what was done and how it was done, and a concise but complete presentation of the test results and conclusions.

3.2 PLANS AND PROCEDURES

The objectives of the test and the planned method of obtaining these objectives should be briefly, but completely, described. Items to be included are:

1. A brief statement, with references if necessary, of any theory pertinent to the test design, including any assumptions made and their justification
2. A description of the test technique and apparatus, including circuits utilized in making measurements, special equipment fabricated for the test, and the accuracy and date of calibration of all test equipment (photographs and diagrams are helpful in this respect)

3. Any precautions taken to assure the accuracy and precision of measurements, including precautions to exclude or limit extraneous variables

4. A description and justification of any deviations from the test plan, the causes thereof, and remedial measures taken

5. A description, with an example if necessary, of how the raw data were converted to the form used for analysis.

As discussed in Sections 2.1 through 2.3, a properly documented pretest plan or test design will include most of the elements of the final report.

3.3 TEST SAMPLES

All basic types of samples should be described. A good technique to follow is to prepare a distinct report section that, for the various types of samples, presents the manufacturer, type or specification number, lot number, origin (factory, distributor, etc.), the number of samples in each category, and method of selection and validation. If useful structural information (such as transistor emitter areas) is available, report it to facilitate data comparisons and to increase the general utility of the data. The importance of this information cannot be overemphasized. Include as an appendix any specification by which parts were selected or have a reference to where such data are available. In addition, any pertinent information about the history of the sample before irradiation, such as previous exposure to radiation, must be noted. Chapters 6, 7, and 8 include suggested standardized formats for reporting data on the samples.

3.4 SAMPLE CONDITIONS DURING MEASUREMENTS OR IRRADIATION

The operational state of the samples and the environmental conditions to which the samples were exposed from the time the samples entered the program until the last measurement was made should be defined in the report. Specifically, this includes such items as electrical operating point; temperature during irradiation, annealing, and measurement; mounting configuration and sample orientation with respect to the incident radiation; dosimeter positions; a description of any potting used; etc. Photographs of equipment setups, mounting fixtures, etc. are recommended.

3.5 RADIATION ENVIRONMENT DESCRIPTION

Documentation of TREE dosimetry should be clear enough so that others can repeat the measurements, perform the same analysis, and apply the environmental description to another effect with possibly a different energy dependence to make response predictions. This implies that the reporting should specify what was actually measured, how the dosimetry values

reported were obtained from the measured dosimetry data, and also any assumptions made in data processing. Section 5.7 treats documentation of the environment in more detail.

3.6 TEST RESULTS

3.6.1 General Requirements

The test results are the most important part of a report. They are the reason the test was performed. It is essential that they be reported as clearly and explicitly as possible. To make the report more comprehensible, the results are usually presented in a condensed tabular or graphical form in the main part of the report. In addition, all of the basic (raw) data should be documented either as an appendix to the main report or in a separate report. Suggested formats for recording test data are given in Chapters 6, 7, and 8. Use of these formats will assist test personnel in remembering to take all the necessary information and will put the data in a standardized form more readily usable by others. Charts, curves, and graphs are very helpful and desirable, but they should only supplement, not replace, basic data tabulations.

In planning a test, a theoretical model is usually selected to predict the effect to be expected. The reduced form of the data should then be chosen on the basis of the theoretical model to reflect the expected dependence upon the relevant parameters. For example, first-order theory says that $1/h_{FE}$ of a transistor should increase linearly with fluence, independent of the initial value of h_{FE} for a given base width. Therefore, for a given transistor, one should plot reduced data of $1/h_{FE}$ versus fluence.

A measurement set is defined as the data taken on a group of samples of the same type in a given combination of test conditions, such as electrical operating point, temperature, and radiation conditions. It is essential that, when the data for a measurement set are presented, all qualifying test conditions be given specifically. If a reported quantity was not measured directly, the method of analysis or evaluation should be given.

3.6.2 Tables and Figures

Each individual sponsoring agency may have a standard format for scientific and technical reporting as well as for tables and figures. A few are listed in References 10 through 12. The following suggestions are intended as a supplement to standard formats to aid in making more effective presentations.

Each figure should be as simple and bold as possible and yet be meaningful without reference to the test. The abscissa and ordinate labels and the figure's title should clearly and concisely describe the figure in terminology consistent with that used in the text. Generally, curves are used to show trends or to compare sets of data; hence, complete cross hatching of the figure with grid lines is unnecessary. If tick marks are used to

indicate subdivisions, the meaning of the tick marks (value of the subdivisions) should be clear. The tick marks should go all the way around the margin of the figure.

Do not overcomplicate the figure by trying to make one figure do the job of two or more. If a figure is meant to represent a collection of data, show enough data points to adequately represent the degree to which the given curve fits the data. If error bars are used, state in the figure what they represent, i.e., standard deviation, range, etc. All independent variables for the data being described should be given with each figure or table. Whenever possible, orient figures and tables in the text in such a manner that the text does not have to be rotated to examine the figures.

3.7 ANALYSIS

A statement should be given as to the constancy of any control samples used. The estimated uncertainty in all important results should be quoted. In specifying errors, the value of one standard deviation is the quantity preferred, although other methods may be used if they are more suitable and are unambiguous. When statistical characterizations are given, a reference that explains the technique involved should be cited.

In summary, a good test report is one that describes all the essential features that must be known to duplicate the test. A majority of this information should be available from a good design, as described in Section 2.2.

CHAPTER 4

RADIATION FACILITIES

4.1 SCOPE

This chapter presents a brief survey of the radiation sources used in TREE testing and gives some general guidelines for source selection. Several classes of radiation sources are omitted from consideration because they fall outside the scope of the preferred procedures of Chapters 6, 7, and 8. The guidelines given here are general and should be used in conjunction with the needs outlined in those chapters.

Only general characteristics are described for the radiation sources that are mentioned. Information on the specific characteristics of a particular machine and its associated facilities is best obtained firsthand from the operator of the radiation facility being considered or from DNA 2432H, TREE Simulation Facilities (Reference 13). The value of the latter document cannot be overemphasized. Time spent in examining the data given in it will greatly enhance the novice's understanding of the capabilities of the different classes of radiation sources most frequently used in TREE testing.

Recommendations for choosing certain machines from a given class of radiation sources are not made. The final choice of the particular facility to be employed rests with the test engineer, who must make that choice after consideration of data requirements, cost, and convenience. Once a source has been tentatively selected, it is important to contact the facility operator (preferably by a scheduled visit) early in the planning stages of a test. Each facility has unique characteristics and restrictions; in fact, these frequently determine the basic structure of a test plan. To intelligently select a facility or plan a test, the test engineer must understand the basic phenomena with which he is dealing. The reader is referred to Chapter 10 of Reference 1 and to basic nuclear physics texts on radiation interactions.

4.2 GENERAL CHARACTERISTICS OF RADIATION SOURCES

From the machine designer's viewpoint, radiation sources are considerably different within each class, but from the operational viewpoint of the test engineer, different sources within a class have many characteristics in common. The common characteristics of several important classes of radiation sources are discussed in the following text.

4.2.1 Nuclear Reactors

For TREE testing considerations, nuclear reactors may be divided into two operational modes: the steady-state mode in which the reactor operates

at a constant power level for long periods of time and the pulsed mode in which the reactor can be pulsed to a high power level for times much less than 1 second.

The radiation parameters associated with pulsed and steady-state reactors vary widely. However, common features may be noted. Gamma dose rate and fast- and slow-neutron fluences are the parameters of primary interest in radiation-effect experiments. They are determined by the reactor power level and by the pulsed-reactor pulse width or by the time of irradiation at a steady-state reactor. Very grossly, the gamma dose rate induces photocurrents in electrically active devices, fast neutrons induce permanent damage, and thermal neutrons are primarily responsible for inducing radioactivity in test samples. Actually, either directly or indirectly, each type of nuclear particle or radiation can produce each type of effect.

Normally, the absolute intensities of the gamma, fast- and slow-neutron fluxes are known for the normal sample positions in reactors. However, some samples can create significant perturbations in the reactor spectra, thus inducing an error in the "known" spectra. In addition, any changes in the core configuration or insertion of other materials in the reactor, particularly the core, can alter the spectra. It is always wise to consult with the facility's technical staff to determine the accuracy of the dosimetry information provided by the facility and to make sure that it represents the current state of the reactor. As a further safeguard, always determine at least the S/Pu ratio to check the reactor's spectra.

Radiation-induced heating of the sample is of concern in some instances. The heating rate is related to the rate of energy deposition from both neutrons and gamma rays and can be calculated by personnel at the radiation facility. As a rule of thumb, provision for cooling the sample may be required when testing in an air void in a steady-state reactor operating at a power level near or above 30 kW. The degree of temperature control required depends on the device parameter involved and the end use of the data.

Thermal neutron shielding of samples inserted in a reactor may be required to limit the formation of radioisotopes in the materials of the experiment. Typically, an experiment will be surrounded or wrapped in a 0.040-inch thick cadmium foil.

4.2.1.1 Pulse Reactors

Pulse reactors are of two types: air cooled and water cooled. These reactors can also be operated in a steady-state mode, but steady-state operation of some air-cooled reactors is discouraged because they produce large fission-product inventories in the reactor core.

The air-cooled reactors are suspended or sit on tables to provide easy access at a convenient height. Water-cooled reactors are generally suspended in a pool of water about 20 feet below the water surface. The volumes of reactor cores vary between about 1 and 10 ft^3. When operating, they produce a neutron and gamma-radiation field in their vicinity, the intensity of which is proportional to the reactor power level. It is possible to suspend test samples in the core of some reactors to maximize the radiation intensity. However, in-core irradiation is usually limited to small samples and the number and type of dosimetry foils that may be used is also limited. Test samples may also be placed at a variety of locations outside the core of both reactor types, resulting in a wide range of radiation intensities.

Pulse reactor facilities are frequently used for neutron/gamma transient-radiation-effects studies and, along with steady-state reactors, are used for permanent neutron-damage studies.

The possible ionization effects of neutrons must be considered when performing a test at a pulse reactor. Usually, the ionization is predominantly a gamma-radiation effect, but neutrons are also efficient ionizers in materials with low atomic numbers. The ionization dose produced by neutrons in silicon is of the order of 3×10^{-11} rads (Si) per n/cm^2 ($E > 10$ keV, Pu, fission). (For 14 MeV monoenergetic neutrons, the value increases to approximately 2×10^{-9} rads (Si) per n/cm^2.) (Reference 3)

Since reactors must be pulsed by a licensed operator, remote pulsing by the test engineer is not allowed. He is given either an electrical signal or a countdown to start the recording instrumentation.

Reference 13 contains definitive descriptions of several pulse reactor facilities. Also see Table 4.2-1 for a summary of pulse reactor facility data.

4.2.1.2 Steady-State Reactors

There are numerous steady-state reactors in use in all parts of the world for experimental purposes. These reactors vary considerably in design and available neutron flux. They are used basically as a source of neutrons.

The principal use of steady-state research reactors (and pulse reactors operated in the steady-state mode) in TREE work is for neutron permanent-damage studies of components. These reactors may often be cost effective for permanent damage tests of components.

A listing of such reactors in the United States is given in Reference 13. The test engineer contemplating the use of such a reactor should contact the facility's operator concerning the availability and applicability of the reactor.

Table 4.2-1. Pulse reactor simulator summary table.

	FACILITY	PEAK PULSE POWER LEVEL, MW	MAX FLUENCE n/cm^2 (E>10 keV)	PEAK PULSE FLUX $n/cm^2/s$ (E>10 keV)	MAX GAMMA DOSE, rads (Si)/pulse	PEAK PULSE GAMMA RATE, rads (Si)/s	n/γ RATIO, $n/cm^2/\gamma$ rad	PULSE WIDTH RANGE, μsec (FWHM)	REPETITION RATE	PULSE REPRODUCIBILITY	WORKING VOLUME IN
1.	Sandia Pulse Reactor (SPR-III) (Kirtland AFB, NM 87115)	118,000	6×10^{14}	8×10^{18}	1.7×10^{5}	2.22×10^{9}	3.6×10^{9}	76 237	2 bursts/hr		7 dia x 20 high
2	Army Pulse Reactor Facility (APRF) (Aberdeen Proving Ground, MD 21005)	6,800 - 150,000	6×10^{14}		3.9×10^{5}	2.4×10^{9}	4.5×10^{9}	45 1,000	105 min	±2 %	4.2 dia x 7.8 high
3	Army Fast Burst Reactor Facility (FBR) (White Sands Missile Range, NM 88002)	65,000	7×10^{13}		2×10^{4}	1×10^{8}		50	1 burst/ 75 min	±5%	50 x 50 x 20 ft chamber
4	White Sands Missile Range Steady State Neutron Generator (SNG) (NM 88002)			7×10^{9}				1 10^{4}	10 10^{5} /pulses sec		
5	Sandia Pulse Reactor (SPR-II) (Kirtland AFB, NM 87115)	89,000	1×10^{15}		1.5×10^{5}		6.6×10^{9}	40 150	1 burst/ 2 hr		1.5 dia x 8 high
6	Lawrence Livermore, Super Kukla Prompt Burst Reactor (Mercury, NV 89023)	160,000 - 400,000	2×10^{15}	5×10^{18}	2.7×10^{5}	7×10^{8}	7.4×10^{9}	400 2,000	1 burst/ day		18 dia x 30 high
7	Northrop Reactor Facility (Triga Mark F) (Hawthorne, CA 90250)	1,800	6.5×10^{14}	1.9×10^{13}	4.3×10^{5}	1.6×10^{4}	1.4×10^{10}	10,000			8 x 8 x 10 ft chamber
8	Pennsylvania State University Breazeale Nuclear Reactor (Triga Mark III) (University Park, PA 16802)	2,000	2.2×10^{14}	2.5×10^{13}	2×10^{6} R	9.6×10^{4}		15,000	4 bursts/hr	±10%	6.5 dia x 36 high
9	General Atomic Triga Reactor Facility (Triga Mark I)	1,100	9.7×10^{14}	5.4×10^{16}	3.0×10^{6}	6.1×10^{7}	3.8×10^{8}	16,000	10 bursts/ hr	±5%	1.25 dia x 24 high
	(Advanced Triga Prototype) (San Diego, CA 92138)	6,700	9.5×10^{14}	1.4×10^{17}	2.8×10^{6}	4.2×10^{8}	4×10^{8}	6,300	10 bursts/ hr	±5%	1.25 dia x 6 high

Table 4.2-1. Continued.

FACILITY	PEAK PULSE POWER LEVEL, MW	MAX FLUENCE n/cm^2 (E>10 keV)	PEAK PULSE FLUX $n/cm^2/s$ (E>10	MAX GAMMA DOSE, rads (Si)/pulse	PEAK PULSE GAMMA RATE, rads (Si)/s	n/γ RATIO, $n/cm^2/\gamma$ rad	PULSE WIDTH RANGE, μsec (FWHM)	REPETITION RATE	PULSE REPRODUCIBILITY	WORKING VOLUME IN
10 Sandia Laboratories Annular Core Pulse Reactor (ACPR) (Kirtland AFB, NM 87115)	9,500	3.7×10^{15}		3.3×10^{6}			65,000	15 bursts/hr	±5%	9 dia x 46 high
11 Sta[illegible]ty of New York at B[illegible]ctor (New[illegible],214)	10		3.15×10^{10}		2×10^{7} R/hr		15,000	3 bursts/hr		6 dia x 100 long
12 AFRRI Reactor Facility (Triga Mark F) (Bethesda, MD 20014)	1,800						10,000	1-3 bursts/hr	±2%	
13 University of Wisconsin Triga Nuclear Reactor Facility (Madison, WI 53706)	12,200						15,000	4 pulses/hr		
14 U C Irvine Dept of Chemistry Triga Reactor (Irvine, CA 92717)	1,000						11,000	6 pulses/hr		
15 Washington State University Reactor (Pullman, WA 99164)	2,000						12,000	6 bursts/hr		
16 U C Triga Mark III (Berkeley, CA 94720)	1,350							4 bursts/hr	±3%	
17 Kansas State University Triga Mark III (Manhattan, KS 66506)	250		10^{16} (E>0.2eV)		2.5×10^{7}					
18 University of Texas at Austin Triga Mark I (Austin, TX)										

4.2.2 Linear Accelerators

In a linear accelerator (LINAC), high-energy electron beams are produced that are useful in TREE studies, both directly and after conversion to bremsstrahlung photons or to photofission neutrons. LINACs are widely used as pulsed radiation sources in TREE studies because of their controllable variable pulse length, intensity, and particle energy.

Direct LINAC electron irradiation is used to produce ionization at higher dose rates than can be obtained with bremsstrahlung. The electron beam can be used directly and focussed on a small item such as a transistor to obtain doses approaching 10^{12} rads (Si)/s. The desired high dose rates are accompanied by the problems of replacement current and secondary emission from surfaces, but these problems are usually resolvable by careful test design. For lower rates, or for larger test item sizes, a bremsstrahlung target may be used. Energies as low as a few MeV up to many tens of MeV are available. Dose-rate variation is obtained by use of scattering foils, by backing the test setup away from the LINAC beam port as needed, or by defocussing the beam within the machine.

Neutrons can be generated by a LINAC via the photofission process, in which photons of energy above about 5 MeV are incident on a U-238 target. However, due to the shape of the bremsstrahlung spectrum and the variation with photon energy of the cross section for the reaction, the LINAC should be operating with at least 25-MeV beam energy for higher efficiency.

The LINAC is a valuable tool for the study of radiation effects because of the following characteristics:

1. Dose rates above 10^{11} rads (Si)/s can be obtained by the use of the direct electron beam.
2. The pulse width and dose rate may be independently varied over a wide range without changing sample position or test configuration.
3. Single or multiple pulses are normally available on command.
4. Short rise and fall-time pulses are the normal operational characteristics.
5. Conversion from electron to gamma radiation is readily accomplished using a bremsstrahlung converter (although the converter will also have a secondary electron output). The bremsstrahlung dose rate obtained will be at least a factor of 100 less than the direct electron dose rate.
6. The LINAC may be used to produce fast neutrons by the photofission process in a suitable target, typically depleted uranium.

The major disadvantage in using the LINAC is the restriction imposed on sample size when the electron beam is used directly.

There are several practical considerations when performing tests at a LINAC. The major ones are:

1. Peak current is achieved at energies somewhat less than the maximum energy.
2. Minimum beam diameters (affecting peak dose rates and maximum sample size) are in the range 0.2 to 2 cm at the beam exit window.
3. In air, the beam diameter expands approximately linearly with distance from the beam exit window; this implies an inverse-distance-squared dose-rate dependence. The angular spread of the beam varies from facility to facility.
4. When testing at any pulsed accelerator, good RF shielding is necessary in the form of shielded boxes to house the test devices, double-shielded cables, and careful and proper one-point grounding. If line drivers are used, care should be taken that neither RF noise nor radiation-induced signals mask the desired signals.
5. Multiple entries to the target (sample irradiation) area are time-consuming and therefore expensive. An average of 5 minutes per entry is typically required to make minor changes in the test configuration. A remotely controlled sample change should be considered for many sample irradiations having similar geometries.
6. Protection of the samples irradiated in the direct electron beam may be required during retuning of the LINAC. The dose delivered to test samples during tuning must be measured and considered in the data analysis. Significant sample heating also can occur.
7. Placement of dosimeters with respect to samples must be planned such that the dosimeters will accurately measure the dose received by the sample without causing a large nonuniformity in the test-sample dose.
8. Beam current-density profiles may change considerably during a long test. Effective pulse-to-pulse monitoring of the beam must be included in the dosimetry plans for a test.
9. A system for locating the beam prior to sample placement is required. Collimators and monitors are in common use for beam location and monitoring.

Polyvinylchloride (PVC) plastic sheets, which darken after irradiation to between 1 and 10 mrads, have been satisfactorily used for this purpose. If a remote television monitor is available at the facility, it is possible to observe scintillations in many plastics as the beam passes through the plastic and thereby check beam stability as machine parameters are varied.

10. It is quite normal to achieve an average of 5 to 6 useful machine hours of operation per 8-hour working day during a test lasting several days.

The characteristics of several LINACs are described in detail in Reference 13. Also see Table 4.2-2 for a summary of LINAC facility data.

4.2.3 Flash X-Ray Machines

Flash X-ray machines generate intense pulses of X-rays (bremsstrahlung) by conversion of electrons produced by discharge of stored electrical energy through a cold cathode tube. These machines are also used as electron-beam generators since the electrons can be used directly for irradiation studies. Flash X-ray sources differ from LINACs in that the electrons are accelerated by an intense pulsed electric field rather than an RF field. By varying many machine design factors, such as stored charge, electron energy (accelerating voltage), circuit parameters, cathode geometry, and target material, a wide range of bremsstrahlung intensities, energies, and beam spatial-distribution profiles may be obtained. However, for a given machine, the pulse width is essentially fixed and only limited variations in photon energy and dose rate are possible.

Various commercial flash X-ray machines produce bremsstrahlung with photon energies varying from 150 keV peak to several MeV peak, the peak energy corresponding to the electron accelerating voltage. The larger flash X-ray machines can usually deliver very high dose rates over large volumes. The bremsstrahlung energy distribution is such that the spectrum maximum usually occurs at less than one-third of the peak energy.

The spatial distribution of dose rate during the pulse generally looks like a "dipole gain lobe." The lobe pattern will vary from burst to burst at short distances from the source. It may even switch from single to multiple lobes during a burst, although this can be minimized by careful machine operation. Thus, the effective bremsstrahlung-source location can change slightly. This effect will often become apparent when dosimetry "beam maps" are performed. Very often, a dosimeter beam map close to the target will show large peaks or valleys in close proximity to one another. This effect is usually not noticeable a few feet from the source where multiple lobes are homogenized.

The beam-switching phenomenon is only of concern when testing within a few feet of the target and only when the time history of the burst (pulse

Table 4.2-2. Linear accelerator simulator table.

	FACILITY	ENERGY RANGE, MeV	MAXIMUM PEAK BEAM CURRENT, amps	ELECTRON DOSE, rad (Si)	ELECTRON DOSE RATE, rad (Si)/s	X-RAY DOSE, rad (Si)	X-RAY DOSE RATE, rad (Si)/s	NEUTRON YIELD, n/pulse	MAX NEUTRON YIELD RATE, n/s	PULSE WIDTH RANGE, μsec	PULSE REPETITION RATE PULSES
1	IRT Corporation LINAC (San Diego, CA 92138)	1 - 25	10	10^6	10^{7} -	200	10^8	5×10^9	5×10^{15}	0.01 - 8	10 - 720
2	NRL LINAC (Washington, DC 20375)	5 - 65	2	4×10^4		1,000		1×10^8		0.03 - 1.4	5 - 360
3	BREL LINAC (Seattle, WA 98124)	3 - 33	2.5		$>10^{11}$		6×10^6	6×10^{10}	7×10^{12}	0.04 6	1 - 550
4	NWEB LINAC (White Sands Missile Range, NM 88002)	2 - 48			6×10^{10}		5×10^8			0 01 - 10	10 - 120
5	EG&G LINAC (Goleta, CA 93017)	1 30	30		$1 5 \times 10^7$		1.8×10^8			5×10^{-5} - 4.5	1 - 360
6	AFFRI LINAC (Bethesda, MD 20014)	13 - 45		10^6	2×10^{11}	15				0.01 5	1 - 120
7	Rome Air Development Center LINAC (Hanscom AFB, MA 01731)	10	2				5×10^8			0 (1 - 4 3	1 - 180
8	Ogden Air Logistics Command LINAC (Hill AFB, VT 84406)	10 - 25	0.5		2×10^{10}		5×10^8			0 04 6	1 - 20
9	LASL PHERMEX (Los Alamos, NM 87544)	27	30							0 2	
10	RPI LINAC (Troy, NY 12181)	>80	>5			210	$1 6 \times 10^9$	$3 2 \times 10^{10}$	1.6×10^{18}	0.007 4.5	1 - 720

shape) is of importance. Many devices do not respond in direct proportion to the pulse amplitude (i.e., their response is not an equilibrium response). For these devices, only the prompt dose is important and the total dose measurement is adequate. Where the pulse shape is required and when testing close to the target, the pulse shape detector must be placed directly at the test sample.

At a flash X-ray source, the energy distribution (spectrum) is a function of time since it requires a finite time for the electron accelerating potential to reach a maximum and to decay to zero. X-ray source configuration, sample packaging, and material in the vicinity of a test sample will cause the photon energy spectrum to vary with location. The spectrum will also differ at various points in a plane perpendicular to the beam direction due to nonuniform absorption in the target material. The magnitude of the fluorescent X-radiation from the target is virtually unknown. In addition, each of these factors may change significantly over the life of the X-ray tube. For all of the above reasons, the spectra available for individual flash X-ray machines are likely to be only rough approximations of the photon energy spectra; further, changes will occur over a period of time.

The pulse width can be varied slightly on some of the high-energy machines, but it is not a simple procedure. The pulse shapes are roughly gaussian or triangular, and the total pulse width is usually more than twice the width at half-amplitude. On some higher energy machines, the cathode configuration can be changed. This alters both the beam half-angle and the distance between the effective origin of the burst and the closest possible sample position (although this distance is often about 2.5 cm).

Since the mass-energy absorption coefficients increase drastically at energies less than about 100 keV for low-atomic-number elements like silicon, it is at sources that have significant low-energy components (especially the low-energy flash X-ray machines) that environmental correlation is most difficult. Lower energy components deposit their energy near the front surface of the test item, resulting in a very nonuniform dose throughout the material. For this reason, it is generally advised that filters be used to suppress the low-energy components to the greatest degree practical. It is possible that, even at sources operating at high nominal energies, there may be a significant low-energy component present due to photons or electrons that have been degraded in energy by scattering. Although some test results indicate that this effect is probably very small, it is nevertheless good practice to eliminate any unnecessary scattering material from the vicinity of the sample.

Radiated noise from the machine and surrounding objects will usually be a serious problem at larger flash X-ray facilities and will be different at each facility and for every instrumentation system. Therefore, shielding will have to be tailored to meet the requirements of each test and design should be flexible enough to permit on-site modifications. At facilities

having larger flash X-ray machines, double- or triple-shielded transmission lines about 40 feet long are usually required and the test items must be enclosed in an RF shield. Low-energy flash X-ray machines are usually small enough to make it more practical to enclose the noise radiating portions of the machine in an RF shield.

Another consideration for the instrumentation system is command pulsing of the X-ray machine by the user. Most machines are equipped with this feature which allows the timing of the occurrence of the X-ray pulse with some event in the test sequence. Although limitations of this feature will differ at each facility, it can be expected that there will be a fixed delay time--the pulse delay will have some uncertainty (the timing jitter) between the command signal and the occurrence of the X-ray pulse.

Detailed descriptions of several flash X-ray facilities are given in Reference 13. Also see Table 4.2-3 for a summary of flash X-ray facility data.

4.2.4 Miscellaneous Sources

Various radiation sources other than those already discussed are sometimes used in TREE studies. Among these are radioactive isotope sources, spent fuel elements from nuclear reactors, steady-state particle accelerators, and high-energy neutron sources.

4.2.4.1 Isotopes

Radioactive isotopes are useful as calibration and standardization tools since they generally have well-known half-lives (and therefore knowable specific activities) and decay schemes (and therefore known radiation types and energies). Co-60 decays with a half-life of 5.3 years, emitting two gamma rays per disintegration of energy 1.17 and 1.33 MeV. A dose rate of 4.1×10^{-3} rad (air)/s, per curie, is observed at 1 foot from a small source of Co-60. Practical irradiation sources have activities of from 1 to several hundred thousand curies. Although isotope sources cannot be used for high-dose-rate simulation, they may be useful and economical for irradiation to high total doses when rate effects are not important or as a source for low-rate radiation-effects studies. Examples of TREE research in which Co-60 irradiation is useful are found in studies of surface effects and equivalence of radiation exposures for permanent bulk damage.

Spent fuel elements can also be used as a source of gamma radiation. Fuel elements from a nuclear reactor always contain a significant buildup of gamma-ray emitting radioactive isotopes after they have been in a reactor for a period of time. Hence, these elements can also be used in instances when low dose rates or total dose are of interest. The dose rate available from a spent fuel element varies according to its type, its reactor history, and the length of time that it has been out of the reactor.

Table 4.2-3. Flash X-ray simulator table.

	FACILITY	TOTAL BEAM ENERGY PER PULSE, joules	PEAK ELECTRON BEAM CURRENT, amps	AVERAGE PARTICLE ELECTRON ENERGY, MeV	PEAK ELECTRON ENERGY FLUENCE PER PULSE, cal/cm^2	MAX. X-RAY INTENSITY/ PULSE, rad (Si)	MAX. X-RAY DOSE RATE, rad (Si)/s	PULSE WIDTH RANGE, ns		PULSE REPETITION RATE	PULSE REPRODUCIBILITY
								ELECTRON MODE	X-RAY MODE		
1	Febetron 705 Electron Beam System, Northrop, Kaman Sciences Lockheed Palo Alto, EG&G	400	5,000	1 4	25	7,000 R		20 50	20	10 s	± 5%
2	Febetron 706 Electron Beam System, Lockheed EG&G, Triangle Institute, Westinghouse	12	7,000	0 5	2	100	4×10^{10}R s	3	3	1 min	± 3
3	ION Physics Corp FX-35 Electron Beam Generator Burlington, MA 01803	1,650		0 4 2 5	220	2 000		35	20		± 5%
4	Boeing FX 75 Electron Beam Generator, Seattle, WA 98124	9,000	60,000	3 5	400	$1 8 \times 10^4$	3×10^{11}R s	29	29	1 2 min	± 10%
5	Harry Diamond Labs FX 45 Electron Beam Generator Adelphi, MD 28783	2,500	25,000	2 4	75	88		25	25	1 7 min	± 4
6	Physics International Pulserad's San Leandro, CA 94577										
	225W	10,000	200 000	0 1 0 7	250	30,000 R		65	65		
	738	6,000		0 7 0 5				50	50		
	1150	40,000		1 4 4 2	100	50,000R	10^{12}	60	60	1 3 min	
	OWL II	110 000	1×10^6	0 3 1 0	520			110			
	PITHON II	Classified									
7	Maxwell Labs San Diego, CA 92123										
	BLACKJACK 3	30 000	550 000	0 7	>1 000			30 60	60	1 45 min	
	BLACKJACK 3 Prime	30,000		1 0				30 60	60		
8	TRW Redondo Beach, CA 90278										
	Vulcan FXR	>15 000	100 000	4 0	> 150	60 000	10^{12}	48	45	1 5 min	
	705 Febetron	400	5 000	2 0	140	7,000		20	20	1 min	

Table 4.2-3. Continued.

FACILITY	TOTAL BEAM ENERGY PER PULSE, joules	PEAK ELECTRON BEAM CURRENT, amps	AVERAGE PARTICLE ELECTRON ENERGY, MeV	PEAK ELECTRON ENERGY FLUENCE PER PULSE, cal/cm^2	MAX. X-RAY INTENSITY/ PULSE, rad (Si)	MAX. X-RAY DOSE RATE, rad (Si)/s	PULSE WIDTH RANGE, ns		PULSE REPETITION RATE	PULSE REPRODUCIBILITY
							ELECTRON MODE	X-RAY MODE		
9 Sandia Labs Albuquerque, NM 87115										
Hermes II	75,000	100,000	9.11	500	4×10^5	8×10^{12}	60	90	3 /m	± 15
RESA	10,000	40,000		400	1.8×10^4	2×10^{12}	20	70	6 /m	± 10
REHYD	36,000	600,000			7 rad (Si)		80	80	1 /m	± 15
10 North Carolina State University Physics Model 940 Electron Beam Generator Raleigh, NC 27650	6,000	80,000	3.5		25,000 R	5×10^{9} R	40	40	1 /m	± 5
11 Harry Diamond Labs Atmospheric Adelphi, MD 20783	2×10^9 (4 beams)	1.2×10^6	8	500	1×10^5	3×10^{13}	100	125	4 /m	
12 Physics International Co. Pulserad 605 X Electron Beam Generator Long Branch, CA 95640	1,200	25,000	2.4	100	38,000	1.9×10^{12}	15	20	1 /m	
13 Raytheon Radiation Facility Sudbury, MA 01776										
730 2650		1,500	2.0		15	2×10^6	50	60		
FX 25	1,200	20,000		120	3,000	1.0×10^{12}	20	20	1 /min	
14 General Electric FX 25 Philadelphia, PA 19101	1,200	2,000	2.0	100	5,000	1.25×10^{11}	20	20	1.2 /min	
15 Rome Air Development Hanscom AFB, MA 01731	800	200	2.0		3,000	1.5×10^{11}	20	20	1.1 /min	
16 Classified Naval Surface Weapons Center Silver Spring, MD 20910	Classified									
17 Classified Naval Research Lab Washington, DC 20375	Classified									

The gamma-ray energy spectra from spent fuel elements is mixed and varies with time; however, the average energy will be about 0.7 MeV.

4.2.4.2 14-MeV Neutron Sources

When a deuterium ion (d) with an energy of a few hundred keV collides with a tritium ion (H^3), a fusion reaction occurs in which a helium ion and a 14-MeV neutron are the end products. Machines are available that utilize this reaction to produce 14-MeV monoenergetic neutrons. Typical usable neutron flux is of the order of 10^{10} n/cm^2/s (Reference 13). There are also sources utilizing a plasma of deuterium and tritium gases that generate 14-MeV neutrons. The user must exercise caution in converting the 14-MeV test results to 1-MeV equivalent since the conversion is not straightforward.

4.2.4.3 Direct Current Accelerators

Van de Graaff, Dynamitron, and other such accelerators are used to produce controlled-energy particles in TREE work for neutron permanent damage, high dose research, and calibration work. Longer pulses of electrons or neutrons can be made than are readily available at a LINAC or other sources by switching the beam on and off or by sweeping it magnetically past the test article. Electron irradiations using a dc accelerator provide a means of high dose or high-rate exposure.

Typical reactions used in these accelerators to produce neutrons include $Be^9(d,n)B^{10}$ for neutrons in the 0.5- to 6-MeV range and $H^3(d,n)He^4$ for 14-MeV neutrons. Target cooling problems go hand-in-hand with increased beam current and flux and may pose a problem in obtaining desired flux over designed volumes at positions near the target.

Typical neutron fluxes per milliampere of beam current that are obtainable are 5×10^{13} n/(s·steradian·mA) from the $H^3(d,n)He^4$ reaction and 1.5×10^{11} n/(s·steradian·mA) from the $Be^9(d,n)B^{10}$ reaction. This leads to total useful energetic neutron fluences on the order of 10^{13} n/cm^2 over an area of a few square centimeters in times on the order of 1 minute for the $H^3(d,n)He^4$ reaction and times on the order of 2 hours for the $Be^9(d,n)B^{10}$ reaction while operating at 1 mA of positive ion current. High currents over extended periods of time are practicable; however, good target cooling is necessary to avoid target material depletion.

In working with dc accelerators, care must be taken in measuring the small currents involved. Electrometers and current integrators are used, and good insulators, guard electrodes, and other such techniques are usually needed.

4.3 SOURCE SELECTION

Some of the major features of various radiation sources were briefly mentioned in the previous section. The characteristics of radiation

facilities that are desirable for typical TREE experiments are presented in this section. Because of the variety of testing considerations involved, it is not feasible to "standardize" research nor to recommend unequivocally a single radiation source for use in TREE studies.

4.3.1 General Considerations

The need for simulation of a given radiation environment to produce a predetermined effect requires careful source selection. The major parameters to be considered are cost, radiation type (generally photons, neutrons, or electrons for TREE work), energy spectrum, and time dependence. Other considerations of a practical nature are discussed under Operational Considerations, Section 4.3.4.

Within the scope of this preferred prodecures document, there are basically two types of device responses of interest: transient response (typically photocurrents generated in the bulk material) and permanent response (damage in either the bulk or surface of the devices). The basic test environment requirements for these responses are given in the following sections.

4.3.2 Transient Response Considerations

Transient responses typically result from photocurrents introduced through ionization phenomena due primarily to photon irradiation. However, neutron ionization can also cause photocurrents of interest. Therefore in most cases, a pulsed source of ionizing radiation should have:

1. Rise and fall times short compared to diffusion times and long enough and with controllable pulse-length capabilities to achieve equilibrium photocurrent in the device under test
2. Sufficient intensity to produce the required range of dose rates in the device (i.e., to obtain data both where I_{pp} is linear with dose rate and at the high rates where nonlinearities appear)
3. Sufficiently energetic photons or electrons to penetrate the case of the device and produce a uniform dose throughout the active volume
4. An energy spectrum sufficiently well-known so that the dose rate in the active volume can be accurately determined by standard methods
5. Spurious RF noise low enough to avoid confusion of effects.

These are ideal characteristics and are not to be found in any one pulsed source.

Many LINAC and flash X-ray machines closely approximate these criteria if proper precautions are taken. The LINAC has the advantages of variable and long pulse width, better-controlled beam diameter, position, intensity, and shot-to-shot performance. The flash X-ray has the advantage of a larger irradiation-volume capability for tests on several devices simultaneously.

There are two other transient responses of devices that can be of concern with some systems. The first response results from short-term annealing of bipolar transistor gain. Because transistor-gain degradation is primarily caused by neutrons, a pulsed source of neutrons with sufficient fluence ($>10^{12}$ n/cm^2) and short duration (depending on response times of interest) is needed. The appropriate pulse width for characterizing this effect will depend upon the system specification to be applied to the part being characterized.

Second, a transient response attributable to surface effects has been observed in some devices. Sources of ionizing radiation with pulse widths that are short with respect to the response times of interest should be used to evaluate the influence of this effect on device response.

4.3.3 Permanent Response Considerations

Permanent responses of devices are attributed to physical-property changes that can persist for long periods of time as compared to the measurement circuit response time. Permanent responses can be grouped into two categories: bulk and surface effects. The bulk effects are due to lattice displacements in the bulk of the material induced by high-energy radiation, primarily neutrons. Surface effects are primarily due to ionizing radiation causing changes in the surface conditions of the bulk material. Therefore, for permanent-bulk-damage tests, a neutron source should have:

1. Sufficient fluence of energetic particles at the test setup position to produce the desired bulk damage
2. A spectrum sufficiently well-known to allow characterization of the spectrum in standard terms by standard methods
3. A known neutron-to-gamma ratio that is high enough so that any effects due to the gamma radiation are negligible in comparison with neutron-induced effects.

Pulsed reactors, some steady-state reactors, and some accelerator-generated neutron sources meet these criteria. Accelerator-generated neutrons may have the energy distribution of a fission spectrum if they are generated in the photofission process, or they may be nearly monoenergetic if a fusion reaction such as the $H^3(d,n)He^4$ reaction is used.

For permanent-surface-effect types of experiments, a source of ionizing radiation that produces a minimal amount of bulk damage is necessary. For electrons in silicon, energies less than about 150 keV meet this requirement. However, if the total dose is less than about 10^6 rads (Si), bulk damage is negligible and higher energy radiations may be utilized. Isotope sources, ion accelerators, LINACs, and flash X-ray machines can all meet these criteria.

4.3.4 Operational Considerations

Once the test engineer has decided upon the type of radiation facility required, the particular facility that will permit attainment of the test objective with the available resources must be selected. The determining factors in this decision are the operational considerations, i.e., those factors that can only be determined by the test engineer. They depend upon such factors as the funds available, expertise in TREE effects testing, the physical dimensions of the test setup, and the accuracy and precision required to obtain the test objectives. A review of Section 2.5, Test Hardware Considerations and Techniques, may be helpful at this time.

One obvious consideration is the cost of using the facility, including rental fees and transportation of personnel and equipment to the facility. This may be related to the support capabilities available at the radiation facility. Costs for using a facility can be obtained by contacting the facility and discussing your requirements with them. This is best left until after the preliminary test design is completed. For a small low-budget test, investigate the possibility of piggy-backing it on another larger test. This is possible when the test conditions of the two are compatible.

Other things to consider are:

1. If a test requires less than a whole day to complete, will the test engineer be charged for a whole day's use of the facility?
2. How flexible is the facility's staff if the test requires work during other than routine business hours?
3. Does the facility have a staff experienced in TREE testing available for consultation?
4. How much assistance will the staff of the facility be able to provide?
5. Will adequate test equipment be available at the facility or will the test engineer have to provide it himself?
6. What dosimetry services can the facility provide?
7. Can an outside vendor be used to provide supplemental dosimetry services for redundancy?

8. The problems of remote operation (including long-cable effects, the possible need for precision test-sample positioning, or frequent setup change) must be considered.

9. The physical size of the test article with respect to the exposure area available must be considered. How uniform is the dose and/or dose rate at the location where the test will be performed, both across the front surface and from the front to the back of the test article? For tests close to a point source, it is usually necessary to prepare a jig to hold the device and dosimeters to assure that they receive the same dose. Trial calculations using the maximum positioning error of the test setup, assuming a $1/R^2$ dose dependence, will show the accuracy required in positioning the components.

10. Are the energy spectrum and/or yield component ratio (n/γ ratio in a reactor, etc.) satisfactory?

11. Can the radiation source be pulsed by a synchronized signal from the test equipment or must this be done by a signal from the facility's operator?

12. What will be the uncertainty in knowing exactly when the pulse will occur?

13. What precautions will be necessary to protect the test setup from unwanted noise at the facility under consideration?

14. Will spurious signals, including charge scattering from the test fixtures and electromagnetic RF noise due to the radiation generator or the radiation itself, be more of a problem at one facility than at another?

15. Is a screen room available? Is it large enough for the planned test?

Most government-owned simulation facilities require justification as to why that facility must be used before permission to use it is granted. They also may require that the tests be related to work on a government contract. When such authorizations involve more than one governmental agency, several weeks or even months of lead time may be necessary. If the material used in a test becomes radioactive during irradiation, a license must be obtained to receive the specific radioisotopes that were generated. A lead time of from a few days to a few months is usually necessary when scheduling a test at a nongovernment-owned facility.

At many facilities, a test plan must be submitted and approved before a firm scheduling commitment will be given. This should specify the limitations (accuracy) of what they can supply. It is the test engineer's responsibility to take these limitations into consideration in the test plan.

CHAPTER 5

DOSIMETRY AND ENVIRONMENTAL CORRELATION

5.1 INTRODUCTION

Dosimetry is the process of measuring and providing a quantitative description of a radiation dose in terms relevant to the radiation effect being studied. In its most general form, the environment can be described by stating the (possibly time-dependent) number of nuclear or atomic particles of various types and energies (the spectrum) that cross a given surface. It is not economically feasible to make such measurements and such complete descriptions are rarely available or required. In mathematical terms, for a radiation spectrum $\phi(E)dE$ and a radiation effect with energy dependence $R(E)$ assumed to be time independent, the total effect produced by the spectrum is

$$R = \int R(E)\ \phi(E)dE. \tag{5-1}$$

For example, if a particular radiation effect of interest has a response, $R(E)$, that is fairly insensitive to energy over the energy range of interest $(R(E) = \text{constant})$, then the total effect is just

$$R \simeq \text{Constant} \int \phi(E)dE \simeq \text{Constant} \times \Phi. \tag{5-2}$$

The integral in Equation 5-2, denoted by Φ, is the total fluence and the particular effect used as the example is one proportional only to the total fluence. Since this effect is independent of spectral shape, the total radiation fluence is the relevant quantity and is all that must be determined when describing the environment. On the other hand, if an effect such as neutron displacement damage in silicon (which is quite dependent on neutron energy) is being studied, the total effect is described by Equation 5-1, in which case both the total fluence and its energy spectrum are relevant and should be determined.

The measurement of a radiation environment also entails the determination of a radiation effect. In this case, a dosimeter with a known response function $D(E)$ which has been calibrated with respect to the radiation field is used and a measurement

$$D = \int D(E)\ \phi(E)dE \tag{5-3}$$

is obtained. If the dosimeter response function, $D(E)$, is approximately proportional to $R(E)$ for the energy range of importance to these integrals, it is a fortuitously appropriate dosimeter. If it is not, other information, such as an estimate of the shape of $\phi(E)$, will be needed to relate the dosimeter reading, D, to the expected effect, R. One measure of the

appropriateness of a detector is how closely its response function is related to the response function for the radiation effect being studied for the type of radiation considered. This same conclusion applies to the appropriateness of dosimetry units, such as the ones defined in Section 5.1.1.

For example, it has been established that the magnitude of bulk ionization effects in silicon is a function only of the ionization energy deposition. Therefore, the appropriate unit for describing ionizing radiation when interested in ionization-induced currents in a silicon device is a unit of energy deposition in silicon, e.g., rad (Si). Any dosimeters whose readings can easily be converted to rad (Si) in a way that is not sensitive to the detailed spectrum of the incident radiation are then useful. By way of contrast, displacement effects in silicon represent a totally different response to the radiation spectrum, and the rad (Si) is an inappropriate unit. In this case, the total fluence and spectral shape or the equivalent fluence of some energy or spectrum of neutrons that would produce the same concentration of displaced atoms in silicon (neutrons/cm^2 (1-MeV equivalent) or neutrons/cm^2 (fission spectrum equivalent)) is frequently used.

Perhaps the most common error made in radiation effects testing is to neglect the effect of the perturbation of the radiation spectrum created by the presence of the test article. It is this perturbed spectrum and not the free-field spectrum that should be used in the correlation or in determining the total radiation fluence from a monitor dosimeter or foil used for the tests. In many cases, it is the zeroth approximation of the true spectrum, i.e., the free field spectrum, that is used.

Before proceeding with a definition of units and descriptions of dosimeters, it is appropriate to comment on two commonly used terms: correlation and simulation. When applied to radiation effects, they are defined as follows:

> Simulation--the production of a particular radiation effect by any means
>
> Correlation--the establishment of the relative intensities of different radiation spectra or other types of stimulation required to produce the same effect.

Simulation does not necessarily imply any need to reproduce a radiation environment, only its effect. If the same effect can be produced by electrical or optical means rather than nuclear radiation, these are valid simulation techniques for that effect. The correlation between radiations must be established separately for each class of effect. For example, the correlation between different energy neutrons is much different for displacement effects than for ionization effects.

5.1.1 Definitions of Units

The Defense Nuclear Agency (DNA) has adopted as standard the definitions of radiation quantities and units in the reports of the International Commission of Radiological Units and Measurements (Reference 14). Several of the more important units and definitions are abstracted in the following paragraphs for convenience to the users of this document. Some units commonly used as a measure of various defined quantities are included.

1. Directly ionizing particles--charged particles (electrons, protons, alpha-particles, etc.) having sufficient kinetic energy to produce ionization by collision.

2. Indirectly ionizing particles--uncharged particles (neutrons, photons, etc.) that can liberate directly ionizing particles or can initiate nuclear transformations.

3. Ionizing radiation--any radiation consisting of directly or indirectly ionizing particles or a mixture of both.

4. Absorbed dose--the quotient of $d\bar{\varepsilon}$ by dm, where $d\bar{\varepsilon}$ is the mean energy imparted by ionizing radiation to the matter in a volume element and dm is the mass of the matter in that volume element.

$$D = \frac{d\bar{\varepsilon}}{dm} \text{ (rads)}.$$

Rad is a unit of absorbed dose and will be used in this document. One rad is the absorption of 100 ergs/g of material being irradiated. The Gray (Gy) has been adopted as the official SI unit. One Gy = 100 rads.

5. Absorbed dose rate--the absorbed dose per unit time interval.

$$\text{Absorbed dose rate} = \frac{dD}{dt} \text{ (rads/s)}.$$

6. Fluence--the quotient of dN by da, where dN is the number of particles that enter a sphere of cross-sectional area da.

$$\Phi = \frac{dN}{da} \text{ (particles/cm}^2\text{)}.$$

7. Flux density (flux) or fluence rate--the quotient of $d\Phi$ by dt, where $d\Phi$ is the measurement of particle fluence in time interval dt.

$$\phi = \frac{d\Phi}{dt} \text{ particles/cm}^2 \cdot \text{s}.$$

8. Energy fluence--the quotient of dE_F by da. dE_F is the sum of the energies, exclusive of rest energies, of all the particles that enter a sphere of cross-sectional area da (dE_F = kinetic energy per particle times the number of particles with that energy).

$$F = \frac{dE_F}{da} \text{ (calories/cm}^2\text{, MeV/cm}^2\text{)}.$$

9. Energy flux density--the quotient of dF by dt where dF is the energy fluence in the time dt.

$$I = \frac{dF}{dt} \left[\text{calories/(cm}^2 \cdot \text{s), MeV/(cm}^2 \cdot \text{s)}\right].$$

10. Exposure--the quotient of dQ by dm, where dQ is the absolute value of the total charge of the ions of one sign produced in air when all the electrons (negatrons and positrons), liberated by photons in a volume element of air of mass dm, are completely stopped in air.

$$X = \frac{dQ}{dm} \text{ (R)}.$$

Roentgen (R) is the unit of exposure.

$$1 \text{ R} = 2.58 \times 10^{-7} \text{ C/g}.$$

(C is the abbreviation for coulomb.)

11. Exposure rate--the quotient of dX by dt, where dX is the increment of exposure in time dt.

$$\text{Exposure rate} = \frac{dX}{dt} \text{ (R/s)}.$$

12. Mass attenuation coefficient--the quotient of dN by the product of ρ, N, and dl, where N is the number of indirectly ionizing particles incident normally upon a layer of thickness dl and density ρ, and dN is the number of particles that experience interactions in this layer.

$$\frac{\mu}{\rho} = \frac{1}{\rho N} \frac{dN}{dl} \ (cm^2/g).$$

13. Mass energy transfer coefficient--the quotient of dE_{tr} by the product of E, ρ, and dl, where E is the sum of the energies of the indirectly ionizing particles incident normally upon a layer of thickness dl and density ρ, and dE_{tr} is the sum of the kinetic energies of all the charged particles liberated in this layer.

$$\frac{\mu_{tr}}{\rho} = \frac{1}{E\rho} \frac{dE_{tr}}{dl} \ (cm^2/g).$$

14. Mass energy-absorption coefficient--

$$\frac{\mu_{en}}{\rho} = \frac{(1 - G)\ \mu_{tr}}{\rho}$$

where G is the proportion of the energy of secondary charged particles that is lost to bremsstrahlung in the material. When the material is air, μ_{en}/ρ is proportional to the quotient of exposure by fluence. μ_{tr}/ρ and μ_{en}/ρ do not differ appreciably unless the kinetic energies of the secondary particles are comparable with or larger than their rest energy.

15. Mass stopping power--the quotient of dE_S by the product of dl and ρ, where dE_S is the average energy lost by a charged particle of specified energy in traversing a path length dl, and ρ is the density of the medium.

$$\frac{S}{\rho} = \frac{1}{\rho} \frac{dE_S}{dl} \ (MeV\ cm^2/g).$$

16. Linear energy transfer--the quotient of dE_L by the product of ρ and dl, where dE_L is the average energy locally imparted to the medium of density ρ by a charged particle of specified energy in traversing a distance of dl.

$$LET = \frac{1}{\rho} \frac{dE_L}{dl} \ (MeV\ cm^2/g).$$

17. Differential energy spectrum--the distribution of energies of particles described respectively as a flux $\phi(E)$ or fluence $\Phi(E)$ of particles having energies in a

range E to E + dE, per unit energy interval, dE (particles/(cm^2·MeV)).

18. Integral energy spectrum--the distribution of energies of particles described as that flux or fluence having energies greater than some specified value (e.g., n/cm^2 (E > 3 MeV)).

19. Fission neutron spectrum--the energy spectrum of neutrons emerging from a fission reaction, usually in thermal neutron-induced fission of U-235.

5.1.2 Weapon and Laboratory Radiation Environment

The radiation environments produced by a nuclear detonation of interest in TREE testing are:

1. Gamma rays, with energies up to a few MeV, primarily emitted as an intense short pulse, but with some contributions later from neutron interactions
2. Neutrons with energies up to 14 MeV, also emitted as a short pulse, but spread in arrival time at a target by the dependence of their speed on energy
3. X-rays, with energies up to several hundred KeV, that reach a target without significant scattering.

The radiation environments produced by laboratory sources for TREE experiments include:

1. Bremsstrahlung X-ray spectra of peak energies of 0.15 MeV up to 10 MeV from flash X-ray machines
2. Bremsstrahlung X-ray spectra of peak energies of 3 MeV up to 75 MeV from LINACs (lower intensities than available from flash X-ray machines)
3. Energetic electrons of energies of up to 75 Mev from LINACs and up to 10 MeV from flash X-rays (ionization energy loss almost independent of energy above 1 MeV; penetration proportional to energy)
4. Fission gamma rays and neutrons from nuclear reactors
5. 14-MeV neutrons from accelerators (pulsed or steady state) using (d,t) reactions
6. Gamma rays from isotope sources such as Co-60.

5.1.3 Types of Radiation Effects and Simulation

The types of radiation effects considered and the relevant parameters describing the radiation environment that most strongly determine the

effects, i.e., what type of average over the spectrum best characterizes the response, are:

1. Bulk ionization effects in semiconductors that depend primarily on the pulse width and the ionizing dose in the semiconductor from a short radiation pulse or on the dose rate in a pulse long compared to the relaxation time.

2. Bulk ionization effects in insulators (conductivity) that depend not only on the dose rate and/or dose for radiation producing lightly ionizing primary or secondary tracks (electrons, photons (i.e., gammas or bremsstrahlung)), but also on linear energy transfer for heavily ionized tracks (such as recoil protons from neutron collisions with hydrogen atoms).

3. Charge-transfer effects (e.g., emission of electrons from surfaces) that depend on particle type and spectrum in a complicated, but calculable, way. (For accurate work, specific theoretical or experimental calibrations of the energy dependence of charge transfer are required.)

4. Displacement effects that depend primarily on the concentration of defects in the target crystal and secondarily on the clustering of displaced atoms. They are produced mostly by neutrons. The neutron-energy dependence of the displacement effectiveness in silicon is shown in Figure 5.1-1 and can be used to calculate the relative effectiveness of different spectra. Neutron damage also has a time dependence that is discussed in Section 6.1.3, Annealing.

In most cases, bremsstrahlung X-rays or electrons are used to simulate the short-pulse ionization effects produced by weapon gamma rays. In some cases, pulsed-reactor gamma rays are used to simulate the longer pulse ionization effects produced by the later arriving neutron-produced gamma rays. Generally, reactor neutrons are used to simulate displacement effects from weapon-spectrum neutrons. 14-MeV neutrons are used to a much lesser degree, primarily to check the expected energy dependence as shown in Figure 5.1-1.

The pulse-width requirements for simulation are determined by the characteristic relaxation time for the effect compared with the weapon produced pulse. Usually, these can be stated as a requirement for the radiation pulse to be either significantly shorter than, or significantly longer than, a characteristic relaxation time.

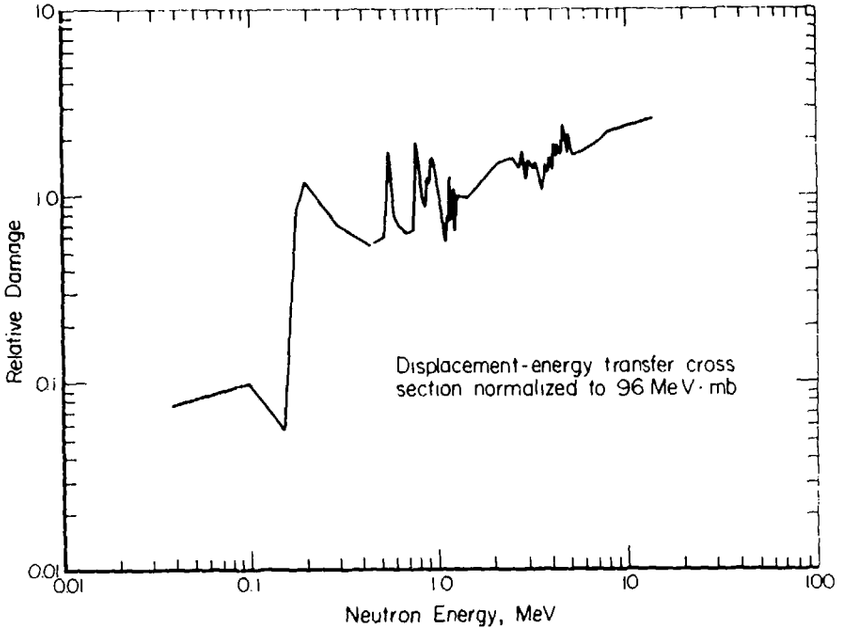

Figure 5.1-1. Relative neutron effectiveness for displacement production (Reference 15). See also Reference 16

In the following sections, the dosimetry techniques are separated into three classes:

1. Neutron measurements, which are primarily applicable to displacement effects studies
2. Photon and electron measurements, which are primarily in support of ionization effects studies
3. Time-dependence monitoring.

5.2 NEUTRON MEASUREMENTS

5.2.1 General Principles

To perform the weighting of different neutron energies by the factors shown in Figure 5.1-1, it is necessary to have the neutron energy spectrum for energies above 10 keV. The contribution to displacement effects from neutrons below 10 keV in weapon or reactor environments is usually taken to be negligible. Many neutron-producing facilities can provide detailed spectral information of the free-field neutron environment. In general, these spectra are determined from data obtained from high-resolution spectrometers (recoil proton, Li^6, He^3, etc.), from low-resolution measurements utilizing activation techniques, or from reactor physics calculations. In general, if the test article is small, there is a good chance the

free-field spectrum will not be significantly perturbed and will be relevant to the test being conducted. If additional spectroscopy measurements are necessary, a decision must be made to determine the accuracies required. For high-resolution measurements, fairly expensive, time-consuming spectrometer measurement should be made. In most cases, however, lower resolution measurements will be acceptable and activation spectroscopy measurements will suffice. The operating power level of a reactor is usually used with known spectral information at usual test positions to determine a first estimate of the neutron fluence during a test. Inasmuch as the techniques for spectrometer measurement are highly dependent upon the instrumentation involved and the calculation of the approximate spectrum is beyond the scope of this manual, no recommended procedures will be given in this document. However, general recommendations are given concerning foil-activation techniques. In addition, Reference 16 contains an excellent discussion of neutron damage measurement considerations.

5.2.2 Foil-Activation Measurements

Foil-activation techniques utilize neutron-induced reactions, for which there is a threshold energy or for which an artificial threshold can be produced by shielding. These neutron-induced reactions produce radioactive isotopes whose emitted radiation can be measured and used to determine the neutron fluence above the threshold. The process is illustrated schematically in Figure 5.2-1. The top curve shows a typical neutron spectrum. The middle curve shows an idealistic response function for a threshold foil. The product of these two functions is shown in the bottom curve. The area under this curve is the total foil response (which is proportional to the foil's radioactivity). It can be seen that the neutrons with energy above E_t contribute to the response, and the effective response coefficient (cross section) is almost a constant, σ_{eff}. Therefore, the foil response is approximately proportional to $\phi(E > E_t)\sigma_{eff}$ (Method E720 of Reference 3).

A method based on irradiating a number of foils with different thresholds has proved to be useful. The limitations to the foregoing approximate analysis are obvious: $\sigma(E)$ is not constant above E_t and E_t itself is a function of the spectral shape. The steeper spectra tend to push E_t downward. In an actual situation, where the cross section is not constant but the spectral shape, $\Phi(E)$, is known, a spectral averaged cross section is obtained from the expression,

$$\sigma = \frac{\int_0^\infty \sigma(E)\,\Phi(E)\,dE}{\int_{E_t}^\infty \Phi(E)\,dE} . \qquad (5\text{-}4)$$

With this average cross section and the measured foil activity, the neutron fluence above the threshold energy, E_t, can be obtained. Since the

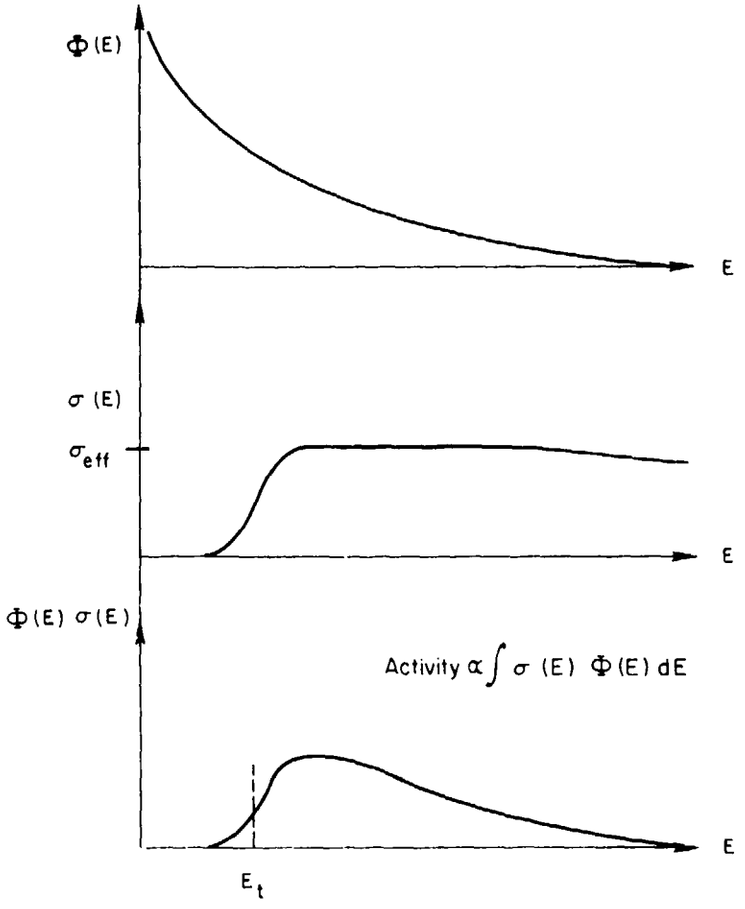

Figure 5.2-1. Threshold foil method.

spectrum is known, the total neutron fluence can be determined. This process is the most common measurement made in neutron effects testing. A commonly used monitor foil material is S-32 which has a threshold energy of approximately 3 MeV. The $Ni^{58}(n,p)Co^{58}$ reaction is also useful. If this method is used, one must ensure that the test setup has not perturbed the spectrum since large errors can unknowingly be introduced.

In situations where the spectral shape is not as well known, a series of threshold foils should be used. By assuming a spectral shape (e.g., a fission spectrum or "best estimate" for the particular reactor), an average cross section can be computed and the fluence above the various thresholds determined, based upon the assumed cross section. A curve of the integral fluence as a function of energy can be determined by this method. From this curve, the ratio of total fluence to that above a monitor foil's threshold (e.g., S-32) can be determined so that further exposures can be

made with the use of only the one monitor foil. Table 5.1-1 presents a list of commonly used foils. If the integral curve obtained in the previous manner differs considerably fron an integral curve of the assumed spectrum, further data evaluation must be done, particularly in the range from 0.01 to 5.5 MeV.

Table 5.1-1. 12.7-mm diameter activation foils (Method E720 of Reference 3).

Reaction	E_t, MeV	E_γ, keV	Gamma/Reaction, (Fission Yield, %)[K]	$T_{1/2}$	Recommended Foil Mass, g	Isotopic Abundance, %	Footnotes
$^{197}Au(n,\gamma)^{198}Au$	0	412	0.96	2.696 days	0.056	100	A B
$^{59}Co(n,\gamma)^{60}Co$	0	1173	1.00	5.26 years	0.057	100	A
		1333	1.00				
$^{55}Mn(n,\gamma)^{56}Mn$	0	847	0.99	2.58 h	0.030	100	A B
		1811	0.27				
$^{235}U(n,f)^{140}La$	0 (0.01)	1596	0.95 (6.29)	40.22 h	0.281	100	A C D
$^{239}Pu(n,f)^{140}La$	0 (0.01)	1596	0.95 (5.24)	40.22 h	0.150	100	A C D
$^{237}Np(n,f)^{140}La$	0.5	1596	0.95 (5.69)	40.22 h	0.580	100	A C E
$^{237}Np(n,f)^{97}Zr$	0.5	743	0.94 (6.01)	17.0 h	0.580	100	A E F
$^{115}In(n,n')^{115m}In$	1.0	336	0.50	4.3 h	0.255	95.7	
$^{238}U(n,f)^{140}La$	1.45	1596	0.95 (6.02)	40.22 h	0.495	100	A C G
$^{232}Th(n,f)^{140}Ba$	1.75	537	0.20 (7.91)	12.8 days	1.066	100	A H
$^{232}Th(n,f)^{97}Zr$	1.75	743	0.94 (4.12)	17.0 h	1.066	100	A F
$^{54}Fe(n,p)^{54}Mn$	2.20	835	1.00	312 days	0.142	5.82	
$^{58}Ni(n,p)^{58}Co$	2.9	811	1.00	70.8 days	0.282	67.8	
$^{32}S(n,p)^{32}P$	2.9	betas	1.00β	14.26 days	4.10	95.0	I
		1710					
$^{24}Mg(n,p)^{24}Na$	6.3	1369	1.00	15.02 h	0.030	79	A
$^{56}Fe(n,p)^{56}Mn$	7.5	847	0.99	2.58 h	0.142	91.7	A J
		1811	0.27				
$^{27}Al(n,\alpha)^{24}Na$	8.7	1369	1.00	15.02 h	0.257	100	A
$^{127}I(n,2n)^{126}I$	11.0	388	0.33	13 02 days	0.657	100	
		666	0.29				
$^{90}Zr(n,2n)^{89}Zr$	14	909	1.00	78.4 h	0.108	51.5	

[A] Cd covers 0.5- to 1-mm thickness.

[B] Use ^{59}Co instead of ^{197}Au and ^{55}Mn for very long irradiations.

[C] 40.23-h daughter of 12.80-day ^{140}Ba. Wait 5 days for maximum decay rate (see ASTM Method E393.)

[D] E_t 0.01 MeV shielded with ^{10}B sphere. [Use of ^{10}B shield is important for soft (Triga) spectra where $\phi(E<0.01$ MeV) will otherwise dominate].

[E] If a ^{10}B sphere is used for the ^{239}Pu foil, then a ^{10}B sphere should also be used for the ^{237}Np foil so that correction for ^{239}Pu impurity in the ^{237}Np foil can be made.

[F] Use ^{97}Zr for low fluence (3×10^{11} to 3×10^{12} n/cm^2). Use peak-shape analysis or measure twice, 7 days apart, to strip off 740-keV ^{99}Mo gamma ray ($T_{1/2}$ = 67 h).

[G] If a ^{10}B sphere is used for the ^{235}U foil, then a ^{10}B sphere should also be used for the ^{238}U foil so that correction for ^{235}U impurity in the ^{238}U foil can be made.

[H] ^{232}Th radioactivity interferes with ^{140}La line.

[I] Requires different detector and calibration technique.

[J] Maximum Mn impurity = 0.001%, Cd covered. Do not use ^{56}Fe foil for long irradiations.

[K] Fission yields are for bombardment with fission-spectrum neutrons (Reference 17). For thermal and 14 MeV, see Reference 18.

Computer codes such as SAND II and SPECTRA have been developed to further extract spectral information from the set of activation data. The SAND II and SPECTRA codes compute both differential and integral spectra, based upon iterative techniques, and utilize the response function differences of the various reactions over the entire sensitive energy regions and other physical information available about the source to obtain these solutions. However, the solutions thus obtained are always nonunique. If the spectral shape is calculated by one of these codes for the particular experimental setup and if no changes in the setup are made, a single monitor foil may be used for subsequent irradiations. It is wise to check to ensure that the spectrum has not changed unknowingly. The accuracy of the neutron fluence measurements with foil activation techniques will be limited by the accuracy of the cross-section knowledge, the calibration of the counting equipment, and the degree of sophistication exercised in reducing the foil activities to fluence information (Method E721 of Reference 3).

The three codes may be obtained from the Radiation Shielding Information Center at Oak Ridge National Laboratory. Evaluated energy-dependent cross sections for neutron detector reactions are also available from the center (SAND II cross-section library format).

Methods for interpreting measured neutron spectra and reporting in terms of equivalent fluence units are given in Section 5.7.

5.3 PHOTON AND ELECTRON MEASUREMENTS

5.3.1 General Principles

For TREE applications, photon and electron measurements are primarily in support of ionization effects testing. Therefore, the dose (or ionization density) in the material of interest is most closely related to the effect. For high-energy electrons and for the Compton effect of high-energy photons and low- or medium-Z material, an approximate rule of thumb (±5 percent) is that the dose is proportional to Z/A of the target material, where A is the mass number. For higher accuracies, even a crude spectral shape used with Equations 5-1 and 5-3 can convert dose measured in any dosimeter, D, to the dose in the material of interest, R, viz.,

$$R = D \frac{\int R(E)\, \phi(E)\, dE}{\int D(E)\, \phi(E)\, dE} . \qquad (5\text{-}5)$$

For electron beam exposures in a known spectrum, dose may be converted from one material to another by using Equation 5-5 and dE/dX values given in the literature (Reference 19).

The use of high-energy electrons (0.5 MeV $\leq$ E $\leq$ 15 MeV) to produce ionization effects is straightforward. Their rate of energy deposition is almost independent of energy and material, Z < 40. The only cautions are that the electron energy needs to be high enough to penetrate the target

and radiative losses must be considered. In addition, thin plates can scatter a small-diameter electron beam into a cone-shaped beam. Therefore, objects in the beam ahead of the target, such as a chassis, must be in place during dosimetry calibration.

The maximum range (depth of penetration) is approximately

$$R_e = 0.412\ E^{(1.265 - 0.0954 \log_e E)} \quad \text{for } 0.01 \text{ MeV} \leq E \leq 3 \text{ MeV}$$

$$R_e = 0.530\ E - 0.106 \quad \text{for } 2.5 \text{ MeV} \leq E \leq 20 \text{ MeV}$$

where

$R_e = \rho\ell$ in gm/cm^2, and E is in MeV,

where ρ is the material density in g/cm^3 and ℓ is thickness in cm.

Photons deposit energy in material primarily through secondary electrons created in photon interactions with matter. Therefore, most of the above discussion on electrons is pertinent to dose deposition by photons.

The response function relating dose deposition to the photon energy is known as the mass absorption coefficient. Figure 5.3-1 shows the mass absorption coefficients for silicon, a typical low-Z material. The absorption coefficients of low-Z dosimetry materials such as calcium fluoride and lithium fluoride are within a factor of 2 relative to silicon over the energy range 150 keV $\leq E \leq$ 1 MeV. Based upon these characteristics, the absorbed dose per unit energy fluence for bremsstrahlung distributions over this energy range is fairly insensitive to the spectral shape, and dose measured in a low-Z dosimeter can be converted quite easily to dose in a low-to-medium-Z material of interest.

Since photons (gamma or X-rays) are indirectly ionizing particles and lose energy through the creation of high-energy electrons that subsequently lose energy through further ionization, extra care must be taken in accounting for lack of electron equilibrium. If a pure photon beam were incident on a slab of material, the energy deposition as a function of depth in the slab would be as shown schematically in Figure 5.3-2. Although the amount of energy initially imparted to the material by photons decreases with depth, the actual dose builds up to a maximum at a depth corresponding to the maximum electron range, then decreases very slowly at the rate of attenuation of the photon beam. This loss of dose to the material near the surface results from the beam not having reached secondary electron equilibrium. At a point corresponding to the maximum electron range and beyond, the beam is in electron equilibrium, meaning that for every secondary electron leaving a small region of interest, another enters the region or, equivalently, the ratio of electrons to photons remains constant. For high photon energies (>200 keV) in low and medium atomic number materials (Z

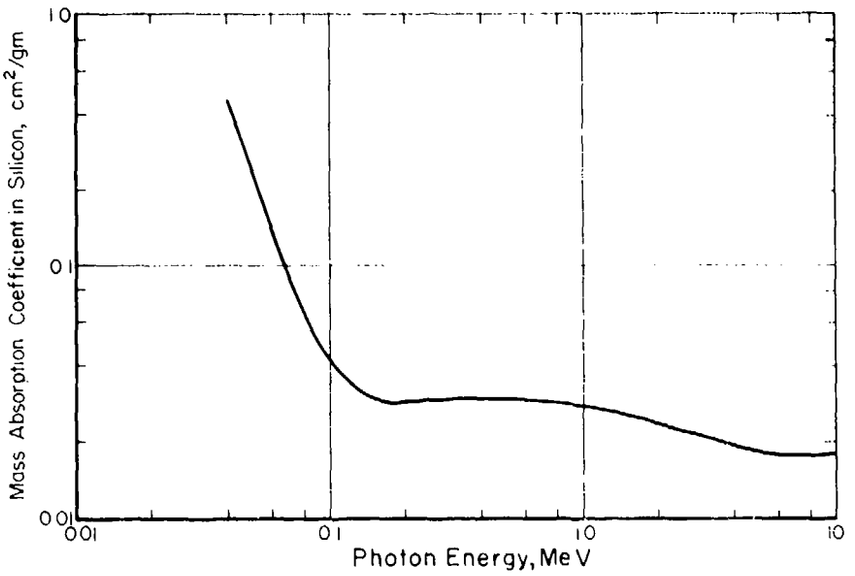

Figure 5.3-1. Mass absorption coefficients for gamma rays in silicon.

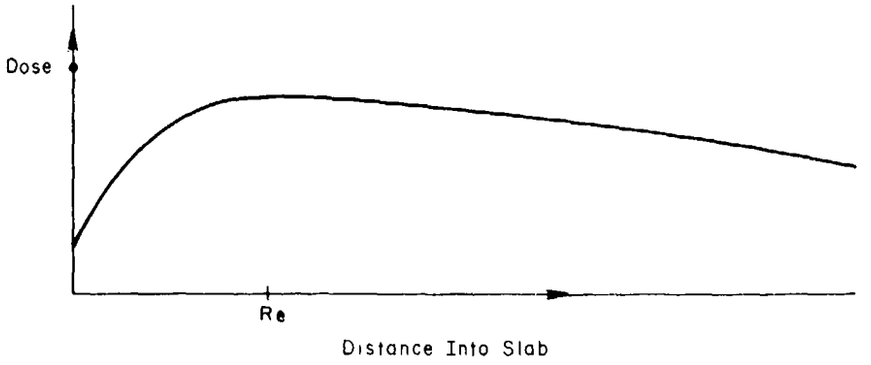

Figure 5.3-2. Energy deposition by photons.

< 40), the ratio of electrons to photons is almost independent of material. At lower energy and higher Z, the ratio changes when the beam goes from one material to another in a similar fashion to that shown in Figure 5.3-2. To avoid complications from nonuniformity of dose and to provide accurate dosimetry, exposures should be performed under conditions of electron equilibrium. Unless electron equilibrium is established correctly in the radiation source, a foil of approximately the correct Z and an electron range thickness should be interposed in front of the target. The same rule applies to the cases of dosimeters.

Dosimeters for use in TREE testing should be calibrated in known spectra to read rads (dosimetry material). Small dosimeters typically read rads (wall material), although for a given spectrum, they may be calibrated to read out in other kinds of rads. This is true of active (say PIN) as well as passive dosimeters, when the dosimeter is too small to establish its own charged-particle-equilibrium in the photon flux. See Methods E666 and E668 of Reference 3 for calculating the absorbed dose.

If nonconducting dosimetry materials or test articles are exposed to intense electron beams characteristic of flash X-ray machines, the effect of the potential buildup in the sample must be evaluated in calculating the actual dose. Method 665 of Reference 3 specifies the procedure for calculating the absorbed dose of materials exposed in a flash X-ray machine, and Method E820 of Reference 3 specifies the procedure for determining absorbed dose rates using electron beams.

5.3.2 Radio-Photoluminescent (RPL) Devices

In RPL devices, irradiation produces stable fluorescence centers that may be stimulated by subsequent ultraviolet illumination to emit visible light. The total light emission is a measure of the absorbed dose in the RPL material (if in electron equilibrium) that was previously exposed.

An example of an RPL dosimeter is a silver metaphosphate glass rod or plate system. These dosimeters can also be used with special energy shields that sufficiently suppress the low-energy response of the high-Z silver by absorption so that the total response is essentially independent of energy, yielding a reading proportional only to exposure (photon fluence) for photon spectra of energy 100 keV < E < 5 MeV. By knowing the total fluence and the spectral shape, Equation 5-1 can be evaluated to determine the dose to any other material. With a thinner shield matching the average Z of the glass, it would measure dose in the glass.

Glass rods should be cleaned and read before irradiation for expected dose <100 rads (glass). They should not be routinely reused. If absolutely necessary, annealing is possible using procedures documented in the literature. Extreme care should be taken to avoid glass-rod chipping. Some fading of glass rods may occur, especially when the rods are subjected to prolonged exposure to ultraviolet light. For accuracy in reading, the system should be calibrated and used by reading rods 24 to 48 hours after exposure.

For high-energy electron-beam dosimetry, the rods should be used directly on or in the test setup without shields; then, the local absorbed dose is measured in rads (glass).

5.3.3 Optical Density Devices

In optical density devices, radiation produces stable color centers that absorb light. Measurements of the optical transmission, usually at a fixed wavelength, can be related to the dose in the active material.

An example of an optical-transmissivity-change dosimeter is a cobalt-glass-chip system. At doses greater than 10^6 rads, saturation is approached and the readings can become very inaccurate. Both an energy-compensation shield and a thermal neutron shield are required when using cobalt-glass chips in a nuclear reactor environment. A bismuth-lead-borate glass also has been developed as a high-level gamma dosimeter for use in mixed gamma-neutron environments.

Other materials used as colorimetric dosimeters include dyed plastics such as blue cellophane, cinemoid films, etc. These should be used within their accurate range ($\sim 10^6$ rads) and corrections may be required at high dose rates. Before using a particular dosimetry system, the rate and environment effects that may be characteristic of the particular system should be determined.

Table 5.3-1 presents the characteristics of some commonly used RPL and optical density devices.

Table 5.3-1. Characteristics of some RPL and optical density devices (Reference 20).

Dosimeter	Range (rads)	Accuracy (percent)	Rate Dependence (rads/s)	Fast-Neutron Response (rads/n-cm^2)
High Z, silver phosphate rods	10^1 to 2×10^4	±10	None to 10^9	$<3 \times 10^{-10}$
Low Z, silver phosphate rods	10^1 to 2×10^4	~±10	None to 10^9	$\sim 6 \times 10^{-9}$
Cobalt glass	10^4 to 4×10^6	±10	None to 10^9	$<3 \times 10^{-10}$
Bismuth glass	10^6 to 10^{10}	±10		Negative

5.3.4 Thermoluminescent Devices (TLDs)

TLD irradiation produces metastable centers that can be induced to emit light by heating. The amount of light is related to the dose in the TLD material. A TLD system consists of the TLDs, the equipment used for preparation of the TLDs, and the TLD reader. Method E668 of Reference 3 describes the procedures for the use of TLDs to determine absorbed ionizing dose in a material.

A commonly used TLD dosimetry system uses manganese doped calcium fluoride (CaF_2:Mn) with a readout unit that heats the exposed material and registers the area under the luminescent peak. The reading procedures are described by Method E668. For low absorbed-dose measurements (<100 rad), dry nitrogen should be flowed through the heating pan area of the reader during readout. TLDs can be annealed and reused. Careful control of the annealing cycle and handling of the TLDs is required to obtain the best dose measurement response. Periodic retesting of the TLDs is necessary to maintain accuracy of the dosimetry system.

Each batch of TLDs should be characterized by the user using the particular reader for the TLD system involved before use in a specific radiation environment. Factors to be considered include the uniformity of TLD response within a batch; reproducibility of individual reusable dosimeter response; and dependence of TLD response on absorbed-dose rate, energy, direction of incident radiation, times between preparation and irradiation, time between irradiation and readout, storage or irradiation temperature, and humidity (see Method E668 of Reference 3).

The TLD reader should be checked regularly for proper operation of the phototubes and heating units. A regular calibration should be made with a Co-60 or other standard source and a log kept to show trends. TLD system manufacturers' recommendations for care of the reader should be followed. To check heating rates and to allow for examination of the entire glow curve, the readout units should be provided with outputs for strip-chart recording of temperature and light output.

The encapsulating material surrounding the TLD material should be thick enough to establish electron equilibrium and should have radiation absorption properties similar to the material in which the absorbed dose is to be determined. TLD materials can be obtained in several forms and chemical compositions. Examples include powders, forms that are extruded, encapsulations in Teflon, etc. Doped calcium fluoride TLDs are commonly available in the form of reusable solid chips.

CaF_2:Mn chips have some significant advantages over some other types and forms of TLDs. The advantages include radiation absorption characteristics similar to silicon, a simple annealing procedure (compared to LiF), ease of handling compared to powders, and a relatively linear absorbed-dose response. A disadvantage in using CaF_2:Mn TLDs is a moderate fading of the TLD response after radiation.

5.3.5 Thin Calorimeters

A thin calorimeter determines the dose by measuring the temperature rise in a small sample of known material. Converting the temperature rise to energy deposition (dose) by the material's specific heat results in a direct determination of the average dose in the sample. If the sample is thin so that it absorbs a negligible fraction of the incident radiation,

and the incident beam is in electron equilibrium for the calorimeter material, the temperature rise is independent of thickness.

The three important elements of a thin calorimeter are the absorber, the temperature sensor, and the thermal isolation. The absorber can be any material, preferably one that has approximately the correct atomic number for the effect being studied and is also a good thermal conductor to assure rapid thermal equilibrium. Metal foils (Be, Al, Fe, Cu, Ag, Pt, Au) have been used successfully as well as thin semiconductor chips (Si, Ge).

The temperature sensor should represent a small perturbation on the absorber. A thermocouple satisfies this criterion well, particularly if it almost matches the atomic number of the absorber. A small copper-constantan thermocouple on a copper foil is a good example. A more sensitive calorimeter results from using a small thermistor as both absorber and temperature sensor. A chemical analysis of the thermistor can establish its effective atomic number, and a calibration against a known material is required to establish the combination of specific heat and temperature coefficient. Care must be taken in assembly to minimize the amount of solder used in attaching leads because this may enhance the amount of higher Z material. Resistance welding can be used to eliminate this problem. If the thermistor is not thin to the radiation, the temperature measurement must be performed for a long enough time to ensure that thermal equilibrium is established within the thermistor (0.1 to 1 second).

In order to accurately measure a small, sudden temperature rise, some degree of thermal isolation is required. The leads to the temperature sensor should be small wire (~3 mils). For single pulse measurements, a block of styrofoam provides good isolation, but the heat lost to the inside layer of styrofoam requires a small correction, particularly for very thin calorimeters. Use of the calorimeter in vacuum also provides excellent isolation. For accurate measurements, especially on a short string of LINAC pulses, the absorber can be suspended in a small evacuated can with water-cooled constant-temperature walls and a thin window for beam entrance. The detailed design depends on the radiation beam being measured and the accuracy requirements. The design may have to take into account scattering from the walls of the chamber. Method F526 of Reference 3 specifies a calorimetric measurement procedure for determining the dose in a single pulse from a LINAC.

For single pulses typical of flash X-ray machines, a cooling curve should be established and exponentially extrapolated to zero time to determine the temperature at the time of the burst.

The response of the calorimeter is calibrated by the specific heat of the absorber and the temperature calibration of the sensor. In electron-beam measurements, if the calorimeter material is the same as the experimental material being tested, the absorbed dose in the experimental

material can be measured directly. If, however, the dose to the calorimeter must be converted to dose in another material of significantly different atomic number, corrections must be made for differences in dE/dX, backscattering, and bremsstrahlung losses.

5.3.6 PIN Detectors

A reverse-biased PIN diode (usually Si) collects charges produced by ionization in the intrinsic semiconductor region. Its calibration is based on the known efficiency for producing electron-hole pairs (3.7 eV/pair in Si) and the active volume of the junction region. The charge collection time is short (on the order of nanoseconds) and, therefore, a PIN diode can be used to measure not only the dose in the semiconductor but also the shape of the radiation pulse (dose rate (Si) versus time). The detector should only be used at low enough dose rates where the linearity is established. At high dose rates ($\sim 10^9$ rads (Si)/s), the internal electric field is modified by the high currents and the output becomes nonlinear. For this and other reasons, a PIN detector is normally limited to dose rates of less than 10^{10} rads (Si)/s. A PIN detector will not correctly measure the dose unless electron equilibrium in the silicon active volume has been established. Many standard commercial detectors can derive measurable portions of their signal from the high Z case or from their tantalum plate contacts. It is possible to obtain degenerate silicon contacts to which the leads are attached or detectors with very thin contacts so that they may be placed in electron equilibrium through the introduction of additional silicon (or aluminum foils). It must be determined if the addition of inactive material to create electron equilibrium for the most energetic portion of a disturbed spectrum has attenuated the low-energy portion of the spectrum and a suitable correction should be made to determine the dose to a thin silicon sample.

PIN diodes, like other semiconductor devices, are subject to degradation due to displacement damage. The damage causes a decrease in the intrinsic silicon lifetime and resistivity resulting in an increase in leakage current. Neutron fluences of $>10^{12}$ n/cm^2 (E > 10 keV, fission) are sufficient to change the calibration of a silicon PIN diode. PIN devices may also be damaged by high-energy gamma dose-induced displacement damage at above 10^4 to 10^5 total rads of such dose. In general, as long as the minority carrier lifetime is much longer (10×) than the collection time, the device will operate satisfactorily.

PIN diodes can also be damaged by high current for long pulses of electrons or photons or by repetitive pulses. Because of the possibility of damage, they should be calibrated routinely and checked by a well-calibrated passive system.

5.3.7 Compton Diode and SEMIRAD

Compton diodes and SEMIRADS are based on the charge transfer of electrons between materials under irradiation. The calibration depends on the spectrum and is not uniquely related to dose in any material, except for a limited range of spectra. The time resolution is excellent and such devices are very useful as pulse-shape monitors at high dose rates. For very high dose rates, Compton diodes are recommended since SEMIRADS will undergo space charge saturation.

5.3.8 Scintillator-Photodiode Detectors

Various organic scintillators having both fast response and a large linear range are available for measurements of ionizing dose rate versus time. Examples are plastics such as Pilot B and NE102 and organic liquids such as NE211 and NE226 which have 2- to 3-nanosecond resolution. At high dose rates, the emitted light is intense so that the photodiode needs to be designed so as to avoid space charge limitation. An FW114 is frequently used with adequate bias voltage to avoid saturation. This combination measures energy deposition in the scintillator, i.e., rads (scintillator). Organic scintillators have been shown to have nonlinear characteristics at high rates ($\sim 10^{11}$ rads/s) and should not be used at rates above this value.

5.3.9 Faraday Cup

A Faraday cup can be used for electron-fluence measurements. The measurements are convertible to rads (Z) entrance-dose units in a material to be inserted in the beam if the incident electron energy is known. Values of electron energy loss rate, dE/dx, are given in Reference 21. When using a Faraday cup to monitor an electron beam, a guard voltage should be applied and a reentrant cup used with a low-Z stopping material, backed up with a higher Z shield material. The incident beam must be collimated and accompanying secondary electrons must be swept out by a magnetic analyzer. For accurate work, the whole cup should be placed in a vacuum. For fast pulsed electron-beam work, if the pulse shape is to be determined, a coaxial cup design matched to the cable impedance may be desirable.

The accuracy of the Faraday cup technique is good enough to warrant its use as a calibration tool. The much greater convenience of a simple, but less accurate, low-Z stopping block current collector also makes this a useful tool in LINAC dosimetry.

5.3.10 Spectrum Monitoring

For TREE facilities, the spectral information accuracy requirements rarely justify detailed photon spectrum measurements. Simpler techniques based on a knowledge of the general source characteristics and some absorption measurements, along with any spectral information provided by the facility operators, are usually adequate.

A combination of dosimeters having different atomic numbers and shielding is recommended for spectral monitoring of the TREE environments; for example, high- and low-Z bare glass rods, or LiF and $CaF_2(Mn)$ in plastic and aluminum container pairs, respectively, to read rads (low Z) and rads (high Z). The dose ratio is a measure of the spectral quality, not of the spectral details. If the ratio is appreciably different from 1.0, the spectrum may contain either low-energy components (<200 keV--a very soft spectrum) or very high energy components (>5 MeV). If there is some doubt considering the source, this point should be checked by measuring the broad-beam absorption curve or first and second half-value layers (HVL) in Al or Cu and comparing it with that for Co-60 (first HVL = 17 g/cm^2 Al or 9 g/cm^2 Cu).

Normally, detailed spectral information is not needed for routine TREE work since the area of interest in gamma-ray effect simulation is the depth-dose distribution and sometimes the linear energy transfer, the absorption coefficients for semiconductors and most insulator materials do not vary much for photon energies in the range 200 keV to 10 MeV, and most useful TREE sources have energies within this range. Gamma-ray simulation facilities should have enough spectral information to be able to convert dose measurements in the dosimetry materials used to absorbed dose in all materials; that is, to approximately evaluate the equations given in Section 5.1.

5.4 PULSE SHAPE MONITORING

It is usually desirable to monitor the radiation pulse shape with a sensor that monitors a quantity proportional to the radiation intensity, but that must be calibrated in terms of the required dosimetry quantity at the sample position. The primary requirements for such a monitor are adequate time resolution, linearity, and proportionability to an appropriate dosimetry quantity. This last requirement can be met most easily if the radiation spectrum is independent of time during the pulse.

Examples of such monitoring measurements are:

1. Tube current measured in flash X-rays (not recommended because the beam energy is time dependent)
2. Current of LINAC electron beam measured with current transformer or secondary emission foil (excellent if beam is energy analyzed and collimated)
3. Peripheral radiation intensity measured with PIN, Compton diode, scintillator, or SEMIRAD (measurement may be sensitive to time-dependent spectrum in flash X-ray and calibration may be affected by scattering from the target)
4. Reactor power pulse monitored with a neutron-sensitive ion chamber (excellent for neutrons, but not good for gammas because of delayed gamma tail)

5. Reactor gamma pulse monitoring with a neutron-insensitive ion chamber.

5.5 RECOMMENDED ENVIRONMENT MEASUREMENTS AND PROCEDURES

It is a recommended practice to provide for routine monitoring of simulation facility dosimetry and environmental measurements whenever possible. This is to ensure that the test data do not become worthless because of failure or loss of the dosimetry services provided by the facility. The monitoring should include at least some of the following procedures:

1. Expose passive dosimeters (or foils) from the simulation facility in a local isotope (Co-60), or other source, along with locally calibrated and read dosimeters (or foils). The facility should then read out its own dosimeters (or foils), and a comparison should be made between the local dose (or fluence) measurements and those of the facility. This process should be extended to cover different types of dosimeters to avoid systematic errors. The principle of this recommendation applies to both gamma-ray doses and neutron exposures.

2. Place passive dosimeters in and on the critical test articles as a check on the facility dosimetry. These dosimeters can be read out later when convenient, presuming that facility dosimetry results are immediately available. When reading dosimeters later, any necessary corrections for fading should be made.

3. Use a calibrated active dosimeter that can be read out along with other signals. This step may be necessary if the simulation facility does not provide immediate dosimetry results.

4. Make an estimate of the perturbation of the free-field spectrum caused by the presence of the test article and the effect of this perturbation on the results of the environment correlation.

It is the responsibility of the test engineer, not the facility operations staff, to determine the adequacy of the radiation measurements made in support of his test. The test engineer should hire an outside dosimetry service if he does not have such services available in-house.

5.5.1 Flash X-Ray Dosimetry

When irradiating circuits or subsystems at flash X-ray facilities, it is recommended that every necessary dose point be monitored by passive

dosimetry on every shot. This is because of the shot-to-shot variations in exposure and in beam position.

It is recommended that high- and low-Z dosimetry pairs be exposed at least occasionally to check beam quality. Also, dosimeters should be used on front, sides, and back of large experiments to check on exposure uniformity and on beam structure and location. If dose to a component or material not in electron equilibrium is needed, the exact configuration should be mocked up with dosimetry material in place of the component and measurements should be made to determine the effect of the nonequilibrium.

For pulse shape and machine diagnostics, active dosimetry should include at least one of the following three diodes:

1. A calibrated scintillator photodiode. A fast scintillant should be used and a high enough voltage applied to the diode so that at expected dose rates, all current is collected to avoid space-charge limitations. If this cannot be done by any other means, the active dosimeter should be moved back from the target to reduce the expected dose rate.

2. A calibrated PIN diode. A high enough voltage should be applied to assure that the PIN diode response is linear, and the load circuit should be arranged so that the detector voltage is not reduced during the pulse to too low a value. Otherwise, the detector should be moved to a lower dose rate position. A possible high-dose circuit involves shorting the output through a current transformer; another involves a low value of load resistance.

3. A calibrated SEMIRAD or Compton diode. If operated actively in the high-exposure rate part of the beam, a gamma-ray SEMIRAD with adequate applied voltage to preclude space-charge limitations or Compton diode may be used.

Active measurements at any TREE facility must be well shielded against RF noise. Cable effects on signal shapes must be evaluated and ground loops must be eliminated (see Section 2.5). Electron-beam dosimetry should be done with a calorimeter if possible. Extreme care must be exercised to assure that samples, dosimeters, etc. are properly grounded so that the potential buildup in the sample does not affect the manner in which energy is deposited.

5.5.2 LINAC Dosimetry

For bremsstrahlung work, the precautions and dosimetry measurements at a LINAC facility are similar to those at a high-energy flash X-ray facility, except that the pulse-to-pulse variability may be much less, and the

spectrum is constant during the pulse if the beam is magnetically analyzed. The collimated electron beam should be monitored on each pulse, preferably with a secondary emission detector or current transformer. This monitor can be calibrated against dose at the sample position using passive dosimeters or a thin calorimeter. Monitoring the beam with a PIN or scintillator detector is not recommended because the direct beam is frequently not available and the peripheral beam is affected by scattering from the target.

For electron-beam work, dosimeters such as RPL glass rods, cobalt glass chips, LiF, or CaF_2 may be calibrated and used without shields to measure the absorbed dose in rads (dosimeter).

If the LINAC beam is not magnetically analyzed and collimated, its energy may change during the pulse, and the bremsstrahlung exposure pulse shape will not be the same as the beam current pulse shape. Also, the pulse observed behind the attenuating or scattering material may be different from the beam current pulse.

5.5.3 Nuclear Reactor Dosimetry

The neutron flux and spectrum at a reactor facility (either bare critical assembly or thermal reactor) depend on the rate of fission in the reactor and the absorbing/scattering geometry. Therefore, the exposure geometry, including absorbers, scatterers, fuel element locations, etc., should be controlled and calibrated. For each exposure geometry (with the test setup in place), a set of threshold foils should be exposed to determine the spectrum shape. Then, for each irradiation, a single foil type should be used to monitor the fluence and its uniformity over the irradiated item. Foil sets should be selected from those listed in Method E720 of Reference 3.

In addition to the neutron fluence measurements, gamma-ray dose determinations should be made to check the n/γ ratio to know what ionizing exposures were given. Any of the passive detectors may be used and should be corrected for neutron dose. A gamma-sensitive SEMIRAD may be used in a fission (but not a fusion) neutron spectrum for an active gamma-ray (dose rate) measurement. Also, for fission reactor work only, an active separation of neutrons and gamma rays is possible using neutron- and gamma-sensitive scintillator photodiodes, if the n/γ ratio is above 10^9 $n/cm^2/\gamma$ rad. The neutron absorbed dose in a material can be calculated using Method E763 of Reference 3; for the gamma absorbed dose, use Method E666.

5.5.4 Selective Shielding

A radiation spectrum may contain components that are undesirable for a particular test. To induce changes in the radiation spectrum, the test article is usually protected by materials that selectively attenuate the undesirable radiation. Although such absorbers have a major effect on a

particular component of the radiation spectrum, it must be remembered that they do affect all components of the radiation, in some cases enhancing one component while removing another.

5.5.4.1 Nuclear Reactor Radiations

Nuclear reactors produce three primary classifications of radiation of concern to TREE--thermal neutrons, fast neutrons, and gamma rays. A reactor does not always produce these radiations in the ratio that is most desirable for a particular test. The alternative is to screen out undesirable portions of the radiation and enhance the desirable.

Thermal neutron shielding limits the formation of undesirable radioisotopes in the test materials. Such induced radioactivity increases the time required for a test setup to cool down to the point where it can be safely handled. In addition, protection of fast neutron foil detectors from thermal neutrons is necessary to minimize competing activation reactions and burnout of reaction products. Materials commonly used for this purpose are boron-10 in the form of Boral (boron carbide and aluminum) or cadmium. The most frequently used thermal neutron shield is cadmium foil, which is typically 0.040-inch thick. Cadmium has the disadvantage that the absorption of thermal neutrons is accompanied by the emission of high-energy gamma rays, adding to the gamma-ray flux.

Fast neutrons are removed from the radiation spectrum by slowing them down to thermal energies, that is, by degrading their energy through multiple collisions with other nuclei until their speeds are comparable to those of the thermal motion of the nuclei of the material. The lower the atomic number of the shielding material, the more efficient the material is in slowing the speed of fast neutrons. Materials such as water, graphite, paraffin, and polyethlene are used for this purpose. A rough rule of thumb is that 1 foot of water reduces fast neutron flux by two orders of magnitude.

The efficiency with which materials absorb gamma rays increases with increasing atomic number and decreases with increasing energy of the gamma ray. For this reason, materials such as lead are used to reduce the gamma-ray flux. The attenuation of gamma rays is also an exponential function of the thickness of the absorbing material. Typically, 4 inches of lead is required to obtain an order of magnitude decrease in the gamma-ray flux in a reactor.

The measure of the quality of the radiation mixture usually used in TREE work is the ratio of the fast neutron flux (in $n/(cm^2 \cdot s)$ ($E > 10$ keV)) to the gamma-ray dose rate (in rads (Si)/s)--the n/γ ratio. In permanent radiation-damage studies, it is usually desirable to maximize the value of this quantity and thus minimize ionization and surface effects. The n/γ ratio can be enhanced by shielding the experiment with lead or

another high-atomic-number material. Normally, alterations of the n/γ ratio are handled by operators of the reactor.

Placing any materials in or near a reactor can seriously affect the performance of the reactor. Check with the facility technical staff when planning a test to make sure that the materials and techniques to be used are acceptable and to determine what selective shielding may be necessary to produce the desired effects.

5.5.4.2 Spectral Filtering

Low-energy photons are attenuated in the case and packaging materials of test samples and burst detectors. This means that the spectrum at the exterior surface of a device may be somewhat different than that in the interior where the active region of the device is located (and where the photocurrents of interest are generated). This alters the relation between the dosimeter dose and the true test sample dose. Also, for a group of similar test samples exposed to the same external (to the case) environment, the differences in case thickness, material, orientation, potting, etc. would lead to an additional measure of disparity in the devices' responses that would not be present in a "harder" (fewer low-energy photons) spectrum such as that of a weapon. Further, the drastic increases in mass-energy absorption coefficients at low energies make it all the more critical that the spectrum be known in the low-energy area, although such information is seldom available.

The problem can be minimized if filters (thin metal sheets) are used to substantially reduce the low-energy photon content of a source spectrum. The problem is greatest at flash X-ray sources, the worst case being the low-energy (300-kVp) machines.

For 600-kVp and higher energy flash X-ray machines, it is recommended that the spectra be cut off at the lower limit to about 60 keV by using a low atomic number (Z) filter or a combination of high- and low-Z materials. A cut-off energy of 30 to 40 keV is more practical for 300- and 400-kVp machines since filtering is an attenuation process and to filter to energies much above 40 keV would reduce the maximum dose rate available from the low-energy machines to a practically unusable value. The filter should be interposed between the source and the sample, preferably right next to the source tube.

In reporting test results, the composition, thickness, and positional sequence with respect to the source should be given for all filtering materials.

5.6 CALIBRATION

Calibration procedures are not discussed in detail in this document. However, the test engineer should adhere to at least the following principles:

1. Neutron foil calibrations can be based on known cross sections, masses of foils, and counting efficiencies calibrated with radioactive standards, or they can be related to exposures of foils to calibrated radiation sources. In either case, the calibration should be related to an NBS standard.

2. Gamma dose calibrations can be related to a standardized Co-60 source or to accurately known quantities such as specific heat of a pure material and thermoelectric voltage of a calibrated thermocouple wire. Since TREE exposures are frequently at high dose rates, the linear range of the dosimeter must be demonstrated up to the dose rates used or else known corrections must be applied. Total dose calibrations based on Co-60 and/or calorimetry, together with linear pulse shape monitors, are recommended. The test engineer is referred to NBS for greater detail in calibration procedures.

5.7 REPORTING AND DOCUMENTATION OF RESULTS

Documentation of TREE dosimetry should be such that the measurements can be repeated and the environmental description can be applied to another effect with possibly a different energy dependence to make a response prediction. This implies that the reporting should specify both what was actually measured and also any assumptions made in data processing.

A frequent omission in reporting is that of adequately describing the characteristics of the radiation facilities used for the test. Lack of this data prevents the reader from correlating the reported radiation effects with test results reported by others. All reported test results should include as a minimum the following types of facility characteristics:

1. Identify the facility and where it is located
2. Specify energy levels for the radiation source
3. Specify pulse widths used, when appropriate
4. Specify distances from energy sources to irradiated samples
5. Specify any special shields and reason for use.

5.7.1 Neutron Environments

A neutron environment causes both displacement damage and ionization effects. Therefore, it is important to measure and report environmental parameters such as fluence and spectrum rather than simply an effect parameter such as gain change in a transistor. It is recommended that the field

parameters of integral fluence be reported with units of n/cm^2 having energies over the thresholds of the foils used, along with other pertinent data concerning the source and the measurement. The recommended basic reporting units are "n/cm^2 (E > threshold energies for the foils used, source spectrum)," or "n/cm^2 (E > 10 keV, foil used; foil/Pu ratio assumed, source spectrum)," or "n/cm^2 (E > any energy, unfold code and foils used)." Differential fluence should be reported as a function of energy with units, $n/(cm^2 \cdot MeV)$ including specifications as to unfold technique and foils used.

Neutron fluence and spectral measurements are often made with foil activation techniques. Also, the environment measurements obtained are often used to calculate an equivalent monoenergetic neutron fluence (Method E722 of Reference 3). The reported data should contain at least the following information:

1. Semiconductor device performance parameter (for example, current gain) degradation being correlated to silicon displacement kerma should be specified.
2. Neutron source as to type and mode of operation during the tests (fast pulse or steady state).
3. Neutron energy-fluence spectrum and how it was determined (Method E721 of Reference 3).
4. Monitor foil employed and the detector system used for counting the foil. If an effective fission cross section for the monitor foil is used, its value should be stated (Method E720 of Reference 3).
5. The displacement portion of the kerma function for silicon should be given or referenced (Method E722 of Reference 3).
6. The method used for determining the average value of the displacement kerma factor ($K_D E_o$) at the specified equivalent energy, E_o, and the value of E_o selected.
7. The method used for evaluating the integrals

$$\phi_{eq}(E_o) = \frac{\int_{E_{min}}^{E_{max}} \phi(E)\ K_D(E)\ dE}{K_D(E_o)}$$

and

$$\phi_{eq}(E_o)/\phi = \frac{\int_{E_{min}}^{E_{max}} \phi(E)\, K_D(E)\, dE}{K_D(E_o) \int_{E_{min}}^{E_{max}} \phi(E)\, dE}$$

where

$\varphi(E)$ = incident neutron energy-fluence spectral distribution

$K_D(E)$ = neutron displacement kerma factor (displacement kerma per unit fluence) as a function of energy

$K_D(E_o)$ = displacement kerma factor at the specified equivalent energy E_o

ϕ_{eq} = the equivalent monoenergetic neutron fluence

$\phi_{eq}(E_o)/\phi$ = the neutron energy spectrum hardness parameter.

The energy limits on the integral are determined by the incident energy spectrum and by the material being irradiated.

8. The values of $\phi_{eq}(E_o)$, $\phi_{eq}(E_o)/\phi$, and $\phi_{eq}(E_o)/M_r$ where $\phi_{eq}(E_o)/M_r$ = the equivalent monoenergetic neutron fluence per unit monitor response, M_r.

Method 722 of Reference 3 gives details of the procedure.

The designer is responsible for validating the operation of his system, so he must correlate the component response data, the test environment data, and the specified threat environment information. He should use an effects curve for the desired effect (displacement or ionization) to relate the effect of measured data test environment to the effect of the specified threat environment on the component or system.

The correlation of a measured environment, $\Phi_m(E)$, with a specified (and possibly degraded by penetration of material) environment, $\Phi_s(E)$, for an effect with energy dependence $\sigma(E)$ follows:

Effect of test environment = $\int \sigma(E)\Phi_m(E)dE$

Effect of specified environment = $\int \sigma(E)\Phi_s(E)dE$.

Comparison of these effects gives the designer information he needs.

5.7.2 Photon and Electron Environments

As discussed in Section 5.3.11, TREE tests in photon environments are generally even less dependent than neutrons upon the need for high-resolution spectral data, but any spectrum information available about the source should be reported. For ionization effects tests, units of rads (material) or rads (material)/s should be used and the method used for obtaining these numbers should be reported.

Reports of photon and electron radiation-hardness testing of electronic devices should include full descriptions of the information illustrated by the following list for TLD dosimetry:

1. The TLD system employed, including the type and physical form of the TLDs, the type of TLD reader, and the annealing procedure used, if any.
2. The results of all performance tests carried out or reference to relevant published studies of the TLD system. As a minimum, such test results should include the sample size, the mean value of the sample responses, the absorbed-dose level, and the standard deviation of the sample response distribution.
3. A description of the procedure for calibrating the absorbed-dose response of the TLD system, including the radiation source type, irradiating geometry, and conditions (for example, absorbed-dose level, absorbed-dose rate, and equilibrium material).
4. A description of the radiation-hardness-test irradiations, including radiation source type, geometry, and conditions (for example, absorbed-dose level, absorbed-dose rate, and equilibrium material), as well as any useful supplemental data (for example, energy spectra).
5. A description of the conversion of TLD response to absorbed dose in the material of interest, including calibration factors, correction factors, and absorbed-dose conversion factors. The absorbed-dose conversion factors would include information such as the radiation absorption characteristics of the material of interest and assumptions or data about the source energy spectrum.
6. An estimate of the overall uncertainty of the results as well as an error analysis of the factors contributing to the random and systematic uncertainties (for an example, see Method E668 of Reference 3).

For other types of dosimeters, the corresponding information should be recorded (Methods E665, E666, and E668 of Reference 3).

CHAPTER 6

TEST PROCEDURES FOR DIODES AND TRANSISTORS

6.1 PERMANENT-DEGRADATION MEASUREMENTS

6.1.1 Scope

This section deals with test procedures for determining the permanent degradation of specific parameters of conventional discrete bipolar transistors, MOS and junction field-effect transistors, semiconductor diodes, and Zener diodes. The procedures outlined are intended for use in mixed neutron-gamma or gamma radiation environments. The recommended procedures that follow have been found to be valid for neutron fluences up to 10^{15} n/cm^2 (E > 10 keV, fission) and gamma doses up to 10^8 rads (Si).

6.1.2 Bulk and Surface Effects

Permanent effects of a mixed neutron-gamma field can be grouped into bulk and surface damage. Carrier-removal and lifetime damage caused by radiation-induced lattice displacements are important categories of bulk damage and are important failure mechanisms in diodes, bipolar transistors, and junction field-effect devices. The buildup of surface charge and the creation of new interface states are important surface effects and are the primary failure mechanisms in MOS transistors. Surface effects also cause device failures in diodes, bipolar transistors, and junction field-effect devices. For example, the low-current transistor gain degradation due to surface effects can be a significant portion of the total gain degradation in a mixed neutron-gamma environment. Damage to semiconductor devices exposed to gamma radiation is primarily due to surface effects. High energy gamma radiation also introduces bulk damage similar to neutron damage at high doses ($>10^6$ rads (Si)). In any particular test, the effects of both bulk and surface damage must be considered. For example, the total current gain degradation of a transistor can be expressed as

$$\left(\Delta \frac{1}{h_{FE}}\right)_{Total} = \left(\Delta \frac{1}{h_{FE}}\right)_{Bulk} + \left(\Delta \frac{1}{h_{FE}}\right)_{Surface} . \qquad (6\text{-}1)$$

Similar expressions can be written for the other parameter changes. Table 6.1-1 shows the relationship between the radiation effects and the important device parameters.

In cases where both bulk and surface damage are expected to be important, tests should be conducted in both mixed neutron-gamma (high n/γ) and pure gamma environments and the effects of bulk and surface damage analytically separated. In cases where bulk damage is the predominant

Table 6.1-1. Permanent effects of radiation on device parameters.

Phenomenon		Junction Diodes	Bipolar Transistors	MOS Field Effect Transistors	Junction Field-Effect Transistors
Bulk effects	Lifetime damage	Reverse-current increase Decrease in switching time Increase in forward voltage (PIN diodes)	h_{FE} decrease at all current levels Reverse-current increase Decrease in switching time	Reverse-current increase	Reverse-current increase
	Carrier removal	Increase in forward voltage Breakdown-voltage change (Zener)	Increase in $V_{CE(SAT)}$, $V_{BE(SAT)}$ h_{FE} decrease at high current levels	I_{DSS}, g_m decrease Threshold-voltage change	I_{DSS}, g_m decrease Change in pinch-off voltage Noise figure increase
Surface effects	Space charge	Reverse-current increase Breakdown-voltage change	h_{FE} decrease at low current levels Reverse-current increase Breakdown-voltage change	Threshold-voltage change Reverse-current increase Breakdown-voltage change	Reverse-current increase Breakdown-voltage change
	Interface states	Reverse-current increase	h_{FE} decrease at low current levels Reverse-current increase	g_m decrease Threshold-voltage change Reverse-current increase	Reverse-current increase Noise-figure increase

effect, a neutron (high n/γ) environment should be used. In cases where surface damage is the predominant effect, a pure gamma environment should be used.

There are also analytical techniques for predicting radiation-induced damage in semiconductor devices. These may be useful for:

1. Estimates of parameter degradation for test planning
2. Design data
3. Developing additional data when testing must be limited.

Analytical techniques for predicting radiation response of semiconductor devices are discussed in References 1, 22, and 23.

6.1.3 Annealing

The radiation-induced parameter changes in semiconductor devices exhibit annealing that is a function of temperature, time, and operating conditions during both irradiation and measurement. Both bulk and surface damage in semiconductor devices can be significantly annealed by injecting carriers during irradiation or measurement or by raising the temperature of the device.

The prompt annealing process, as measured by device parameter changes as a function of time, is termed "rapid" or "transient" annealing. This process is most dramatically evidenced by an initial reduction in transistor current gain followed by a partial recovery, all within a small fraction of a second. The initial reduction in gain can be equivalent to that associated with a fluence many times as large as that actually measured. To measure rapid-annealing effects, it is necessary to irradiate the device with a neutron pulse short compared with the earliest time of interest and to operate the device actively during and after irradiation. A pulsed reactor can best be used for this type of test. Surface damage introduced by ionizing radiation can also undergo rapid annealing. Semiconductor devices exhibit an additional recovery trend along a scale of hours or days following irradiation. This is termed long-term annealing and is a definite function of temperature, whereas rapid annealing is usually considered complete within about 1,000 seconds after irradiation.

Since radiation damage is subject to annealing, it is important to keep accurate records of time, temperature, and operating conditions during and after irradiation.

6.1.4 Radiation-Source Considerations

Radiation sources normally used to determine the permanent radiation damage of semiconductor devices include pulsed nuclear reactors, steady-state nuclear reactors, and low-dose-rate gamma sources. Other sources of

neutrons such as fast-neutron generators, van de graaff machines, linear accelerators (LINACs), and synchrotrons are sometimes used in radiation-effects studies. Radiation-source considerations are discussed in Chapter 4; dosimetry techniques are discussed in Chapter 5.

6.1.5 Parameters to be Discussed

The important device parameters discussed in this document are summarized for bipolar transistors and diodes in Table 6.1-2 and for field-effect devices in Table 6.1-3. Readily achievable measurement accuracies and the relative importance of each parameter for some device categories are also given (also see Reference 4). The degree of device characterization will depend on the actual data requirements for a particular application. Selection of parameters to be measured, the number of times a parameter is measured, and the accuracies required must be based upon the requirements of the test and the specific circuit application of the device.

Table 6.1-2. Bipolar-transistor and diode parameter requirements--permanent degradation.

Device Category	Important Parameters and Readily Achievable Measurement Accuracy[a]								
	h_{FE} h_{fe} ±5%	$V_{CE(sat)}$ $V_{BE(sat)}$ ±5%	I_{CBO} I_{EBO} ±5%(b)	V_{BE} ±2%	t_r t_s t_f ±10%	V_z ±5%	I_R ±5%	t_{rr} ±10%	V_z ±0.1%
Power transistors	(1)	(2)	(3)	(4)					
Switching transistors	(1)	(2)	(4)	(5)	(3)				
Linear transistors	(1)	(2)	(3)	(4)	(5)				
Matched-pair transistors	(2)	(4)	(3)	(1)					
Switching diodes and rectifiers						(1)	(2)	(3)	
Reference diodes						(2)			(1)

(a) Numbers in parentheses indicate relative parameter priority.
(b) Function of the magnitude of the currents.

Table 6.1-3. Field-effect-transistor parameter requirements--permanent degradation.

Device Category	Important Parameters and Readily Achievable Measurement Accuracy(a)				
	g_m ±5%	I_{DSS} $I_{DS(ON)}$ ±5%	V_T ±5%	I_{GSS} $I_{DS(OFF)}$ ±10%(b)	$V_{DS(ON)}$ ±5%
JFET					
Amplifier	(1)	(2)	(3)	(4)	(3)
Analog switch	(5)	(1)	(2)	(4)	(3)
MOSFET					
Digital switch	(5)	(2)	(1)	(4)	(3)
Analog	(2)	(3)	(1)	(4)	(5)

(a) Numbers in parentheses indicate relative parameter priority.
(b) Function of the magnitude of the currents.

Transistor gain-bandwidth product, f_T, or the delay time, t_d, are usually of interest in radiation-effects studies because these parameters are useful in the prediction of gain degradation and quality-assurance applications. Several methods are available to measure these parameters, including measurement of small signal gain or phase shift as a function of frequency, bridge and delay time methods, the measurement of scattering parameters, etc. The particular method selected will depend on the ultimate application of the data, the method of data interpretation, and the characteristics of the device to be tested.

Tables 6.1-2 and 6.1-3 do not include some other device parameters usually found in electrical specifications because, for most devices, changes in these parameters are seldom significant at radiation levels of interest ($\sim 10^{14}$ n/cm^2 (E > 10 keV, fission) and 10^6 rads (Si)). In addition, a number of fundamental parameters not discussed here are of interest for obtaining accurate transistor models used in computer simulation of electronic-circuit behavior. Procedures for making electrical measurements of parameters not listed in Tables 6.1-2 and 6.1-3 can be found in Reference 4 and in numerous papers in the literature.

6.1.6 Specific Test Procedures

This section describes specific preferred test procedures for measuring the parameters in Tables 6.1-2 and 6.1-3. In addition, several basic test-facility and test-design decisions not related to the measurement of a particular parameter must be made when planning for a test. These are discussed in Section 2.5.

Specific test procedures are given for pre- and post-exposure and in-situ measurements. Generally, the selection of either method is optional for permanent damage characterization of semiconductor devices. Transient annealing measurements after a neutron pulse and surface effects measurements require in-situ tests.

There are some data which should be taken that are common to all the tests discussed in this section. These are:

1. Neutron fluence, neutron spectrum, and gamma dose (or gamma dose rate) in the locale of each group of samples for each irradiation
2. The irradiation time period and the time period between irradiation and measurement
3. Ambient temperature during irradiation and measurement
4. The expected accuracy and precision of the measurements
5. Complete description of the test circuitry and equipment.

In-situ tests should also include:

1. Time history of the irradiation rates
2. Time history of irradiation-chamber temperature.

Additional information on the requirements for data reporting is given in Section 6.3.

Parametric measurements can be made using the steady-state method or the pulsed method. The simplest technique is to apply steady-state ac or dc sources to the test circuit and observe the desired response while varying one or more of the sources in discrete steps. As power dissipation increases, the junction temperatures increase rather dramatically, altering many of the parameters of the device. The pulsed method of parameter measurement minimizes changes in junction temperature and may also be used to simulate actual operating conditions for a particular circuit design. A simple and relatively fast method of obtaining many parameters is to use a curve tracer to sweep out a family of device characteristics and display them on an oscilloscope. Both steady-state and pulsed measurements can be made by this method. This method typically yields data with an uncertainty of at least 5 percent, so it is not recommended for critical design data purposes.

The choice of a particular measurement method must involve consideration of the ultimate circuit application of the device (if known), accuracy requirements, cost limitations, the number of measurements to be made, and methods of data reduction. Regardless of the particular method chosen, conditions should be identical for pre- and postirradiation measurements,

as far as possible. When a large number of measurements are planned, consideration should be given to automating the measurements and the data reduction procedure. Although such methods are not described here, the suggested measurement circuitry can be modified to allow for automated measurement schemes and machine-oriented data reduction.

The preferred techniques in the following section are based on the procedures given in References 3 and 4. The exact circuit configurations shown are suggested setups; many variations are allowable without sacrificing the ultimate worth of the data obtained. All circuit configurations are given for npn transistors and n-channel FETs. Changes that must be made for application to pnp transistors and p-channel FETs should be obvious.

Certain portions of the illustrated circuit configurations are assumed to be isolated from the radiation environment. Such isolation is either indicated by cabling for in-situ tests or is understood for preexposure/postexposure tests. Care must be taken to assure the existence of that isolation.

6.1.6.1 Transistor Current Gain, h_{FE}

h_{FE} is the common-emitter dc current gain of a transistor. It is defined as the ratio of the dc collector current (less the common emitter-leakage current, I_{CEO}) to the base current when the transistor is connected in the common-emitter configuration.

$$h_{FE} = \frac{I_C - I_{CEO}}{I_B} . \qquad (6\text{-}2)$$

Usually the leakage current is negligible compared to the base and collector currents and $h_{FE} = I_C/I_B$. Measurement of h_{FE} requires an accurate measurement of the base and collector currents at a given temperature and operating point.

h_{FE} and the rate of degradation of h_{FE} are current dependent. Therefore, unless specific requirements dictate otherwise, it is suggested that all h_{FE} measurements be made with the emitter current or the collector current maintained constant. This is normally most convenient for design and instrumentation purposes. Also, to be meaningful, h_{FE} should be measured with the transistor operating in the normal active region. The saturation-active-region boundary may be difficult to identify for high-voltage transistors, especially after neutron irradiation. h_{FE} also depends on V_{CE}, especially at operating points near the saturation region and at high current levels. If possible, for each of several values of V_{CE}, h_{FE} data should be taken at as many bias levels as are sufficient to construct h_{FE} versus I_E or I_C curves over the full operating range of the device. Since the saturation voltage increases with neutron fluence,

it may not be possible to attain the pretest operating point after irradiation. In addition, with I_C or I_E held constant, the V_{CE} for active operation increases approximately exponentially with neutron fluence such that h_{FE} measurements may be made in active and partial saturation in the same test, which greatly complicates the h_{FE} degradation model.

The value of h_{FE} after neutron irradiation will be lower than the pretest value. Therefore, with I_E or I_C constant, the posttest base current for a given operating point will be larger than the pretest base current. If the posttest h_{FE} is very low, care should be taken not to exceed the base-emitter dissipation rating when attempting to achieve the pretest operating point.

The preferred methods for making steady-state and pulsed h_{FE} measurements are described by Method F528 of Reference 3 and Methods 1017, 1019, and 3076 of Reference 4. Figure 6.1-1 shows the circuit schematics for various collector current ranges. Figure 6.1-1a is used for steady-state measurements for collector currents under 100 μA; Figure 6.1-1b uses a pulsed voltage source for collector currents in the range of 100 μA to 100 ma; and Figure 6.1-1c is used for collector currents greater than 100 ma.

The basic procedure involves driving sufficient current, I_B, into the base of a transistor to achieve the desired collector current, I_C, at the required collector-emitter voltage, V_{CE}. The magnitude of the base current is measured and the gain calculated. The three test circuits in Figure 6.1-1 allow tests over a wide range of collector currents. Measurements and calculations are repeated for all collector-current values of interest. The test engineer must decide on the following for each test:

1. Collector currents, I_C, at which the measurements are to be made
2. Collector-emitter voltage, V_{CE}, to be used when making the measurements
3. Ambient temperature at which the tests are to be made.

Figure 6.1-2 shows the minimum acceptable pulse width for making the pulsed measurements using the circuits in Figures 6.1-1b and 6.1-1c.

The steady-state and pulse measurement methods are applicable to in-situ measurements when modified to include the required cables between the instrumentation and the test sample. Proper termination of all cables is a requirement.

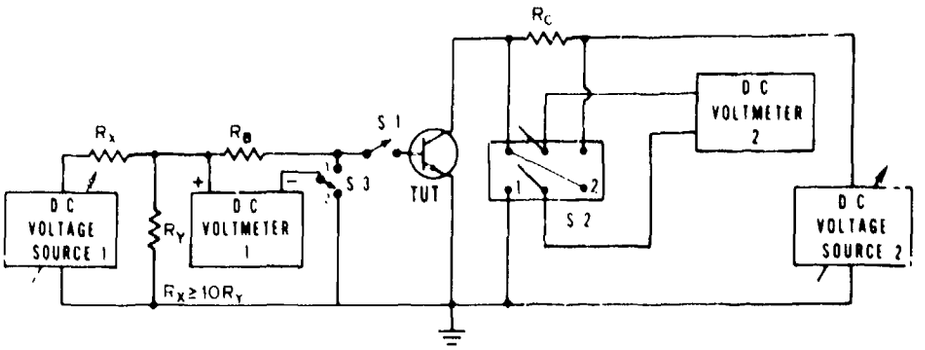

a. Circuit 1

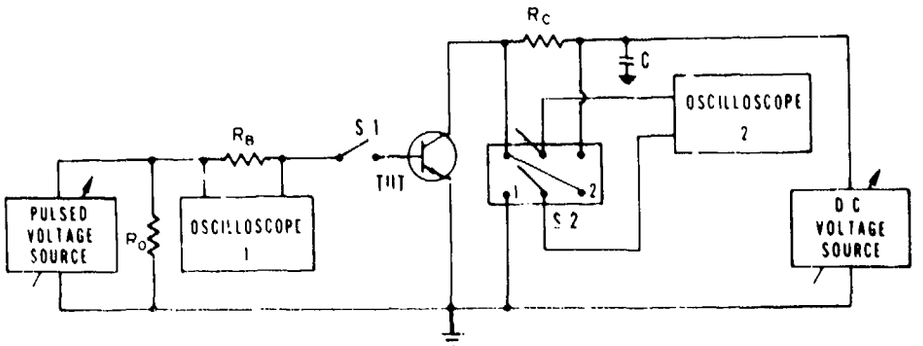

b. Circuit 2

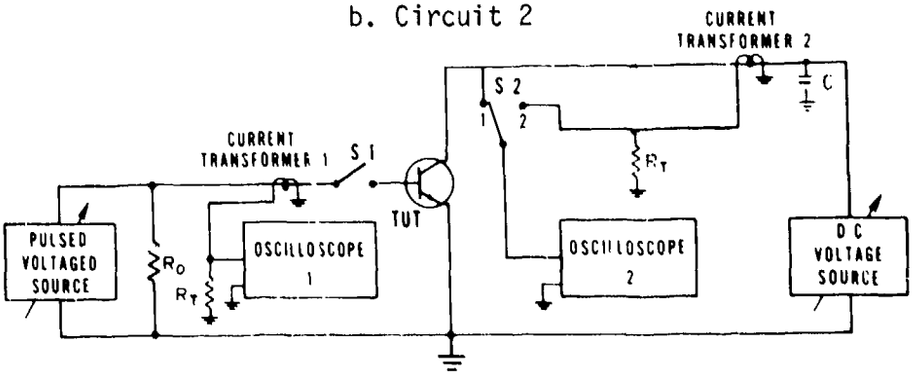

c. Circuit 3

Note: Capacitor C in Circuits 2 and 3 is a bypass capacitor that is used if required.

Figure 6.1-1. Schematics of h_{FE} measurement circuits (Method F528 of Reference 3).

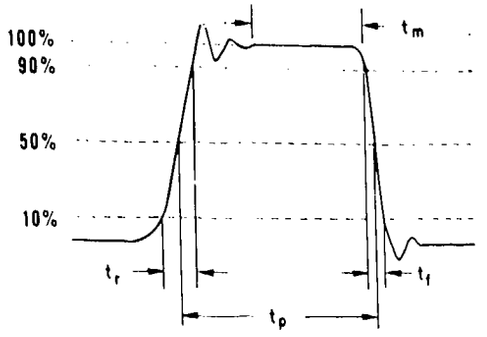

Note: t_m must be at least equal to $t_p/3$.

Figure 6.1-2. Minimum pulse width, t_p, for use in h_{FE} test measurements (Method F528 of Reference 3).

Figure 6.1-3 shows a data report form that can be used with the circuits shown in Figure 6.1-1 (Method F528 of Reference 3).

An arrangement for making rapid annealing measurements of h_{FE} is shown in Figure 6.1-4. A constant current source is used to maintain the selected emitter current during measurements. The trigger signal is used to maintain the device in the cutoff or active region as determined by the test requirements. The emitter current, I_E, and V_{CC} must be selected so that the required transistor operating point is achieved. The voltage V_B is monitored on an oscilloscope to provide an indication of the base current. Direct measurement of the collector current is generally not required when a constant emitter current source is used. The bypass capacitor is used to provide a stiff collector voltage and minimize oscillations (the large value bypass capacitor should be shunted by a small value low-inductance disc capacitor). The trigger signal also triggers the measuring equipment. A useful reference for timing is the incidence of the neutron pulse. A pre- and postburst sweep are required to establish initial and final h_{FE} values and reveal any scope drift problems that could compromise calibration.

Transient-annealing measurements are complicated by variations of the ambient temperature and by the photocurrents generated by the gamma radiation accompanying a neutron pulse. For meaningful data analysis, the temperature and the gamma dose rate must be monitored during a rapid-annealing experiment. Note that from 1 to 10 percent of the maximum gamma dose rate can persist for milliseconds after the neutron pulse. For this reason, extreme care should be exercised in analyzing rapid-annealing data. Measurements should be taken as specified in Method 1018 of Reference 4 to properly record the annealing data.

Page of

h_{FE} TEST REPORT FORM

Test Operator

Date

Test Equipment	Manufacturer	Model No	Serial No	Calibration Date

Circuit 1
1. D-C Voltage Source 1
2. D-C Voltage Source 2
3. D-C Voltmeter 1
4. D-C Voltmeter 2

Circuit 2
1. Pulsed Voltage Source
2. D-C Voltage Source
3. Oscilloscope 1 Preamp
4. Oscilloscope 2 Preamp

Circuit 3
1. Pulsed Voltage Source
2. D-C Voltage Source
3. Oscilloscope 1 Preamp
4. Oscilloscope 2 Preamp
5. Current Transfer 1
6. Current Transfer 2

a. Cover page

Page .. of .

h_{FE} REPORT FORM

Test Operator ..... Date .....

Transistor Type ..... Lot No. ..... Serial No. .....

Circuit 1

T_{CEO} Data: V_{CE} = ..., R_C = ..., V_{BC} = ..., I_{CEO} = ...

R_{SHUNT} Data: V_{BY} = ..., V_{BB} = ..., R_{SHUNT} = ...

V_{CE}	I_C (spec)	V_{BYT}	R_{BB}	R_C	V_{BC}	I_C (calc)	R_B	V_{BB}	I_B (calc)	h_{FE} (calc)	T_A (°C)

Circuit 2: t_p = ... µs, Pulse Rate = ... pps

V_{CE}	I_C (spec)	R_C	V_{BC}	I_C (calc)	R_B	V_{BB}	I_B (calc)	h_{FE} (calc)	T_A (°C)

Circuit 3: t_p = ... µs, Pulse Rate = ... pps

V_{CE}	I_C (spec)	I_C (meas)	I_B (meas)	h_{FE}	T_A (°C)

b. Data page (one such page is required per TUT)

Figure 6.1-3. Data report form.

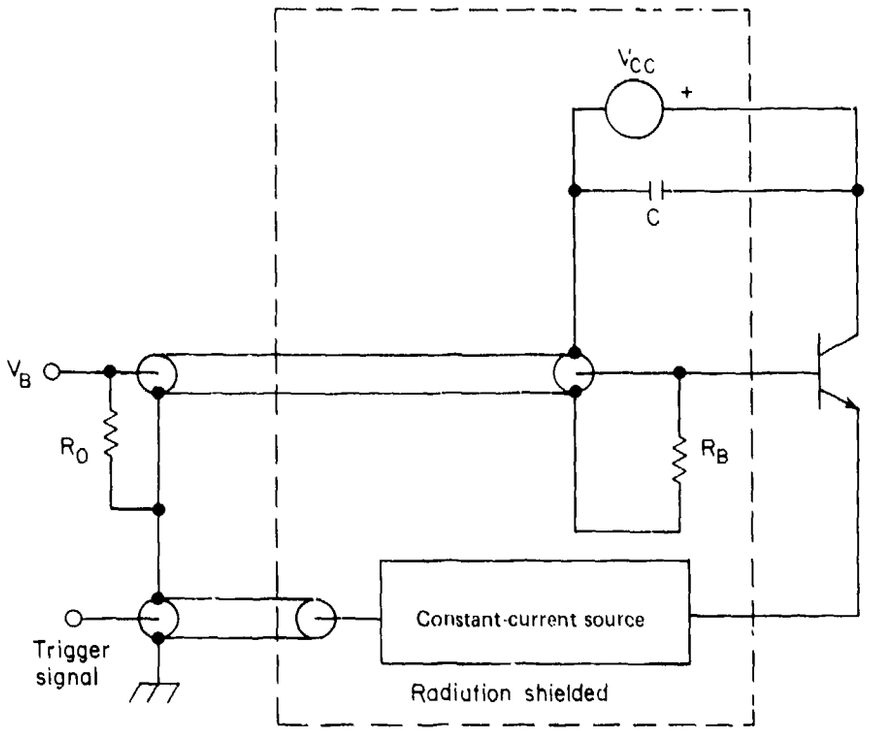

$$h_{FE} \approx \frac{I_E R_O R_B}{V_B(R_O + R_B)} - 1$$

Figure 6.1-4. Rapid-annealing h_{FE} measurement circuit.

6.1.6.2 Transistor Small-Signal Current Gain, h_{fe}

h_{fe} is the small-signal, short-circuit, forward current gain of a transistor operating in the normal active region when connected in the common-emitter configuration. The value of h_{fe} is determined by an accurate measurement of the ratio of the a-c collector current, i_c, to the base current, i_b, at a given temperature and operating point.

A steady-state technique for pre- and posttest measurements using sinusoidal excitation is shown in Figure 6.1-5. This circuit shown is based on Method F632 of Reference 3. Capacitors C_1, C_2, and C_3 are selected to be short circuits at the test frequency to effectively couple and bypass the test signal. The inductor impedance at the test frequency should be large compared with the small-signal input impedance, h_{ie}, of the transistor. The test engineer must specify the test frequencies and the test voltages and currents at which the measurements are to be made. Data to be recorded include the bias conditions, the test frequency, and the values of i_c and i_b. Then

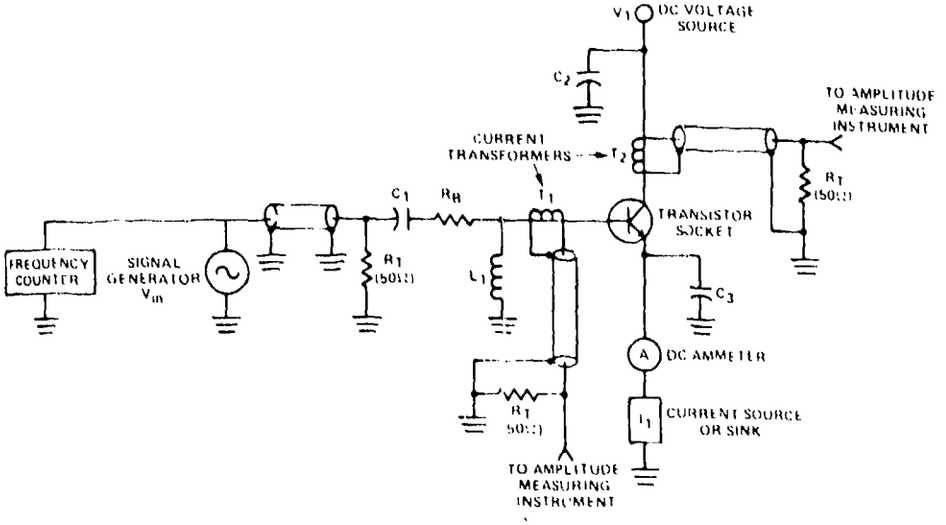

Figure 6.1-5. Steady-state measurement circuit.

$$h_{fe} = \frac{i_c}{i_b} . \qquad (6\text{-}3)$$

The circuit of Figure 6.1-5 is usable for frequencies up to approximately 100 MHz if the following precautions are taken during construction (Method F632 of Reference 3):

1. The generator and all cables must be properly terminated
2. All lead lengths must be kept to a minimum
3. The components must have suitable characteristics at the test frequency
4. The base and collector circuits must be shielded from each other and from extraneous RF interference.

Pulsed h_{fe} measurements are usually not required in radiation-effects work and, thus, no specific recommendations are made.

In-situ measurements can be made using the circuit shown in Figure 6.1-5 by inserting cables between the transistor socket in the irradiation chamber and the measuring equipment. Three coaxial or shielded cables should be used. All cables should possess a common-ground connection. The frequency used for in-situ test should be limited by consideration of cable effects at the higher frequencies.

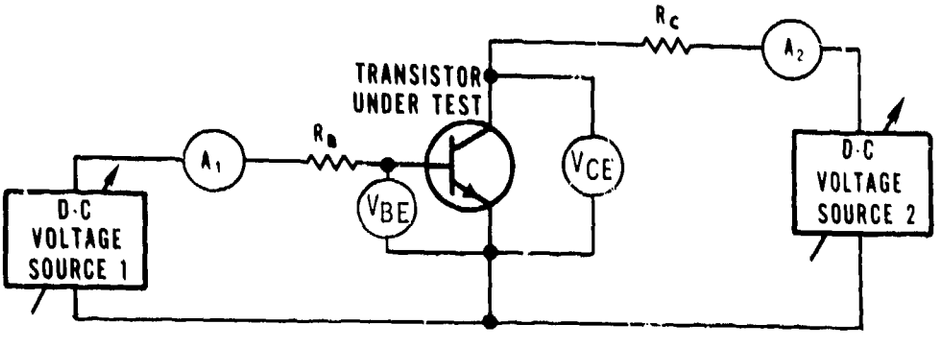

a. dc method

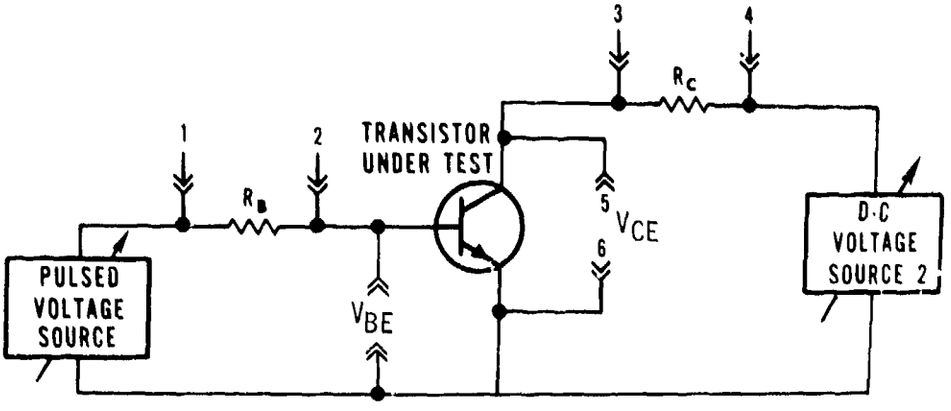

b. Pulsed method using the resistor-sampling technique

Figure 6.1-6. $V_{CE(SAT)}$ test circuits (Method F570 of Reference 3).

active region. The V_{BE} measurement is important for the case of matched-pair devices operated in the normal active region as a differential amplifier. For this mode of operation, the curves of I_C versus V_{BE} are matched.

It is necessary to measure the I_C versus V_{BE} dependences of both devices of a matched-pair at collector currents extending from low currents (~10 μA) to currents somewhat larger than that at which h_{FE} is a maximum. The number of current levels at which these measurements should be made is a function of the useful current range of the particular device type. The optimum technique for measurements on matched-pair devices is to directly monitor the differential base-emitter voltage as a function of neutron fluence.

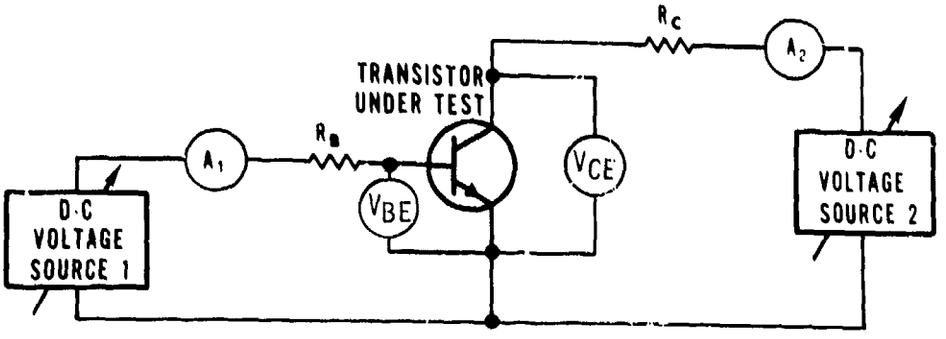

a. dc method

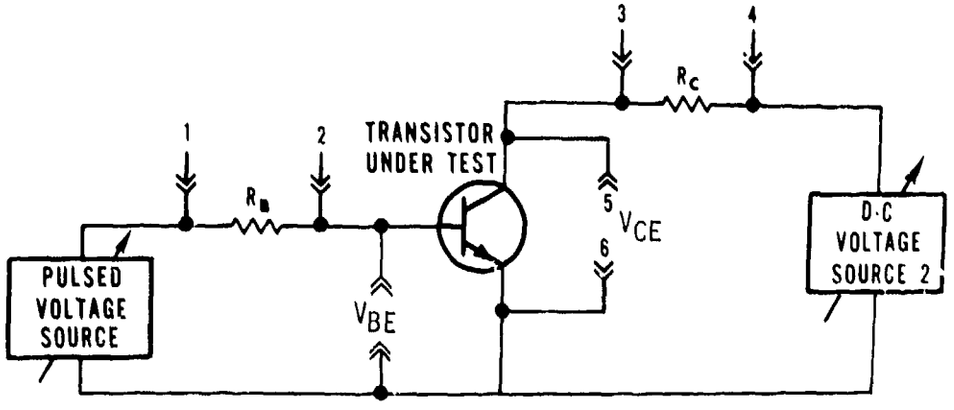

b. Pulsed method using the resistor-sampling technique

Figure 6.1-6. $V_{CE(SAT)}$ test circuits (Method F570 of Reference 3).

active region. The V_{BE} measurement is important for the case of matched-pair devices operated in the normal active region as a differential amplifier. For this mode of operation, the curves of I_C versus V_{BE} are matched.

It is necessary to measure the I_C versus V_{BE} dependences of both devices of a matched-pair at collector currents extending from low currents (~10 μA) to currents somewhat larger than that at which h_{FE} is a maximum. The number of current levels at which these measurements should be made is a function of the useful current range of the particular device type. The optimum technique for measurements on matched-pair devices is to directly monitor the differential base-emitter voltage as a function of neutron fluence.

Either steady-state or pulsed methods may be employed to measure these characteristics. The circuits of Figure 6.1-6 can be used to measure V_{BE}. These circuits can also be modified for differential V_{BE} measurements.

Since the I_C-V_{BE} characteristic is quite temperature sensitive, it is mandatory to keep the sample temperature constant during measurement. This can be accomplished by using a heat sink and avoiding a high duty cycle. Significant changes in these characteristics can result from simply handling the sample.

In-situ measurements may be performed by simply modifying the circuit configurations to include the required cables between the device and the instrumentation.

6.1.6.5 Transistor Leakage Currents, I_{CBO} and I_{EBO}

I_{CBO} is the reverse leakage current of a transistor collector-base junction when the emitter is unconnected. I_{EBO} is the reverse leakage current of a transistor emitter-base junction when the collector is unconnected.

I_{CBO} and I_{EBO} are determined by accurate measurements of leakage currents as functions of reverse-bias voltages. Since both leakage currents are functions of bias voltage, measurements at two or three operating points are usually adequate (one measurement should be at a bias voltage that is a large fraction of the junction breakdown voltage). The reverse bias must be less than the junction breakdown voltage to prevent damage to the transistor.

A steady-state measurement of I_{CBO} is illustrated in Figure 6.1-7. I_{EBO} is measured by interchanging the collector and emitter connections. V_R is an adjustable dc voltage source ($V_R < BV_{CBO}$) and M is an instrument capable of accurate current measurements down to picoamperes. Recorded data include V_R and I_{CBO}. The procedure is based on Method 3036 of Reference 4. (See also Method F769 of Reference 3.)

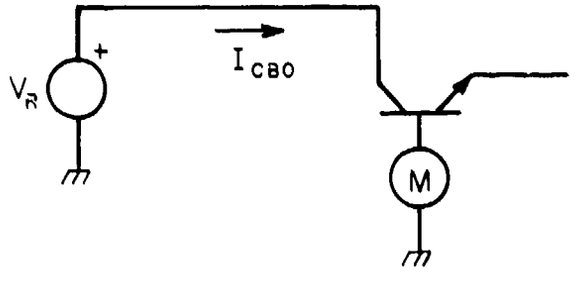

Figure 6.1-7. Steady-state I_{CBO} measurement circuit.

The currents to be measured are normally extremely small; therefore, extreme caution must be exercised when making these measurements. Problems may be encountered due to stray leakage currents and fields. It is recommended that the pre- and posttest measurements be made in a test fixture having shielded wiring that is well insulated from ground. Considerable changes in I_{CBO} and I_{EBO}, due to their temperature sensitivity, can result from simply handling the sample.

An extension of the steady-state technique of Figure 6.1-7 to in-situ measurements is shown in Figure 6.1-8. I_{EBO} is measured by interchanging the collector and emitter connections.

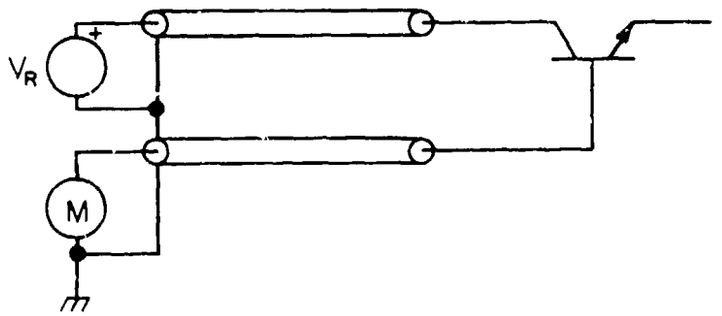

Figure 6.1-8. In-situ steady-state I_{CBO} measurement circuit.

In addition to the recommendations given for pre- and postirradiation measurements, the leakage current in the measurement circuit should be determined without a sample attached. This current must be subtracted from the currents recorded during I_{CBO} and I_{EBO} measurements. The degree of uncertainty of in-situ data can be reduced by assuring that the cables are of the same type, from the same manufacturer, from the same lot if possible, and have the same radiation history.

6.1.6.6 Transistor Switching Times, t_r, t_s, and t_f

t_r, t_s, and t_f are the rise time, storage time, and fall time, respectively, of the collector-current pulse as measured when the transistor is driven into saturation and returned to the cutoff mode. These three switching times are precisely defined in the literature and are functions of the test circuit elements as well as normal and inverted dc current gains and cutoff frequencies. Any specification of measurement technique involves specifying circuit component values as well as collector and turnon and turnoff base currents. Because of the wide range of device types suitable for switching applications, it is impractical to determine a preferred procedure that would satisfy manufacturers as well as users. The measurement procedure should be dictated by the intended device application

or the specific requirements of the test data (see Method 3251 of Reference 4). When making measurements of the switching characteristics of transistors, the limitations and accuracy of the particular measurement scheme and the specific test equipment used should be carefully reviewed.

6.1.6.7 Diode Forward Voltage, V_F

V_F is the voltage across a diode under conditions of forward bias. The information normally required is a curve of V_F versus I_F, the forward current. Diode forward-voltage drop should be measured at several current levels over the operating range of the device.

The measurement techniques and precautions that must be taken are very similar to those for transistor base-emitter voltage, V_{BE}. The basic configuration is shown in Figure 6.1-9.

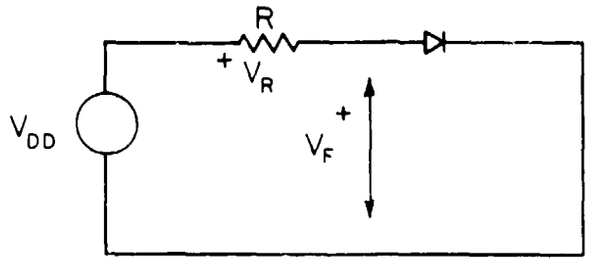

Figure 6.1-9. Basic V_F measurement circuit.

Method 4011 of Reference 4 gives the procedure. The supply voltage, V_{DD}, is adjusted to obtain the specified value of forward current through the diode. R is a precision sampling resistor to measure the forward current, I_F. A switch may be added in series for pulsed operation if junction heating is a problem. Recorded data should include V_{DD}, R, V_F, V_R, and pulse data if applicable. This technique is applicable to both conventional and Zener diodes.

6.1.6.8 Diode Zener Voltage, V_Z

V_Z is the Zener breakdown voltage of a diode at a particular current I_Z, which is a function of the device application. The measurement of V_Z should be made at a constant current level and constant temperature at the specific operating points. In addition, measurements can also be made at several temperatures to provide a measure of the effect of radiation on the temperature coefficient. Some devices have rather large temperature coefficients of Zener voltage; hence, temperature control is usually required.

The considerations, procedures, and precautions of measurement of I_R are identical to those for measurements of I_{CBO} and I_{EBO} given in Section 6.1.6.5 (see Method 4016 of Reference 4 and Method F769 of Reference 3).

6.1.6.10 Diode Reverse-Recovery Time, t_{rr}

t_{rr} is the reverse-recovery time of a diode, as defined in Figure 6.1-11.

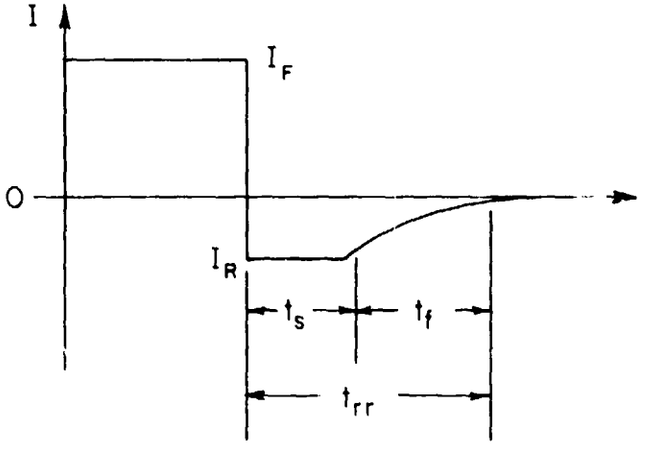

Figure 6.1-11. Diode reverse-recovery characteristics.

The recovery time, t_f, is usually limited by the series resistance and capacitance in the circuit. Because of this, t_s is the important switching parameter to measure. However, to give designers an estimation of the total reverse-recovery time for different circuits, it is recommended that both t_s and t_f be recorded, along with the values of I_F and I_R. The diode switching characteristic may be measured using a standard circuit such as the one in Figure 6.1-12 (Method 4031 of Reference 4). V_{DD} is an adjustable dc voltage source used to forward bias the diode. The diode is turned off by a negative pulse from the pulse generator. Advantages of this measurement circuit are:

1. The pulse generator is always properly terminated.
2. The diode may be turned on for a time long compared with the diode response times, thus eliminating effects of pulse width on switching times. However, I_F must be low enough to minimize heating effects.
3. Measurements may be easily made over a range of I_F/I_R for a given value of I_F.

The rise times of the pulse generator and the oscilloscope must be small compared with the diode response times.

The considerations, procedures, and precautions of measurement of I_R are identical to those for measurements of I_{CBO} and I_{EBO} given in Section 6.1.6.5 (see Method 4016 of Reference 4 and Method F769 of Reference 3).

6.1.6.10 Diode Reverse-Recovery Time, t_{rr}

t_{rr} is the reverse-recovery time of a diode, as defined in Figure 6.1-11.

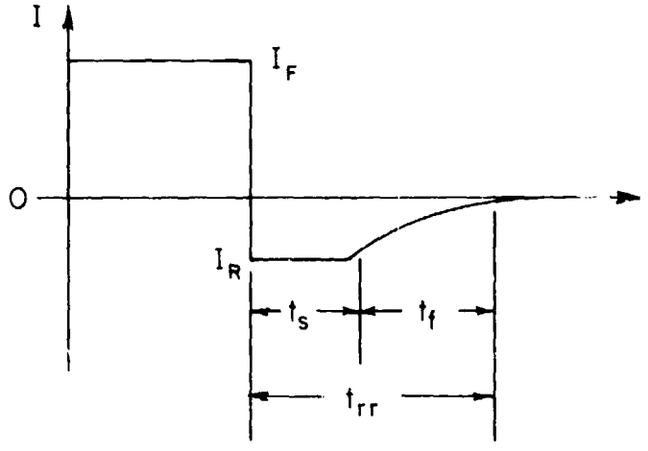

Figure 6.1-11. Diode reverse-recovery characteristics.

The recovery time, t_f, is usually limited by the series resistance and capacitance in the circuit. Because of this, t_s is the important switching parameter to measure. However, to give designers an estimation of the total reverse-recovery time for different circuits, it is recommended that both t_s and t_f be recorded, along with the values of I_F and I_R. The diode switching characteristic may be measured using a standard circuit such as the one in Figure 6.1-12 (Method 4031 of Reference 4). V_{DD} is an adjustable dc voltage source used to forward bias the diode. The diode is turned off by a negative pulse from the pulse generator. Advantages of this measurement circuit are:

1. The pulse generator is always properly terminated.
2. The diode may be turned on for a time long compared with the diode response times, thus eliminating effects of pulse width on switching times. However, I_F must be low enough to minimize heating effects.
3. Measurements may be easily made over a range of I_F/I_R for a given value of I_F.

The rise times of the pulse generator and the oscilloscope must be small compared with the diode response times.

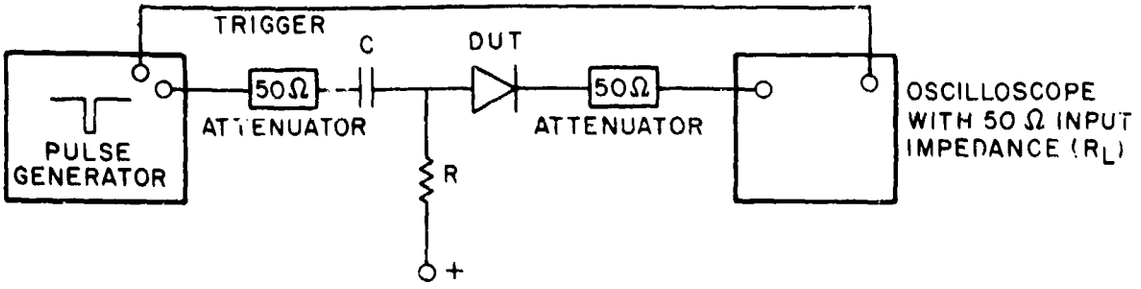

Figure 6.1-12. Basic t_{rr} measurement circuit.

Since t_s is related to I_F/I_R, measurements should be made at values of I_F and I_R particularly applicable to the ultimate device application or to the individual diode types as specified by the manufacturer. Recorded data should include V_{DD}, R, I_F, I_R, t_s, and t_f.

6.1.6.11 FET Drain Currents, I_{DSS} and $I_{DS(ON)}$

I_{DSS} is the zero-gate-voltage drain current measured in the pinchoff region of a field-effect transistor. In JFETS, I_{DSS} is a measure of the maximum drain current at which the device can operate. For MOSFET devices that operate in both the enhancement and depletion modes, $I_{DS(ON)}$ is defined as the drain current in the pinchoff region when the gate is biased for maximum channel conduction. I_{DSS} and $I_{DS(ON)}$ are determined by an accurate measurement of the drain current at the specified operating point and temperature. I_{DSS} is measured for devices operating in the depletion mode only (JFET). $I_{DS(ON)}$ is measured for devices that operate in the enhancement and depletion modes (MOSFET).

Since I_{DSS} and $I_{DS(ON)}$ depend on the drain-source voltage, V_{DS}, data should be taken at operating points in the range between the pinchoff voltage, V_p, and the drain-source breakdown voltage, BV_{DS}. Measurements are usually made for values of V_{DS} near V_p, BV_{DS}, and $BV_{DS}/2$ unless specific requirements dictate otherwise.

Figure 6.1-13 shows circuit schematics for making steady-state I_{DSS} and $I_{DS(ON)}$ measurements. V_{DS} and V_{GS} are adjustable voltage sources used to set the proper operating point. $V_{GS} = 0$ for I_{DSS} measurements and is set for rated maximum conduction for $I_{DS(ON)}$ measurements. V_{DS} must be greater than the pinchoff voltage. R_D is chosen so that $V_D \ll V_{DS}$ to monitor I_D. The circuit is based on Method 3413 of Reference 4. Recorded data should include values for V_{DS}, V_{GS}, R_D, and V_D.

The circuits shown in Figure 6.1-13 can be adapted for pulsed operation by replacing the V_{DS} voltage source with a pulse generator and by

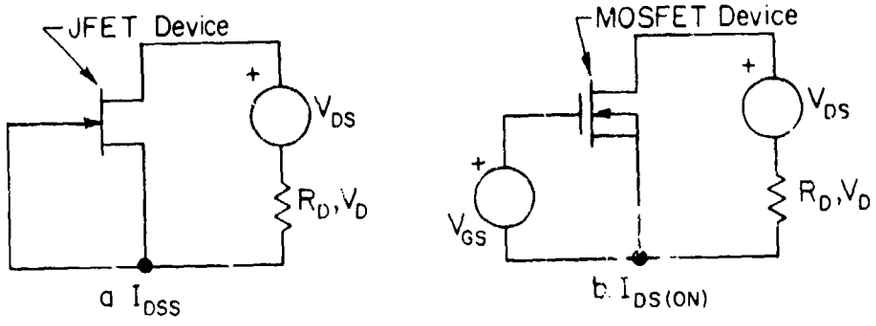

Figure 6.1-13. Steady-state I_{DSS} and $I_{DS(ON)}$ measurement circuit.

monitoring the voltage across R_D on a suitable oscilloscope. Pulsed measurements are usually preferred since device heating is minimized. Pulsed measurements are mandatory when the required operating points cannot be obtained in a steady-state measurement scheme without exceeding the dissipation ratings of the device.

The above procedures are applicable to in-situ measurements when modified to include the required cables between the instrumentation and the test sample.

6.1.6.12 FET Threshold Voltage, V_T

The threshold voltage, V_T, is defined as the gate-to-source voltage at which the drain current is reduced to the leakage current. The linear threshold voltage is measured under very low sweep rate or dc conditions when the FET is operating in the linear region with a typical drain voltage, V_D, of approximately 0.1 volt (Method F617 of Reference 3 and Method 1022 of Reference 2). The saturated threshold voltage is measured in a similar manner but with the FET operating in the saturated region with a typical drain voltage of approximately 10 volts (Method F618 of Reference 3).

The measurement method is applicable to both enhancement and depletion mode MOSFETs and for both silicon on sapphire (SOS) and bulk-silicon MOSFETs. It is for use primarily in evaluating the response of MOSFETs to ionizing radiation and, for this reason, the test differs from conventional methods for measuring threshold voltages.

The radiation-induced change in V_T is the most important radiation-induced failure mode for MOSFETs. Changes in V_T in MOSFETs are caused primarily by ionizing radiation. In addition, the changes in V_T of MOSFETs is a strong function of gate bias applied during irradiation. To be meaningful, MOSFETs should be irradiated with the particular bias condition required by the application. If no operating point is specified, MOS devices

should be irradiated at several bias conditions (both positive and negative that include typical operating conditions).

Changes in V_T for both JFET and MOSFET devices can be measured with the circuit shown in Figure 6.1-14. MOSFETs can be operated in either the enhancement or depletion mode. JFETS operate in the depletion mode. By changing the polarities of the supplies, p-channel devices can be tested with the same arrangement.

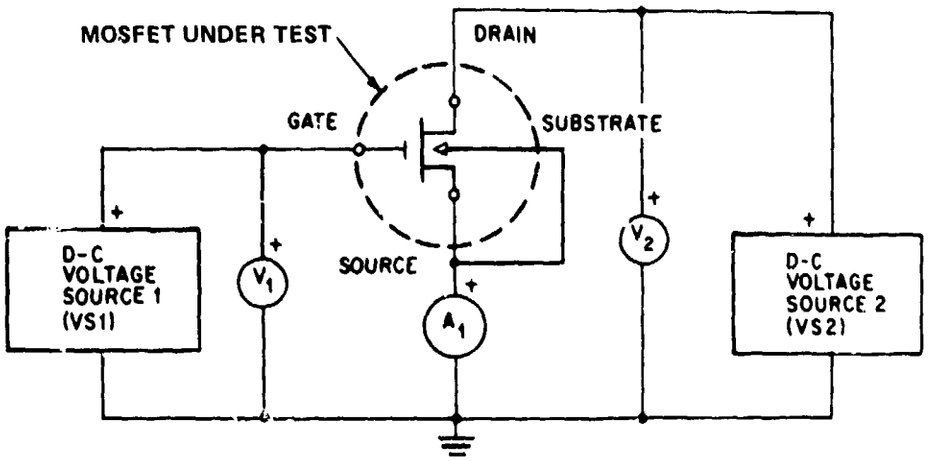

Figure 6.1-14. V_T test circuit for n-channel MOSFETs.

The threshold value is determined by measuring the drain-source current of the device under test at several values of gate voltage for a fixed drain-source voltage, V_2. For linear threshold measurements, a linear plot of the drain current as a function of gate voltage is made. The maximum tangent to the resulting curve is extrapolated to the gate-voltage axis or to the voltage independent line representing the drain-leakage current. This intercept is the threshold voltage (see Figure 6.1-15). For saturated threshold measurements, the square root of the difference of the drain current and the leakage current is plotted on a linear scale as a function of gate voltage. The maximum tangent intercept extrapolated to the gate voltage axis is the threshold value. Data to be recorded include the measured values of drain-leakage current, I_L, drain voltage, V_D, gate voltage, V_G, threshold voltage, V_T, and a curve such as shown in Figure 6.1-15 (References 2 and 3).

Measurements can be performed in situ if suitable cables are included between the sample and the instrumentation.

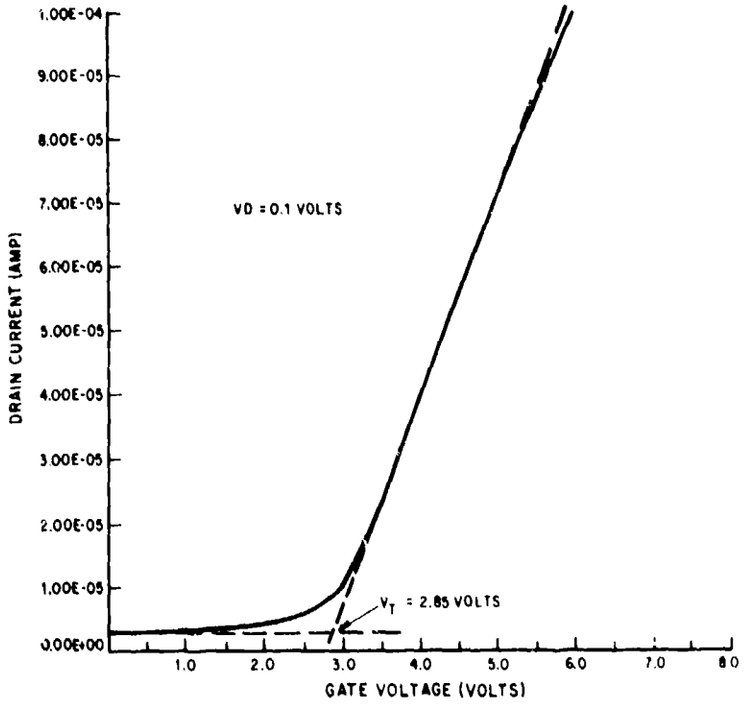

Figure 6.1-15. Typical V_T data for an n-channel enhancement device.

6.1.6.13 FET Forward Transconductance, g_m

g_m is the small-signal, forward transconductance of a field-effect transistor defined by $g_m = \partial I_D/\partial V_{GS}|V_{DS}$. The magnitude of g_m is determined by an accurate measurement of a small change in drain current for a given small change in gate voltage at a given temperature and operating point (the slope of plots of I_D versus V_{GS}).

g_m is an increasing function of drain current having its maximum value at I_{DSS} or $I_{DS(ON)}$. There is little dependence on V_{DS} provided the device is operated in the pinchoff region. For the selected values of V_{DS}, g_m data should be taken over the full operating range of the device to construct g_m versus I_D curves. Irradiation decreases I_{DSS}; thus, some pretest operating points may not be achieved after irradiation. Unless specific requirements dictate otherwise, it is suggested that all g_m measurements be made with V_{GS} maintained constant.

A steady-state technique for g_m measurement that employs sinusoidal excitation is shown in Figure 6.1-16. V_{GS} and V_{DS} are used to set the operating point. To hold V_{DS} nearly constant, V_o should be as small as can accurately be measured. I_D is a meter used to establish the dc drain current. R_D is a small resistor chosen to be much less than the FET

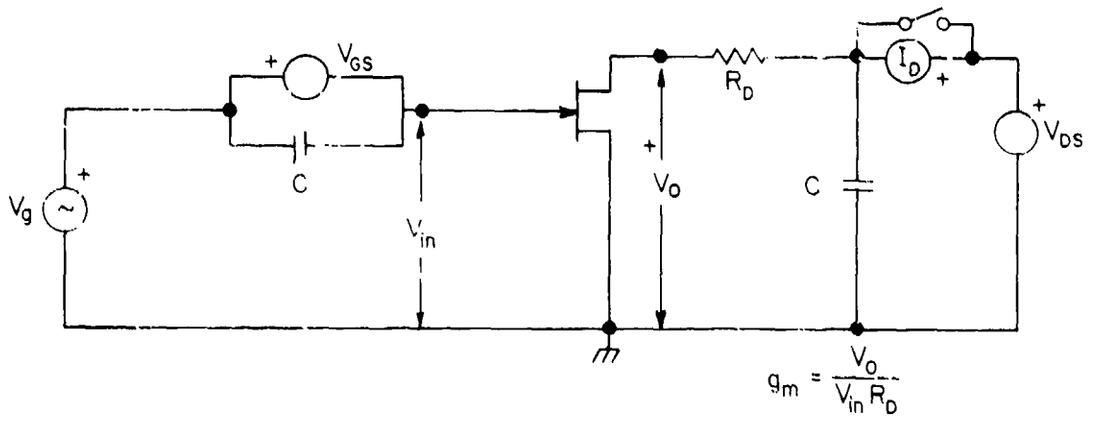

Figure 6.1-16. FET small-signal g_m measurement circuit.

dynamic output resistance. Data to be recorded should include V_{GS}, V_{DS}, I_D, V_{in}, V_D, and the test frequency.

Usually, g_m measurements are made at 1 kHz. However, if the proper precautions are taken, the circuit in Figure 6.1-16 can be used up to 25 MHz (see Section 6.1.6.2). In-situ measurements can be made if the proper cables are provided. The procedure is based on Method 3455 of Reference 4.

6.1.6.14 FET Leakage Currents, I_{GSS} and $I_{DS(OFF)}$

I_{GSS} is the gate leakage current of a field-effect transistor with the drain shorted to the source. $I_{DS(OFF)}$ is the drain source current with the channel off. I_{GSS} and $I_{DS(OFF)}$ are determined in a manner similar to the leakage currents for transistors (Section 6.1.6.5). Measurement arrangements for determining I_{GSS} are shown in Figure 6.1-17. I_{GSS} is normally measured for JFET devices while $I_{DS(OFF)}$ is measured for MOS devices. V_{GS} is used to set the required reverse bias voltage while the leakage current is measured with an instrument capable of current measurement down to picoamperes. Measurements should be made with test fixtures having shielded wiring that is well insulated from ground. The ambient temperature of the samples should be held constant. Method F616 of Reference 3 details the procedure for MOSFET devices. A test circuit for MOSFETs is shown in Figure 6.1-18.

6.1.6.15 FET Drain-Source Saturation Voltage, $V_{DS(ON)}$

$V_{DS(ON)}$ is the dc voltage between the drain and source of a FET operating in a specified condition in the resistance region ($V_{DS} < V_p$) that describes the nonlinear voltage drop due to the resistance of the channel in series with the drain and source. This parameter is of primary importance for switching applications. Measurements should be made at the

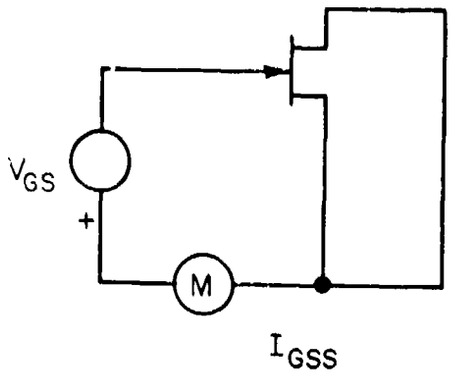

Figure 6.1-17. FET leakage current measurement circuit.

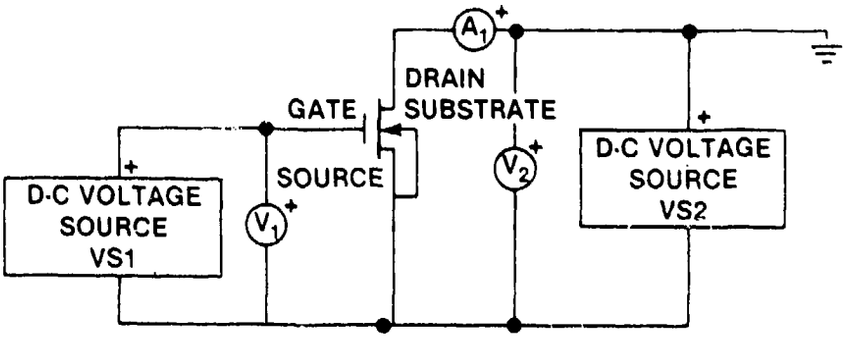

Figure 6.1-18. Drain leakage current test circuit for n-channel enhancement mode MOSFETs.

particular operating point of interest. It is desirable to measure $V_{DS(ON)}$ as a function of V_{GS} for various values of I_D. Steady-state and pulsed measurements may be made using the same configuration as shown in Figure 6.1-13, except that the operating points are chosen in the resistance region and the drain source voltage is measured directly (see Method 3405 of Reference 4).

Care must be taken during steady-state measurements to avoid excessive temperature buildup and the associated change in device characteristics.

6.2 TRANSIENT RESPONSE MEASUREMENTS

6.2.1 Scope

This section deals with experimental procedures for determining the time history of primary photocurrents, I_{pp}, generated within conventional discrete bipolar transistors, MOS and junction field-effect transistors, semiconductor diodes, and Zener diodes when they are exposed to sources of

ionizing radiation. Extrapolation of the procedures set forth here for application to other devices and/or other kinds of radiation should be performed with great care. The procedures have been found to be valid for ionizing-radiation dose rates as great as 10^{10} rads (Si or Ge)/s. The procedures may be used for measurements at dose rates as great as 10^{12} rads (Si or Ge)/s; however, extra care must be taken.

6.2.2 Analytical Techniques

This document is primarily concerned with techniques for radiation-effects testing. However, the designer should also be aware of theoretical and empirical techniques for predicting primary photocurrent in semiconductor devices. These analytical techniques may be applicable when an estimate of I_{pp} must be made in preparation for future testing, when less accurate results will suffice for preliminary design data, or when testing must be limited but more data are required. In these approaches, nondestructively measured electrical parameters are employed to calculate probable photocurrents and radiation storage times within specified confidence limits (see Reference 1 for further information).

6.2.3 Radiation Source Considerations

The radiation sources used to obtain transient response data are LINACs and flash X-ray machines. Additional details on these radiation sources are discussed in Chapter 4 and Reference 13.

The LINAC is a very flexible machine and thus is an extremely useful radiation source for characterization of the radiation response of semiconductor devices. A wide range of pulse width can be obtained and dose rates can be independently varied over a wide range without changing the sample position or test configuration. For virtually all transistor and diode types, LINAC pulse widths of 0.01 μs result in nonequilibrium photocurrents. However, a 4-μs pulse is several times the dominant minority-carrier lifetime in most transistor and diode types. In such cases, the photocurrent amplitude near the end of the LINAC pulse is a good approximation to the equilibrium (steady-state) value. At high dose rates ($\geq 10^9$ rads (Si)/s), the LINAC beam diameter is generally too small (0.5 to 2 cm at the beam exit window) to test more than one sample at a time, so tests are normally structured as a sequence of individual measurements.

Flash X-ray machines are available in a variety of maximum voltage ratings, energy delivery capabilities, a wide range of radiation intensities, and beam spatial distributions. With larger machines, it is possible to monitor several components simultaneously. Typically, four to eight samples are monitored, the limitation being primarily on the amount of instrumentation available. Comparative tests between samples exposed in the same

burst are readily performed but should be supported by careful dosimetry of each sample. Generally, it is advisable to structure a test to group all similar measurements so that a minimum of operational changes is required. Since the pulse width of most flash X-ray machines is shorter than or comparable to device time constants, nonequilibrium photocurrents are generated in flash X-ray tests.

6.2.4 Parameters to be Discussed

The most valuable ionization-effects data for the designer are specifications of the primary photocurrents as functions of time at various conditions of fixed-voltage bias in response to known ionizing-radiation dose-rate profiles. In diodes, a single photocurrent, designated i_{pp}, is of interest. In transistors, two photocurrents are of interest. The collector-base photocurrent is designated i_{ppc}; the emitter-base photocurrent is designated i_{ppe}. In the majority of cases, i_{ppe} is neglected because its value is small relative to the value of i_{ppc}. In some instances, the secondary photocurrent, i_{s}, in transistors and the radiation storage time, t_{sR}, in diodes and transistors may be of interest. In field-effect transistors, the transient response includes the drain pn junction primary photocurrent, i_{ppd} (since the FET device is symmetric, a similar photocurrent i_{pps}, is generated at the source), the channel response, and the influence of charge emission and ionization currents generated in the gate circuit on the drain current by gain action in the field-effect transistor. The procedures described here are applicable to the measurement of all these parameters.

The effect of ionizing radiation on semiconductor devices is illustrated by the generalized pn junction defined in Figure 6.2-1. The primary photocurrent, i_{pp}, flows in the direction shown and is a function of radiation dose rate, $\dot{\gamma}$, and dose, γ, in the device material, the reverse-bias voltage, V_R, and time, t. It is also a function of the type and energy spectrum of the incident ionizing radiation. In many cases, several of these dependencies will not be strong and may be neglected.

A typical primary-photocurrent response to a rectangular pulse of ionizing radiation is shown in Figure 6.2-2. There exists a dose dependence of i_{pp} immediately after onset of the radiation. This dependence disappears with increasing time and becomes a pure dose-rate dependence near the end of the radiation pulse when the primary photocurrent assumes a steady-state value, I_{pp}. The value of I_{pp} for a particular dose rate and the device relaxation time are valuable information as they aid in the extrapolation to weapon-pulse response of a particular device. For short radiation pulses, the steady-state photocurrent of a particular device may not be achieved. Under short-pulse conditions, the primary photocharge, Q_{pp}, and the device relaxation time for a particular dose will be employed as the generalized parameter of a particular pn junction. Note that Q_{pp} for

When an operating transistor is exposed to transient ionizing radiation, a current pulse is observed in the external circuit. This current pulse, which may be orders of magnitude larger than that of a diode with comparable dimensions, can reach a peak value at a time later than the radiation peak and can, in some cases, continue for times of the order of milliseconds. This characteristic behavior of transistors is the result of the action of the transistor amplifying properties on the primary radiation-induced photocurrents. The electrical action of the transistor creates a secondary photocurrent, i_{sp}, that is produced by the accumulation of excess carriers in the base region as a result of the flow of primary photocurrents across the pn junctions of the device. The steady-state value of i_{sp} is approximately equal to $h_{FE}i_{pp}$. Its magnitude can be substantially modified by an external base impedance. The presence of the internal base resistance limits the ultimate reduction of i_{sp}. The amplitude and response duration of i_{sp} also depend on the collector load resistance and depletion capacitance.

Transistors tend to be driven into saturation by pulses of high-intensity gamma radiation, which results in minority-carrier storage. The length of time a transistor remains in saturation is defined as the radiation-storage time, t_{sR}, as illustrated in Figure 6.2-2. For most transistors, t_{sR} is a function of radiation dose rate and the external base-emitter impedance. i_{sp} and t_{sR} in transistor circuits can usually be determined with reasonable accuracy using circuit-analysis techniques and a knowledge of device electrical parameters when the primary-photocurrent profiles are known. If measurement of i_{sp} and t_{sR} is required, the radiation response must be measured in the particular circuit application of interest.

6.2.5 Test Considerations

This section discusses some considerations for transient-response testing that are independent of the particular radiation source to be used. See also Section 2.5 for a general discussion of test considerations.

The effective dose to a semiconductor junction can be altered by changing the orientation of the test device with respect to the irradiating beam. Most transistors and diodes can be considered "thin samples" and their responses are independent of orientation. High power devices may have thick-walled cases or mounting studs that can act to shield the semiconductor chip, reducing the dose received. Care must be taken in the mounting of such devices.

The dose rate range over which measurements are to be made must be specified for the particular device. Measurements should be made over a wide range of dose rates because some devices exhibit a nonlinear photocurrent response due to saturation effects and injection level effects on lifetimes. In the case of bipolar transistors, a component of secondary photocurrent may be introduced into the measurements. The nonlinearities are usually observed at the higher dose rates ($\dot{\gamma} \geq 10^6$ rads (Si)/s).

When an operating transistor is exposed to transient ionizing radiation, a current pulse is observed in the external circuit. This current pulse, which may be orders of magnitude larger than that of a diode with comparable dimensions, can reach a peak value at a time later than the radiation peak and can, in some cases, continue for times of the order of milliseconds. This characteristic behavior of transistors is the result of the action of the transistor amplifying properties on the primary radiation-induced photocurrents. The electrical action of the transistor creates a secondary photocurrent, i_{sp}, that is produced by the accumulation of excess carriers in the base region as a result of the flow of primary photocurrents across the pn junctions of the device. The steady-state value of i_{sp} is approximately equal to $h_{FE}i_{pp}$. Its magnitude can be substantially modified by an external base impedance. The presence of the internal base resistance limits the ultimate reduction of i_{sp}. The amplitude and response duration of i_{sp} also depend on the collector load resistance and depletion capacitance.

Transistors tend to be driven into saturation by pulses of high-intensity gamma radiation, which results in minority-carrier storage. The length of time a transistor remains in saturation is defined as the radiation-storage time, t_{sR}, as illustrated in Figure 6.2-2. For most transistors, t_{sR} is a function of radiation dose rate and the external base-emitter impedance. i_{sp} and t_{sR} in transistor circuits can usually be determined with reasonable accuracy using circuit-analysis techniques and a knowledge of device electrical parameters when the primary-photocurrent profiles are known. If measurement of i_{sp} and t_{sR} is required, the radiation response must be measured in the particular circuit application of interest.

6.2.5 Test Considerations

This section discusses some considerations for transient-response testing that are independent of the particular radiation source to be used. See also Section 2.5 for a general discussion of test considerations.

The effective dose to a semiconductor junction can be altered by changing the orientation of the test device with respect to the irradiating beam. Most transistors and diodes can be considered "thin samples" and their responses are independent of orientation. High power devices may have thick-walled cases or mounting studs that can act to shield the semiconductor chip, reducing the dose received. Care must be taken in the mounting of such devices.

The dose rate range over which measurements are to be made must be specified for the particular device. Measurements should be made over a wide range of dose rates because some devices exhibit a nonlinear photocurrent response due to saturation effects and injection level effects on lifetimes. In the case of bipolar transistors, a component of secondary photocurrent may be introduced into the measurements. The nonlinearities are usually observed at the higher dose rates ($\dot{\gamma} \geq 10^6$ rads (Si)/s).

As the effective volume for the generation of photocurrent in semiconductor devices includes the space-charge region, i_{pp} may be dependent on applied voltage. At voltages near the breakdown voltage, i_{pp} increases sharply because of avalanche multiplication in the junction. If the device application is known, measurements of i_{pp} should be made at the specified bias voltage. If the application is not known, the bias dependency should be checked by first making measurements at one-half the rated breakdown voltage, followed by measurements at a bias of 1 volt. If the results do not agree within ±20 percent, additional measurements should be made at a bias voltage 0.8 times the rated breakdown voltage (Method F448 of Reference 3).

From an engineering standpoint, the error introduced into an i_{ppc} measurement when the emitter lead is open is seldom significant, since $i_{ppe} << i_{ppc}$ for most geometries. In cases where a more accurate representation of transistor radiation response is desired, such as obtaining data for computer-aided circuit analysis, the emitter-base junction photocurrent, i_{ppe}, must also be measured. The relationships of the collector and emitter photocurrent generators for transistor modeling are expressed in terms of the measured primary photocurrents as follows (Reference 24):

$$I_{pC} = \frac{i_{ppc} - \alpha_N i_{ppe}}{1 - \alpha_N \alpha_I} \tag{6-4}$$

$$I_{pE} = \frac{i_{ppe} - \alpha_I i_{ppc}}{1 - \alpha_N \alpha_I} \tag{6-5}$$

where i_{ppc} and i_{ppe} are the measured primary photocurrents, and α_N and α_I are the normal and inverse current gain. To reduce the magnitude of any error, measurements can be made with both junctions reverse biased, thus prohibiting transistor action. If this is done, the voltage-bias conditions should be reported in test results.

In field-effect devices, a proper drain-photocurrent measurement, i_{ppd}, requires the source be shorted to the drain. If the source is open-circuited, additional current flow in the drain circuit due to the source photocurrent, i_{pps}, is observed. Since ionizing radiation induces photocurrents across both drain and source junctions, i_{pps} will flow through the channel region and add to the observed photocurrent. At low currents where i_{pps} is less than the maximum channel current, the observed drain current is equal to the sum of $i_{ppd} + i_{pps}$. At high currents where i_{pps} is greater than the channel can supply, the observed current is limited to the sum of i_{ppd} and the maximum channel current.

6.2.6 Spurious Currents

The radiation sources and fields used in TREE testing can act as a source of spurious currents. The currents arising from air ionization,

secondary emission, and cable currents are important in semiconductor device testing since these currents effectively place a lower limit on the magnitude of signal photocurrents that can be measured accurately. These sources must be eliminated or accounted for in all device testing. A discussion of noise suppression is included in Section 2.5.

Typical spurious current levels indicate that devices whose steady-state photocurrent is at least 10^{-11} A·s/rad (Si) present no particular difficulty from spurious currents. Devices whose steady-state photocurrents are less than 10^{-11} A·/rad (Si) require individually tailored experimental procedures to reduce the noise level in radiation tests so that useful photocurrent measurements can be made.

The spurious current due to air ionization can be easily checked by measuring the current while irradiating the test fixture in the absence of a test device. Air ionization contributions to the observed signal are proportional to the applied field. The effects of air ionization external to the device may be minimized by coating exposed leads with a thick layer of paraffin, silicone rubber, or nonconductive enamel. Measurements can also be made in a vacuum.

Spurious currents due to secondary emission are not proportional to the applied field. These currents may be minimized by shielding of the surrounding circuitry and irradiating the minimum area necessary to ensure irradiation of the test device. Reasonable estimates of the current magnitude can be made based on the area of metallic target materials irradiated. Values are generally less than 10^{-12} A·s/cm^2·rad.

6.2.7 Specific Test Procedures

Preferred test circuits are given here for the measurement of semiconductor-junction primary photocurrent, i_{pp}. Two basic techniques are illustrated--the resistor-sampling method and the current-probe method. Either one- or two-lead measurements are applicable to these basic techniques. In addition, a resistor sampling circuit applicable for field-effect devices is illustrated. Although the measurement techniques for field-effect transistors are essentially the same as those for bipolar transistors and diodes, some specific procedures and precautions are given to complement the basic measurement techniques as they apply to field-effect devices.

Adequate documentation of the methods and results of transient-effects tests is essential. The following data should be recorded for each device tested (additional procedures outlining the format for data reporting are given in Section 6.3):

1. Device identification
2. Date of test and operator
3. Identification of test facility and all test equipment

4. Description of test circuit, including shielding and grounding schemes
5. Type of ionizing radiation, including the energy spectrum
6. Description of irradiation pulse shape monitor
7. Dosimetry technique
8. Radiation pulse shape and width
9. Dose rate in the sample, rads (material)/s
10. Accumulated dose in the sample, rads (material)
11. Test circuit current with device removed
12. Test circuit response data
13. Sample orientation
14. Ambient temperature
15. Pictorial record of $i_{pp}(t)$
16. Values of I_{pp}
17. Device relaxation time, if calculated.

In the following test circuits, the single-point grounding philosophy is recommended whenever possible. If adjustment of the bias voltage from the instrumentation is not required, the power-supply cables can be eliminated by the use of batteries located in the exposure room. These batteries should be well shielded from the radiation. In general, lead lengths should be as short as possible to minimize inductance. Resistors and capacitors with suitable high-frequency characteristics should be used. In addition, all wiring and components should be RF shielded and cables should be bundled together.

6.2.7.1 Resistor-Sampling Methods

The primary photocurrent may be measured by the circuits shown in Figure 6.2-3 (Method F448 of Reference 3). For most tests, the configuration of Figure 6.2.3a is appropriate. The resistors R_2 serve as high-frequency isolation and must be at least 20Ω. The capacitor C supplies the charge during the current transient. Its value must be large enough so that the decrease in voltage during a current pulse is less than 10 percent. Capacitor C should be paralleled by a small (0.01 μF) low-inductance capacitor to ensure that possible inductive effects of the large capacitor are offset. Resistor R_o provides proper termination for the coaxial cable used for the signal lead. When photocurrents are large, the configuration of Figure 6.2-3b is necessary. R_1 is a small-value resistor to keep the signal small so as to maintain the bias across the junction within 10 percent of its nominal value during test. The response characteristics of this circuit must be adequate to ensure that the current signal is accurately displayed. The adequacy of the test circuit is evaluated by

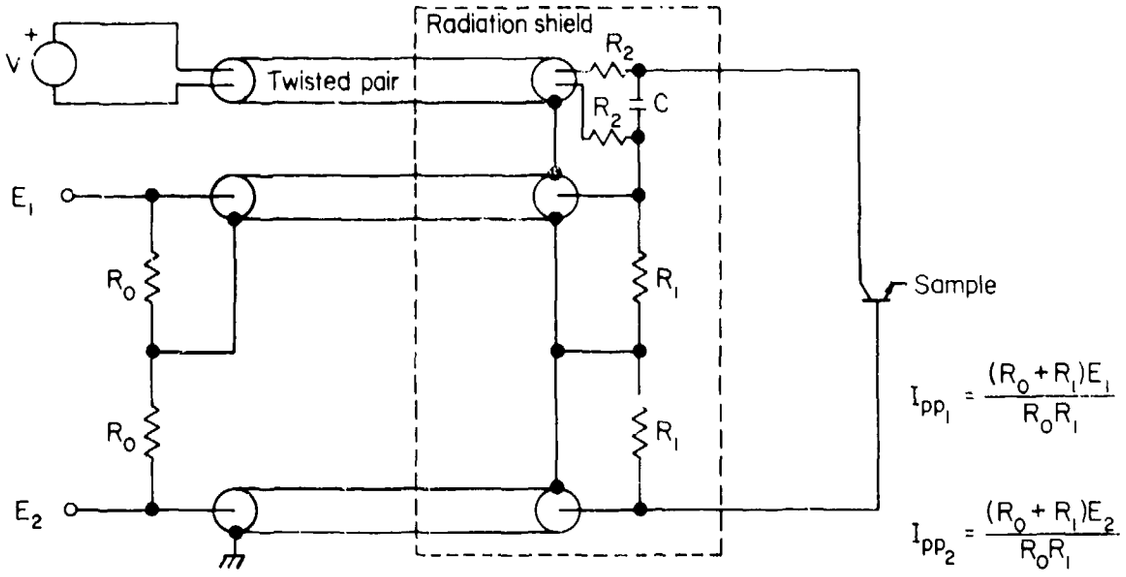

Figure 6.2-4. Two-lead resistor-sampling photocurrent measurement circuit.

6.2.7.2 Current-Probe Methods

The primary photocurrent may be measured directly by using a current probe (Method F448 of Reference 3). This technique is used when minimum deviation of the operating point is required. Figure 6.2-5 shows the circuit configuration. R_2 and C have the same significance as in the resistor-sampling circuit, but it may be required that the signal cable monitoring the current transformer be matched to the characteristic impedance of the probe, in which case R_0 would have this impedance, which is specified by the current probe manufacturer. The current probe must have sufficient bandwidth to ensure that the current signal is accurately displayed. Low-frequency response must be checked so that the droop is less than 5 percent for the radiation pulse width used. Rise time must be less than 10 percent of the radiation pulse width. When monitoring large photocurrents, care must be taken that the ampere-microsecond saturation of the current probe is not exceeded.

The measurement circuits illustrated in Figures 6.2-3 through 6.2-5 can be adapted for the measurement of secondary photocurrent and radiation storage time by interchanging the emitter and base terminal of the transistor. External base and collector resistors are added as specified by the basic data requirements. Unless specific data requirements dictate otherwise, it is suggested that the base terminal be connected to the emitter through a high-resistance (minimum stray capacitance) circuit such that the current flowing out of the base is a negligible portion of the total base current ($R_B \sim 10^5$ ohms). In addition, measurements should be made with a minimum collector resistance required to obtain an accurate sample of the

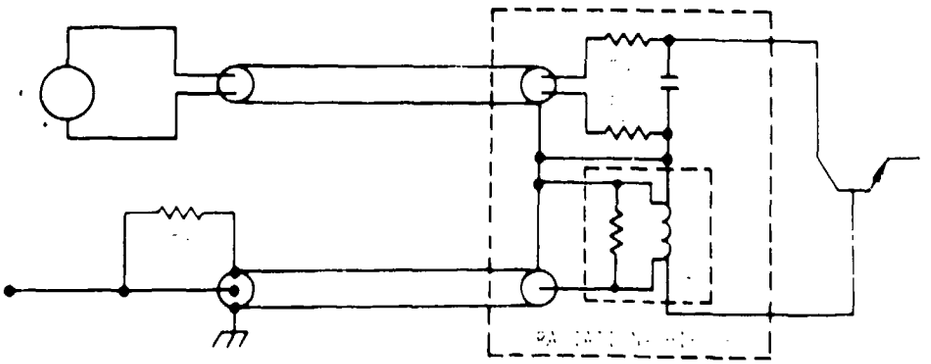

Figure 6.2-5. Current-probe photocurrent measurement circuit.

collector current. Care should be exercised in the construction of the secondary photocurrent test circuit to minimize the stray capacitance at the base and collector terminals of the evice under test. In particular, the capacitance associated with the external base resistance must be minimized to reduce the time constant of the base circuit.

6.2.7.3 Measuring Nonequilibrium Transient Photocurrents

There is a widespread use of ionizing sources with radiation pulses that are shorter than the time required for the device under test to achieve equilibrium. These photocurrents are dependent upon the characteristics of the excitation source as well as the characteristics of the device itself.

A standard measurement procedure described in Method F675 of Reference 3 provides a means of ensuring that all influencing factors enter the measurement in the same manner. The procedures to be followed are similar to those described in Sections 6.2.7.1 and 6.2.7.2. A series RC network is added from each lead of the bias supply to ground in Figures 6.2-3 through 6.2-5. The resistors terminate cable reflections in the power supply line and the capacitors are dc blocking capacito . Figure 6.2-6 shows the modified test circuit.

6.2.7.4 Measurement Method for FETs

In field-effect transistors, it is necessary to specify the response of the channel and the influence of charge emission and ionization currents generated in the gate circuit (package response) in addition to the primary photocurrent. The package response influences the drain current by gain action in the field-effect device. In general, the drain photocurrent and the channel response can be measured independently from the package response by irradiating samples where secondary-emission and air-ionization currents are minimized. The package response can be independently

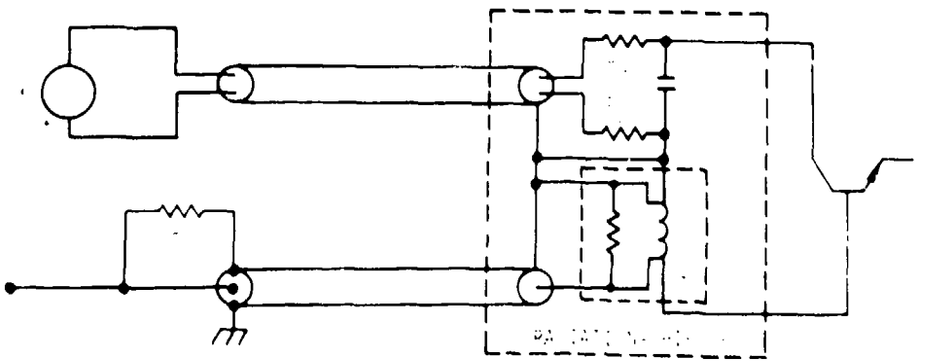

Figure 6.2-5. Current-probe photocurrent measurement circuit.

collector current. Care should be exercised in the construction of the secondary photocurrent test circuit to minimize the stray capacitance at the base and collector terminals of the evice under test. In particular, the capacitance associated with the external base resistance must be minimized to reduce the time constant of the base circuit.

6.2.7.3 Measuring Nonequilibrium Transient Photocurrents

There is a widespread use of ionizing sources with radiation pulses that are shorter than the time required for the device under test to achieve equilibrium. These photocurrents are dependent upon the characteristics of the excitation source as well as the characteristics of the device itself.

A standard measurement procedure described in Method F675 of Reference 3 provides a means of ensuring that all influencing factors enter the measurement in the same manner. The procedures to be followed are similar to those described in Sections 6.2.7.1 and 6.2.7.2. A series RC network is added from each lead of the bias supply to ground in Figures 6.2-3 through 6.2-5. The resistors terminate cable reflections in the power supply line and the capacitors are dc blocking capacito . Figure 6.2-6 shows the modified test circuit.

6.2.7.4 Measurement Method for FETs

In field-effect transistors, it is necessary to specify the response of the channel and the influence of charge emission and ionization currents generated in the gate circuit (package response) in addition to the primary photocurrent. The package response influences the drain current by gain action in the field-effect device. In general, the drain photocurrent and the channel response can be measured independently from the package response by irradiating samples where secondary-emission and air-ionization currents are minimized. The package response can be independently

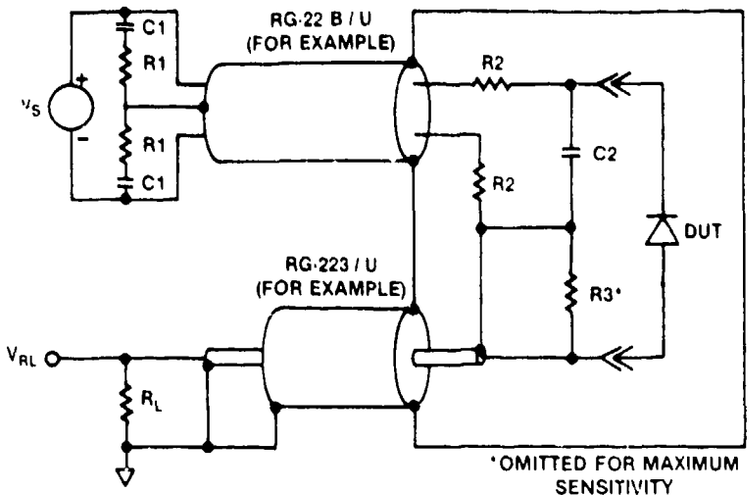

Figure 6.2-6. Resistor sampling nonequilibrium photocurrent measurement circuit.

determined by irradiating "dummy packages." These devices consist of FET metallization pattern put down on an oxidized silicon chip and encapsulated in identical packages as the active samples.

Figure 6.2-7 shows a circuit for measurement of the transient drain and gate currents of field-effect devices. The circuit can be used for measurements on JFET and MOSFET devices. V_D and V_G are the drain and gate bias supplies, the transient currents are measured by sampling resistors R_D and R_G, R_2 is selected for high-frequency isolation, and C provides the power supply bypass capacitance. E_1 and E_2 are photographed on a suitable oscilloscope.

The sampling resistor in the drain circuit should be kept as small as possible to avoid causing circuit saturation of i_{pp} at high dose rates due to an effective reduction of the bias voltage across the junction. If the voltage drop across R_D is more than 10 percent of the supply voltage, the sampling resistor should be reduced or replaced by a current probe. To increase the sensitivity of the measurement circuit, $R_D > R_0$ may be required. In this case, a line driver should be used to match impedance between the cable and the sampling resistor. The sampling resistor, R_G, must also be selected as small as possible to prevent flow of secondary photocurrent. In JFET devices, the transient gate current is approximately twice the drain current (since the source photocurrent also flows in the gate lead). In MOSFET devices, the photocurrents are generated by the drain- and source-substrate junctions, and thus only the dielectric-response, air-ionization, and secondary-emission currents flow in the gate lead.

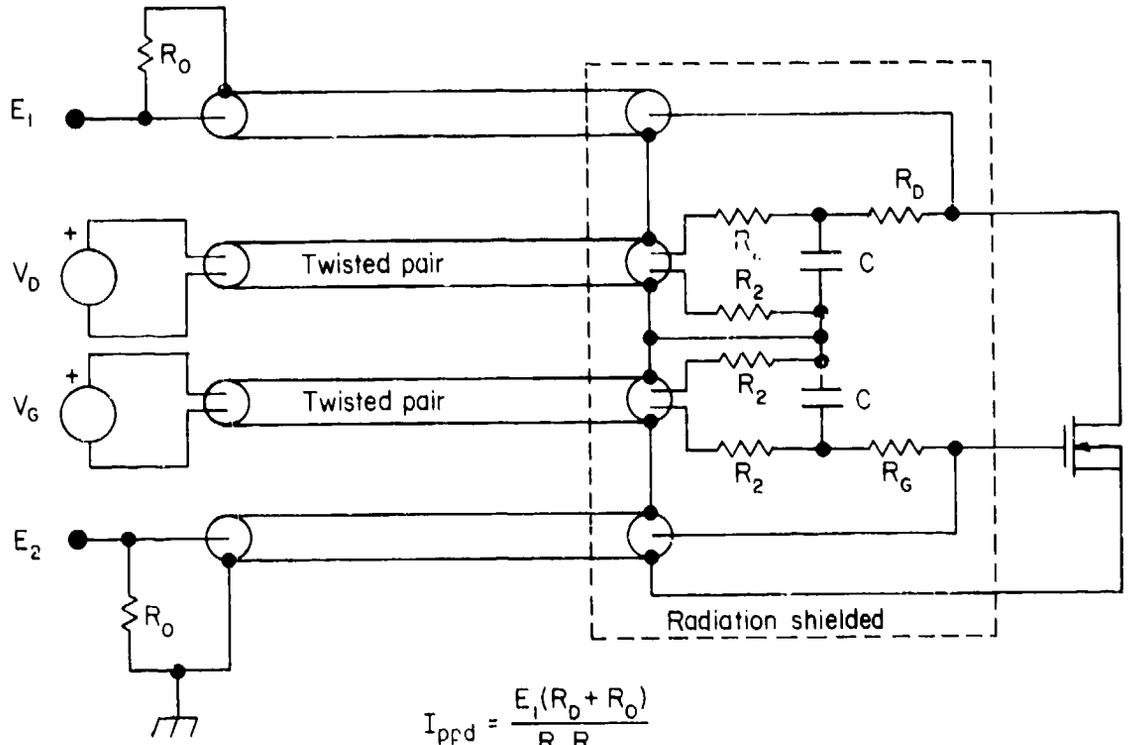

$$I_{ppd} = \frac{E_1(R_D + R_O)}{R_D R_O}$$

$$I_{ppg} = \frac{E_2(R_G + R_O)}{R_G R_O}$$

Figure 6.2-7. Drain and gate transient response measurement circuit for FET devices.

The major bias conditions of interest in field-effect devices are the pinchoff and cutoff regions. The drain photocurrent is measured in the cutoff region (V_D = 0, V_G variable beyond the threshold voltage). The channel response is measured by biasing the FET device in the pinchoff region. The measured current in the drain lead is then the sum of drain photocurrent and the channel response. Secondary photocurrents can be measured by varying the drain and gate resistance. Note that the source terminal is connected to the drain when making drain-photocurrent measurements. If the source is left floating, the magnitude of the drain current will increase due to the source photocurrent.

6.3 DATA REPORTING

6.3.1 General

The general information required in most reports of TREE tests is discussed in Chapter 3, Documentation Requirements. Information requirements

covered in that section include reporting of the experimental procedure, a description of the facilities used, the documentation of the dosimetry, and a complete description of the samples irradiated. Included in this section are specific data requirements for tests involving transistors and diodes and standardized formats for reporting the data. Figure 6.3-1 shows a sample data format that can be used to present the genera' information for each irradiation test.

Device Type(s): _____

Facility: _____ Date of Test: _____

Dosimetry Method(s): _____

Irradiation Temperature: _____

Experimental Configuration: _____

Electrical Condition During Irradiation: _____

(Specify device bias condition and the circuit diagram, including all test equipment and grounding scheme used during in-situ measurement.)

Additional Comments:

Figure 6.3-1. Sample format for general test information.

In addition to the irradiation procedure, basic types of samples should be described. A good technique is to have a distinct data sheet that presents for the various device types the manufacturer, type or specification number, lot number, origin (factory, distributor, etc.), and method of selection and validation. If useful electrical and structural information (such as power rating and junction areas) is available, it should be

reported to facilitate data comparisons and to increase the general utility of the data. A suggested parts tabulation sheet is illustrated in Figure 6.3-2.

Information to be Included				Useful Information					
Serial No.	Unit Designation in Test	Manufacturer	Date of Manufacture and/or Purchase	Device Batch and Lot No.	Maximum Current Rating	Maximum Voltage Rating	Junction Area(s)	Device Application	Comments

Figure 6.3-2. Sample format for tabulating parts data.

A statement should be given as to the constancy of any control samples used. The estimated uncertainty in all important results should be quoted. In specifying errors, the value of one standard deviation is the quantity preferred, although other methods may be used if they are more suitable and unambiguous. When statistical characterizations are given, at least a reference should be cited that explains the techniques involved in their calculation.

6.3.2 Permanent-Damage Data

Device parameter data should be tabulated for each measurement set, giving the parameter measured, the irradiation level at which the measurement was made, and the operating condition of the device during measurement. Note that preirradiation parameter values must be included. Usually the preirradiation measurements performed on the test device are of two types: those in which important radiation-induced changes are expected to occur (see Tables 6.1-2 and 6.1-3) and other measurements that may help to characterize the device. In addition to these measurements, it is desirable to perform other measurements by which the particular device can be characterized. Sample data formats for tabulating measured parameter values are given in Figure 6.3-3 for diodes, bipolar transistors, and field-effect devices. As supplementary information to parameter data, the measurement procedure should be reported. Specifically, this includes the measurement-circuit diagram, a list of the measurement equipment, a statement regarding the accuracy and/or precision of the data, etc.

Graphs showing the radiation-induced changes in the measured parameter values are very desirable and complement the tabulated data. The method employed for the graphical presentation of data depends on the method of data analysis and the objectives of the experiments. As a general

Device Type: _____

Date: _____

Unit Desig	V_F at I_F		I_R at V_R		V_Z, ΔV_Z at I_Z			t_{rr} at I_F	I_R		Neutron Fluence	Total Dose	Temp
	V	mA	μA	V	V	V	mA	ns	mA	mA	n/cm² (1-MeV Eq.)	rad(Si)	°C

a. Diodes

Device Type:

Date:

Unit Desig	Parameters									Test Conditions								Neutron Fluence	Total Dose	Comments
	h_{FE} h_{fe}	$V_{CE(SAT)}$ $V_{BE(SAT)}$	I_{CBO} I_{EBO}	V_{BE}	f_T	t_d	t_r	t_s	BV_{CBO} BV_{EBO} BV_{CEO}	I_C	I_L	I_B	V_{CE}	V_{CB}	V_{EB}	I_C I_B	Freq.	Temp			
		V	nA	mV	MHz	ns	ns	ns	V	mA	mA	mA	V	V	V		Hz	°C	n/cm² (1-MeV Eq.)	rad(Si)	

b. Bipolar transistors

Device Type: _____

Date: _____

Unit Desig	Parameters					Test Conditions						Neutron Fluence	Gamma Dose	Comments
	I_{DSS} $I_{DS(ON)}$	V_T	g_{fs}	I_{GSS} $I_{DS(OFF)}$	$V_{DS(ON)}$	V_{DS}	V_{GS}	ID	Freq.	T	V_{GS} During Exposure			
	mA	V		mA	V	V	V	mA	Hz	°C	V	n/cm² (1-MeV Eq.)	rad(Si)	

c. Field-effect transistors

Figure 6.3-3. Sample formats for recording permamant-effects data.

guideline, it is recommended that parameter measurements made at a specified operating point should be plotted as a function of radiation exposure. Parameters that are measured at several operating points at each fluence level should be plotted as a function of the parameter varied to change the operating point. The result will be a family of curves for the various radiation exposures.

Figure 6.3-4 shows an example of h_{FE} curves. h_{FE} is plotted as a function of collector current prior to irradiation and at the two neutron fluences at which measurements are made. To aid in interpolation, it would be helpful to show intermediate fluence levels between curves at one or more current values such as the 10^{12} n/cm^2 point at I_C = 10 mA. These points can be determined by interpolating on a curve of h_{FE} versus neutron fluence at a selected current level.

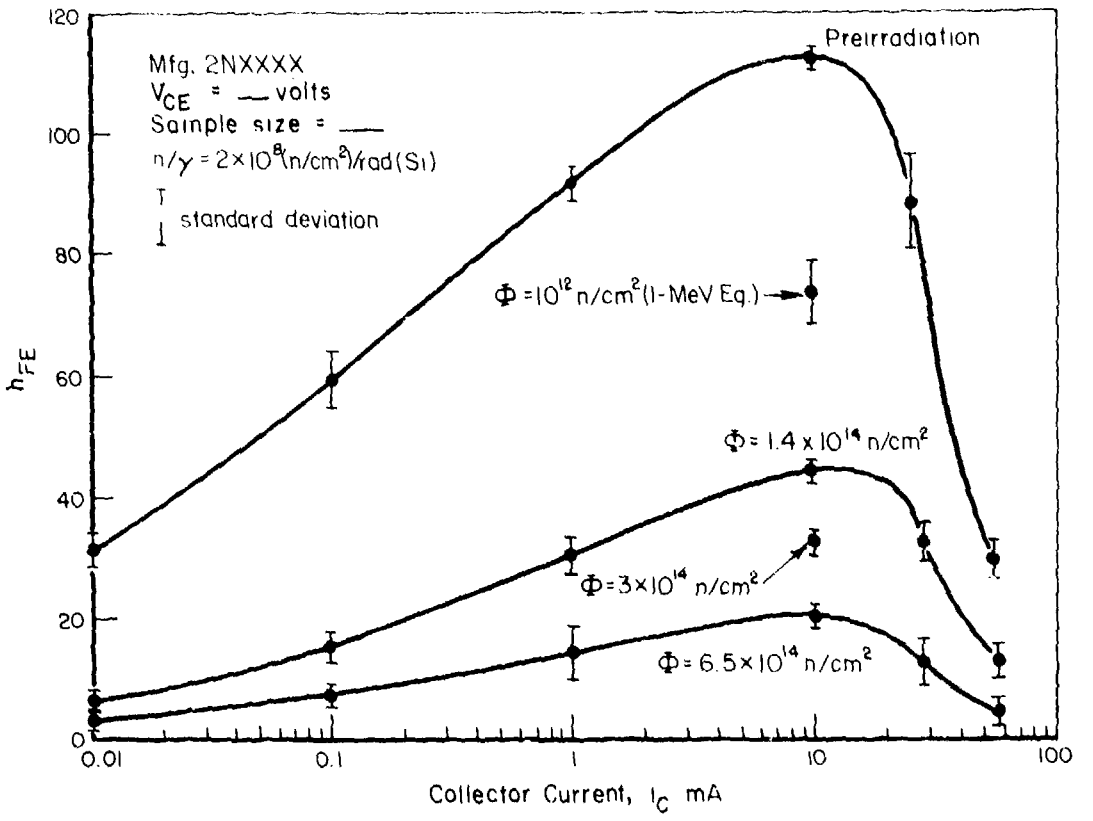

Figure 6.3-4. Format for reporting h_{FE} permanent-damage data.

Similar methods can be used to report permanent-effects data on field-effect devices and diodes. A curve showing the change in threshold voltage, ΔV_T, as a function of the gate bias at several gamma dose levels

is recommended for radiation tests on MOSFET devices. Permanent-effects data on diodes could include a family of curves showing the forward voltage versus forward current at various neutron fluences.

Consideration should also be given to calculating the constants for the radiation-damage models that are presently being used (i.e., the lifetime damage constant or the carrier-removal damage constant).

6.3.3 Ionization-Effects Data

The measured ionization response data of semiconductor devices should be tabulated in a format similar to the one described for permanent-effects data. Sample data formats are given in Figure 6.3-5 for diodes, bipolar transistors, and field-effect devices. Electrical device characterization data that are likely to be correlated with the radiation response, such as the storage time of a transistor, should also be recorded.

The graphical presentation of ionization-effects data as a complement to tabulated data is very desirable. A typical format for the graphical presentation of steady-state primary photocurrent, I_{pp}, as a function of ionizing-radiation dose rate is shown in Figure 6.3-6. For each device type on which ionizing-radiation data are reported, there should be an illustration showing a typical response as a function of time and displaying the leading and trailing edges of the pulse. The pulse shape should be given in sufficient detail to permit pulse-width scaling of peak photocurrent. The dose rate at which the response shape was taken should be indicated on the I_{pp} versus $\dot{\gamma}$ curve. In the event the shape of the I_{pp} response changes appreciably with dose rate, additional illustrations of response should be shown and areas of the I_{pp} curve to which they apply should be indicated.

The graphical and pictorial data that should be developed for general use include:

1. i_{pp} as a function of time
2. Steady-state I_{pp} versus $\dot{\gamma}$ and device relaxation time
3. Q_{pp} versus γ and device relaxation time
4. i_{pp} or Q_{pp} versus voltage
5. Equilibrium I_{sp} and t_{sR} versus $\dot{\gamma}$.

Device Type: _____

Date: _____

Unit Desig	Rev. Bias	I_{pp}	Q_{pp}	τ	t_{sR}	I_Z	V_Z	ΔV_Z	Dose Rate	Dose	Pulse Width	Comments
	V	mA	Q	μs	μs	mA	V	V	rad(Si)/s	rad(Si)	μs	

a. Diodes

Device Type: _____

Date: _____

Unit Desig	V_{CB}	V_{EB}	I_{ppc}	I_{ppe}	Q_{ppc}	Q_{ppe}	τ_{CB}	τ_{EB}	I_{sp}	t_{sR}	Dose Rate	Dose	Pulse Width	Comments
	V	V	mA	mA	Q	Q	μs	μs	mA	μs	rad(Si)/s	rad(Si)	μs	

b. Bipolar transistors

Device Type: _____

Date: _____

Unit Desig	V_D	V_G	I_{ppd}	I_{ppg}	Q_{ppd}	Q_{ppg}	τ_D	τ_G	I_{sp}	t_{sR}	Dose Rate	Dose	Pulse Width	Comments
	V	V	mA	mA	Q	Q	μs	μs	mA	μs	rad(Si)/s	rad(Si)	μs	

c. Field-effect transistors

Figure 6.3-5. Sample formats for recording ionization-effects data.

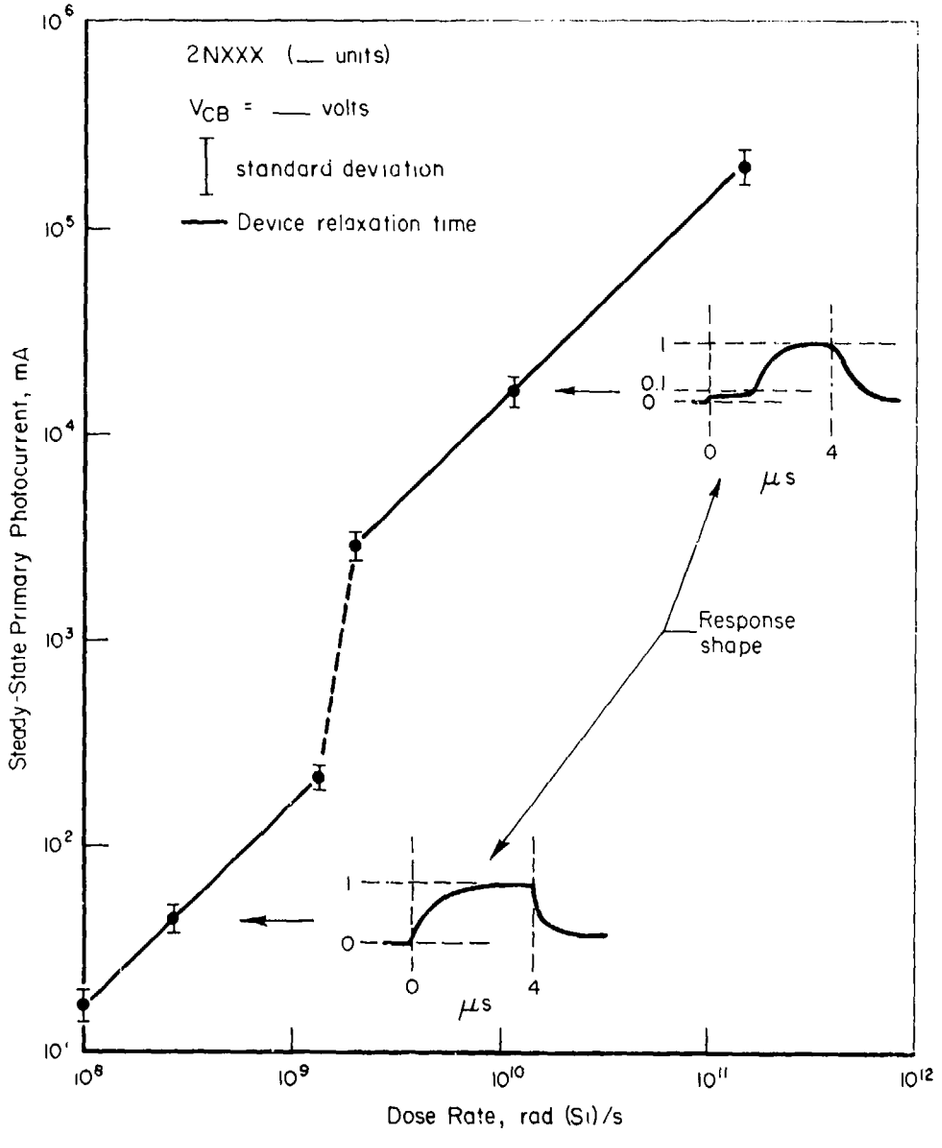

Figure 6.3-6. Format for reporting primary-photocurrent data.

CHAPTER 7

TEST PROCEDURES FOR CAPACITORS

7.1 SCOPE

This chapter discusses the procedures for determining the currents and voltages in charged and uncharged capacitors exposed to a transient radiation environment. While permanent changes such as degradation of the dielectric or physical distortion of the capacitor are observed in some capacitor parameters, the most important effects are due to ionization within the capacitor structure and are, therefore, transient. The mechanisms of the capacitor response will not be described in this chapter. It is recommended that the user familiarize himself with the appropriate sections of Reference 1.

7.2 PARAMETERS TO BE MEASURED

7.2.1 Conductivity

For the most common capacitance values, the predominant effect on a charged capacitor exposed to radiation is the induced conductivity in the capacitor dielectric. An exception to the dominance of the conductivity has been observed in capacitors with very low capacity (10 to 100 pF), where the secondary-emission signal may be larger than the conductivity signal (Section 7.3). The radiation-induced conductivity tends to cause a discharge of the capacitor, producing a current in the capacitor-charging circuit. Both the magnitude and the time dependence of this conductivity are of interest.

Figure 7.2-1 shows currents in a typical charged capacitor resulting from radiation photoconductivity response due to a square pulse of radiation. The photoconductivity response is usually divided into prompt and delayed components. The prompt component occurs simultaneously with the radiation and disappears at the termination of the pulse. Delayed components persist following the cessation of radiation, decaying with characteristic relaxation times which may be a function of the dose deliver d by the radiation pulse.

The conductivity in the dielectric is given by

$$\sigma = \sigma_0 + \sigma_r \ ,$$

where σ_0 = leakage conductivity of the dielectric and σ_r = radiation-induced conductivity. Normally, σ_0 is small enough so that it can be neglected.

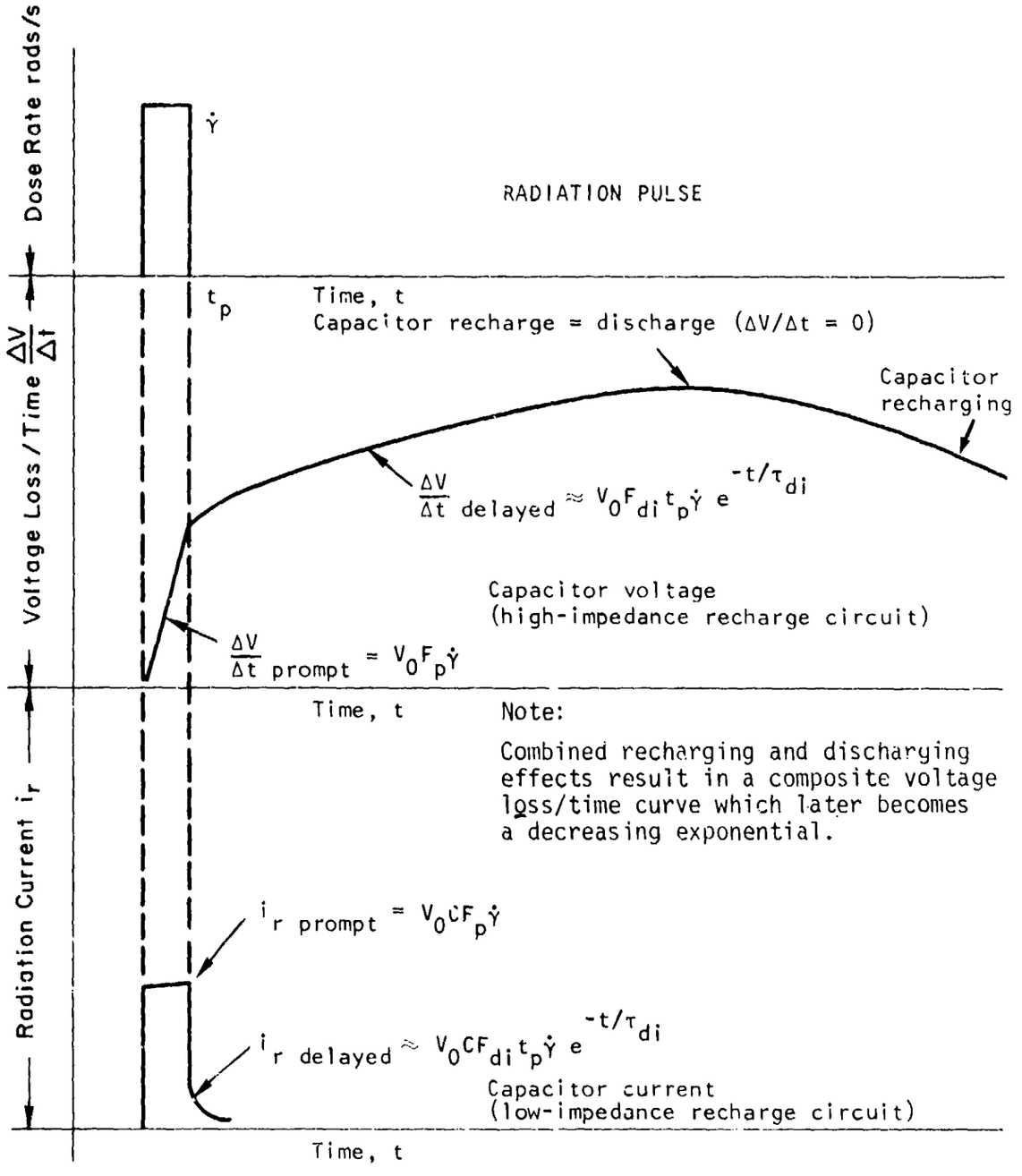

Figure 7.2-1. Capacitor photoconductivity characteristics.

The experimentally determined parameter is the current in the dielectric as a function of time, i(t), which is related to the conductivity $\sigma_r(t)$ by

$$i(t) = \frac{CV_0}{\varepsilon\varepsilon_0}\sigma_r(t) \ , \tag{7-1}$$

where C is the capacitance, ε is the relative dielectric constant, and ε_0 is the permittivity of free space.

The radiation-induced conductivity can be written

$$\sigma_r = \sigma_p + \sum_i \sigma_{di} \ , \tag{7-2}$$

where, for short-pulsed radiation,

$$\sigma_p = F_p(\gamma)\dot{\gamma} \ , \tag{7-3}$$

$$\sigma_{di} = F_{di}(\alpha)\int_{-\infty}^{t} \dot{\gamma}(t')[\exp -(t - t')/\tau_{di}]dt' \ , \tag{7-4}$$

where

$$\alpha = \gamma, \ t_p < \tau_{di}; \ \alpha = \dot{\gamma}\tau_{di}, \ t_p > \tau_{di} \ . \tag{7-5}$$

In these equations,

σ_r = radiation-induced total conductivity

σ_p = prompt portion of the conductivity

σ_{di} = i^{th} delayed conductivity component

$F_p(\gamma)$ = prompt conductivity fitting parameter that may be a function of total dose

$\dot{\gamma}$ = instantaneous dose rate during the pulse

$F_{di}(\alpha)$ = fitting parameter of the i^{th} delayed component, and a function of the dose rate times the pulse width ($\dot{\gamma}t_p = \gamma$) if the pulse width is shorter than the i^{th} decay constant, or the dose rate times the decay time for pulse widths longer than the decay constant

τ_{di} = decay constant of the i^{th} delayed component, which may vary during the decay.

The parameters in Equation 7-9 can be related to those in Equations 7-3 and 7-4 through

$$F_{d1} = \frac{\varepsilon\varepsilon_0}{V_{BI}} \frac{A_1}{\gamma} \left[\frac{1}{\tau_1} - \frac{1}{RC}\right] \tag{7-10}$$

$$F_{d2} = \frac{\varepsilon\varepsilon_0}{V_{BI}} \frac{A_2}{\gamma} \left[\frac{1}{RC} - \frac{1}{\tau_2}\right]$$

$$\tau_{d1} = \tau_1 , \quad \tau_{d2} = \tau_2 ,$$

where

$$\gamma = \int_0^{t_p} \dot{\gamma} dt$$

V_{BI} = built-in voltage.

F_p is determined as described in Section 7.7, Data Analysis.

7.2.3 Space-Charge Polarization--First Pulse Effects

The buildup and discharge of space charge in the dielectric during radiation testing are very important phenomena that can greatly affect the results of capacitor testing.

A "polarization effect" that is attributed to space-charge buildup within the dielectric material due to nonuniform trapping has been observed with most capacitors, particularly with Mylar, paper, mica, polycarbonate, and tantalum oxide devices. The effect is manifested in several ways. One of these is an apparent decrease in the induced conductivity with sequential radiation pulsing. Charge transfer across the dielectric during a radiation pulse builds up a space-charge field opposing the applied electric field. If the applied electric field is then removed, subsequent radiation pulses result in a current in the external circuit that is opposite in direction to that observed with the field applied. This is caused by the discharge of the space-charge field. Similarly, if the electric field is reversed rather than removed after the space charge has been built up, the space-charge field enhances the applied field and a larger current results than would normally be observed. Thus, the first pulse at a given polarity of voltage produces the largest response.

Saturation of the polarization effect, where no further decrease in the charge transfer is observed with subsequent radiation pulses, occurs after

The parameters in Equation 7-9 can be related to those in Equations 7-3 and 7-4 through

$$F_{d1} = \frac{\varepsilon\varepsilon_0}{V_{BI}} \frac{A_1}{\gamma} \left[\frac{1}{\tau_1} - \frac{1}{RC}\right] \tag{7-10}$$

$$F_{d2} = \frac{\varepsilon\varepsilon_0}{V_{BI}} \frac{A_2}{\gamma} \left[\frac{1}{RC} - \frac{1}{\tau_2}\right]$$

$$\tau_{d1} = \tau_1 , \quad \tau_{d2} = \tau_2 ,$$

where

$$\gamma = \int_0^{t_p} \dot{\gamma} dt$$

V_{BI} = built-in voltage.

F_p is determined as described in Section 7.7, Data Analysis.

7.2.3 Space-Charge Polarization--First Pulse Effects

The buildup and discharge of space charge in the dielectric during radiation testing are very important phenomena that can greatly affect the results of capacitor testing.

A "polarization effect" that is attributed to space-charge buildup within the dielectric material due to nonuniform trapping has been observed with most capacitors, particularly with Mylar, paper, mica, polycarbonate, and tantalum oxide devices. The effect is manifested in several ways. One of these is an apparent decrease in the induced conductivity with sequential radiation pulsing. Charge transfer across the dielectric during a radiation pulse builds up a space-charge field opposing the applied electric field. If the applied electric field is then removed, subsequent radiation pulses result in a current in the external circuit that is opposite in direction to that observed with the field applied. This is caused by the discharge of the space-charge field. Similarly, if the electric field is reversed rather than removed after the space charge has been built up, the space-charge field enhances the applied field and a larger current results than would normally be observed. Thus, the first pulse at a given polarity of voltage produces the largest response.

Saturation of the polarization effect, where no further decrease in the charge transfer is observed with subsequent radiation pulses, occurs after

one or more pulses, depending on the capacitor and on the dose delivered in each pulse. Decreases of 50 to 70 percent for mica, 10 to 20 percent for tantalum oxide, and 30 percent for Mylar have been observed due to this space-charge buildup during radiation pulsing. Test results indicate that the degree of polarization is dose dependent.

To examine the polarization and its effect on zero-applied-voltage signals, it is recommended that the magnitude of the polarization be determined as follows:

1. With an applied voltage, expose the capacitor to successive radiation pulses until saturation of the polarization is achieved. Note the dose for saturation.
2. Discharge the space-charge field (depolarize) by pulsing the radiation at zero applied volts until the normal zero-volt signal is achieved.
3. Reapply the voltage and, with radiation pulses of 1/10 to 1/20 of saturation dose each, measure the signal as a function of dose.
4. When saturation is reached, remove the voltage and measure the zero-volt signal as a function of dose.

Conductivity data should be taken using the first pulse at a given voltage. Each pulse with the voltage applied should be followed by a sufficient number of pulses (10 or more) at zero applied volts to restore the device to its normal condition before the next measurement is performed.

Stored charge effects that produce anomalous first-pulse responses are sometimes seen in electrolytic (e.g., tantalum) capacitors. Measurements of response of these capacitors should always include repeat measurements of the first level tested as a check for these effects.

7.3 GENERAL TEST CONSIDERATIONS

7.3.1 Test Specimens

The materials and construction of commercially available capacitors may be the primary source of uncertainty in the results when these devices are irradiated. Capacitors whose measurable electrical characteristics are very nearly equal will respond very differently to a radiation pulse. Random sampling from various production lots is advisable to obtain representative results in the basic characterization of a capacitor type.

The orientation of the capacitor specimen is critical in linear accelerator (LINAC) and flash X-ray studies since it can influence the uniformity of dose deposition. It is generally advisable to orient the capacitor so that the beam will penetrate the specimen perpendicular to the

capacitor's major axis. The conductivity due to highly ionizing particles may have a strong dependence on the orientation of the capacitor plates and dielectric to the incident flux.

The positioning of the test specimens for pulsed-reactor studies may not be as critical as for other studies, except for consistency, since neutron and gamma radiations are very penetrating. It is recommended that the capacitor be oriented with its major axis perpendicular to a straight line extending through the center of the reactor core.

7.3.2 Temperature

The monitoring and recording of the temperature to obtain adequate data for analysis is especially important for capacitors since the radiation-induced effect may be temperature dependent. Special temperature studies may even require the continuous monitoring of the temperature. Directly attaching thermistors or thermocouples to the test capacitor is the recommended method for measuring temperature. Possible degradation of the temperature sensor must be a consideration when performing these tests since it also is exposed to the radiation.

7.3.3 Voltage Dependence

The voltage dependence of the radiation-induced response should be measured at each exposure level of interest. Both polarities of voltage should be applied, if possible, with the usual precautions for depolarization between each data point. Unusual behavior in the voltage dependence is a good diagnostic for "maverick" capacitors or improperly operating test circuitry.

Since the induced current is voltage dependent, care must be taken to ensure that an excessive change in the voltage operating point does not occur during the radiation transient. Test circuits using sampling resistors are normally prone to this problem since a sizable radiation-induced current can cause a significant voltage drop across the sampling resistor. Even with low-impedance systems, such as current probes, problems can occur at very high dose rates or with devices exhibiting a high level of response. Voltage-stabilizing capacitors, to be used in parallel with the voltage source, should be selected to maintain the source voltage to within ±5 percent during the radiation pulse.

7.3.4 Spurious Currents

Noise suppression is discussed in Section 2.5. Of particular importance to capacitor testing are those currents arising from cable currents, air ionization, and secondary emission. These sources must be eliminated or accounted for in all capacitor testing.

7.4 RADIATION SOURCE CONSIDERATIONS

LINACs are the most useful single source for dielectric characterization. Pulse widths within the nanosecond to microsecond range are obtainable and the pulse height can be changed for each pulse width, allowing dose and dose rate to be varied independently. Flash X-ray machines are also used as electron-beam generators for testing dielectrics. An advantage of the flash X-ray machine over the LINAC is the larger irradiation volume capability that permits simultaneous tests on several devices. Chapter 4 describes each of these machines and the selection criteria.

Pulsed reactors are also used to characterize the radiation response of capacitors. In reactor testing, the capacitor response results from a mixed neutron-gamma field due to the mixing of the effects of the isolated electron pairs and the highly ionized particles from the (n,p) reactions. The proton effects are especially important in organic dielectrics. Lead and polyethelyne shields can be placed between the radiation source and the exposed component to help separate the neutron and gamma effects. The pulsed reactor is useful for characterizing dielectrics with relatively long time constants for the delayed component. Reactor selection criteria are discussed in Chapter 4.

7.5 RECOMMENDED APPROACHES

The two recommended approaches for determining the response of charged capacitors to transient radiation are a voltage- or charge-loss technique, with the data interpretation in terms of $\Delta V/V_0$; and current-measurement techniques, with the data being interpreted in terms of the photoconductivity-equation parameters.

The $\Delta V/V_0$ approach (charge loss) measures the amount of charge transferred to the plates of the capacitor as a function of time. Although the prompt current, I_p, is generally much larger than the delayed current, I_d, the prompt charge, $\sim I_p t_p$, may be of the same order as the delayed charge, $\sim I_d \tau_d$, if t_p is chosen to be much less than τ_d. Thus, for short pulses, the charge-measurement technique requires less dynamic range in the instrumentation than the current-measurement technique. The charge method is well suited for delayed-conductivity-component measurements and is recommended when the delayed charge transport is important. Care must be taken in these measurements that the voltage across the capacitor does not change by more than about 10 percent. Since spurious signals are difficult to identify by their time dependence in this technique, such signals must be carefully eliminated.

When fast-time-resolution measurements are desired or when the prompt current pulse is most significant, the current-measurement technique is recommended. Spurious signals are also more readily identified with the

fast time resolutions available with this technique. The instrumentation for current measurements should have a wide dynamic range.

7.6 SPECIFIC TEST PROCEDURES

"First-pulse" effects should always be kept in mind when testing capacitors. The unbiased response should be measured for the first few irradiation pulses to check for stored charge release. Conductivity data should be taken on thoroughly depolarized capacitors. After each exposure with applied voltage, the capacitor should be pulsed with zero applied bias until the zero-volt signal is constant from pulse to pulse.

7.6.1 Parameter Variations

A systematic variation of the important factors is required when performing tests whose purpose is the basic characterization of a dielectric. This is accomplished by holding relevant variables constant except the one under study. For example, to determine a voltage dependence, all other variables such as the incident dose rate, the pulse width, and temperature are controlled to avoid confusing effects from variations occurring in one or more of these parameters with the effect of voltage.

The single-parameter-variation tests that are the most important in capacitor testing are:

1. Dose-rate dependence. Each of several capacitors should be exposed to a wide range (preferably at least 100:1) of dose rates while the dose is held constant. This test is limited to a LINAC as the radiation source; flash X-ray sources are not suitable since the pulse width is fixed.

2. Dose dependence. Each of several capacitors should be exposed to a series of pulse widths while the dose rate is held constant. This test is limited to a LINAC as the radiation source because of the availability of variable pulse widths.

3. Voltage dependence (to verify the direct proportionality of response current to applied voltage). This test should be performed on at least one sample of a given type.

4. Capacitance (to verify the direct proportionality of response current to capacitance). Capacitors within a specific type or family group, covering a range of capacitance values but having the same working voltage, can be tested. With careful test structuring, this information can be obtained from the analyses of other tests.

5. Temperature dependence. This test should be performed on several samples of dielectric types known to be temperature sensitive.

6. Reproducibility. This test should be performed on a few individual samples under random test conditions. Some redundancy should also be included; i.e., several different samples should be measured under the same test conditions to estimate the precision of measurement and the sample-to-sample variations.

It should not be inferred that all these tests have to be performed for a complete test. Perform only those tests that will satisfy the test objectives. Variation testing as described above requires a rather large matrix or sequence of measurements. Therefore, multiple-channel testing is desirable when the radiation source and economics permit.

7.6.2 Basic Requirements

The transient response of a capacitor due to photoconductivity is determined from measurement of capacitor voltage loss or the radiation-induced current. Analysis of the data from either measurement will produce the required photoconductivity parameters. A supplementary measurement is the replenished charge that is the integral of the radiation-induced current.

Radiation-induced current transients are monitored by two methods: measuring the voltage drop across a sampling resistor in series with the device and measuring the output of a current transformer (current probe) used in the circuit. Capacitor-voltage-loss transients are monitored by measuring the voltage across the test device.

Adequate data for interpretation of the test results is essential. The basic requirements for data common to all tests are:

1. Identification of all test equipment
2. Accuracy of all test equipment
3. Radiation pulse shape (LINAC and flash X-ray)
4. Neutron spectrum (pulsed reactors)
5. Instrument scale factors
6. Capacitor orientation with respect to the beam or reactor core
7. Exact circuit configuration, including grounding scheme
8. Ambient temperature measurement
9. Dosimetry.

7.6.3 Capacitor-Voltage-Loss Measurements

Figure 7.6-1 illustrates the recommended circuit for measuring capacitor voltage loss, ΔV, during exposure to transient radiation. Use of this circuit and/or measurement should be limited to experiments involving radiation-pulse widths and intensities (i.e., dose/pulse) such that the capacitor voltage loss does not introduce significant error in the analysis ($\Delta V \leq 10$ percent). The limiting factor in the analysis is the assumption of a constant applied voltage. In Figure 7.6-1, V_0 is the bias voltage, R is the load resistance, C_2 is the power supply bypass capacitor, and R_2 is for high-frequency isolation ($R_2 \geq 20\Omega$). C_2 must be large enough to supply the transient current during radiation. The time constant $2R_2C_2$ should be larger than any time constant of interest.

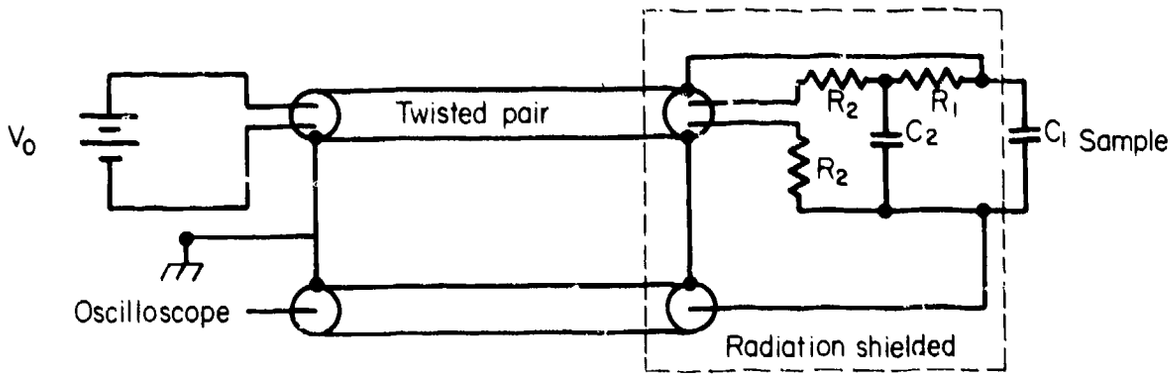

Figure 7.6-1. Voltage-measurement circuit.

The voltage-measurement circuit is essentially an "open" circuit technique and requires that the capacitor recharge time constant be long ($R_1C_1 >> \tau_d$). This means that after one circuit time constant, R_1C_1, the capacitor voltage change should still be greater than two thirds of the peak response. If this is not the case, the resistance value of R_1 should be increased to meet this circuit requirement. Note that since R_1 is in the ground leg of the circuit, the oscilloscope system can be dc coupled and R_1 can be made as large as necessary.

Data to be recorded in addition to those listed in Section 7.6.2 include C, R_1, V_0, and ΔV versus time.

7.6.4 Sampling Resistor Technique for Short-Pulse Measurements

Figure 7.6-2 illustrates the recommended circuit for measuring radiation-induced current by the resistor method. This circuit is used when maximum sensitivity is required or when the time duration of the transient current exceeds the pulse-width capability of current probes. R_o is the cable termination impedance, C_2 is the power supply bypass capacitor, and R_1 is the load resistance. R_1 is selected to satisfy one of the following criteria:

1. For best pulse response, R_1 should equal R_o.
2. For maximum sensitivity, R_1 may be omitted.
3. When operating, point deviations must be held to a minimum and sensitivity is not critical, R_1 may be very small. Note that the conductivity current-induced voltage across the resistors R_1 equals the change in voltage across the test capacitor and should be kept to 1 percent or less of the applied voltage.

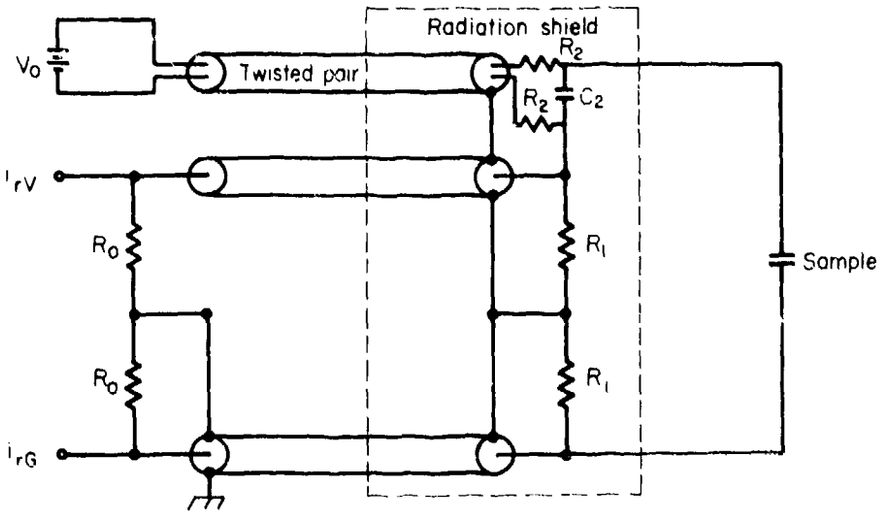

i_{rV} = radiation current in voltage lead of sample
i_{rG} = radiation current in ground lead of sample

Figure 7.6-2. Current-measurement circuit using sampling resistor.

If a good radiation-insensitive amplifier system is available, its insertion in the signal-measuring cables near the sample allows the option of increasing R_1 for enhanced sensitivity or desired integration.

Data to be recorded in addition to those listed in Section 7.6.2 include C, R_1, R_o, i_r versus time, and V_0. This circuit eliminates noise in the output cables and the spurious signal due to the symmetric component of the charge emission. It does not eliminate any unsymmetric component of the charge emission. In some installations, the low side of the capacitor can be grounded and the ground signal eliminated.

7.6.5 Current-Probe Sampling

The recommended circuit for measuring the radiation-induced current by the current-probe method is illustrated in Figure 7.6-3. This circuit is used when minimum deviation of the operating point is required. R_o is the cable termination impedance chosen to match the current probe, CT is a current transformer with a suitable response characteristic, and C_2 is the power supply bypass capacitor. A series resistance may be required to eliminate oscillations when performing some measurements. A compromise between desired high-speed response and the reduction of oscillation must be sought with this circuit.

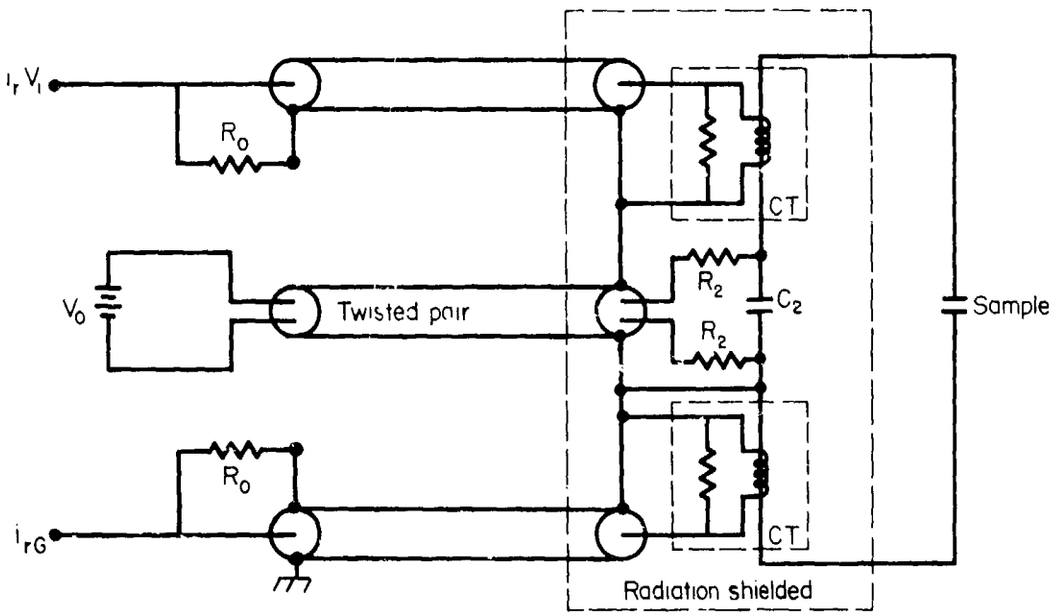

Figure 7.6-3. Current-measurement circuit using current transformers.

Data to be recorded in addition to those listed in Section 7.6.2 include C, R_o, i_r versus time, V_0, and the current transformer identification. This circuit is usually not suited for longer term delayed component measurements.

7.6.6 Replenished-Charge Measurement

The most commonly used technique for determining replenishment charge is the measurement of capacitor voltage loss in a long-time constant circuit (see Section 7.6.3). This technique covers a very large dynamic range in current and time. Other methods of determining this parameter, which is the integral of the radiation-induced current, are by manually extracting the information from a photograph of the current display or by electronically integrating the current signal as shown in Figure 7.6-4.

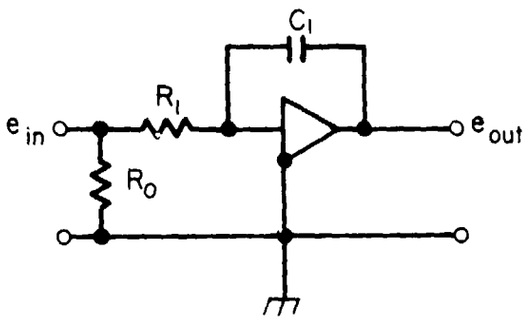

Figure 7.6-4. Charge-integration measurement circuit.

The required period of integration can be determined experimentally by integrating a known current. The time constant of the integrator, determined by R_1 and C_1, must be very long when compared with the period of integration in order to have a negligible loss of charge during the period of integration. Charge is determined from the following relation:

$$\int V_{in} dt = V_{out}(R_1 C_1) \quad . \tag{7-11}$$

7.6.7 Direct Measurement of i_r for Pulsed-Reactor Tests

Differentiation of the current through the sampling resistor (V_R/R_1) yields a direct indication of i_r as a function of time. Figure 7.6-5 illustrates the recommended differentiation circuit. R_i and C_i are chosen so their product nearly equals the circuit time constant T, R_f and C_i are chosen so that $R_f C_i$ is small enough for accurate differentiation, and C_2 is the power supply bypass capacitor.

Data to be recorded in addition to those listed in Section 7.6.2 include C, R_i, C_i, R_f, di/dt, and V_0.

The operational amplifier is used as a differentiator on one oscilloscope channel to measure di/dt, while another channel uses a conventional

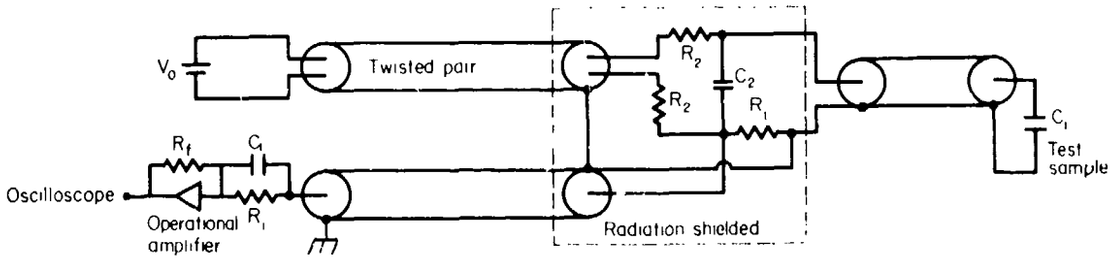

Figure 7.6-5. Circuit for direct measurement of i_r, long pulses.

preamplifier to record voltage. The induced current, i_r, is then determined from

$$i(t) = i_r(t) + R_1 C_1 \frac{di}{dt} . \qquad (7\text{-}12)$$

A background test should be performed, prior to the testing of capacitors to determine if the noise level that may be associated with the analog differentiation of this circuit is excessive.

As an aid to accurate analysis of the transient effects data, a time-mark generator should be used to accurately determine the time correlation between the radiation burst and component behavior in this method of measurement. Timing marks should be superimposed on all oscilloscope traces taken during a particular reactor pulse. In addition, one timing mark should be placed between two others near the center of the trace to act as a master time mark. This method allows for the absolute determination of simultaneity among the oscilloscope traces taken during a single reactor pulse.

7.7 DATA ANALYSIS

A variety of analytical methods have been used to determine critical characterizing parameters from the measured response of common dielectric capacitors to the transient radiation environment. The following analytical methods are relatively straightforward in concept and application. They are basically applicable to all radiation sources, with the exception that any analysis with capacitor voltage loss data, $\Delta V/V_0$, should be limited to short radiation pulses (LINAC and flash X-ray). Although other methods may be appropriate for data analyses, deviations from these preferred procedures must be justified.

7.7.1 Determination of F_p from Voltage-Loss Data

For a short square radiation pulse ($t_p \ll \tau_d$), F_p can be determined from capacitor voltage loss or radiation-induced current data through the following relationship:

$$\frac{1}{V_0}\frac{dV}{dt} = F_p \dot{\gamma} = i_r/CV_0 \ , \qquad (7\text{-}13)$$

where

$\frac{dV}{dt}$ = slope during pulse (see Figure 7.2-1)

V_0 = applied voltage.

7.7.2 Determination of F_d from Voltage-Loss Data

Analysis involving more than one delayed component of conductivity requires curve fitting for separation of the components in the observed composite decay. However, it is estimated that for 95 percent of circuit analysis problems, a single exponential function describing the delayed photoconductivity is adequate.

Therefore, assuming a single delayed component, σ_d, and short pulses ($t_p << \tau_d$) of constant dose rate,

$$\sigma_d \sim F_d \dot{\gamma} t_p e^{-t/\tau_d} \qquad t > t_p. \qquad (7\text{-}14)$$

For a short time following the pulse,

$$F_d = \frac{1}{V_0 \dot{\gamma} t_p}\frac{\Delta V}{\Delta t} \ , \qquad (7\text{-}15)$$

where $\Delta V/\Delta t$ is the constant slope of the observed curve immediately following the pulse.

7.7.3 Determination of Decay-Time Constant from Voltage-Loss Data

The high resistance (R_1) in series with the battery in the capacitor voltage-loss circuit (Figure 7 6-1) restricts the flow of recharging current to the capacitor. Thus, current flow due to the delayed conductivity immediately following the radiation pulse is essentially from the capacitor storage:

$$i_0 = C_1 \frac{\Delta V}{\Delta t} \qquad t_p < t << \tau_d \ . \qquad (7\text{-}16)$$

At the time of maximum response, t_m, the capacitor recharge and discharge currents are equal and $\Delta V/\Delta t = 0$ (Figure 7.2-1). The current, $i(t_m)$, is obtained by dividing the maximum voltage at this instant in time by the series resistance, R_1. The decay time constant, τ_d, is determined from these parameters through the following relationship:

$$\tau_d = \frac{t_m}{\ell n \left(\frac{i_0}{i(t_m)} \right)} \quad . \tag{7-17}$$

7.7.4 Parameter Determination from Radiation-Induced-Current Data

For a short square radiation pulse ($t_p << \tau_{di}$), F_p can be determined from the radiation-induced current data:

$$i_r = \varepsilon\varepsilon_0 C_1 V_0 \left[F_p \dot{\gamma} + \sum_i F_{di} \gamma e^{-(t-t_p)/\tau_{di}} \right] . \tag{7-18}$$

where γ is the dose in the pulse and $t = 0$ corresponds to the beginning of the pulse. For $t = t_p$,

$$F_p = i_r / \varepsilon\varepsilon_0 C_1 V_0 \dot{\gamma} \quad . \tag{7-19}$$

The prompt component can then be subtracted from the signal, and F_{di} and τ_{di} unfolded by standard graphical techniques.

7.7.5 Special Considerations for Electrolytic Capacitors

The built-in voltage, V_{BI}, modifies the response of electrolytic capacitors and some special considerations apply.

The value of V_{BI} can be determined by irradiating the capacitors at a low dose rate (e.g., with a Co^{60} source) with one end grounded and the other end connected to a high-impedance voltmeter ($\sim 10^{11} \Omega$ to ground). The voltage across the capacitor will rise to a saturation value approximately equal to V_{BI}.

The recommended circuit is shown in Figure 7.6-2 where $R_1 C >> t_p$. The data can be readily fitted to Equation 7-9.

The parameter F_p can be calculated from

$$\frac{1}{V_0 + V_{BI}} \frac{dV}{dt} = F_p \dot{\gamma} \quad . \tag{7-20}$$

To determine the conductivity parameters for an applied voltage from fitting Equation 7-9, simply replace V_{BI} in Equation 7-10 by $V_0 + V_{BI}$. Note that since V_{BI} is less than a few volts, it can be neglected for large values of V_0.

7.7.6 Special Considerations in the Analysis of Data from Flash X-Ray Studies

The burst shape at a flash X-ray cannot be described well in closed form (mathematically). This means that the analysis must be based on approximate descriptions of the burst shape or computer-aided numerical techniques.

The most common technique is to assume that the flash X-ray pulse is adequately represented by a square wave that has a pulse width equal to the flash X-ray pulse width at half-maximum amplitude. The effective dose rate for the square wave is determined from the dose delivered in the flash X-ray pulse.

A more satisfactory technique is to use a computer and a curve-fitting technique. A numerical description of the actual flash X-ray burst shape is applied to Equation 7-16 using estimated values for the conductivity parameters. The resulting radiation-induced current as a function of time is then applied to the measurement circuit equation, usually Equation 7-10, to obtain a prediction of the circuit current as a function of time. After comparing the predicted and measured responses, refinements can be made in the estimated values of the conductivity parameters. Successive passes with this procedure will lead to an accurate determination of the desired parameters. This iterative technique is expensive and time consuming but probably most accurate. It is important that the response measurements be relatively free from spurious current effects.

7.7.7 Special Considerations in Analysis of Data from Pulsed Reactor Studies

The general characteristics of the radiation-induced conductivity will be discussed in terms of the induced current, i_r. During the initial rise of the radiation pulse, i_r is proportional to the dose rate, $\dot{\gamma}$, modified by the dose dependence of F_p. If the F_p is a constant in this time interval, a semilog plot of i_r and $\dot{\gamma}$ versus time will indicate the same period for both quantities, provided they are actually proportional. They would be proportional for this interval since the dose rate, $\dot{\gamma}$, is rising exponentially. The function F_p can be determined from LINAC data if it is not constant. For an exponentially rising burst shape, a semilog plot of i_r and $\dot{\gamma}$ versus time is shown in Figure 7.7-1, where F_p = constant and indicates equal periods for the initial rise.

The induced current is not proportional to $\dot{\gamma}$ at the later times in the burst; it does not decrease as rapidly as the dose rate (Figure 7.7-1). The magnitude of the current at the start of the decay is much larger than the current that can be induced by the residual radiation existing at this time. It would be expected that the current would decay exponentially with a time constant equivalent to the circuit time constant. However, it is

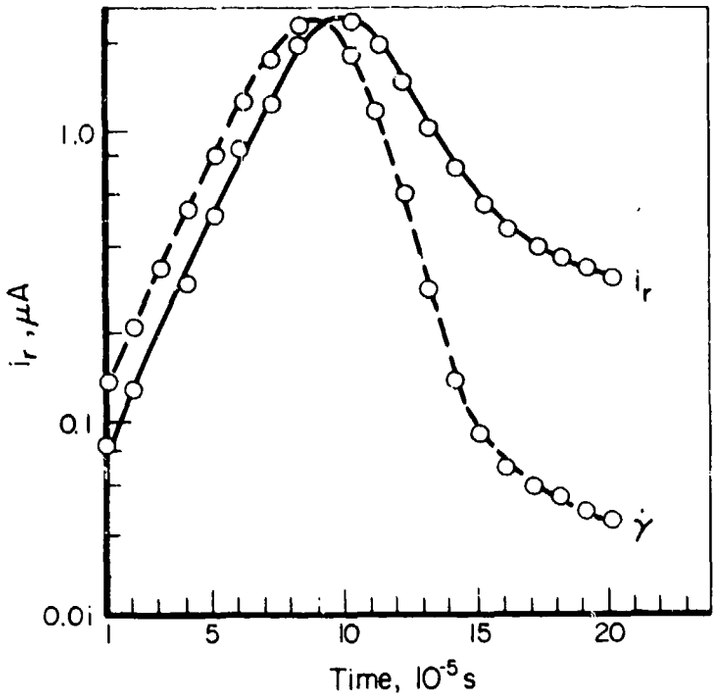

Figure 7.7-1. Sample i_r and $\dot{\gamma}$ during a pulsed reactor burst.

evident from the figure that i_r maintains a value that is disproportionately large compared with that during the major portion of the burst. This is clearly indicative of a delayed component in i_r. This delayed component, τ_d, is then determined from the slope of this semilog plot over the chosen measurement time interval.

7.8 DATA REPORTING

If the test was conducted as a simple proof test, the test circuit and temperature during irradiation should be given along with the beam energy and pulse width of the machine. A reproduction of the pulse shape is desirable. Any procedure used to reduce spurious currents should be described in detail. For each sample, the applied voltage, capacitance, working voltage, dose rate, and dose (in rads (dosimeter)) are required along with the maximum circuit current achieved. The bias history of the capacitor should also be reported. It is recognized that proof-test data are generally of little value to anyone other than the user, but by reporting the data in this way, their usefulness and validity can be better assessd.

For basic dielectric-characterization tests, the method of analysis should be described. In addition to the information given above, the following information is also required for each sample: the derived values of

Serial No.	Rated Capacitance, μF	Tolerance, ± %	Working Voltage	Case Size	Manufacturer	Measured Capacitance @1 kc, μF	Date of Manufacture	Date of Purchase	Unit Designation in Test

a. Parts tabulation

Date _____

Unit Designation	V, ± volts	Dose Rate, rads (Si)/s	Dose, rads (Si)	Pulse Width, μs	T, C	F_p/ϵ_0, rad^{-1}	F_{d1}, Ω-cm/rad	τ_1, μs	F_{d2}, Ω-cm/rad	τ_2, ms	Etc.

b. Capacitor ionization-effects data

Figure 7.8-2. Sample data formats.

If measurements were made to determine the relative neutron ionization effectiveness, the shield arrangements and the neutron-to-gamma ratios obtained should be presented, along with any neutron-spectrum measurement results. For each sample, the neutron fluxes, the proportionality constant, F, and the ratio of the neutron-induced current to the total current should be given.

Serial No.	Rated Capacitance, μF	Tolerance, ± %	Working Voltage	Case Size	Manufacturer	Measured Capacitance @ 1 kc, μF	Date of Manufacture	Date of Purchase	Unit Designation in Test

a. Parts tabulation

Date__ _____

Unit Designation	V, ± volts	Dose Rate, rads (Si)/s	Dose, rads (Si)	Pulse Width, μs	T, C	F_p/ϵ_0, rad^{-1}	F_{d1}, Ω-cm/rad	τ_1, μs	F_{d2}, Ω-cm/rad	τ_2, ms	Etc.

b. Capacitor ionization-effects data

Figure 7.8-2. Sample data formats.

If measurements were made to determine the relative neutron ionization effectiveness, the shield arrangements and the neutron-to-gamma ratios obtained should be presented, along with any neutron-spectrum measurement results. For each sample, the neutron fluxes, the proportionality constant, F, and the ratio of the neutron-induced current to the total current should be given.

CHAPTER 8

INTEGRATED CIRCUITS

8.1 SCOPE

This chapter discusses procedures for determining the response of integrated circuits (ICs) to the nuclear-weapon environment. The integrated circuits are grouped into two general classes--digital and linear--although some interface circuits do not fall clearly into either class. Within these two classes, some additional distinctions are made as to the circuit function, design, and construction. Each integrated circuit type is designed to perform a specific task. The tests for the integrated circuit should be designed to evaluate its capability of performing this task. This chapter cannot cover all possible combinations of integrated circuits and parameters to be measured; it will present pertinent material from which specific tests necessary to characterize a particular integrated circuit type can be developed. In developing a test plan for these devices, it is important that the reader utilize the guidelines presented in this chapter and also utilize the information in Chapters 6, 7, and 8 of the Design Handbook for TREE (Reference 1) to estimate the gross response of the integrated circuit.

8.2 PERMANENT-DEGRADATION MEASUREMENTS

8.2.1 Neutron Damage in Integrated Circuits

Neutron interactions with silicon result in a reduction of the minority carrier lifetime causing a decrease of bipolar transistor gain, an increase in junction leakage currents, and a shift in junction voltages. A secondary effect, important at large neutron fluences, is carrier removal, which causes an increase in diode and transistor bulk resistances, a decrease in transistor gain at high currents, an increase in transistor saturation voltage, and changes in the equilibrium carrier concentration in majority carrier devices. The most significant of these changes is the degradation of transistor gain. Typically, the observed degradation in integrated circuit performance such as loss of fanout capability, loss of circuit gain, increased offset current, or changes in input biasing primarily reflects the loss in gain of the circuit transistors. Furthermore, the integrated circuit parameters just mentioned and the device's switching characteristics are sensitive to the rapid annealing phenomena (Chapter 8 of Reference 1).

8.2.2 Total Ionizing Dose Damage in Integrated Circuits

Large doses of ionizing radiation cause a positive space charge to accumulate within the oxide passivation layer and can cause an increase in

the density of interface states. These phenomena affect bipolar transistor gain, junction leakage current, junction breakdown voltages, and threshold voltages for MOS devices. Total dose effects are sensitive to bias conditions during irradiation. In addition, some annealing of total ionizing dose damage does occur.

Total ionizing dose effects on MOS digital-circuits cause a shift of the gate turn-on or threshold voltage of the transistors. The primary circuit response is a shift in the input threshold voltage and output levels. The failure level for these circuits depends strongly on the circuit design and the manufacturing process.

The effect of total ionizing dose on linear circuits results in changes of input offset voltage, input impedance, and input bias current.

8.2.3 Annealing

The annealing in integrated circuits may be quite different from that exhibited by simpler discrete devices due to changing internal operating conditions. In bipolar integrated circuits, most of the rapid annealing is due to the rapid annealing of the bipolar transistors. In MOS devices, the radiation-induced space charge in the $Si-SiO_2$ interface is characterized by a rapid annealing phase following the radiation burst. Rapid annealing is seen in digital circuits as a change in propagation delay, changes in source and sink currents, and threshold voltage changes. For linear amplifiers, rapid annealing affects the circuit gain and bias current.

In addition to rapid annealing, the radiation-induced parameter changes in integrated circuits exhibit some degree of long-term annealing as a result of room-temperature storage and continued operation. This room-temperature annealing is particularly important when characterizing surface effects. It is important that a record be maintained of the time and the bias conditions between irradiation and measurement.

8.2.4 Temperature

The electrical performance of integrated circuits can be significantly affected by temperature. For example, in digital circuits the lower the temperature, the smaller the gain margin and the less neutron degradation the circuit will be able to tolerate. Typically, integrated circuit temperature responses are larger than the changes due to thermal annealing and/or the difference due to the temperature dependence of the neutron damage. Therefore, it is possible to irradiate integrated circuits at a fixed temperature, such as room temperature, and to later measure their responses over the specific temperature range of operation. However, in the case of rapid annealing, the annealing factor is a strong function of irradiation temperature. Therefore, separate sets of data should be taken for rapid annealing of circuit response at each ambient temperature of interest.

Method 1017 of Reference 2 specifies exposure and storage temperatures for neutron irradiation, and Method 1019 specifies temperatures for total dose irradiation.

8.2.5 Parameters to be Measured

8.2.5.1 Digital Circuits

The output response of digital circuits is a nonlinear function of gain degradation and threshold voltage shifts. Threshold voltage shifts are a measure of the noise margin of a particular device. The electrical parameters most indicative of gain and noise margins are the voltage and current levels at the input and output terminals and the transfer characteristic between input and output. The voltage and current characteristics are useful since they tend to show circuit changes occurring before those changes significantly affect specified circuit operation. Input and output voltage and current levels should be measured for both logic states and should cover all possible loading configurations for the particular application under consideration. The discrete points that are generally characterized include high and low input current and voltage levels, output short circuit current, unsaturated output sink current, and high and low output voltage levels.

The number of parameters measured and the operating conditions during measurement and irradiation will be determined by the data requirements. Table 8.2-1 summarizes the operating configurations for the various digital circuit "black-box" tests usually of interest to the system designer for the assessment of neutron and total dose effects on digital integrated circuits. The effects of neutrons on integrated circuit switching performance and propagation delay are strongly dependent on the capacitance in the measuring circuit. To obtain consistent test results, the circuit configurations recommended by MIL-STD-883B should be used for all measurements (Reference 2).

8.2.5.2 Linear Circuits

Modern linear integrated circuit devices use two major types of technologies--bipolar with dielectric isolation, and MOS/SOS. Bipolar devices are affected predominately by neutrons; the MOS technologies are more sensitive to total dose effects. The most widely used linear/analog circuit functions are operational amplifiers, A/D and D/A converters, voltage comparators, and voltage regulators.

The primary cause of linear circuit failure is transistor gain degradation. This degradation is characterized by radiation-induced changes in the transfer characteristics. The more significant changes occur in the current gain, input bias current, and the input offset voltage and current. Parameters of interest are listed in Table 8.2-2.

JFET input stages are not subject to significant gain degradation, but other parameters, such as offset voltage and leakage current, may change significantly.

In general, a large variety of test configurations is available for linear circuits. The configuration used should be dictated by the objective of the study being conducted. Repeatable circuit operating conditions and biasing should be set for the pretest measurements. With linear circuits in particular, it may be difficult to maintain the same conditions for measurement during and after exposure because of the changing circuit characteristics due to the radiation. As an example, general circuit gain measurements on linear circuits should be made with an open-loop configuration where possible. If stable measurements in the open-loop configuration are marginal, it may not be possible after exposure to repeat them. In that case, closed-loop configuration with a minimum feedback should be used.

8.2.6 Test Considerations

This section discusses the general test considerations for permanent-damage integrated circuit parameter measurements. Basic test-design decisions and considerations, which are not specifically related to the measurement of a particular parameter, must be made when planning for any radiation testing. These are discussed in Chapter 2. The user should review that chapter prior to proceeding with specific integrated circuit tests.

Neutron and gamma permanent-damage testing is normally performed in steps. A series of pretest electrical parameter values should be measured to form a data base. Automated test equipment is best for these tests, since a minimum of 10 samples of each device type should be tested so that the results are statistically significant. It is common to make 15 to 30 different measurements on each sample. For integrated circuits, the parameters specified in Tables 8.2-1 and 8.2-2 should be considered. The tester must always be aware that when measuring the permanent damage caused by neutron or gamma irradiation, very precise measurements must be taken because it is the difference in pre- and posttest measurements that is significant. In general, extreme care must be taken to obtain satisfactory measurement precision. Control devices should always be used, and the measurement precision should be reported along with the radiation data. Important variables that should be controlled include external temperature, heat dissipation during test, oscillation, socket and lead resistance, changes in instrumentation condition and accuracy, and the time and temperature between irradiation and measurements.

After the pretest data have been recorded, the devices should be exposed to a fluence that gives about 10 to 15 percent of the estimated gain degradation. A few unirradiated control devices for each type of device should also be tested to monitor nonradiation-induced changes. These

JFET input stages are not subject to significant gain degradation, but other parameters, such as offset voltage and leakage current, may change significantly.

In general, a large variety of test configurations is available for linear circuits. The configuration used should be dictated by the objective of the study being conducted. Repeatable circuit operating conditions and biasing should be set for the pretest measurements. With linear circuits in particular, it may be difficult to maintain the same conditions for measurement during and after exposure because of the changing circuit characteristics due to the radiation. As an example, general circuit gain measurements on linear circuits should be made with an open-loop configuration where possible. If stable measurements in the open-loop configuration are marginal, it may not be possible after exposure to repeat them. In that case, closed-loop configuration with a minimum feedback should be used.

8.2.6 Test Considerations

This section discusses the general test considerations for permanent-damage integrated circuit parameter measurements. Basic test-design decisions and considerations, which are not specifically related to the measurement of a particular parameter, must be made when planning for any radiation testing. These are discussed in Chapter 2. The user should review that chapter prior to proceeding with specific integrated circuit tests.

Neutron and gamma permanent-damage testing is normally performed in steps. A series of pretest electrical parameter values should be measured to form a data base. Automated test equipment is best for these tests, since a minimum of 10 samples of each device type should be tested so that the results are statistically significant. It is common to make 15 to 30 different measurements on each sample. For integrated circuits, the parameters specified in Tables 8.2-1 and 8.2-2 should be considered. The tester must always be aware that when measuring the permanent damage caused by neutron or gamma irradiation, very precise measurements must be taken because it is the difference in pre- and posttest measurements that is significant. In general, extreme care must be taken to obtain satisfactory measurement precision. Control devices should always be used, and the measurement precision should be reported along with the radiation data. Important variables that should be controlled include external temperature, heat dissipation during test, oscillation, socket and lead resistance, changes in instrumentation condition and accuracy, and the time and temperature between irradiation and measurements.

After the pretest data have been recorded, the devices should be exposed to a fluence that gives about 10 to 15 percent of the estimated gain degradation. A few unirradiated control devices for each type of device should also be tested to monitor nonradiation-induced changes. These

control devices should be measured each time the test devices are measured and, from the observed changes in the controls, the uncertainty for each parameter can be determined. Parameter measurements should be made between each radiation exposure and the process should be repeated until degradation is about 90 to 95 percent in the parameter of interest. A new set of dosimeters should be used for each exposure level. Since the effects are cumulative, each additional exposure will have to be determined to give the specified total accumulated fluence. In the case of neutron exposure, correlation to a 1-MeV equivalent dose is required (Reference 2). Notice that the testing should be performed until significant (minimum 50 percent) or near total degradation is achieved. This permits the calculation (interpolation) of the device degradation over all applicable fluences. Using this technique, the data, if stored and available to others, can be of considerable value.

Data that should be taken on all tests are listed below. This list should be considered as a minimum requirement when planning a test. Specific test programs may require additional data. The data should include:

1. Part type number--including the serial number, manufacturer, controlling specification, date code, and other identifying numbers given by the manufacturer
2. Radiation test date
3. Quantities of each part type to be tested
4. Electrical test conditions from pretest through posttest
5. Electrical parameters to be measured during exposure tests
6. Electrical parameters to be measured in pre- and postexposure tests
7. Criteria for pass, fail, record actions on tested parts
8. Criteria for anomalous behavior designation
9. Radiation exposure levels--neutron, gamma dose (or gamma dose rate) for each irradiation
10. Radiation exposure time period and time periods between exposure and measurements
11. Ambient temperature during exposure and measurement
12. Expected accuracy and precision of the measurements
13. Radiation dosimetry requirements

14. Parameter measurement circuits for other than specified electrical test circuits

15. The test data

16. For in-situ tests--time history of the radiation rates and the test chamber temperature

17. Test instrument descriptions and settings.

Test procedures for permanent-damage measurements have been developed and are contained in Reference 2. Method 1017 specifies the test considerations for measuring degradation of integrated circuits when exposed to the neutron environment. Method 1019 specifies the procedures for evaluating integrated circuit degradation from steady-state total dose effects in an ionizing radiation environment.

Dosimetry procedures for use in neutron and total dose testing have been formulated. These are described in Reference 3. Methods E720, E721, E722, and E763 are applicable for neutron fluence determination, and Methods E665, E666, E668, and F526 are applicable to total dose measurements. These procedures, or their equivalents, should be used when testing integrated circuits.

When exposing circuits in a biased state, it is desirable to operate them in a manner typical of the intended application, taking into account the expected operational pulse width as compared to the pulse width of the simulation facility. Circuits whose operation is static during exposure may operate differently after irradiation than if they were operated continuously throughout the exposure. An example of such an effect would be a flip-flop left in a single state during irradiation. The possibility of unsymmetric output characteristics should be taken into account by characterizing both states of all outputs of such circuits.

8.2.7 Specific Digital Circuit Test Procedures

8.2.7.1 Static Terminal Measurements

A useful technique for determining the permanent degradation of digital integrated circuits is the measurement of the current and voltage characteristics of the input and output terminals. These measurements are readily performed with automated integrated circuit testers such as the Fairchild 5000. Alternately, a curve tracer can also be used to make the same measurements.

Figures 8.2-1 through 8.2-6 illustrate the basic measurement configurations for measuring the terminal parameters listed in Table 8.2-1. The methods are based on the appropriate procedures of Reference 2 and apply to TTL, DTL, RTL, ECL, and MOS digital integrated circuits. The test conditions must be specified for each type of device and each measurement.

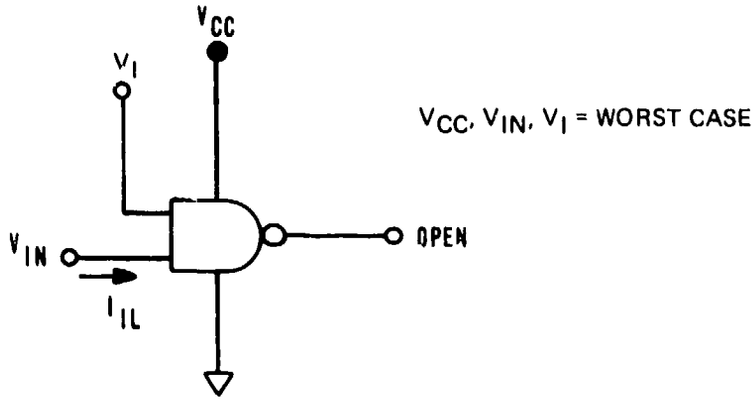

Figure 8.2-1. Low-level input current, I_{IL}.

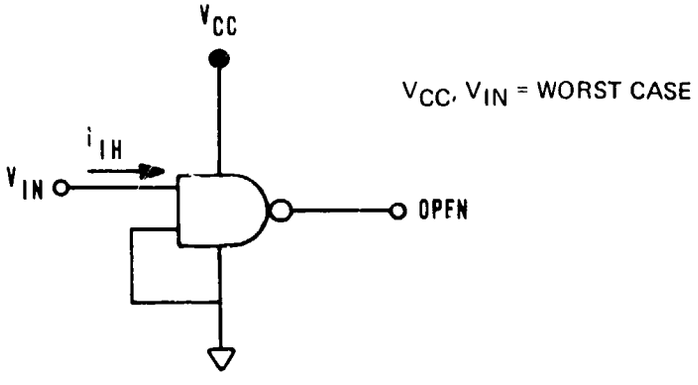

Figure 8.2-2. High-level input current, I_{IH}.

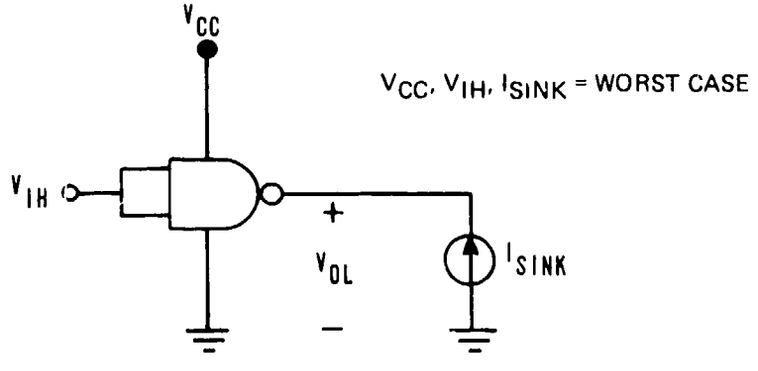

Figure 8.2-3. Low-level output voltage, V_{OL}.

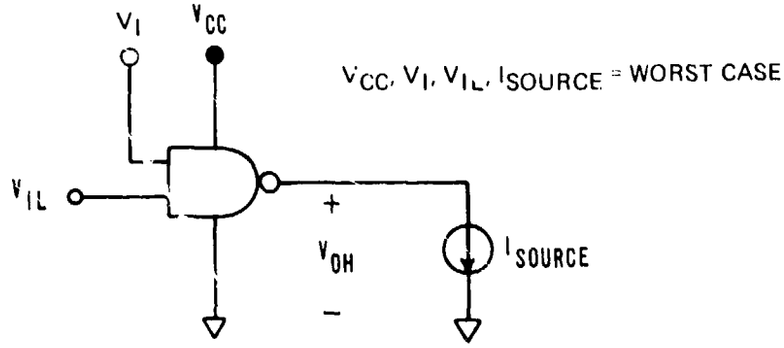

Figure 8.2-4. High-level output voltage, V_{OH}.

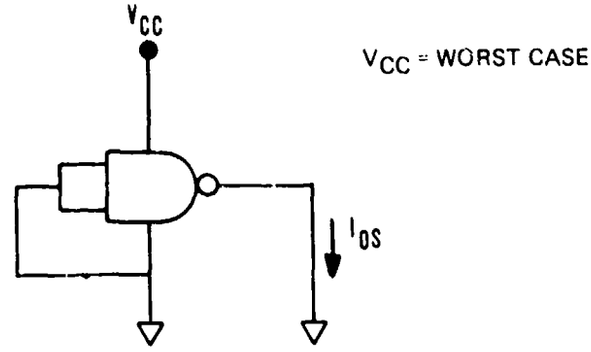

Figure 8.2-5. Output short circuit current, I_{OS}.

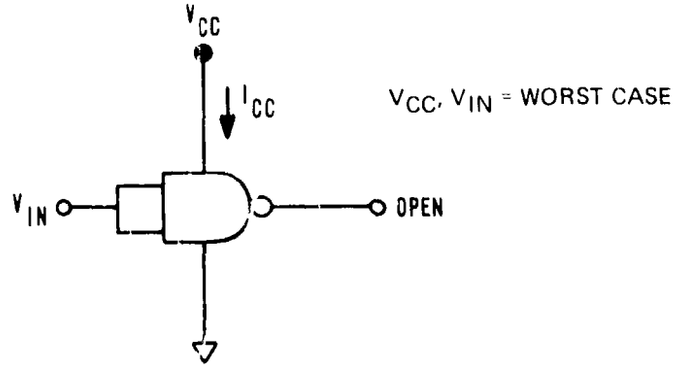

Figure 8.2-6. Power supply current, I_{CC}.

These may be derived from a procurement document, manufacturer's specification sheets, or specific application requirements, depending on the purpose of the test. The specified parameters include test temperature, power supply voltage, and voltage and current levels of the untested terminals and the terminals under test.

The test configurations shown are for +5V TTL logic gates. Appropriate polarity changes must be made for other types of logic. Specified load conditions at the terminals shall meet the requirements of Method 3002 of Reference 2. For in-situ measurements, it is necessary to include shielded cabling between the device under test and the measurement equipment. The effects of the cabling must be measured and taken into account when evaluating the data. See Section 2.5 for cabling considerations.

The high- and low-level input voltages can be determined by either Method 3006 or 3007, depending on the type of circuit. For an inverting gate, the configuration of Figure 8.2-3 is used; for a noninverting gate, the configuration shown in Figure 8.2-4 is used. Appropriate voltage measuring equipment must be used to assure that the input voltage level that results is the appropriate worst-case output voltage level ($V_{OH(MIN)}$ or $V_{OL(MAX)}$). Similarly, the low-level output current can be determined by using Method 3011 (Figure 8.2-5) and forcing the output terminal to the specified value of V_{OL}.

A useful parameter for evaluating neutron-induced degradation of TTL devices is the unsaturated sink current at the output terminals. This current is closely related to the gain of the output transistor and changes smoothly as the device degrades. It shows larger changes at moderate radiation levels than the standard electrical parameters. The procedure for measuring unsaturated sink current is similar to the method for measuring the low-level output voltage (Figure 8.2-3 and Method 3007 of Reference 2). A significant difference is that the output terminal being tested is subjected to voltage pulses of sufficient magnitude to pull the output transistor out of saturation. The corresponding current pulses are then measured. Method F676 of Reference 3 describes the entire procedure. Figure 8.2-7 shows the test circuit setup.

A typical output current-voltage characteristic of a TTL circuit in the zero state is shown in Figure 8.2-8 along with an illustration of neutron-induced degradation. While the offset voltage, V_{OS}, and the saturation resistance, R_{SAT}, both increase, the major effect is the reduction in output current, I_{OL}. Similar curves can also be made for the output current in the one state and at the input terminal. However, neither of these curves is as useful in design as the zero state output curve.

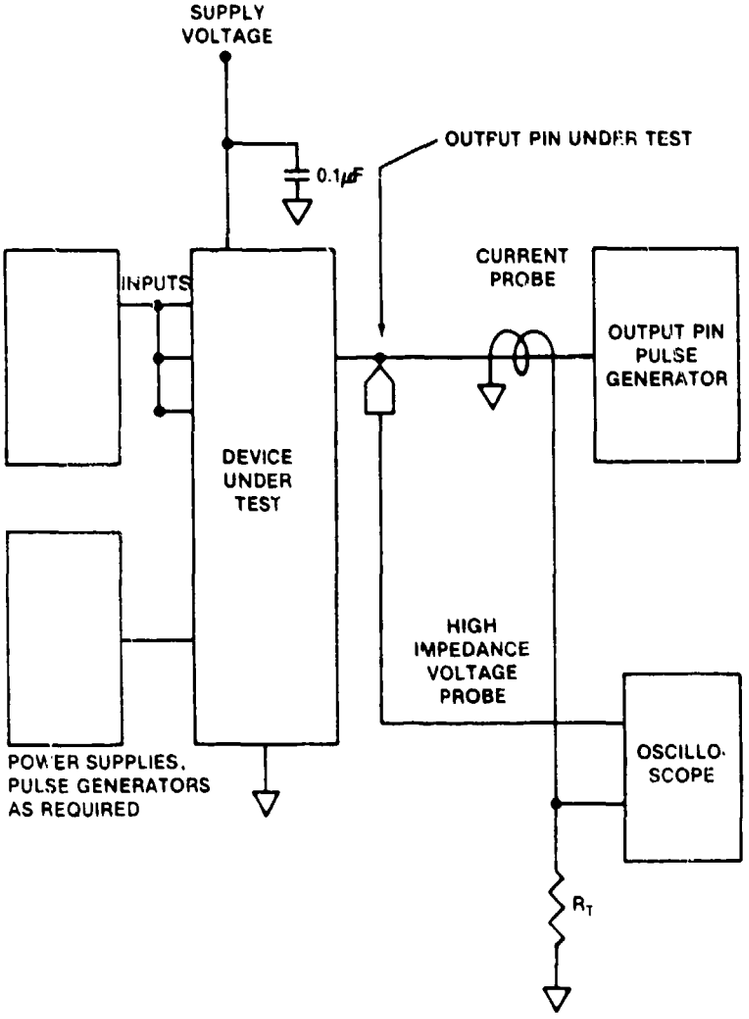

Figure 8.2-7. Test circuit for unsaturated sink current measurement.

If switching time measurements must be taken for a critical system application, it is recommended that changes in switching time due to neutron and total dose degradation be reported along with the appropriate current-voltage measurements for the circuits. The reason for this is that switching times are sensitive to load capacitance and, often, the data can be extended to other capacitive load conditions if the output current-voltage data are available.

Figure 8.2-9 shows the recommended circuit for measuring propagation delay. The test conditions must be specified for each type of device. These include the limits of t_{PHL} and t_{PLH}, the driving signal parameters (t_{THL}, T_{TLH}, high level, low level, pulse width, repetition rate), power supply voltages, and test temperatures. Switching times can be measured using substantially the same circuit. Figure 8.2-10 shows the output transition time measurement parameters according to Method 3004 of Reference 2.

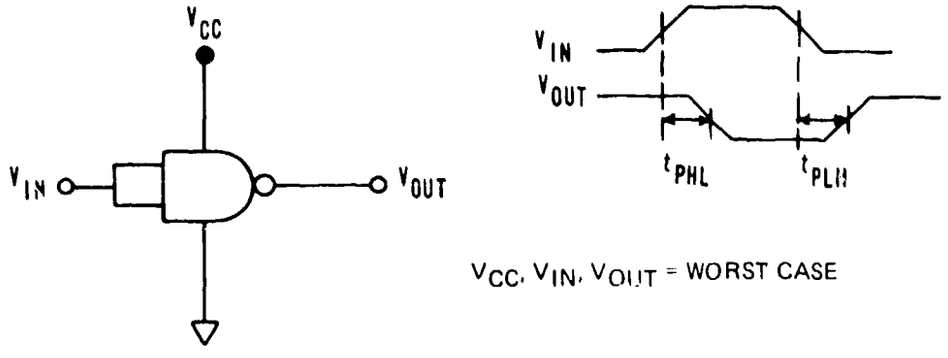

Figure 8.2-9. Propagation delays, t_{PHL} and t_{PLH}.

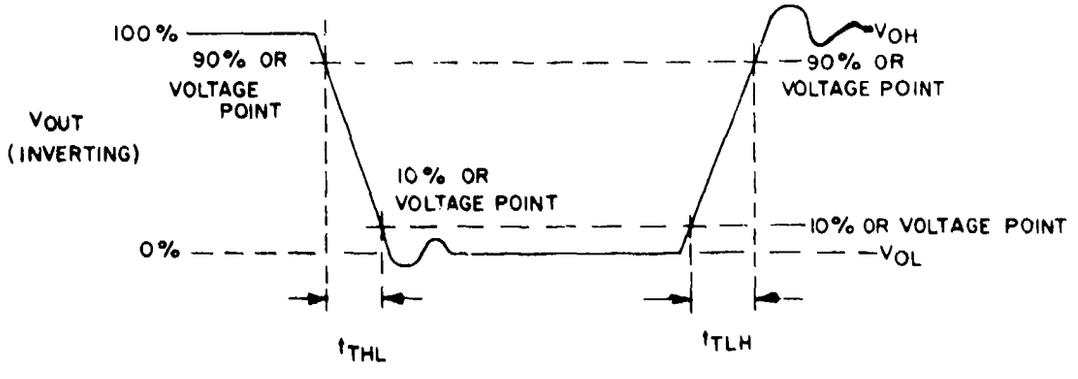

Figure 8.2-10. Transition time measurements, t_{THL} and t_{TLH}.

If switching time measurements must be taken for a critical system application, it is recommended that changes in switching time due to neutron and total dose degradation be reported along with the appropriate current-voltage measurements for the circuits. The reason for this is that switching times are sensitive to load capacitance and, often, the data can be extended to other capacitive load conditions if the output current-voltage data are available.

Figure 8.2-9 shows the recommended circuit for measuring propagation delay. The test conditions must be specified for each type of device. These include the limits of t_{PHL} and t_{PLH}, the driving signal parameters (t_{THL}, T_{TLH}, high level, low level, pulse width, repetition rate), power supply voltages, and test temperatures. Switching times can be measured using substantially the same circuit. Figure 8.2-10 shows the output transition time measurement parameters according to Method 3004 of Reference 2.

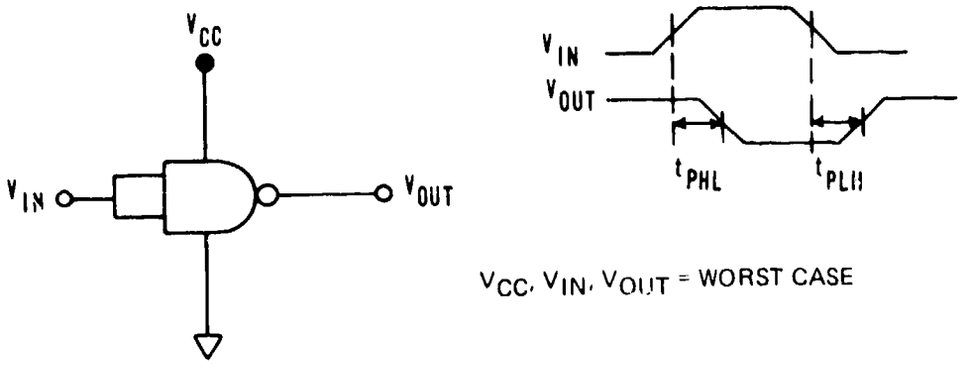

Figure 8.2-9. Propagation delays, t_{PHL} and t_{PLH}.

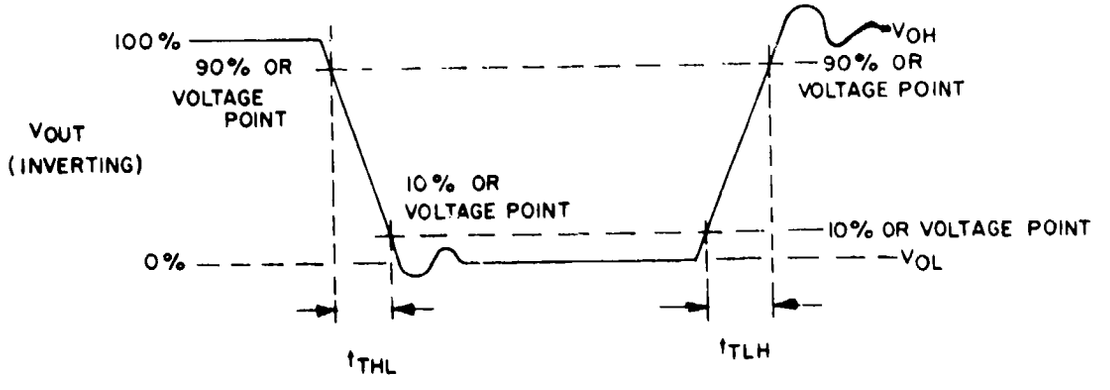

Figure 8.2-10. Transition time measurements, t_{THL} and t_{TLH}.

8.2.7.3 Rapid Annealing Measurement

There are two parameters and two possible bias conditions under which one might wish to obtain an indication of rapid annealing in a digital circuit when testing in a neutron or total dose environment. The circuit could be biased or unbiased during irradiation. The effects that result from the two conditions should be different because, in one case, all internal devices are off and, in the other, only certain devices are exposed while off. Parameters of primary interest are propagation delay and source and sink currents. The measurement circuit to be used should be like those previously specified for characterization of these parameters with the addition of a mechanism for removal of power during exposure. When performing these tests, it must be understood that the transient annealing measurements are complicated by the photocurrents generated by the gamma radiation accompanying a neutron pulse. For meaningful data analysis, the gamma dose rate must be monitored during a rapid annealing experiment. Note that from 1 to 10 percent of the maximum gamma dose rate can persist for milliseconds after the neutron pulse. For this reason, extreme care should be exercised in analyzing rapid annealing data. Method 1019 of Reference 2 specifies test setup and site requirement considerations for annealing measurements for steady-state total dose effects.

8.2.8 Specific Linear Circuit Test Procedures

8.2.8.1 Terminal Measurements

The procedures for measuring linear circuit degradation due to neutron or total dose exposure are essentially the same procedures followed for normal usage characterization. For in-situ measurements, an important precaution is to ensure that the devices will not oscillate when operated at the end of long cables. It may be necessary to utilize line drivers to avoid excessive loading of the device outputs (see Chapter 2). The test methods outlined in Reference 2 with the necessary modifications are recommended as the preferred procedures for permanent-damage evaluation. As with digital circuits, it may be feasible to use automated test equipment for some measurements.

Figures 8.2-11 through 8.2-13 illustrate the basic measurement configurations for measuring the parameters listed in Table 8.2-2. The procedures apply to both bipolar and MOS devices. Test conditions must be specified for each type of circuit and each measurement. These are derived from a procurement document, manufacturer's specification sheets, or specific application requirements, depending on the purpose of the test. The specified parameters include test temperature, power supply voltages, maximum and minimum values of the input and output currents and voltages, the value of the test circuit components, and other appropriate performance specifications.

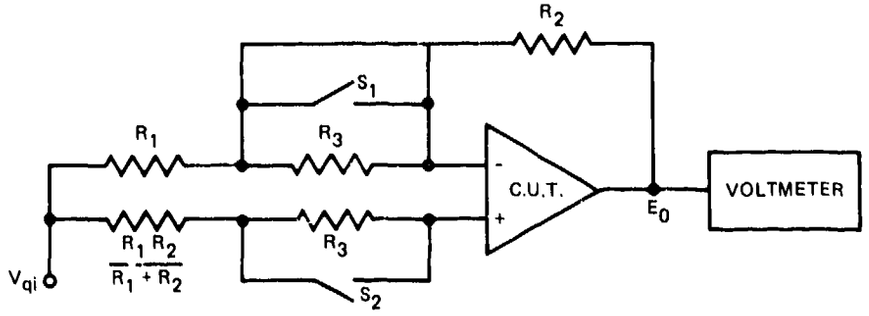

Figure 8.2-11. Circuit for input offset voltage and current, and input bias current.

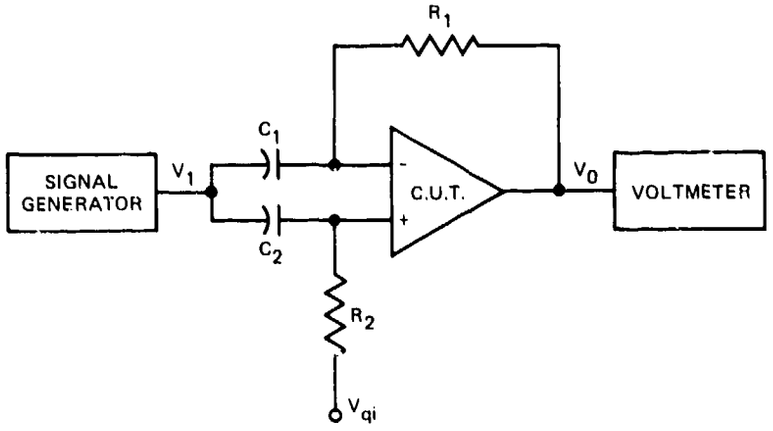

Figure 8.2-12. Common mode rejection ratio test circuit.

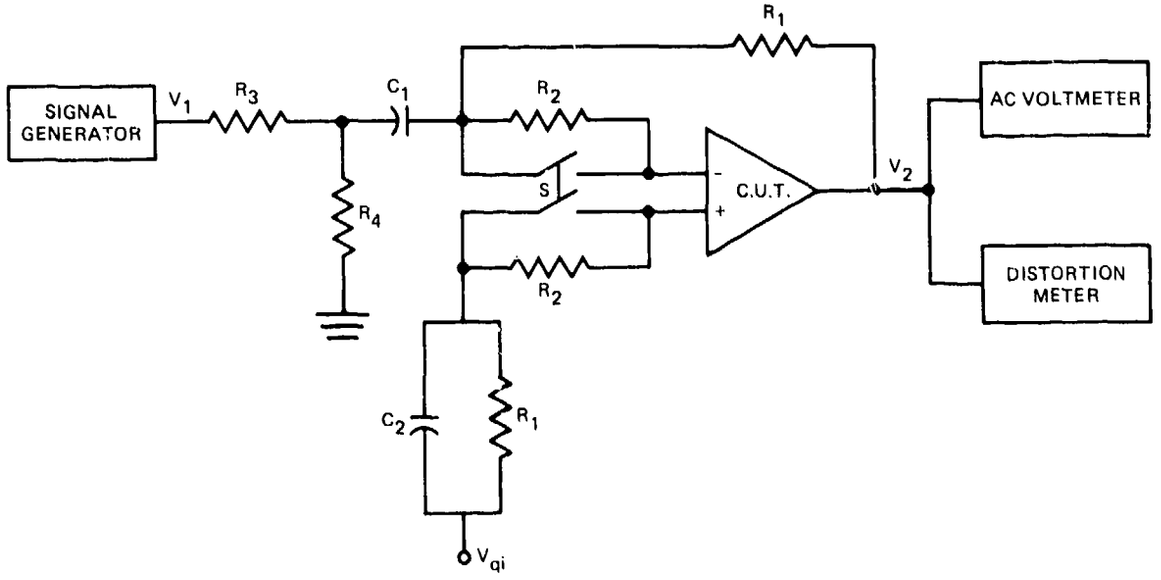

Figure 8.2-13. Gain, dynamic range, and input impedance measuring circuit.

Figure 8.2-11 shows a test configuration that can be used to measure input offset voltage and current and input bias current. R_2 is chosen to be less than the nominal input impedance but large enough not to load the amplifier; R_3 is a convenient value less than the nominal input impedance; and R_2/R_1 is the smaller of 100 or 10 percent of the open-loop gain. The configuration is shown for a differential amplifier; by removing one half of the input network, it is adaptable to single input circuits. Input offset voltage is measured with switches S_1 and S_2 closed. The value is:

$$V_{iO} = \frac{R_1}{R_2} (E_O - V_{qO}) \quad . \tag{8-1}$$

For input offset current, E_{O1} is measured with S_1 and S_2 closed; E_{O2} is measured with S_1 and S_2 open. Then:

$$I_{iO} = \frac{R_1}{R_2} \frac{E_{O1} - E_{O2}}{R_3} \quad . \tag{8-2}$$

The input bias current is determined by measuring E_{O1} with S_1 open and S_2 closed, and E_{O2} with S_1 closed and S_2 open. Then:

$$I_{in} = \frac{R_1}{R_2} \frac{E_{O1} - E_{O2}}{2R_3} \quad . \tag{8-3}$$

Figure 8.1-12 shows a test configuration for measuring the common mode rejection ratio of a linear amplifier. R_1 is a value less than the nominal input impedance of the circuit under test and large enough not to load the circuit. $R_2 \approx R_1$, $C_2 \approx C_1$, and $2\pi f R_1 C_1 \geq$ (10 × open-loop gain). The common mode voltage gain is $A_C = V_O/V_1$ at the frequency of interest. Then, the common mode rejection ratio is:

$$CM_{rr} = 20 \log \frac{\text{open-loop voltage gain}}{\text{common mode voltage gain}} \quad . \tag{8-4}$$

Figure 8.2-13 shows a test circuit for measuring the open-loop voltage gain, the dynamic range (output voltage swing), and the input impedance. It also provides the bandwidth and distortions, if desired. A differential input configuration is shown, but single ended measurements can be made by removing the circuitry on the positive input terminal. R_2 is equal to the minimum specified input impedance. R_1 is chosen not to load the circuit under test. The open-loop gain is measured with switch S closed. V_1 is increased until V_2 is a specified value. Then, the open-loop gain, A_d, is:

$$A_d = \frac{V_2}{V_1} \frac{R_3 + R_4}{R_4} \quad . \tag{8-5}$$

The dynamic range is determined simultaneously. Distortion will increase as the output voltage exceeds the specified dynamic range. Input impedance is determined by observing that the drop of V_2 is less than 6 dB when switch S is opened at a given test frequency.

8.2.8.2 Rapid Annealing Measurements

When performing rapid annealing tests in a neutron or total dose environment, two considerations are necessary. The first is to determine whether the circuit is to be biased or unbiased during exposure. If the circuit is to be continuously biased during irradiation, then the appropriate circuit as described in Section 8.2.8.1 will be sufficient. If, on the other hand, the circuit is to be unbiased during exposure, the circuits described above will have to be modified so that the circuit under test can be turned on quickly. In addition, it is necessary to characterize the circuit's response to turn-on both before irradiation and immediately after the rapid anneal. A line driver may be needed to avoid excessive loading of the device outputs. It must also be understood that transient annealing measurements are complicated by the photocurrents generated by the gamma radiation accompanying the neutron pulse.

8.3 TRANSIENT-RESPONSE MEASUREMENTS

8.3.1 Transient Effects

Transient effects in integrated circuits are due to the generation of excess charge carriers that cause changes in circuit currents and voltages. The results of these changes can be temporary (transient) or permanent (catastrophic). In both digital and linear circuits, the transient responses appear primarily as output voltage pulses, output voltage state changes, or power supply current surges. The magnitude and duration of these effects depend on the type of component in the circuit, the type of component isolation, the circuit configuration, and the loading of the circuit. Relative magnitudes of device response for use as testing guidelines can be obtained from Chapter 8 of Reference 1.

8.3.1.1 Metalization and Junction Burnout

High current surges that are induced in integrated circuits by transient radiation may cause junction burnout or metalization failure because of power dissipation in the device. Metalization burnout usually occurs at locations where thinning of the metalization occurs, such as sharp bends or when the metalization crosses over a step in the surface oxide. Detailed discussion of the various IC failure modes is beyond the scope of this document. Chapter 10 of Reference 1 gives some details and cites a number of references.

Circuits containing diffused resistors are more susceptible to metalization failure and junction burnout because the resistor value drops significantly during a high-intensity transient pulse. Junction-isolated circuits are also more prone to burnout problems because the substrate photocurrent is very large, and there will be large transient currents at high radiation levels.

8.3.1.2 Integrated Circuit Latchup

There are two types of radiation-induced latchup: a hard latchup and an incipient latchup. A hard latchup results in a sustained functional failure. The erroneous operational condition can be corrected by cycling the bias power supply if burnout has not occurred in the interim. Incipient latchup is characterized by a functional failure that is not sustained but lasts longer than can be explained by normal circuit time constants.

Four latchup-type mechanisms have been identified in integrated circuits. They are four-layer (pnpn) latchup, second breakdown, sustaining voltage breakdown, and circuit lockup. Similar failure characteristics are exhibited by other circuit failures such as offset voltage shifts and long capacitive discharge times (linear circuits). The mechanisms of integrated circuit latchup are discussed in Chapter 8 of Reference 1. Four-layer latchup is the one most commonly found in modern integrated circuits.

It has also been observed that, in some devices, latchup occurs over only a restricted range of dose rates. At dose rates above and below this range, latchup does not occur. This phenomenon is termed a "latchup window" (Reference 25). The possibility of this phenomenon occurring for certain devices must be taken into consideration when testing for latchup.

Identification of a latchup susceptible integrated circuit is accomplished by identifying erroneous operating states immediately after radiation exposure by exercising the device with a functional test (Method 1020 of Reference 2).

8.3.2 Parameters to Measure

The most important ionization-effects data for the system designer are specifications of transient output response as a function of dose rate for fixed bias conditions and known ionizing-radiation dose-rate profiles. In addition, the power supply transient due to excessive current drain is a parameter of interest to the designer. Significant power-supply transients occurring in a system can cause changes in circuit bias conditions that could lead to latchup or an unexpected system response.

The output and supply current transient responses can be characterized by either a voltage or a current measurement method. A method for measuring latchup response is also described in the following section.

8.3.3 Test Considerations

General test considerations for transient response measurements are discussed in Section 2.5. Some additional test considerations relating specifically to integrated circuits are presented in this section as an aid in designing transient response tests.

A minimal pretest check is always necessary to verify that the intended sample is electrically and mechanically satisfactory. For samples used to generate basic design data for a system, it should be established that all samples meet the p[illegible] or application specifications for that part number prior to testing. Device permanent damage can occur due to electrical or radiation accidents or photocurrent stresses. The risk is greater in tests at high dose rates (greater than 10^9 rads (Si)/s). It is recommended that tests be made before and after irradiation to verify satisfactory electrical response.

The response of integrated circuits depends upon the radiation pulse width. When measuring responses to a pulse of ionizing radiation, it is helpful to know the time required to establish photocurrent equilibrium in the circuit during irradiation. Figure 8.3-1 illustrates the dependence of the circuit radiation response on the pulse width for a typical circuit. The circuit response is dose dependent when the pulse width is less than the equilibrium time, and usually dose-rate dependent when the pulse width is greater than the equilibrium time. The circuit equilibrium time can be determined from a set of data such as that shown in Figure 8.3-1, or from a measurement of the unsaturated response to a square pulse of uniform intensity whose pulse width is greater than the equilibrium time. Such a response will look similar to the plot in Figure 8.3-2 where the abscissa is time instead of pulse width.

It is important to recognize that the transient responses of a circuit to radiation are sensitive to electrical loading of both the input and output. Many digital circuits are sensitive to excessive capacitive loading; this problem is greater for circuits with high output resistance. For this reason, many digital circuits are most sensitive to ionizing radiation at low fanout; hence, they should be tested in this condition for worst-case results. The transient radiation failure threshold can increase by a factor of two to three for higher fanout conditions.

Linear circuits also are influenced by electrical loading. Generally, one of the most sensitive portions of linear integrated circuits is the response of the input stages, since any changes in circuit performance are amplified by the gain of the amplifier stages. The photocurrent may develop significant voltage drop if it must flow through a high impedance. For differential amplifiers, the mismatch in the source impedances at the inputs can greatly affect the transient response. Highly unbalanced source resistances make the circuit more sensitive to radiation. Circuits that typically have widely differing source impedances (such as operational amplifiers) should be tested using the highest input impedance condition.

The response of other components in the circuit application sometimes can cause problems. For example, a tantalum capacitor placed at the input of an op-amp and loaded with only a high dc resistance will have a long-term voltage buildup after radiation. This will also affect the amplifier output. A measurement of the circuit impedance will help to determine if the circuit response is sensitive to loading variations. When the response is sensitive to loading, at least two values of load impedance should be used to determine the output impedance during irradiation.

Table 8.3-1 summarizes general loading and operating configurations that could be used for determining device response. The responses should be measured at each terminal for devices with more than one input and output. Digital circuit loads must meet the requirements of Method 3002, and dynamic drive sources for digital circuits must be specified in accordance with Method 3001 of Reference 2.

Table 8.3-1. Loading and operating configurations for circuit response testing in pulsed ionizing environments.

Circuit Type	Response Measured at	Loading	Output Operating Configuration
Digital	Output	Fanout 1	1 State 0 State
	Input	Low Impedance High Impedance	0 State 1 State
	Other Access Nodes	High Impedance	1 State 0 State
	Power Supply	--	--
Linear	Output	Low Impedance High Impedance Low Impedance High Impedance	Open Loop[a] Open Loop[a] Closed Loop Closed Loop
	Input	Low Impedance High Impedance	-- --
	Dual Inputs	Worst-Case Mismatch	--
	Other Access Nodes	High Impedance	--
	Power Supply	--	--

[a]Not always possible.

The response of other components in the circuit application sometimes can cause problems. For example, a tantalum capacitor placed at the input of an op-amp and loaded with only a high dc resistance will have a long-term voltage buildup after radiation. This will also affect the amplifier output. A measurement of the circuit impedance will help to determine if the circuit response is sensitive to loading variations. When the response is sensitive to loading, at least two values of load impedance should be used to determine the output impedance during irradiation.

Table 8.3-1 summarizes general loading and operating configurations that could be used for determining device response. The responses should be measured at each terminal for devices with more than one input and output. Digital circuit loads must meet the requirements of Method 3002, and dynamic drive sources for digital circuits must be specified in accordance with Method 3001 of Reference 2.

Table 8.3-1. Loading and operating configurations for circuit response testing in pulsed ionizing environments.

Circuit Type	Response Measured at	Loading	Output Operating Configuration
Digital	Output	Fanout 1	1 State 0 State
	Input	Low Impedance High Impedance	0 State 1 State
	Other Access Nodes	High Impedance	1 State 0 State
	Power Supply	--	--
Linear	Output	Low Impedance High Impedance Low Impedance High Impedance	Open Loop[a] Open Loop[a] Closed Loop Closed Loop
	Input	Low Impedance High Impedance	-- --
	Dual Inputs	Worst-Case Mismatch	--
	Other Access Nodes	High Impedance	--
	Power Supply	--	--

[a]Not always possible.

For linear circuits, the test conditions depend on the type of device and on the specific applications. Specific details must be included in the test specifications.

When using repetitive pulsing, high dose rates, and/or long pulse widths, large total doses may build up in the devices being tested. A dose of about 10^4 rads (Si) is the threshold beyond which some devices may incur significant permanent damage. When this threshold is exceeded, the dose should be reported and a clear identification made of the data obtained above the threshold.

When testing to determine threshold values, it is suggested that a few devices be checked to determine the relative location of the threshold. The remaining devices can then be tested over a more limited dose or dose rate range to establish specific threshold values.

An additional problem arises when the operation of the circut under test must be synchronized with the radiation pulse. It is not always possible to remotely pulse the radiation source to coordinate the desired radiation with circuit operation. Some facilities do provide an equipment trigger signal; however, there is usually an inherent variation (jitter) in the delay between the actual trigger signal received at the test equipment and the radiation pulse, making synchronization difficult. The facility operator should be consulted to determine whether the jitter time of the trigger signal is acceptable for a particular test (Reference 13).

Adequate documentation of the test methods and the results of transient-effects testing is extremely important. The following data should be recorded for each radiation test as a minimum:

1. Device identification
2. Date of test and operator
3. Description of test facility
4. Description of all test equipment
5. Description of test circuit including physical configuration, shielding, and grounding
6. Type of ionizing radiation
7. Energy spectrum of the incident radiation
8. Radiation-pulse shape
9. Radiation-pulse width
10. Dose rate in the device
11. Accumulated dose in the device
12. Ambient temperature
13. Test circuit current with device removed

14. Test circuit response data
15. Voltage bias on the device
16. Device orientation
17. Case connections
18. Values of photocurrent for each data set
19. Pictorial presentation of device response
20. Relaxation time, if calculated.

8.3.4 Specific Test Procedures for Digital and Linear Circuits

The voltage and current measurement techniques discussed in this section are basically the same as those described in Section 6.2 for discrete semiconductor devices. Note that very often several measurements are made simultaneously when testing integrated circuits. For example, output voltage, input current, and power supply current may need to be observed at the same time.

The material presented here outlines basic testing principles. It is the responsibility of the user to correctly adapt the appropriate material to his unique requirements to assure that all data are taken in accordance with established Military and ASTM radiation testing standards.

8.3.4.1 Voltage Measurements of Device Response

A block diagram of a typical circuit for voltage measurement during ionization testing is shown in Figure 8.3-3. The cable between the circuit under test and the line driver should be kept short to minimize capacitive loading and replacement currents. The power supply capacitor C must be large enough to supply the transient current and remain a stiff voltage source during the radiation transient. The time constant R_2C must be large compared to the period of the noise signal induced in the long cable. A convenient method of checking this is to drive the circuit input using a pulser. Cabling and active instrumentation in the exposure area must be shielded. If a digital circuit is to be checked at both output levels, a relay or solid-state switch should be incorporated in the measurement circuitry to change the input bias level.

Active line drivers are frequently employed in these measurements as illustrated in Figure 8.3-3. These must be carefully designed so that the linearity, input impedance, dynamic range, capacitive loading, transient response, radiation response, and other characteristics do not affect the accuracy of the test. These problems are discussed in Section 2.5. Often the signal must be reduced to a value that can be handled by the measuring equipment. In this case, attenuators are needed.

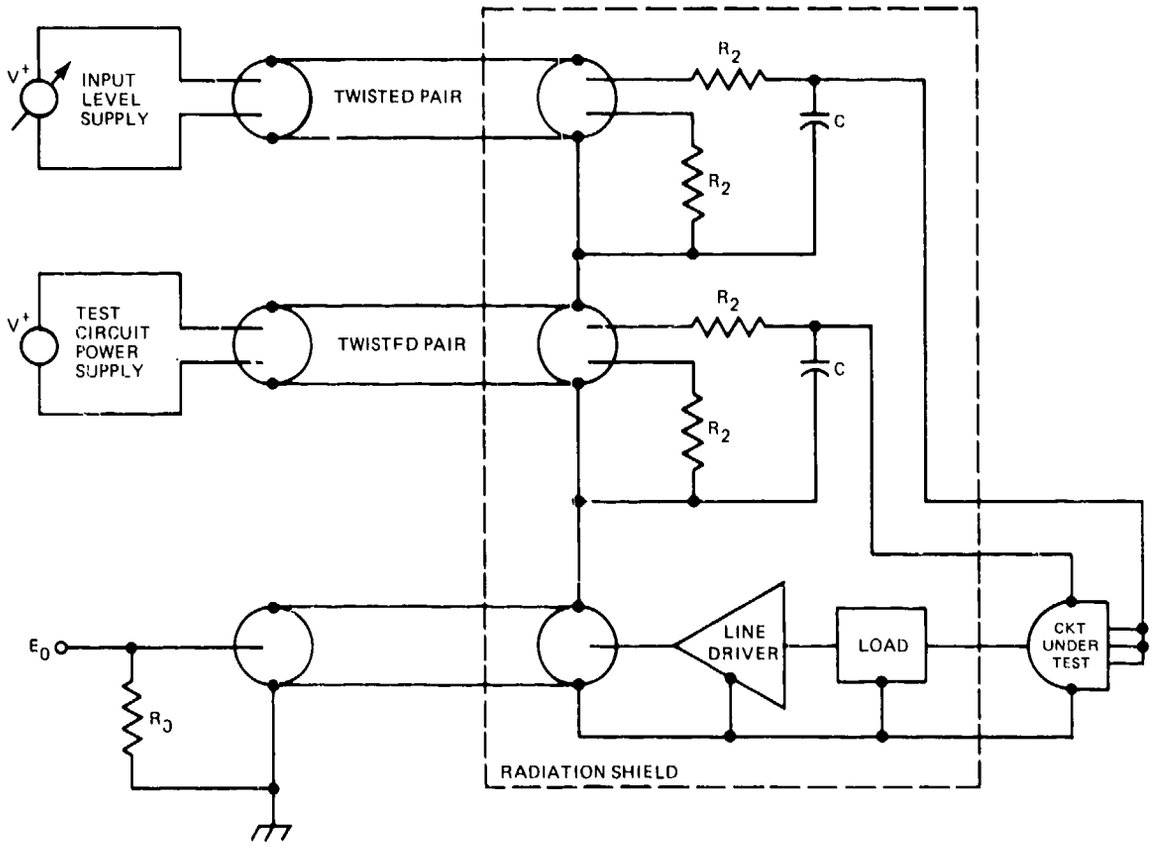

Figure 8.3-3. Typical test configuration for transient ionization testing of digital integrated circuits.

Figure 8.3-4 shows a linear circuit test configuration using the same measurement circuit principles shown in Figure 8.3-3. Dose rate response measurement procedures are given in Method 1023 of Reference 2 and Method F773 of Reference 3.

Differential measurements can be used in radiation testing; however, careful selection of suitable test equipment capable of recording responses to narrow fast-rise-time radiation pulses is necessary. Cable lengths must be closely matched. The physical cable location and the voltage applied to the common conductor must be chosen to minimize replacement current effects. The effects of the source impedance of the device being tested on the spurious voltage due to a replacement current must also be taken into account.

8.3.4.2 Current Measurement of Device Response

The two basic preferred test circuits for the measurement of device current photoresponses--the resistor-sampling method and the current-probe

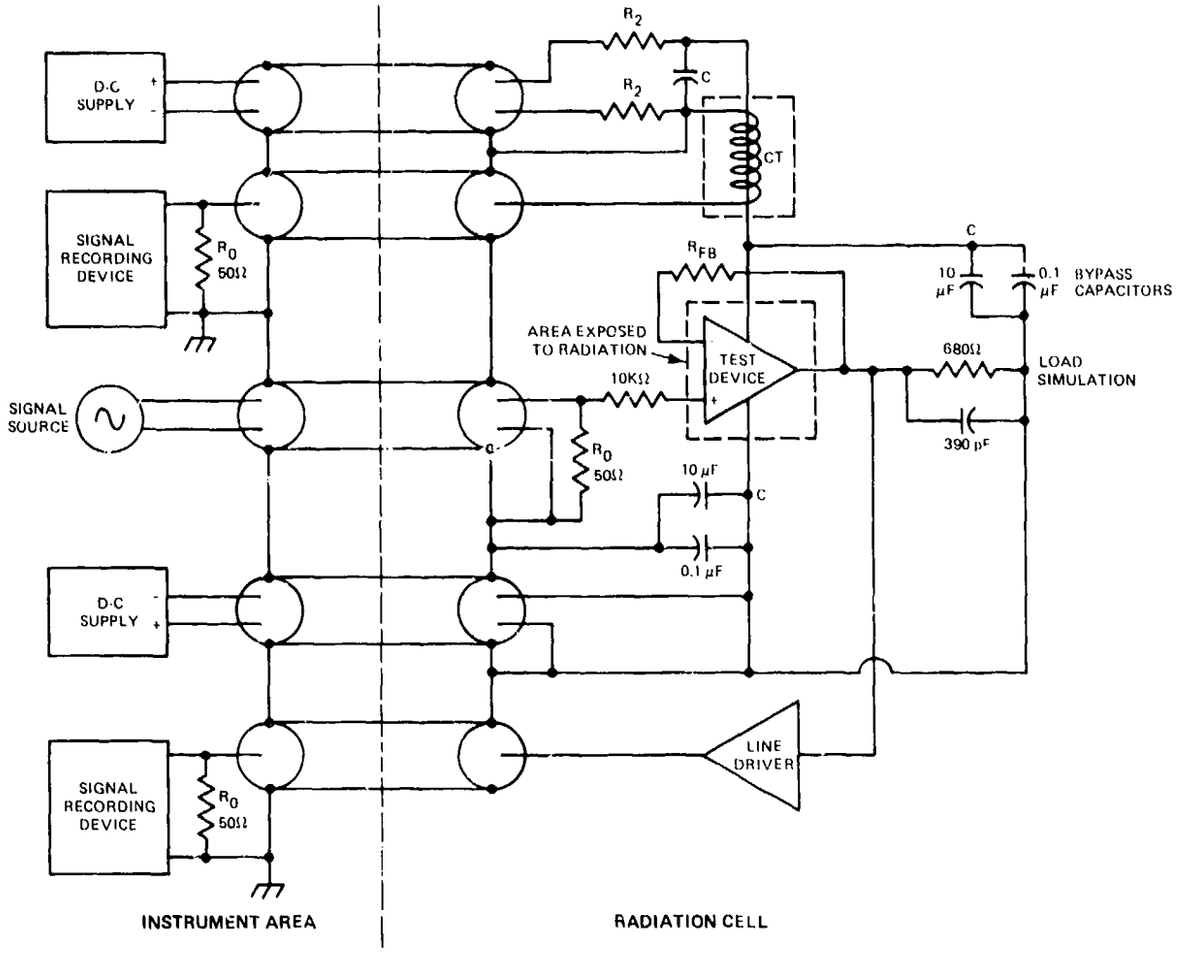

Figure 8.3-4. Example of a test circuit for transient ionization testing of a linear circuit.

method--are discussed in Section 6.2. The circuits shown in Figures 6.2-3 and 6.2-4 can be adapted for use with integrated circuits as shown in Figure 8.3-5. Resistors R_1, R_2, and R_3 are selected for high-frequency isolation but are small enough to permit proper dc current in the test device; capacitors C_1, C_2, and C_3 are for bias-supply bypass; R_0 is equal to the characteristic cable impedance; and V is the bias voltage source. I_{pp} is measured by the current probe, CT, and recorded on an oscilloscope.

The current-probe technique is used when minimum deviation of the operating point is required. Although this method of measuring current is less sensitive than the resistor sampling technique, it is capable of measuring larger currents. The upper limit of the measurement is dependent upon the

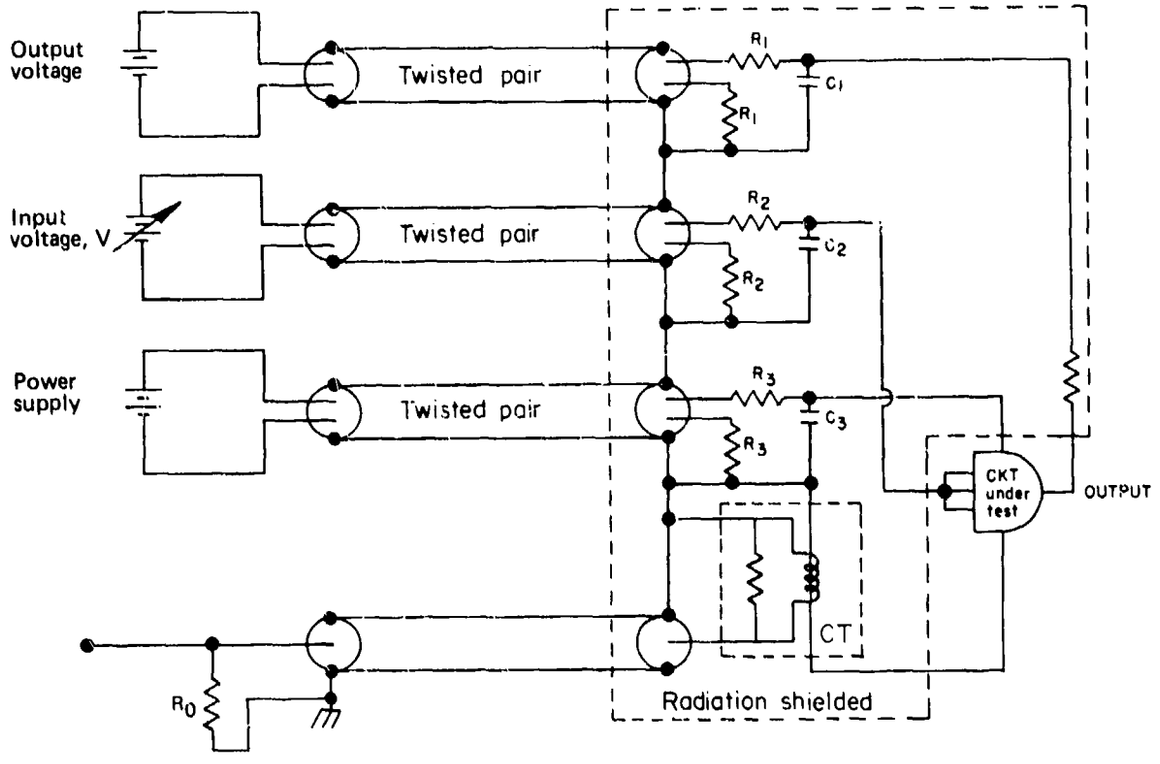

Figure 8.3-5. One-lead, current-probe measurement circuit.

saturation limit of the current probe; low-frequency response of such probes must be checked when using wide pulse widths. Insertion impedance of the probe should be considered. The probe should always be positioned between the bypass capacitor and the circuit under test.

The system power supply voltage may drop during the ionizing radiation exposure due to an excessive transient current drain. It may also be important to record the power supply current of the circuit under test. This measurement is particularly important for junction-isolated integrated circuits.

Figure 8.3-4 illustrates the use of a current probe to measure power supply current of a linear circuit. The procedure detailed in Method F448 of Reference 3 should be followed in all cases.

8.3.4.3 Dose Rate Threshold for Upset of Digital Integrated Circuits

The dose rate threshold for a digital integrated circuit is that dose rate that causes either an instantaneous change in the output voltage

beyond some specification limit or a change of state of any stored data. The test circuit for determining the upset threshold dose rate is substantially the same as the one shown in Figure 8.3-3. Method 1021 of Reference 2 and Method F744 of Reference 3 give the exact procedure to follow when making this measurement.

The procedure for determined integrated circuits (circuits whose outputs are unique functions of the input) is to first bias the device with the outputs in the HIGH state. It is then exposed to stepped increases of dose rate exposure in accordance with a specified test plan until the lowest dose rate is determined which causes the specified voltage transient for any of the monitored outputs. Power supply peak transient current is also monitored. The test is repeated with the outputs biased in the LOW state.

For nondetermined integrated circuits (circuits whose output is not a unique function of the inputs), specified patterns of ones and zeros are monitored for changes as well as the specified voltage transients for any of the outputs.

The items to be specified for testing include the device type, test circuit parameters, upset voltage level definitions, bias conditions, total dose restrictions, radiation pulse, and applicable failure criteria. For nondetermined devices, the patterns of ones and zeros to be stored must also be specified.

8.3.4.4 Radiation-Induced Latchup Testing

Two procedures have been developed to evaluate transient radiation-induced integrated circuit latchup. The first is an analytical technique valid for both bipolar junction-isolated and dielectrically-isolated integrated circuits (Method F774 of Reference 3). The procedure involves examining the integrated circuit device itself, composite drawings of the device, electrical schematics, and chip photographs to identify the four-layer paths in the device. If there are no four-layer paths in the circuit, or no four-layer paths properly biased to sustain latchup, then it can be concluded with a high level of confidence that the integrated circuit is free from latchup. If neither of these conclusions can be reached, then the circuit must be radiation tested to determine if it is free from latchup. Finally, in some cases, a direct conclusion can be reached that the circuit is susceptible to latchup. In all cases, a radiation verification test should be used in conjunction with the analysis to verify the results of the analysis when latchup is not indicated.

The second procedure specifies actual gamma dose rate testing to determine integrated circuit latchup. Method 1020 of Reference 2 describes the detailed requirements for these tests. The tests are nondestructive and

devices that pass the test may be used as production hardware. A block diagram of the recommended test setup is shown in Figure 8.3-6.

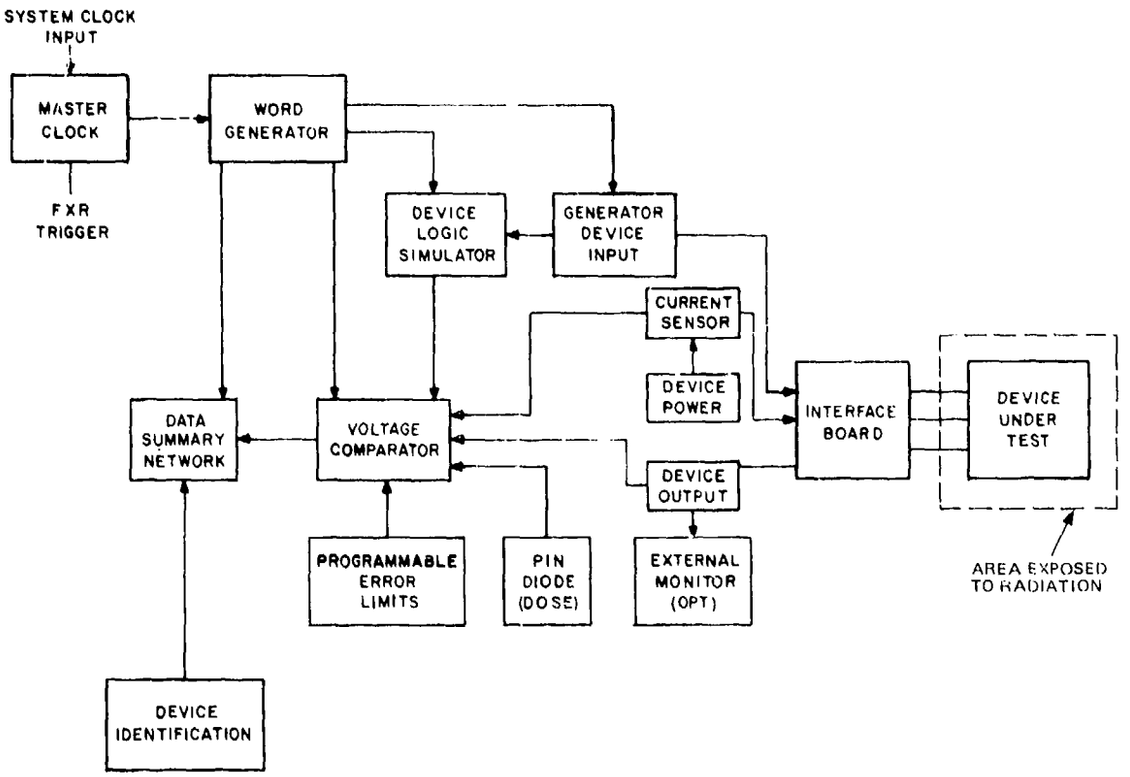

Figure 8.3-6. Recommended latchup test system.

There are two groups of digital integrated circuit devices to be considered when testing for latchup. These are determined devices whose output is a unique function of the input and changes when the input changes (e.g., NAND gates), and nondetermined devices whose output is not a function of the input (e.g., a J-K flip-flop that changes output state only with the clock signal). Failed determined devices are those whose output is not in a proper logic state or that fails to respond properly to a change in input after radiation. Nondetermined devices that fail the latchup test are those that do not respond properly to the second change in input after radiation. The second change is used since the first change in input may not change the output if it has already changed due to radiation. However, the second change of input must change the output.

For linear circuits, there are two preferred methods for verifying proper device operation. The first method involves a visual examination of oscilloscope photographs of the circuit output responses before and

after radiation exposure to determine the failure status. The second method uses preset comparators to evaluate the device output. At least two different input levels are applied to the test device. The corresponding output levels are fed into the preset comparators for failure evaluation.

Medium- and large-scale integrated circuits normally have more output states than can be practically monitored. An evaluation must be made of the actual device application requirements to identify the input/output functions pertinent to the latchup test.

Test requirements to be specified include the device types, parameters to be measured, device operating conditions during test, time intervals between exposure and functional tests, radiation dose and limits, and temperature. Data reporting shall include at least an identification of parts by serial number and the pass/fail status data. Careful data recording is essential.

8.4 DATA REPORTING

8.4.1 General

The general information required in most reports of TREE tests is given in Chapter 3. Information requirements covered in that section include reporting of the test procedures, description of the facilities used, documentation of the dosimetry, and a complete description of the samples irradiated. Included here are specific data requirements for tests involving integrated circuits and standardized formats for reporting the data. Figure 8.4-1 shows a typical data format that can be used to present the general information for each irradiation test.

In addition to the irradiation procedure, basic types of samples should be described. A good technique to employ is to provide a separate data sheet that presents the manufacturer, type of specification number, lot number, origin (factory, distributor, etc.), and method of selection and validation for the various device types. If useful electrical and structural information (such as power rating and junction areas) is available, it should be reported to facilitate data comparisons and to increase the general utility of the data. A typical parts tabulation sheet is illustrated in Figure 8.4-2.

A statement should be given as to the consistency of any control samples used. The estimated uncertainty in all important results should be quoted. In specifying errors, the value of one standard deviation is the quantity preferred, although other methods may be used if they are more suitable and are unambiguous. When statistical characterizations are given, the techniques involved in their calculation should be explained--at least by a reference.

Due to the large variety of integrated circuits and the number of tests that can be performed on them, specific test conditions cannot be defined

Device Type(s): _____

Facility: _____ Date of Test: _____

Dosimetry Method(s): _____

Irradiation Temperature: _____

Experimental Configuration: _____

Electrical Condition During Irradiation: _____

(Specify device bias condition and the circuit diagram, including all test equipment and grounding scheme used during in situ measurement.)

Additional Comments:

Figure 8.4-1. Sample format for general test information.

Information to be Included				Useful Information				
Serial Number	Unit Designation in Test	Manufacturer	Date of manufacture and/or Purchase	Device Batch and Lot Number	Maximum Current Rating	Maximum Voltage Rating	Device Application	Comments

Figure 8.4-2. Sample format for tabulating parts data.

on the data sheet itself. Therefore, a separate record is recommended for documenting the measurement conditions by device pin number for each integrated circuit test. Figure 8.4-3 is a suggested format for recording measurement conditions. The test designation is necessary to identify each individual test on the data sheets. Either a standard test designation or a number may be used.

In addition to recording the test conditions, a test diagram with bias conditions specified should be included.

8.4.2 Permanent-Damage Data

It is recommended that device parameter data be tabulated for each set of measurements giving the parameters measured, the irradiation level at which the measurements were made, the operating condition of the device during measurement, and any additional test conditions. Note that preirradiation parameter values must be included. A sample data format for tabulating measured parameter values is given in Figure 8.4-4. As supplementary information to parameter data, the measurement procedure should be reported. Specifically, this includes the measurement-circuit diagram, a list of the measurement equipment and a statement regarding the accuracy and/or precision of the data.

Type: _____

Date: _____

Test	Operating Conditions On Pin																
Desig	1	2	3	4	5	6	7	8	9	10	11	12	13	14	15	16	Comments

Figure 8.4-3. Sample format for recording integrated circuit measurement conditions.

Type: _____

Date: _____

Unit Desig	Test Desig	Gamma Dose rads (Si)	Neutron Fluence n/cm² (1-MeV Eq)	Measurement and Test Conditions	Value	Measurement and Test Conditions	Value	Measurement and Test Conditions	Value	Measurement and Test Conditions	Value

Figure 8.4-4. Sample format for recording permanent-effects data.

Graphs showing the radiation-induced changes in the measured parameter values are very desirable and complement the tabulated data. The method employed for the graphical presentation of data depends on the method of data analysis and the objectives of the experiments. As a general guideline, it is recommended that parameter measurements made at only one operating point should be plotted as a function of radiation exposure. Parameters that are measured at several operating points at each fluence level should be plotted as a function of the parameter varied to change the operating point. The result will be a family of curves for the various radiation exposures. Figure 8.4-5 shows an example of TTL output voltage changes due to neutron exposure. Similar curves can be developed for devices sensitive to total dose exposure.

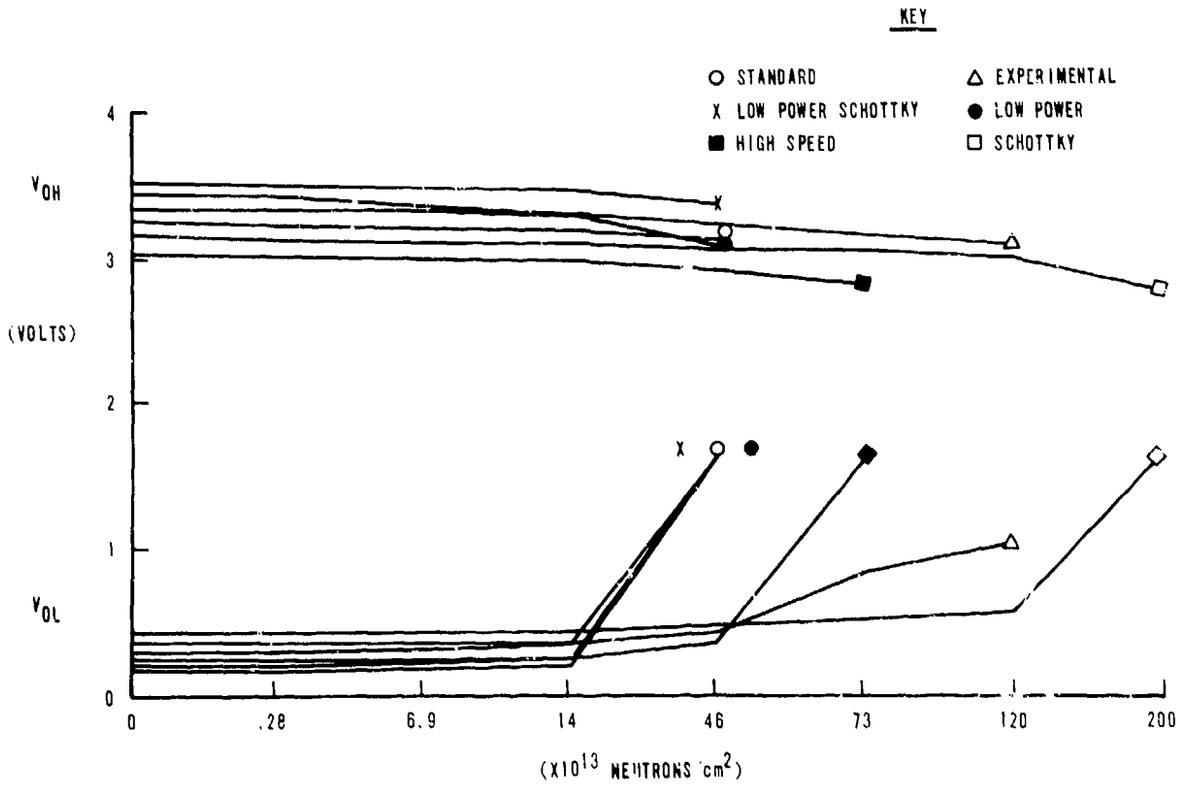

Figure 8.4-5. TTL output voltage versus neutron fluence (Reference 26).

8.4.3 Transient Radiation Exposure Data

The measured ionization response of integrated circuits should be tabulated in a fashion similar to the format described for permanent-effects data. A sample data format for tabulating ionizing data is given in Figure 8.4-6. Consideration should also be given to reporting complementary

electrical-characterization data measured before radiation exposure that are likely to be correlated with the radiation response.

Type: _____

Date: _____

Unit Desig	Test Desig	Thres. Def.	Rad(Si) Dose	μs Nom. Pulse Width	Rad(Si)/s Dose Rate	(mA) ΔI PIN__	ΔI PIN__	Δ... PIN__	ΔI_{GND} PIN__	(V) ΔV PIN__	ΔV PIN__	ΔV PIN__	ΔV PIN__

Figure 8.4-6. Integrated circuit ionization-effects data.

The graphical presentation of ionization-effects data as a complement to tabulated data is very desirable. A typical format for the graphical presentation of the transient response as a function of dose rate is shown in Figure 8.4-7. For each device type on which radiation data are reported, an illustration or oscilloscope photograph should show a typical response as a function of time and display the leading and trailing edges of the pulse. The dose rate at which the illustration was taken should be indicated. If the shape of the response changes appreciably with dose rate, additional illustrations of response should be shown and the areas of the response curve to which they apply should be indicated.

Similar graphical data can be developed for other circuit parameters for both digital and linear integrated circuits. Figure 8.4-8 shows the variation of the important recovery time parameter of a linear amplifier after radiation exposure.

8.5 TESTING CONSIDERATIONS FOR MSI AND LSI DEVICES

The principles of testing to determine the radiation response of integrated circuit devices discussed in the preceeding sections are applicable to devices of much greater complexity than simple gate circuits or basic operational amplifiers. These devices are generally referred to as medium-scale integrated (MSI), large-scale integrated (LSI), and very large-scale integrated (VLSI) circuits. Such devices normally contain many more output states than can be practically monitored during test. Many of these devices can only be evaluated on a pass/fail basis and most require unique test setups; however, the appropriate test standards referred to in this chapter must be a part of any such test setup and must be adhered to in all cases (References 2 and 3).

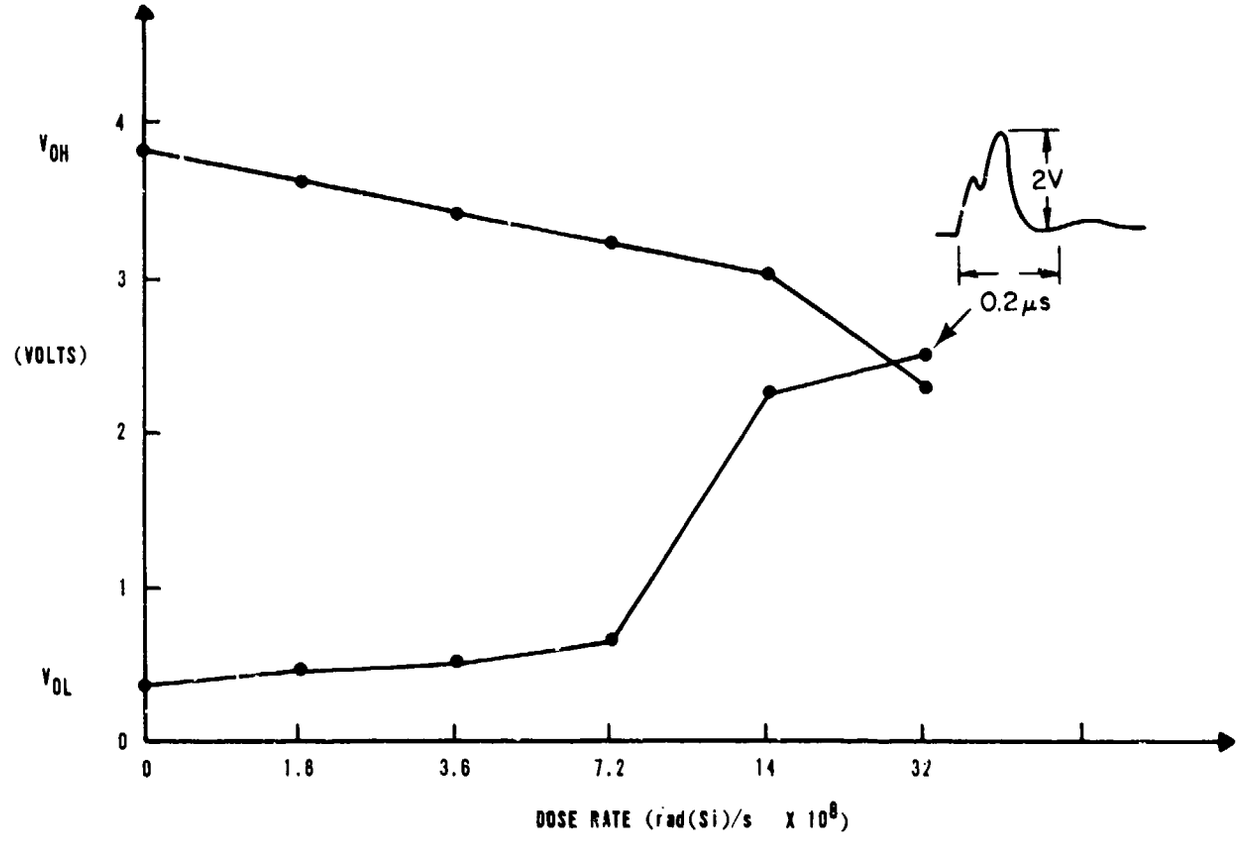

Figure 8.4-7. Transient radiation response of a TTL NAND gate (insert shows a typical output response waveform) (Reference 26).

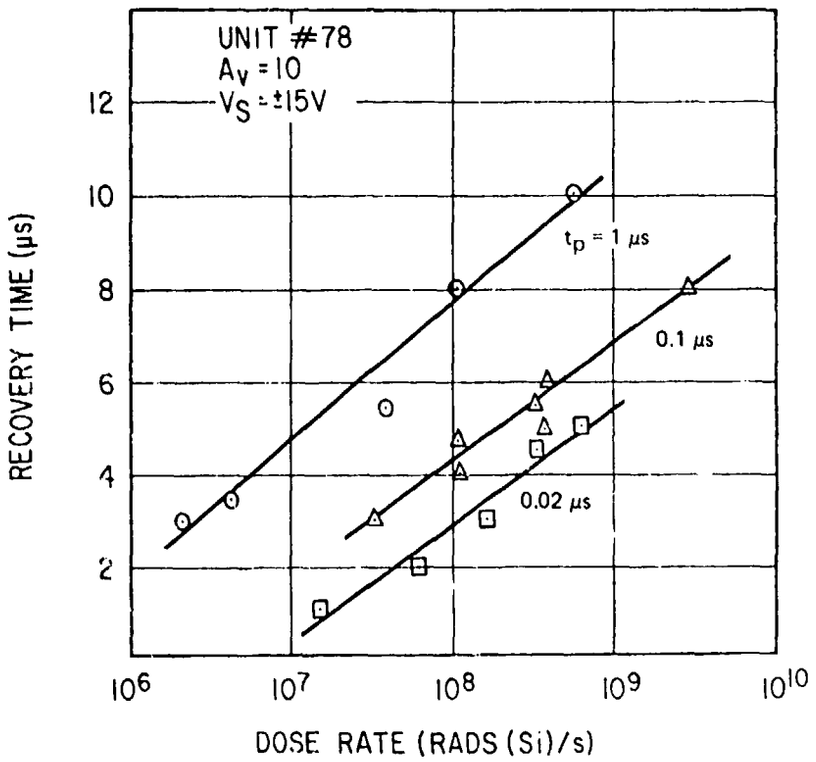

Figure 8.4-8. Amplifier recovery time as a function of ionizing dose rate for three radiation pulse widths (Reference 27).

Automated LSI test systems are usually rather large and immobile. They are readily adaptable to permanent-damage measurements where devices can be tested, exposed to a given quantity of radiation, and then tested again. They are not well suited for in-situ testing for transient error detection or for pulsed radiation exposure measurements. A useful approach that has been developed for memories and microprocessors is based on comparing a device under test to a reference device pin for pin. This approach uses procedures defined to systematically test a device and identify malfunctions in a comprehensive, but not exhaustive, way. For example, if two registers on the same chip can be separately loaded into the accumulator, and if data from one register can be properly added to the contents of the accumulator, then it is not necessary to test the proper addition of data from the second register. The following paragraph describes an instrumentation setup that has been developed for testing microprocessors.

Microprocessors may contain thousands of transistors and thousands of interconnections with only 40 connections available for measurements. The perfect test for such devices would be to manipulate the instructions and

available control pins to put the internal devices into all possible state combinations. Such a 100-percent test would consume far more time than is acceptable. An evaluation of the device application must be made to help identify the input/output functions to be monitored; compromises must be made to use a test program that directs the device under test to execute a representative number of different types of functions.

A block diagram of an instrumentation setup that has been developed to evaluate microprocessor response to radiation exposure is shown in Figure 8.5-1 (Reference 28). The procedure is to compare the functioning of two identical microcomputer systems driven by a common system clock and executing identical instruction set listings. One microcomputer is a reference system and the other is the support system for the microprocessor being exposed to the radiation. A comparator circuit detects any differences in the outputs of the microprocessor under test and the reference microprocessor. The measurements monitor only the functioning of the device under test on a pass/fail basis, not the device parameter variations. The test techniques and instrumentation are quickly adaptable to a variety of microprocessors. A more complete description of the procedures and the instrumentation is given in Reference 28.

Similar test setups can be developed for testing other types of LSI devices. It is the responsibility of the user to thoroughly consider the requirements of his system when devising specific test procedures in accordance with the established standards.

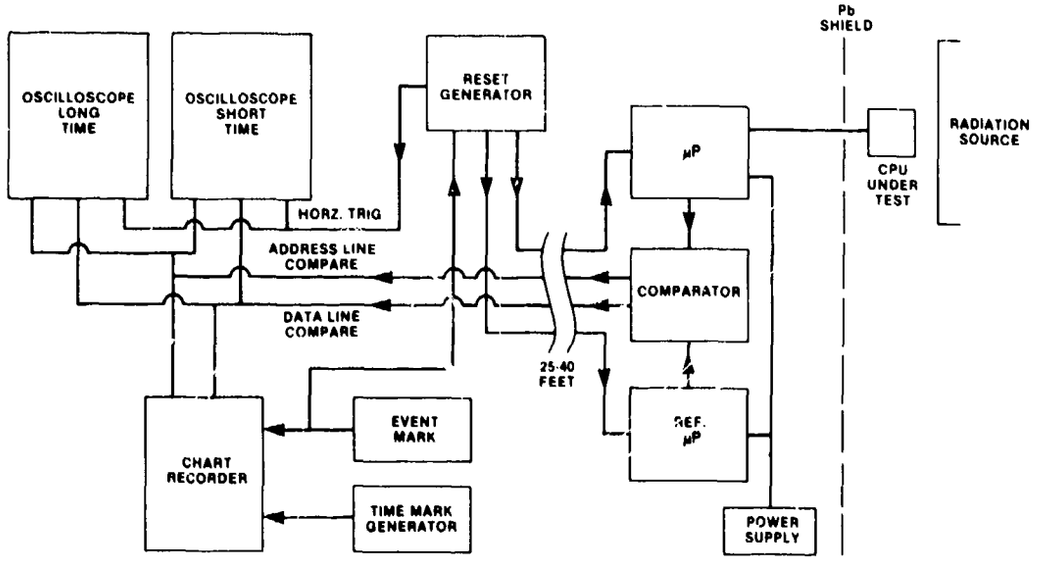

Figure 8.5-1. Block diagram of instrumentation setup (Reference 28).

CHAPTER 9

REFERENCES

1. Design Handbook for TREE (U), DASIAC, Unpublished.

2. Test Methods and Procedures for Microelectronics, MIL-STD-883B, 31 August 1977 (U).

3. Annual Book of ASTM Standards--Parts 43 and 45, American Society for Testing and Materials, 1980 (U).

4. Test Methods for Semiconductor Devices, MIL-STD-750B, 27 February 1970 (U).

5. Wilkes, S.S., Mathematical Statistics, John Wiley, New York, 1962 (U).

6. Hold, A., Statistical Theory With Engineering Applications, John Wiley, New York, 1967 (U).

7. General Specification for Semiconductor Device, MIL-S-19500F, 15 December 1977 (U).

8. General Specification for Microcircuits, MIL-M-38510D, 31 August 1977 (U).

9. Caldwell, R.S., et al., Symposium on Transient Radiation Effects and Techniques for Circuit Hardening (U), The Boeing Company, Unpublished.

10. Standards for DNA Scientific and Technical Reports, Defense Nuclear Agency, Washington, D.C., 16 July 1979 (U).

11. Format Requirements for Scientific and Technical Reports Prepared by or for the Department of Defense, MIL-STD-847A, 31 January 1973 (U).

12. Preparation of Test Reports, MIL-STD-831, 28 August 1963 (U).

13. TREE Simulation Facilities--Second Edition, DASIAC, DNA 2432H, 1 January 1979 (U).

14. ICRU Report 19--Radiation Quantities and Units, International Commission on Radiation Units and Measurements, Washington, D.C., 1976 (U).

15. Holmes, R.R., et al., Weapons Effects Studies, Volume II, Radiation Effects on Interceptor Electronics, Bell Telephone Laboratories, 1 October 1970 (U).

16. Verbinski, V., and C. Cassapakia, Simultaneous Neutron Spectrum and Transistor-Damage Measurements in Diverse Neutron Fields: Validity of $D_{Si}(E_n)$, NRL Memo Report 3929, 16 March 1979 (U).

17. Mach, M.E., and B.F. Rider, Compilation of Fission Product Yields, Vallecitos Nuclear Center, Pleasanton, CA, NEDO-12154-1, 1974 (U).

18. ANL 5800, Reactor Physics Constants, Argonne National Laboratory, Argonne, IL, February 1969 (U).

19. Berger, M.J., and S.M. Seltzer, Tables of Energy Losses and Ranges of Positrons and Electrons, NASA Technical Report SP-3012, 1964 (U).

20. Humpheries, K.C., A Review of Some Passive Dosimetry Methods Used in Radiation-Effects Studies With Fast Burst Reactors, USAEC Publication CONF-69-0102, p. 508, 1969 (U).

21. Energy Loss of Electrons and Positrons, NBS Circular 577 (U).

22. Price, W., et al., Total-Dose Hardness Assurance Guidelines for Semiconductor Devices, Jet Propulsion Laboratory, Pasadena, CA, DNA 5905F, 1 February 1982 (U).

23. Namenson, A., et al., Piece Part Neutron Hardness Assurance Guidelines for Semiconductor Devices, DNA 5910F, 6 October 1981 (U).

24. Messenger, G., and E. Steele, Statistical Modeling of Semiconductor Devices for the TREE Environment, IEEE Transactions on Nuclear Science, Vol. NS-15, 133, December 1968 (U).

25. Snowden, D., and J. Harrity, DNA Support Services, IRT Corporation, San Diego, CA, DNA 5516F, 31 January 1981 (U).

26. Knoll, M.G., Companion Study of the Five Transistor-Transistor-Logic (TTL) Families and Emitter Coupled Logic (ECL). Air Force Weapons Laboratory, Kirtland Air Force Base, NM, AFWL-TR-78-5, May 1978 (U).

27. MacDougall, J.S., et al., Development of a Radiation Hardened Operational Amplifier, Fairchild Camera and Instrument Corporation, Mountain View, CA, AFCRL-72-0558, August 1972 (U).

28. Wilkin, N.D., Ionizing Radiation Susceptibility of Microprocessors, Harry Diamond Laboratories, Adelphi, MD, HDL-TR-1949, April 1981 (U).

DISTRIBUTION LIST

DEPARTMENT OF DEFENSE

Armed Forces Radiobiology Rsch Institute
ATTN: J. Hsieh

Assistant to the Secretary of Defense
Atomic Energy
ATTN: Military Applications
ATTN: Executive Assistant

Command & Control Tech Ctr
ATTN: C-330
ATTN: C-310

Defense Advanced Rsch Proj Agency
ATTN: R. Reynolds
ATTN: S. Roosild
ATTN: J. Fraser

Defense Communications Engineer Ctr
ATTN: Code R720, C. Stansberry
ATTN: Code R410

Defense Electronic Supply Ctr
ATTN: DEFC-ESA

Defense Intelligence Agency
ATTN: DT-1B
ATTN: DB-4C, Rsch, Phys Vuln Br

Defense Logistics Agency
ATTN: DLA-SE
ATTN: DLA-QEL, J. Slattery
ATTN: DLA-SEE, F. Harris

Defense Nuclear Agency
3 cy ATTN: RAEV, TREE
4 cy ATTN: TITL

Defense Tech Info Ctr
12 cy ATTN: DD

Field Command Defense Nuclear Agency
Det 1
Lawrence Livermore Lab
ATTN: FC-1

Field Command
Defense Nuclear Agency
ATTN: FCTT, W. Summa
ATTN: FCTT
ATTN: FCTXE
ATTN: FCPF, R. Blackburn
ATTN: FCPR

Joint Chiefs of Staff
ATTN: C3S Evaluation Office, HDOO

National Communications System
ATTN: NCS-TS, D. Bodson
ATTN: NCS-TS

Under Secretary of Defense for Rsch & Engrg
ATTN: Strategic & Space Sys (OS)
ATTN: Strat & Space Sys (OS), C. Knowles
ATTN: Strat & Theater Nuc Forces, B. Stephan

DEPARTMENT OF DEFENSE (Continued)

National Security Agency
ATTN: P. Deboy
ATTN: T. Neal
ATTN: R. Light
ATTN: T. Brown
ATTN: K. Schaffer
ATTN: T. Livingston
ATTN: G. Daily
ATTN: R-52, O. Van Gunten

DEPARTMENT OF THE ARMY

Aberdeen Proving Ground
ATTN: S. Harrison

Applied Sciences Div
ATTN: R. Williams

BMD Advanced Technology Ctr
ATTN: ATC-O, F. Hoke
ATTN: ATC-T

BMD Systems Command
ATTN: BMDSC-HW, R. Dekalb
ATTN: BMDSC-AU, R. Webb
ATTN: BMDSC-AV, J. Harper
ATTN: BMDSC-HW

Deputy Chief of Staff for Rsch Dev & Acq
ATTN: G. Ogden

Fort Huachuca
ATTN: Tech Ref Div

Harry Diamond Labs
ATTN: DELHD-NW, J. Bombardt
ATTN: R. Reams
ATTN: DELHD-NW-P, T. Flory
ATTN: DELHD-NW-RA
ATTN: P. Winokur
ATTN: DELHD-NW-R, F. Mclean
ATTN: DELHD-NW-R, B. Dobriansky
ATTN: DELHD-NW-EA, J. Miletta
ATTN: DELHD-NW-RA, W. Vault
ATTN: DELHD-NW-P
ATTN: DELHD-NW-R, C. Self
ATTN: DELHD-NW-R, T. Oldham
ATTN: DELHD-NW-R, H. Eisen
ATTN: J. Vallin
ATTN: C. Fazi
ATTN: L. Harper
ATTN: T. Taylor
ATTN: DELHD-NW-RC, J. McGarrity
ATTN: T. Conway
ATTN: T. Griffin
ATTN: DELHD-NW-EC, Chief Lab 21000
ATTN: DELHD-NW-RC, E. Boesch
ATTN: DELHD-NW-RH

US Army Armor & Engineer Board
ATTN: ATZK-AE-AR, J. Dennis

DEPARTMENT OF THE ARMY (Continued)

US Army Armament Rsch Dev & Cmd
ATTN: DRDAR-LCA-PD
ATTN: DRDAR-LCN-F
ATTN: DRDAR-TSI-E, A. Grinoch
ATTN: DRDAR-TSS, Tech Div

US Army Ballistic Rsch Labs
ATTN: DRDAR-BLV, D. Rigotti
ATTN: DRDAR-BLB, W. Van Antwerp
ATTN: DRDAR-BLT

UA Army Chemical School
ATTN: ATZN-CM-CS

US Army Communications R&D Cmd
ATTN: DELET-IR, E. Hunter
ATTN: DRSEL-NL-RO, R. Brown
ATTN: DRSEL-CT-HDK, A. Cohen

US Army Communications Sys Agency
ATTN: CCM-RD-T, S. Krevsky

US Army Engineer Div, Huntsville
ATTN: HNDED-ED, J. Harper

US Army Intelli ence & Sec Cmd
ATTN: IARDA-OS, R. Burkhardt

US Army Material & Mechanics Rsch Ctr
ATTN: DRXMR-HH, J. Dignam
ATTN: DRXMR-B, J. Hofmann

US Army Mobility Equip R&D Cmd
ATTN: DRDME-E, J. Bond, Jr

US Army Nuclear & Chemical Agency
ATTN: MONA-MS, H. Wells
ATTN: MONA-WE
ATTN: Library

US Army Rsch Office
ATTN: R. Griffith

US Army Signal Warfare Lab, VHFS
ATTN: K. Erwin

US Army Test and Evaluation Comd
ATTN: DRSTE-EL
ATTN: DRSTE-FA

US Army TRADOC Sys Analysis Actvy
ATTN: ATAA-TFC, O. Miller

US Army Training and Doctrine Comd
ATTN: ATCD-Z

US Army White Sands Missile Range
ATTN: STEWS-TE-NT, M. Squires
ATTN: STEWS-TE-AN, T. Arellanes
ATTN: STEWS-TE-AN, A. De La Paz
ATTN: STEWS-TE-AN, J. Meason
ATTN: STEWS-TE-N, K. Cummings
ATTN: STEWS-TE-AN, R. Hays
ATTN: STEWS-TE-AN, R. Dutchover

USA Night Vision & Electro-Optics Lab
ATTN: DRSEL-NV-SD, J. Carter
ATTN: DRSEL-NV-SD, A. Parker

DEPARTMENT OF THE ARMY (Continued)

USA Missile Command
ATTN: Hawk Project Officer, DRCPM-HALR
ATTN: DRCPM-PE-EA, W. Wagner
ATTN: DRSMI-SF, H. Hendricksen
3 cy ATTN: Doc Sec

XM-1 Tank System
ATTN: DRCPM-GCM-SW

DEPARTMENT OF THE NAVY

Naval Air Systems Cmd
ATTN: AIR 5324K
ATTN: AIR 350F
ATTN: AIR 310

Naval Avionics Ctr
ATTN: Code 8415, D. Repass

Naval Electronic Systems Cmd
ATTN: Code 50451
ATTN: PME 117-21
ATTN: NAVELEX 51024, C. Watkins
ATTN: Code 5045.11, C. Suman

Naval Intelligence Support Ctr
ATTN: NISC, Library

Naval Ocean Systems Ctr
ATTN: Code 7309, R. Greenwell
ATTN: Code 4471

Naval Postgraduate School
ATTN: Code 1424, Library

Naval Sea Systems Cmd
ATTN: SEA-06J, R. Lane
ATTN: SEA-04531

Naval Surface Weapons Ctr
ATTN: F31, J. Downs
ATTN: Code WA-52, R. Smith
ATTN: Code F30
ATTN: Code F31
ATTN: Code F31, K. Caudle
ATTN: Code F31, F. Warnock

Naval Weapons Ctr
ATTN: Code 343, FMA6A2, Tech Svcs

Naval Weapons Evaluation Fac
ATTN: Code AT-6

Naval Weapons Support Ctr
ATTN: Code 70242, J. Munarin
ATTN: Code 3073, T. Ellis
ATTN: Code 6054, D. Platteter
ATTN: Code 605, J. Ramsey

Nuclear Weapons Trng Group, Pacific
ATTN: Code 32

Office of the Deputy Asst Secretary of the Navy
ATTN: L. Abella

Office of the Deputy Chief of Naval Ops
ATTN: OP 985F

DEPARTMENT OF THE NAVY (Continued)

Naval Rsch Lab
ATTN: Code 6635, G. Mueller
ATTN: Code 6814, M. Peckerar
ATTN: Code 6611, E. Petersen
ATTN: Code 6816, E. Richmond
ATTN: Code 6510, H. Rosenstock
ATTN: Code 6813, N. Saks
ATTN: Code 6611, P. Shapiro
ATTN: Code 6612, D. Walker
ATTN: Code 6612, R. Statler
ATTN: Code 4020, J. Adams
ATTN: Code 6603, J. McElhinney
ATTN: Code 6680, D Nagel
ATTN: Code 6816, R. Hevey
ATTN: Code 4040, J. Boris
ATTN: Code 6611, A. Campbell
ATTN: Code 6682, D. Brown
ATTN: Code 6683, C. Dozier
ATTN: Code 6601, E. Wolicki
ATTN: Code 6810, J. Davey
ATTN: Code 6611, J. Ritter
ATTN: Code 6814, D. McCarthy
ATTN: Code 6701
ATTN: Code 2627
ATTN: Code 6816, H. Hughes
ATTN: Code 6673, A. Knudson
ATTN: Code 6813, W. Jenkins
ATTN: Code 6613, R. Lambert
ATTN: Code 6600, J. Schriempf
ATTN: Code 6612, G. McLane
ATTN: Code 6816, D. Patterson
ATTN: Code 6816, G. Davis
ATTN: Code 6813, J. Killiany
ATTN: Code 6611, L. August
ATTN: Code 6653, A. Namenson
ATTN: Code 6610, R. Marlow
ATTN: Code 6680, D. Nagel

Office of Naval Rsch
ATTN: Code 220, D. Lewis
ATTN: Code 414, L. Cooper
ATTN: Code 427

Strategic Systems Project Office
ATTN: NSP-2301, M. Meserole
ATTN: NSP-27334, B. Hahn
ATTN: NSP-2701, J. Pitsenberger
ATTN: NSP-27331, P. Spector
ATTN: NSP-2430, J. Stillwell

DEPARTMENT OF THE AIR FORCE

Aeronautical Systems Div
ATTN: ASD/ENESS, P. Marth
ATTN: ASD/ENACC, R. Fish
ATTN: ASD/YH-EX, J. Sunkes
ATTN: ASD/ENTV, L. Robert

Air Force Geophysics Lab
ATTN: PHG, M/S 30, E. Mullen
ATTN: SULL
ATTN: SULL, S-29
ATTN: PLIG, R. Filz

Air Force Inscitute of Technology
ATTN: ENP, J. Bridgeman

DEPARTMENT OF THE AIR FORCE (Continued)

Headquarters
Air Force Systems Command
ATTN: DLCAM
ATTN: DLW

Air Force Tech Applications Ctr
ATTN: TAE

Air Force Wright Aeronautical Lab
ATTN: POE-2, J. Wise
ATTN: POD, P. Stover

Air Force Wright Aeronautical Lab
ATTN: TLA
ATTN: LTE
ATTN: LPO, R. Hickmott
ATTN: TEA, R. Conklin
ATTN: DHE-2
ATTN: DHE

Air Logistics Command
ATTN: MMETH, R. Blackburn
ATTN: MMIFM, S. Mallory
ATTN: MMETH
ATTN: MMGRW, G. Fry
ATTN: OO-ALC/MM
ATTN: A. Cossens
ATTN: MMEDD

Air University Library
ATTN: AUL-LSE

Assistant Chief of Staff
Studies & Analyses
2 cy ATTN: AF/SAMI, Tech Info Div

Ballistic Missile Office
ATTN: ENSN, H. Ward
ATTN: ENBE
ATTN: SYST, L. Bryant
ATTN: ENMG
ATTN: SYDT
ATTN: ENSN M. Williams
ATTN: ENSN
ATTN: ENSN, J. Tucker

Headquarters
Electronic Systems Div, IN
ATTN: INDC

Foreign Technology Div
ATTN: TQTD, B. Ballard
ATTN: PDJV

Office of Secretary of the Air Force
ATTN: Dir

Rome Air Dev Ctr
ATTN: RBR, J. Brauer
ATTN: RBRP, C. Lane
ATTN: RDC, R. Magoon

Sacramento Air Logistics Ctr
ATTN: MMEAE, R. Dallinger

DEPARTMENT OF THE AIR FORCE (Continued)

Rome Air Dev Ctr
ATTN: ESR, P. Vail
ATTN: ESE, A. Kahan
ATTN: ESR, J. Bradford, MS 64
ATTN: ESR, W. Shedd
ATTN: ESR/ET, E. Burke MS 64
ATTN: ESR, B. Buchanan

Space Div
ATTN: AQT, S. Hunter
ATTN: AQM
ATTN: YB
ATTN: YD
ATTN: YE
ATTN: YGJ, R. Davis
ATTN: YG
ATTN: YK
ATTN: YKA, C. Kelly
ATTN: YKS, P. Stadler
ATTN: YLS
ATTN: YLS, L. Darda
ATTN: YL
ATTN: YLVM, J. Tilley
ATTN: YN
ATTN: YR
ATTN: YV

Strategic Air Command
ATTN: NRI-STINFO, Library
ATTN: XPFS, M. Carra

Tactical Air Command
ATTN: XPG

3416th Tech Training Squadron, ATC
ATTN: TTV

Air Force Weapons Lab
ATTN: NTYC
ATTN: NTYC, J. Ferry
ATTN: NTYCT, J. Mullis
ATTN: NTYC, R. Maier
ATTN: NTYEE, C. Baum
ATTN: NTYCT, R. Tallon
ATTN: SUL
ATTN: NTYC, M. Schneider

DEPARTMENT OF ENERGY

Department of Energy
Albuquerque Operations Office
ATTN: WSSB, R. Shay
ATTN: WSSB

OTHER GOVERNMENT AGENCIES

Central Intelligence Agency
ATTN: OSWR/STD/MTB, A. Padgett
ATTN: OSWR/NED
ATTN: OSWR, T. Marquitz

Department of Transportation
Federal Aviation Admin
ATTN: ARD-350

NASA
ATTN: J. Murphy

OTHER GOVERNMENT AGENCIES (Continued)

NASA
ATTN: Code 710.2, D. Haykin, Jr
ATTN: Code 310, W. Womack
ATTN: Code 660, J. Trainor
ATTN: Code 701, W. Redisch
ATTN: Code 695, M. Acuna
ATTN: Code 724.1, M. Jhabvala
ATTN: Code 311.3, D. Cleveland
ATTN: Code 311A, J. Adolphsen
ATTN: Code 601, E. Stassinopoulos
ATTN: Code 5301, G. Kramer
ATTN: Code 654.2, V. Danchenko

NASA
ATTN: EG02
ATTN: L. Hamiter
ATTN: M. Nowakowski
ATTN: H. Yearwood

NASA
ATTN: M. Baddour

NASA
ATTN: G. Deyoung

NASA Headquarters
ATTN: Code D, W. McGinnis
ATTN: Code DP, B. Bernstein
ATTN: Code DP, R. Karpen

Department of Commerce
National Bureau of Standards
ATTN: T. Russell
ATTN: C. Wilson
ATTN: R. Scace
ATTN: Code A305, K. Galloway
ATTN: Code A353, S. Chappell
ATTN: Code A347, J. Mayc-Wells
ATTN: Code A361, J. French
ATTN: Code C216, J. Humphreys
ATTN: Code A327, H. Schafft

NATO

NATO School, SHAPE
ATTN: US Documents Officer

DEPARTMENT OF ENERGY CONTRACTORS

University of California
Lawrence Livermore National Lab
ATTN: Tech Info Dept, Library
ATTN: L-156, R. Kalibjian
ATTN: L-156, J. Yee
ATTN: L-153, D. Meeker
ATTN: W. Orvis
ATTN: L-389, R. Ott
ATTN: L-10, H. Kruger

Los Alamos National Lab
ATTN: J. Freed
ATTN: D. Lynn
ATTN: C. Spirio
ATTN: D. Wilde
ATTN: MS D450, B. McCormick

DEPARTMENT OF ENERGY CONTRACTORS (Continued)

Sandia National Lab
ATTN: Div 2144, W. Dawes
ATTN: Div 2143, H. Sander
ATTN: Org 9336, J. Renken
ATTN: Div 2143, H. Weaver
ATTN: Org 2150, J. Hood
ATTN: T. Wrobel
ATTN: Org 2100, B. Gregory
ATTN: Div 4232, L. Posey
ATTN: Div 1732, G. Baldwin

DEPARTMENT OF DEFENSE CONTRACTORS

Advanced Microdevices, Inc
ATTN: J. Schlageter

Advanced Research & Applications Corp
ATTN: R. Armistead
ATTN: T. Magee
ATTN: L. Palkuti

Advanced Research & Applications Corp
ATTN: A. Larson

Aerojet Electro-Systems Co
ATTN: P. Lathrop
ATTN: D. Toomb
ATTN: SV/8711/70
ATTN: D. Huffman

Aerospace Corp
ATTN: W. Crane, A2/1083
ATTN: R. Slaughter
ATTN: J. Reinheimer
ATTN: J. Wiesner
ATTN: A. Carlan
ATTN: R. Crolius
ATTN: H. Phillips
ATTN: W. Kolasinski, MS/259
ATTN: D. Schmunk
ATTN: D. Fresh
ATTN: V. Josephson, MS-4-933
ATTN: C. Huang
ATTN: J. Stoll
ATTN: S. Bower
ATTN: P. Buchman
ATTN: R. Crolius
ATTN: B. Blake
ATTN: I. Garfunkel
ATTN: G. Gilley

Aerospace Industries Assoc of America, Inc
ATTN: S. Siegel

Ampex Corp
ATTN: D. Knutson
ATTN: J. Smith

Analytic Svcs, Inc
ATTN: P. Szymanski
ATTN: J. O'Sullivan
ATTN: A. Shostak

Applied Systems Engrg Dir
ATTN: J. Retzler, Nuc S/V Mang

DEPARTMENT OF DEFENSE CONTRACTORS (Continued)

AVCO Systems Div
ATTN: D. Fann
ATTN: C. Davis
ATTN: W. Broding
ATTN: D. Shrader

Battelle Memorial Institute
ATTN: R. Thatcher

BDM Corp
ATTN: S. Meth
ATTN: C. Stickley

BDM Corp
ATTN: R. Antinone
ATTN: D. Wunsch
ATTN: Marketing

Beers Assoc, Inc
ATTN: S. Ives
ATTN: B. Beers

Bell Labs
ATTN: R. McPartland
ATTN: D. Yaney

Bendix Corp
ATTN: Doc Con

Bendix Corp
ATTN: M. Frank

Bendix Corp
ATTN: E. Meeder

Boeing Aerospace Co
ATTN: MS-81-36, W. Doherty
ATTN: D. Mulkey
ATTN: MS-2R-00, C. Rosenberg
ATTN: MS-2R-00, A. Johnston
ATTN: C. Dixon
ATTN: MS-2R-00, T. Arimura
ATTN: MS-81-36, P. Blakely
ATTN: MS-2R-00, E. Smith

Boeing Co
ATTN: D. Egelkrout
ATTN: H. Wicklein
ATTN: 8K-38
ATTN: R. Caldwell

Booz, Allen and Hamilton, Inc
ATTN: R. Chrisner

Burr-Brown Rsch Corp
ATTN: H. Smith

Burroughs Corp
ATTN: Product Evaluation Lab

Cincinnati Electronics Corp
ATTN: L. Hammond
ATTN: C. Stump

DEPARTMENT OF DEFENSE CONTRACTORS (Continued)

California Institute of Technology
ATTN: D. Nichols, T-1180
ATTN: R. Covey
ATTN: P. Robinson
ATTN: J. Bryden
ATTN: F. Grunthaner
ATTN: A. Shumka
ATTN: W. Price
ATTN: K. Martin
ATTN: W. Scott

Charles Stark Draper Lab, Inc
ATTN: P. Greiff
ATTN: A. Schutz
ATTN: J. Boyle
ATTN: R. Bedingfield
ATTN: R. Ledger
ATTN: A. Freeman
ATTN: D. Gold
ATTN: Tech Library
ATTN: R. Haltmaier
ATTN: W. Callender
ATTN: N. Tibbetts

Clarkson College of Technology
ATTN: P. McNulty

Computer Sciences Corp
ATTN: A. Schiff

Control Data Corp
ATTN: T. Frey
ATTN: D. Newberry, BRR 142

University of Denver
ATTN: Sec Officer for F. Venditti

Develco, Inc
ATTN: G. Hoffman

Dikewood
ATTN: Tech Library for L. Davis

E-Systems, Inc
ATTN: K. Reis

E-Systems, Inc
ATTN: Div Library

Eaton Corporation
ATTN: A. Anthony
ATTN: R. Bryant

Electronic Industries Assoc
ATTN: J. Kinn

Exp & Math Physics Consultants
ATTN: T. Jordan

University of Florida
ATTN: H. Sisler

FMC Corporation
ATTN: M. Pollock

Ford Aerospace & Communications Corp
ATTN: K. Attinger
ATTN: J. Davison
ATTN: Tech Info Svcs

DEPARTMENT OF DEFENSE CONTRACTORS (Continued)

Ford Aerospace & Communications Corp
ATTN: D. Newell
ATTN: D. Cadle
ATTN: E. Hahn

Franklin Institute
ATTN: R. Thompson

Garrett Corp
ATTN: H. Weil

General Dynamics Corp
ATTN: O. Wood
ATTN: R. Fields, MZ2839

General Electric Co
ATTN: Tech Info Ctr for L. Chasen
ATTN: J. Peden
ATTN: J. Andrews
ATTN: R. Casey
ATTN: R. Benedict
ATTN: Tech Library
ATTN: J. Palchefsky, Jr
ATTN: W. Patterson
ATTN: D. Tasca

General Electric Co
ATTN: L. Hauge
ATTN: B. Flaherty
ATTN: J. Reidl
ATTN: G. Bender

General Electric Co
ATTN: G. Gati, MD-E184

General Electric Co
ATTN: C. Hewison
ATTN: J. Gibson
ATTN: D. Cole

General Electric Co
ATTN: D. Pepin

General Research Corp
ATTN: A. Hunt
ATTN: E. Steele
ATTN: R. Hill
ATTN: Tech Info Ofc

George Washington University
ATTN: A. Friedman

Georgia Institute of Technology
ATTN: Res & Sec Coord for H. Denny

Goodyear Aerospace Corp
ATTN: Sec Con Station

Grumman Aerospace Corp
ATTN: J. Rogers

GTE Microcircuits
ATTN: F. Krch

Harris Corp
ATTN: C. Davis
ATTN: W. Abare
ATTN: E. Yost

DEPARTMENT OF DEFENSE CONTRACTORS (Continued)

Harris Corp
ATTN: C. Anderson
ATTN: J. Schroeder
ATTN: B. Gingerich, MS-51-120
ATTN: D. Williams, MS-51-75
ATTN: Mgr Linear Engrg
ATTN: J. Cornell
ATTN: T. Sanders, MS-51-121
ATTN: Mgr Bipolar Digital Eng

Hazeltine Corp
ATTN: C. Meinen
ATTN: J. Okrent

Honeywell, Inc
ATTN: F. Hampton
ATTN: D. Neilsen, MN 14-3015
ATTN: J. Moylan
ATTN: R. Gumm

Honeywell, Inc
ATTN: J. Zawacki
ATTN: C. Cerulli
ATTN: R. Reinecke
ATTN: J. Schafer
ATTN: MS 725-5
ATTN: H. Noble

Honeywell, Inc
ATTN: Tech Library

Honeywell, Inc
ATTN: L. Lavoie

Honeywell, Inc
ATTN: D. Herold, MS-MN 17-2334
ATTN: D Lamb, MS-MN 17-2334
ATTN: R. Belt, MS-MN 17-2334

Hughes Aircraft Co
ATTN: CTDC 6/E110
ATTN: D. Binder
ATTN: K. Walker
ATTN: R. McGowan

Hughes Aircraft Co
ATTN: E. Smith, MS V347
ATTN: E. Kubo
ATTN: W. Scott, S32/C332
ATTN: A. Narevsky, S32/C332
ATTN: D. Shumake

Hughes Aircraft Co
ATTN: R. Henderson

Hughes Aircraft Co
ATTN: P. Coppen
ATTN: MS-A2408, J. Hall

IBM Corp
ATTN: Electromagnetic Compatability
ATTN: T. Martin
ATTN: Mono Memory Systems
ATTN: H. Mathers

IBM Corp
ATTN: J. Ziegler

DEPARTMENT OF DEFENSE CONTRACTORS (Continued)

IBM Corp
ATTN: O. Spencer
ATTN: L. Rockett, MS 110-020
ATTN: A. Ederfeld
ATTN: MS 110-036, F. Tietze
ATTN: W. Doughten
ATTN: N. Haddad
ATTN: W. Henley
ATTN: H. Kobecha
ATTN: S. Saretto

IIT Research Institute
ATTN: I. Minoel
ATTN: R. Sutkowski

Illinois Computer Rsch, Inc
ATTN: E. Davidson

Institute for Defense Analyses
ATTN: Tech Info Svcs

Intel Corp
ATTN: T. May

International Tel & Telegraph Corp
ATTN: A. Richardson
ATTN: Dept 608

IRT Corp
ATTN: J. Harrity
ATTN: R. Judge
ATTN: M. Rose
ATTN: N. Rudie
ATTN: Physics Div
ATTN: MDC
ATTN: Systems Effects Div
ATTN: R. Mertz

JAYCOR
ATTN: R. Stahl
ATTN: J. Azarewicz
ATTN: M. Treadway
ATTN: L. Scott
ATTN: T. Flanagan
ATTN: R. Berger

JAYCOR
ATTN: E. Alcaraz
ATTN: R. Sullivan

JAYCOR
ATTN: R. Poll

Johns Hopkins University
ATTN: R. Maurer
ATTN: P. Partridge

Johns Hopkins University
ATTN: G. Masson, Dept of Elec Engr

Kaman Sciences Corp
ATTN: Dir Science & Technology Div
ATTN: J. Erskine
ATTN: W. Rich
ATTN: C. Baker
ATTN: N. Beauchamp

DEPARTMENT OF DEFENSE CONTRACTORS (Continued)

Kaman Tempo
ATTN: DASIAC
ATTN: W. McNamara
ATTN: R. Rutherford
4 cy ATTN: M. Espig

Kaman Tempo
ATTN: W. Alfonte

Kinon, John M
ATTN: J. Kinon

Litton Systems, Inc
ATTN: G. Maddox
ATTN: F. Motter
ATTN: J. Retzler

Lockheed Missiles & Space Co, Inc
ATTN: Reports Library
ATTN: J. Crowley
ATTN: F. Junga, S2/54-202
ATTN: J. Smith

Lockheed Missiles & Space Co, Inc
ATTN: D. Wolfhard
ATTN: K. Greenough
ATTN: B. Kimura
ATTN: L. Rossi
ATTN: S. Taimuty, Dept 81-74/154
ATTN: G. Lum
ATTN: Dr G. Lum, Dept 81-63
ATTN: J. Cayot, Dept 81-63
ATTN: P. Bene
ATTN: J. Lee
ATTN: E. Hessee
ATTN: A. Borofsky, Dept 66-60, B/577N

M.I.T. Lincoln Lab
ATTN: P. McKenzie

Magnavox Advanced Products & Sys Co
ATTN: W. Hagemeier

Magnavox Govt & Indus Electronics Co
ATTN: W. Richeson

Martin Marietta Corp
ATTN: H. Cates
ATTN: J. Tanke
ATTN: W. Janocko
ATTN: TIC/MP-30
ATTN: W. Brockett
ATTN: R. Yokomoto
ATTN: J. Ward
ATTN: R. Gaynor
ATTN: MP-163, W. Bruce
ATTN: S. Bennett
ATTN: P. Fender
ATTN: MP-163, M. Redmond

McDonnell Douglas Corp
ATTN: Library
ATTN: R. Kloster, Dept E451
ATTN: M. Stitch, Dept E003
ATTN: D. Dohm
ATTN: T. Ender, 33/6/618
ATTN: A. Munie

DEPARTMENT OF DEFENSE CONTRACTORS (Continued)

Martin Marietta Denver Aerospace
ATTN: D-6074, G. Freyer
ATTN: Goodwin
ATTN: M. Shumaker
ATTN: E. Carter
ATTN: Rsch Library
ATTN: P. Kase
ATTN: MS-D6074, M. Polzella

University of Maryland
ATTN: H. Lin

McDonnell Douglas Corp
ATTN: J. Holmgrem
ATTN: R. Lothringer
ATTN: J. Imai
ATTN: D. Fitzgerald
ATTN: P. Bretch
ATTN: M. Onoda
ATTN: M. Ralsten
ATTN: P. Albrecht

McDonnell Douglas Corp
ATTN: Tech Library

Messenger, George C
ATTN: G. Messenger

Mission Research Corp
ATTN: M. van Blaricum
ATTN: C. Longmire

Mission Research Corp
ATTN: D. Alexander
ATTN: D. Merewether
ATTN: R. Pease
ATTN: R Turfler

Mission Research Corp
ATTN: B. Passenheim
ATTN: J. Raymond

Mission Research Corp
ATTN: J. Lubell
ATTN: R. Curry
ATTN: W. Ware

Mitre Corp
ATTN: M. Fitzgerald

Mostek
ATTN: MS 640, M. Campbell

Motorola, Inc
ATTN: A. Christensen

Motorola, Inc
ATTN: C. Lund
ATTN: L. Clark
ATTN: O. Edwards

National Academy of Sciences
ATTN: National Materials Advisory Board

University of New Mexico
ATTN: H. Southward

DEPARTMENT OF DEFENSE CONTRACTORS (Continued)

National Semiconductor Corp
ATTN: F. Jones
ATTN: J. Martin
ATTN: A. London

New Technology, Inc
ATTN: D. Divis

Norden Systems, Inc
ATTN: D. Longo
ATTN: Tech Library

Northrop Corp
ATTN: J. Srour
ATTN: Z. Shanfield
ATTN: P. Eisenberg
ATTN: A. Kalma
ATTN: S. Othmer
ATTN: A. Bahraman

Northrop Corp
ATTN: P. Gardner
ATTN: L. Apodaca
ATTN: D. Strobel
ATTN: P. Besser
ATTN: T. Jackson
ATTN: E. King, C3323/WC
ATTN: S. Stewart

Pacific-Sierra Research Corp
ATTN. H. Brode, Chairman SAGE

Palisades Inst for Rsch Svcs, Inc
ATTN: Secretary

Physics International Co
ATTN: Div 6000
ATTN: J. Huntington
ATTN: J. Shea

Power Conversion Technology, Inc
ATTN: V. Fargo

R & D Associates
ATTN: C. Rogers
ATTN: W. Karzas

Rand Corp
ATTN: C. Crain

Raytheon Co
ATTN: G. Joshi
ATTN: T. Wein
ATTN: J. Ciccio

Raytheon Co
ATTN: A. Van Doren
ATTN: H. Flescher

RCA Corp
ATTN: V. Mancino

RCA Corp
ATTN: R. Killion

DEPARTMENT OF DEFENSE CONTRACTORS (Continued)

RCA Corp
ATTN: L. Napoli
ATTN: D. O'Connor
ATTN: Office N103
ATTN: G. Hughes
ATTN: R. Smeltzer
ATTN: L. Minich

RCA Corp
ATTN: E. Schmitt
ATTN: L. Debacker
ATTN: W. Allen

RCA Corp
ATTN: W. Heagerty
ATTN: E. Van Keuren
ATTN: J. Saultz
ATTN: R. Magyarics

Rensselaer Polytechnic Institute
ATTN: R. Gutmann
ATTN: R. Ryan

Research Triangle Institute
ATTN: M. Simons

Rockwell International Co
ATTN: V. Michel
ATTN. V. De Martino
ATTN: V. Strahan
ATTN: A. Rovel
ATTN: J. Pickel, Code 031-BB01
ATTN: R. Pancholi
ATTN: C. Klein
ATTN: GA50, IC/L, G. Green
ATTN: J. Blandford
ATTN: K. Hull
ATTN: J. Bell

Rockwell International Corp
ATTN: TIC D/41-092, AJ01
ATTN: D. Stevens

Rockwell International Corp
ATTN: A. Langenfeld
ATTN: TIC 106-216

Rockwell International Corp
ATTN: T. Yates
ATTN: TIC BA08

Sanders Assoc, Inc
ATTN: L. Brodeur
ATTN: M. Aitel

Science Applications, Inc
ATTN: D. Millward
ATTN: J. Spratt
ATTN: L. Scott
ATTN: V. Verbinski
ATTN: V. Orphan
ATTN: R. Fitzwilson
ATTN: D. Strobel
ATTN: D. Long
ATTN: J. Naber

DEPARTMENT OF DEFENSE CONTRACTORS (Continued)

Science Applications, Inc
ATTN: J. Swirczynski
ATTN: N. Byrn
ATTN: C. Cheek

Science Applications, Inc
ATTN: J. Wallace
ATTN: W. Chadsey

Science Applications, Inc
ATTN: D. Stribling

Scientific Research Assoc, Inc
ATTN: H. Grubin

Signetics Corp
ATTN: J. Lambert

Singer Co
ATTN: Tech Info Ctr
ATTN: J. Brinkman
ATTN: J. Laduca
ATTN: R. Spiegel

Sperry Corp
ATTN: Engrg Lab

Sperry Corp
ATTN: J. Inda

Sperry Flight Systems
ATTN: D. Schow

Sperry Rand Corp
ATTN: R. Viola
ATTN: C. Craig
ATTN: F. Scaravaglione
ATTN: P. Maraffino

SRI International
ATTN: A. Whitson

Sundstrand Corp
ATTN: Research Dept

Sylvania Systems Group
ATTN: L. Pauplis
ATTN: C. Thornhill
ATTN: L. Blaisdell
ATTN: W. Dunnet

Sylvania Systems Group
ATTN: H. Ullman
ATTN: P. Fredrickson
ATTN: H & V Group
ATTN: C. Ramsbottom

Strategic Systems Div
ATTN: J. Waldron

Systron-Donner Corp
ATTN: J. Indelicato

Teledyne Brown Engrg
ATTN: D. Guice
ATTN: T. Henderson
ATTN: J. McSwain

DEPARTMENT OF DEFENSE CONTRACTORS (Continued)

Teledyne Systems Co
ATTN: R. Suhrke

Texas Instruments, Inc
ATTN: R. Stehlin
ATTN: R. Carroll, MS 3143
ATTN: R. McGrath
ATTN: T. Cheek, MS 3143
ATTN: E. Jeffrey, MS 961
ATTN: F. Poblenz, MS 3143
ATTN: D. Manus

TRW Electronics & Defense Sector
ATTN: W. Willis
ATTN: F. Friedt
ATTN: P. Gardner
ATTN: A. Witteles, MS R1/2144
ATTN: D. Clement
ATTN: P. Guilfoyle
ATTN: Vulnerability & Hardness Lab
ATTN: P. Reid, MS R6/2541
ATTN: H. Holloway
ATTN: M. Ash
ATTN: W. Rowan
ATTN: E. Hennecke
ATTN: J. Bell
ATTN: R. Kingsland
ATTN: H. Volmerange, R1/1126
ATTN: Tech Info Ctr
2 cy ATTN: R. Plebuch
2 cy ATTN: O. Adams

TRW Electronics & Defense Sector
ATTN: C. Blasnek
ATTN: F. Fay
ATTN: J. Gorman
ATTN: R. Kitter

TRW Systems and Energy
ATTN: R. Mathews
ATTN: B. Gililland
ATTN: G. Spehar

Vought Corp
ATTN: Tech Data Ctr
ATTN: Library
ATTN: R. Tomme

Westinghouse Electric Corp
ATTN: E. Vitek, MS 3200
ATTN: MS 3330
ATTN: J. Cricchi
ATTN: L. McPherson
ATTN: N. Bluzer
ATTN: MS 330, D. Grimes
ATTN: H. Kalapaca

Westinghouse Electric Corp
ATTN: S. Wood